The internal cranial anatomy of *Champsosaurus lindoei* and its functional implications

by

Thomas William Dudgeon

A thesis submitted to the Faculty of Graduate and Postdoctoral Affairs
in partial fulfilment of the requirements for the degree of

Master of Science

in

Earth Sciences

Carleton University
Ottawa, Ontario

Abstract

Although *Champsosaurus* is well-known in Late Cretaceous and Paleocene deposits of North America, their cranial anatomy is poorly understood. Here, a well-preserved skull of *Champsosaurus lindoei* is described in detail using high-resolution micro-CT scanning. This confirms the presence of the putative neomorphic bone, which may be homologous with the pre-existing stapes, or developed through incomplete fusion of dermatocranial ossification centres. The ventral openings on the skull of *Champsosaurus* relate to the fenestrae ovales, an unusual configuration that may be convergent with other aquatic reptiles. Overall, the endocranial anatomy of *Champsosaurus* is typical for a basal diapsid. The morphology of the pars inferior of the inner ear suggests that *Champsosaurus* were capable of detecting sound underwater, and geometric morphometric analyses of the semicircular canals suggests that they were specialized for detecting head movements in an aquatic environment. Taken together, these results suggest that *Champsosaurus* were well adapted for an aquatic lifestyle.

Acknowledgements

I would like to thank Dr. Jordan Mallon and Dr. Hillary Maddin for their supervision and guidance throughout this project, Dr. Michael Ryan and Dr. Emily Standen for their invaluable feedback, and Dr. David Evans for helping to develop this project and for his advice and assistance along the way. I would like to thank Dr. Danielle Fraser and Bassel Arnaout for patiently teaching me R. Thanks to the staff and students of Carleton University, especially to the Carleton University Palaeontology students, for their support and encouragement.

Thanks also to the staff of the Canadian Museum of Nature, Royal Ontario Museum, and the Royal Tyrrell Museum for providing access to their collections. For helpful discussions, I thank Dr. Jason Anderson, Dr. Michael Coldwell, and Dr. Tetsuto Miyashita. Thanks to G. Sobral and the Museum für Naturkunde, K. Andrzewski, M. Polcyn, K. Chapelle, S. Lautenschlager, and H. Maddin for providing CT data, F. Gaidies for CT scanning the *Pantherophis* specimen, and the University of Texas CT Facility and the Alta Vista Animal Hospital for CT scanning CMN 8920 and CMN 8919, respectively.

Special thanks to Zoe Landry, Andrew Dodge, Emmett Janssens, and Eric Guitard, for their moral support and assistance with colour identification. Finally, I would like to thank Mom, Dad, Becky, Zoe, and Gabby for their constant love and support.

Table of Contents

List of Tables

List of Illustrations

List of Appendices

Chapter 1: A review of Choristodera (Diapsida)

Introduction

Choristoderes are a group of small to medium-sized (15 cm – 3 m long) diapsid reptiles that lived from the Middle Jurassic to the Miocene of Laurasia (Gao and Fox, 1998; Matsumoto et al., 2013). These animals were primarily aquatic (Katsura, 2010), preying on fish and other aquatic organisms (Matsumoto et al., 2009). The exact phylogenetic position of Choristodera within Diapsida is debated due to the sudden appearance of derived choristoderes in Upper Jurassic deposits, and an absence of specimens from their early evolutionary history (Matsumoto and Evans 2010; Matsumoto and Evans 2016). Of the two main clades within Diapsida (Neodiapsida and Araeoscelidia; Gaffney 1980; Evans 1988), Evans (1990) noted that choristoderes share more features with Neodiapsida, with the exception of the palatal dentition and absence of the mandibular retroarticular process. Many early phylogenies placed Choristodera as stem neodiapsids or as the sister-group to Neodiapsida (Evans, 1988; Gao and Fox, 1998; Rieppel and Reisz, 1999; Modesto and Sues, 2004), but recent reconstructions that include newly described basal choristoderes place Choristodera in a polytomy with Lepidosauromorpha and Archosauromorpha (Figure 1.1; Ezcurra 2016; Simoes et al., 2018).

At present, 12 genera are attributed to Choristodera (Figure 1.2; Matsumoto et al., 2013): *Cteniogenys* (Middle Jurassic, Euramerica; Evans 1990), *Coeruleodraco* (Late Jurassic, China; Matsumoto et al., 2019), *Lazarussuchus* (Miocene, Europe; Hecht, 1992;

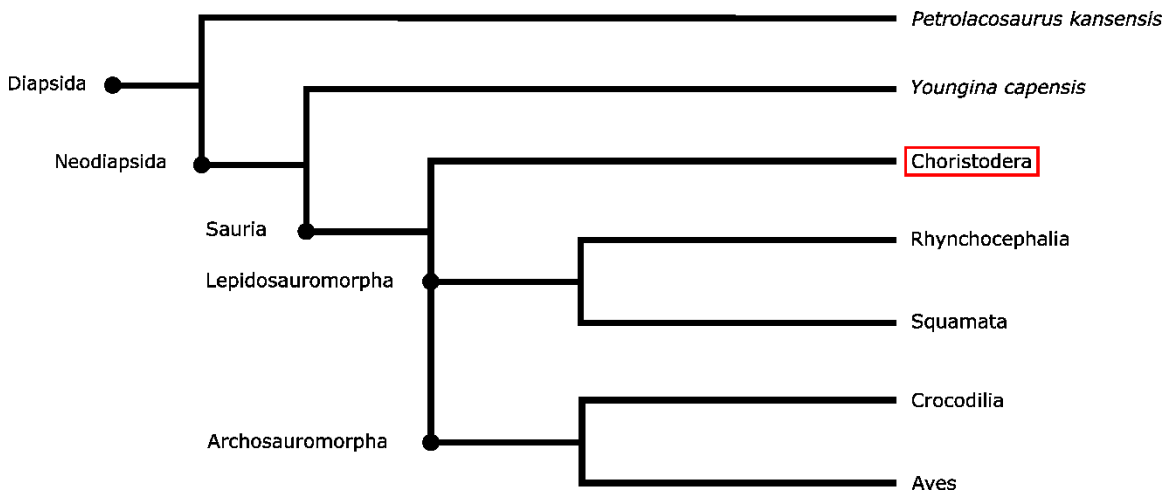

Figure 1.1: A phylogeny of Sauria with Choristodera highlighted in red (based on Ezcurra 2016).

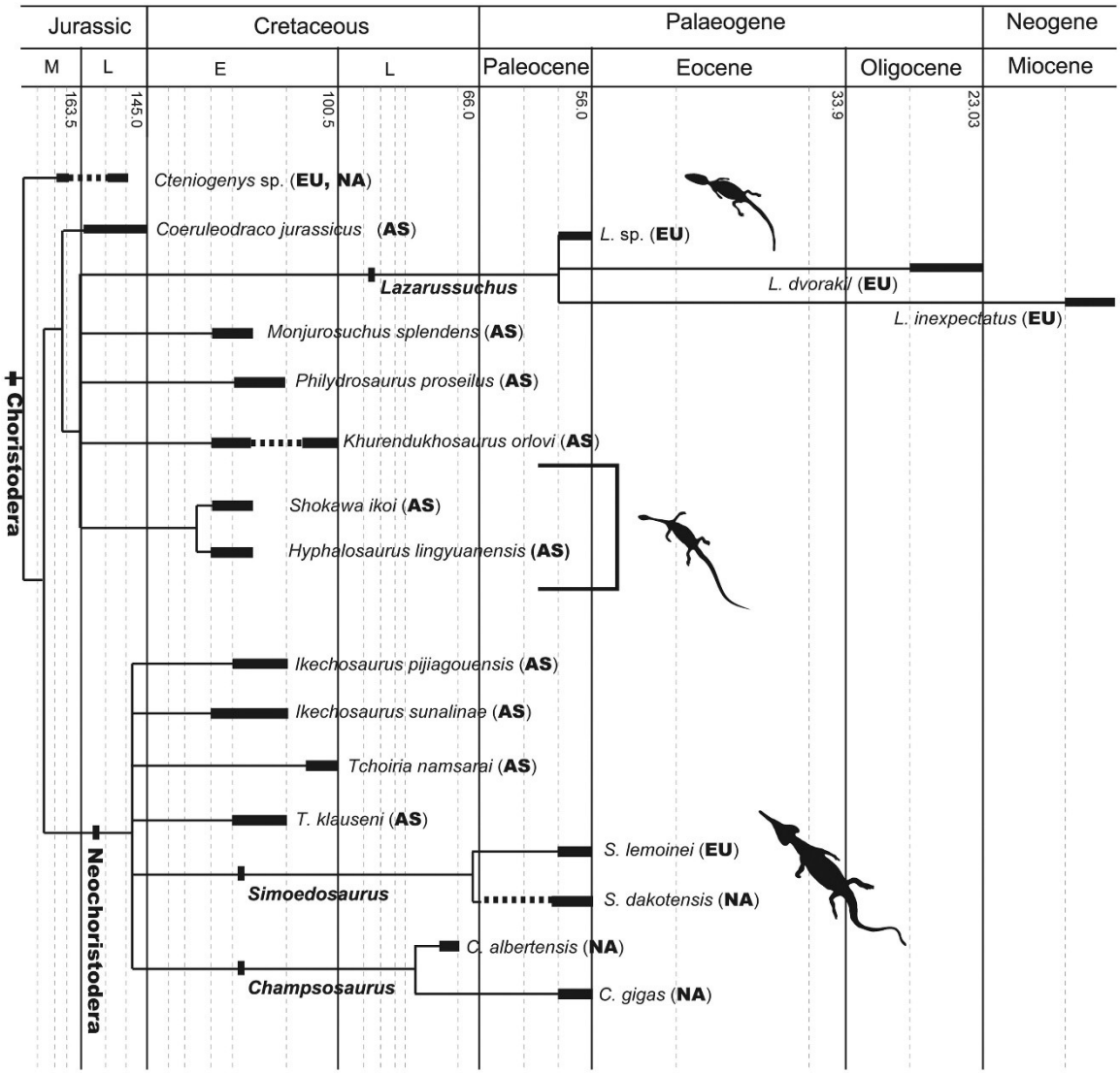

Figure 1.2: Time-calibrated phylogeny of Choristodera (from Matsumoto et al., 2019). Silhouettes indicate choristoderan morphotypes. Dotted vertical lines represent stages. Thick black horizontal lines are used when the age of the locality is identified only to stage, and thick dotted black lines indicate the estimated range. Square bracket left of the middle silhouette indicates taxa with that morphotype. Abbreviations: AS, Asia; EU, Europe; NA, North America.

Evans and Klembara, 2005), *Monjurosuchus* (Early Cretaceous, China and Japan; Gao et al., 2000; Matsumoto et al., 2007), *Philydrosaurus* (Early Cretaceous, China; Gao and Fox, 2005), *Shokawa* (Early Cretaceous, Japan; Evans and Manabe, 1999), *Hyphalosaurus* (Early Cretaceous, China; Gao et al., 1999), *Khurendukhosaurus* (Early Cretaceous, Mongolia; Sigogneau-Russell and Efimov, 1984; Skutschas 2008; Matsumoto et al., 2009), *Ikechosaurus*, *Tchoiria* (Cretaceous, China and Mongolia; Efimov, 1975; Sigogneau-Russell, 1981a), *Simoedosaurus*, and *Champsosaurus* (Late Cretaceous-earliest Eocene, Europe and North America; Gao and Fox 1998).

The interrelationships of these genera are poorly resolved, but there is strong support for the monophyletic relationship of *Champsosaurus*, *Simoedosaurus*, *Tchoira*, and *Ikechosaurus* (Figure 1.2). Together, these taxa form the group Neochoristodera (Evans and Hecht 1993), and are characterized, in part, by their larger size (2 – 3 m long), elongated snout, and expanded temporal region (see Systematic Palaeontology section for diagnostic features). Choristoderes that are basally positioned to Neochoristodera are informally referred to as non-neochoristoderes.

Gao and Fox (1998) provided the most recent review of Choristodera, where they discussed *Cteniogenys*, *Simoedosaurus*, and *Champsosaurus*, described new material from the Cretaceous of North America that may pertain to *Cteniogenys*, and erected a new species of *Champsosaurus* from Dinosaur Provincial Park, *C. lindoei*. Since this review by Gao and Fox (1998), nine new genera have been attributed to Choristodera; however, an updated review of Choristodera incorporating these more recent advances has not been conducted. The purpose of this chapter is to provide a systematic review of the current status of Choristodera based on the literature, with emphasis on the most diverse and well-known

choristodere genus, *Champsosaurus*, which is the focus of this thesis. Current problematic aspects of choristoderan nomenclature are discussed, such as the implications of the invalidity of the type species for *Champsosaurus*, *C. annectens*, and the absence of phylogenetic definitions for Choristodera and Neochoristodera. I will then provide a discussion of recent choristodere discoveries that shed light on the palaeobiology of these enigmatic animals, and discuss avenues for further research that form the remainder of this thesis.

Institutional Abbreviations

AMNH, American Museum of Natural History, New York, New York; BDL, Menat Museum Bord du Lac, Menat, Puy-de-Dôme, France; CAGS, Chinese Academy of Geological Sciences, Beijing, China; CMN, Canadian Museum of Nature, Ottawa, Ontario; GMV, Geological Museum of China, Beijing, China; IGM, Geological Institute of the Mongolian Academy of Sciences, Ulan Bataar, Mongolia; IVPP, Institute of Vertebrate Paleontology and Paleoanthropology, Beijing, China; ROM, Royal Ontario Museum, Toronto, Ontario; TMP, Royal Tyrrell Museum of Palaeontology, Drumheller, Alberta; SMM, The Science Museum of Minnesota, St. Paul, Minnesota; UALVP, Laboratory for Vertebrate Paleontology, Department of Biological Sciences, University of Alberta, Edmonton, Alberta.

Systematic Palaeontology

Class Reptilia Laurenti, 1768
Subclass Diapsida Osborn, 1903
Order Choristodera Cope, 1884b

Type genus – *Champsosaurus* Cope, 1876.

Attributed genera – *Cteniogenys*, *Coeruleodraco*, *Lazarussuchus*, *Monjurosuchus*, *Philydrosaurus*, *Hyphalosaurus*, *Shokawa*, *Khurendukhosaurus*, *Simoedosaurus*, *Tchoiria*, *Ikechosaurus*, *Champsosaurus*.

Temporal and spatial distribution – Middle Jurassic to Miocene of North America, Europe, and Asia (Matsumoto et al., 2019). Haddoumi et al. (2016) described fragmentary material from the Bathonian (Late Jurassic) of North Africa that may pertain to a basal choristodere. If true, this would be the first choristodere material described outside of Laurasia, extending the geographic range of Choristodera to northern Gondwana.

Diagnosis – The diagnosis of Choristodera has changed substantially over time as new taxa are discovered and attributed to it. Choristodera was initially diagnosed by little to no ossification in the sacral vertebrae, and no fusion between the vertebral centra and the neural arches (Cope 1884b). This diagnosis was made when only *Champsosaurus* and *Simeodosaurus* were known. Following the discovery of *Tchoiria* (Efimov 1975) and *Ikechosaurus* (Sigogneau-Russell 1981), the diagnosis of Choristodera was updated by Evans (1988) to: (1) confluent nares; (2) slender nasals fused at the midline; (3) prefrontals meeting in midline, separating nasals from frontals; (4) no supratemporal ossification; (5) no postparietal; (6) palatal elements covered by a shagreen of teeth; (7) sub-thecodont marginal teeth; (8) long gavial-like snout; (9) fused postorbitofrontal; (10) T-shaped interclavicle with

bulbous stem. The diagnosis of Choristodera dramatically changed following the discovery of *Cteniogenys* (Evans 1990). Gao and Fox (1998) stated that the character matrix from Evans (1990) provides as many as 19 synapomorphies of Choristodera, but Evans' (1990) character matrix only reports three characters that are definitively shared across all known choristoderes including *Cteniogenys*: (1) prefrontals meeting the midline; (2) dorsal process of maxilla inrolled medially; (3) and vomers meeting the maxillae laterally, extending the length of the hard palate and displacing the choanae posteriorly. The 16 extra synapomorphies reported by Gao and Fox (1998) were likely included because they were ambiguous in only one taxon.

Gao and Fox (1998), in a comprehensive review of Choristodera, updated the diagnosis to include seven characters: (1) external nares terminal and confluent; (2) nasals fused, elongated more than half the length of the snout (this character is a putative synapomorphy for the group as it cannot be scored for the basal *Cteniogenys*); (3) basipterygoid process and cotyle reduced, and basipterygoid and pterygoid tightly sutured; (4) neomorph forming part of lateral wall of braincase and medial wall of the temporal fossa (this character was tentative because the neomorph had only been inferred in *Cteniogenys* through facets in neighboring bones); (5) vertebral centrum amphiplatyan with notochordal canal closed; (6) neural arches separate from centra during maturity (choristoderans share this character with other aquatic reptile groups); (7) sacral and caudal ribs free from vertebrae.

However, more recent discoveries show that some of these characters are now non-diagnostic for all choristoderes. Newer material of *Khurendukhosaurus* (Matsumoto et al., 2009) shows that this species fused their neurocentral sutures in maturity, resulting in the

once diagnostic feature of Choristodera, and iconic feature of *Champsosaurus* (character 6 of Gao and Fox 1998: neural arches separate from centra into maturity), to be non-diagnostic of the whole clade. Additionally, the discovery of *Philydrosaurus* (Gao and Fox 2005) shows that these choristoderes have paired nares, a feature later found in *Hyphalosaurus* (Gao and Ksepka 2008), indicating that confluent nares (character 1 of Gao and Fox 1998) is not a feature uniting Choristodera.

Despite the subsequent discovery of several genera since Gao and Fox (1998), the diagnosis for Choristodera has not been revised. Matsumoto et al., (2019) provided nine characters to assign *Coeruleodraco* to Choristodera: (1) median contact of the elongated prefrontals, separating nasals from frontals; (2) dorsal flange of the maxilla inflected medially; (3) absence of a parietal foramen; (4) squamosal expanded posterior to the occipital condyle; (5) conical sub-thecodont teeth; (6) a slender dentary with anteroposteriorly elongated grooves on the labial surface; (7) additional sacral vertebrae; (8) expanded spine tables on the vertebrae; (9) amphiplatyan vertebral centra. Although not a formal diagnosis, these are the most current and accurate synapomorphies that unite Choristodera. A formal re-evaluation of choristoderes, integrating this convoluted history of diagnoses, is still needed to consolidate the diagnostic features of the group.

Remarks – *Cteniogenys*, *Coeruleodraco*, *Lazarussuchus*, *Monjurosuchus*, and *Philydrosaurus* are characterized by a relatively small body (approximately 30-40 cm long), with a short neck and skull, giving them a lizard-like appearance. *Shokawa* and *Hyphalosaurus* also possess a short snout, but have remarkably elongate necks, giving them a nothosauriform body plan (Matsumoto and Evans 2010). *Khurendukhosaurus* has an inferred similarity to *Hyphalosaurus*, but the exact shape of the skull or length of the neck is not

known (Matsumoto and Evans 2010). *Ikechosaurus*, *Tchoiria*, *Simoedosaurus*, and *Champsosaurus* are relatively large choristoderes (2-5 m long) that possess short necks (relative to the nothosauriform choristoderes) and highly elongated snouts with posteriorly expanded temporal fenestrae. *Pachystropheus* (Jurassic, Europe, von Huene 1935; Storrs and Gower, 1993; Storrs et al., 1996), *Irenosaurus* (Early Cretaceous, Mongolia, Efimov, 1979), and *Liaoxisaurus* (Early Cretaceous, China, Gao et al., 2005) have been described as distinct choristoderan genera; however, these conclusions have been met with skepticism due to poor preservation, and a strong morphological similarity with other established choristoderes, which suggest they may be synonymous. Matsumoto and Evans (2010) divided Choristodera into three distinct morphotypes: the short necked brevirostrines, the long necked brevirostrines, and the short necked longirostrines. These morphotypes are not necessarily monophyletic, and may simply reflect a similarity in overall morphology due to convergence in some lineages.

Family Cteniogenidae Seiffert, 1973

Type genus – *Cteniogenys* Gilmore, 1928.

Temporal and spatial distribution – Same as type genus.

Diagnosis – Same as the type genus.

Genus *Cteniogenys* Gilmore, 1928

Type species – *Cteniogenys antiquus* Gilmore, 1928.

Type locality and horizon – Late Jurassic (Kimmeridgian-Tithonian), Morrison Formation, Como Bluff, Quarry 9, Wyoming (Gilmore, 1928).

Temporal and spatial distribution – Middle Jurassic (Bathonian), Kirtlington Mammal Bed, Oxfordshire, England (Evans 1990); Middle Jurassic (Bathonian), Kilmaluag Formation, Scotland (Evans and Waldman, 1996); Late Jurassic (Kimmeridgian), Morrison Formation, Wyoming, Utah, South Dakota (Chure and Evans, 1998; Foster and Trujillo, 2000); Late Jurassic (Kimmeridgian), Guimarota Lignite mine, Portugal (Seiffert 1973; Evans 1989; Gao and Fox 1998); Late Cretaceous (mid-upper Campanian), Dinosaur Park Formation, Alberta, Canada (Gao and Fox 1998).

Diagnosis – From Gao and Fox (1998): (1) no contact between premaxillae and nasals; (2) orbits narrow and elongate; (3) frontals subrectangular; (4) dorsal process of maxilla prominent, confined to anterior part of maxilla, and slightly inrolled dorsally; (5) prefrontal short, widened, having elongate palatal process.

Remarks – *Cteniogenys* was a relatively small (approximately 15 cm long; Evans and Hecht 1993; Figure 1.3), amphibious reptile. The holotype species, *C. antiquus*, was first described by Gilmore (1928), who described them as lizards based solely on isolated dentaries from Como Bluff, Wyoming (Upper Jurassic). This interpretation was further supported by Estes (1983) and Seiffert (1973) who identified new material from Guimarota, Portugal (Middle Jurassic). Evans (1989) described new specimens of *Cteniogenys* from the Kurlington

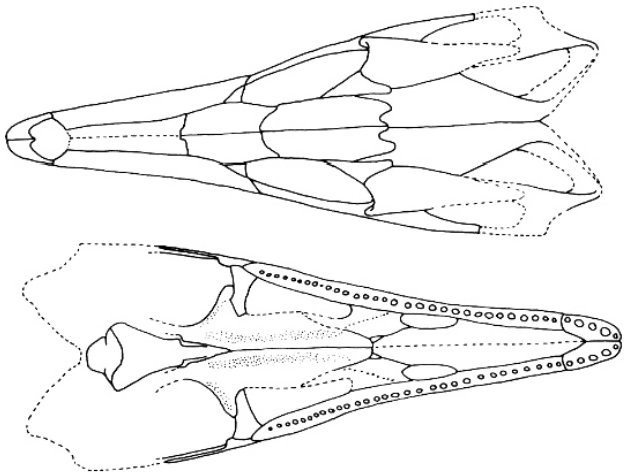

Figure 1.3: Reconstructed line drawing of the dorsal and ventral view of the skull of *Cteniogenys* (modified from Evans 1990).

Mammal Bed, Britain (Middle Jurassic) and identified these animals as belonging to Choristodera based predominantly on the presence of confluent nares.

The skull of *Cteniogenys* has typical proportions for a basal diapsid, with only slight elongation in the preorbital region (Evans 1990). Based on the shape of the skull, the temporal fenestrae were likely large, but the posterior end of the skull was not preserved, so the relative size of these structures is not known. *Cteniogenys* also had a palatal dentition and posteriorly placed choanae, a feature typically seen in aquatic reptiles. The hypothesis that these animals were aquatic is supported by the dorsoventrally flat profile of the skull, and elongation of the preorbital region. A feature unique to *Cteniogenys* among choristoderes is that the confluent narial opening faces dorsally, and is bordered by the maxillae as well as the premaxillae (in contrast to other choristoderes, where the nares face anteriorly and are bordered solely by the premaxillae).

Evans (1990) described *Cteniogenys* as having many features in common with the more derived choristoderes of the Cretaceous and Palaeogene, although retaining a more generalized, non-choristoderan body plan. This lead Evans (1990) to conclude that the body plan of *Cteniogenys* is likely representative of the basal body plan of Choristodera, a hypothesis that has been supported with the subsequent discovery of new specimens and taxa, and the generation of updated phylogenetic reconstructions. Gao and Fox (1998) attributed material from the Upper Cretaceous of Alberta, Canada (Oldman Formation) to *Cteniogenys*; however, this has been met with skepticism as the material is highly fragmented with poor diagnostic features and is comparatively late with respect to all known *Cteniogenys* material (Matsumoto et al., 2009; Matsumoto and Evans 2010).

Genus *Coeruleodraco* Matsumoto et al., 2019

Type species – *Coeruleodraco jurassicus* Matsumoto et al., 2019.

Type locality and horizon – Late Jurassic (Oxfordian), Tiaojishan Formation, Hebei Province, China (Matsumoto et al., 2019).

Temporal and spatial distribution – Same as for the type, and only known specimen.

Diagnosis – (1) paired external narial openings; (2) unossified parasphenoid rostrum; (3) short nasal lacking contact with maxilla; (4) small lower temporal opening that is longer than high; (5) tubercular sculpture along the posterior margin of the squamosal; (6) cervical neural spine tables expanded; (7) well developed entepicondyle on the humerus with distinct rounded distal tubercle; (8) ischiadic plate with a posterodorsal process; (9) distally expanded fan-like caudal ribs fused to vertebrae (Matsumoto et al., 2019).

Remarks – The holotype of *Coeruleodraco* provides the best evidence for the presence of the putative neomorphic bone in non-neochoristoderes. Other non-neochoristoderes have allowed researchers to infer the presence of the neomorph through facets in the neighboring bones, but *Coeruleodraco* appears to have it preserved. The type specimen is the best preserved early choristodere from the Jurassic, and exemplifies the ancestral choristoderan body plan.

The discovery of *Coeruleodraco* updated the framework of choristoderan phylogeny, placing *Cteniogenys* as a sister taxon to all other choristoderes and grouping all other non-neochoristoderes together (Matsumoto et al., 2019). The statistical support for a monophyletic Neochoristodera is strong (bootstrap value of 88; Matsumoto et al., 2019), but the placements of *Cteniogenys* at the base of Choristodera (bootstrap value of 21; Matsumoto

et al., 2019) and the remaining non-neochoristoderes in a polytomy with Neochoristodera (bootstrap value of 3; Matsumoto et al., 2019), are weakly supported. Matsumoto et al., (2019) did not comment on the weak support for these groups, but it is likely the poor representation of early choristoderes that limits understanding of the group's early evolutionary history.

Genus *Lazarussuchus* Hecht, 1992

Type species – *Lazarussuchus inexpectatus* Hecht, 1992.

Attributed species – *L. inexpectatus*, *L.* d*voraki*

Type locality and horizon – Late Oligocene-early Miocene (Armissan), Armissan quarry, France (Hecht, 1992).

Temporal and spatial distribution – Paleocene (Selandian-Thanetian) to early Miocene (Armissan), France, Czech Republic, Germany (Hecht, 1992; Evans and Klembara, 2005; Bohme 2008; Matsumoto et al., 2013).

Diagnosis – Hecht (1992) distinguished this genus from other choristoderes on the basis of 13 autapomorphies that were also used to diagnose the type species *L. inexpectatus*: (1) elongated paired dorsal nares set high on snout; (2) nares separated at midline by reduced nasals and premaxilla; (3) broad squamosal-postorbital bar; (4) premaxilla spine lengthened posteriorly; (5) tooth rows on the pterygoid and palatine consist of isolated large teeth; (6) osteodermal ossifications around border of supratemporal fenestra and on the temporal arch; (7) complex rugose ornamentation on most skull bones; (8) cervical ribs broad, flattened and expanded with large capitulum in relation to tuberculum; (9) postzygapophoseal tubercle on

cervicals; (10) weak accessory vertebral articulation below postzygapophysis; (11) no trunk intercentra; (12) ectepicondylar groove bridged to form foramen; (13) unguals narrow and not flattened.

Remarks – The discovery of *Lazarussuchus* (Hecht 1992) was significant for choristoderan systematics because this genus is found in upper Oligocene-lower Miocene deposits, despite having a basal choristoderan body plan. Until the discovery of *Lazarussuchus*, the youngest choristoderes were *Champsosaurus* and *Simoedosaurus* from the upper Palaeocene of North America and Europe; however, the discovery of *Lazarussuchus* pushes the temporal range of Choristodera to as recent as 30 Ma (a difference of nearly 25 Ma; Hecht 1992). Additionally, *Champsosaurus* and *Simoedosaurus* are both highly derived choristoderes of relatively large body size (2-5 m long), possessing an elongated snout and greatly expanded temporal fenestrae. *Lazarussuchus*, on the other hand, is relatively small (approximately 30 cm long; Hecht 1992; Figure 1.4) and shows a basal choristodere skull morphology more similar to that of *Cteniogenys* of the Jurassic (Evans and Hecht 1993). Hecht (1992) described *Lazarussuchus* as a prime example of Jablonski's (1986) "Lazarus Effect", where a taxon reappears in the fossil record long after it was believed to have gone extinct. This led Hecht (1992) to name the genus *Lazarussuchus*, meaning "Lazarus crocodile", and the holotype specific epithet *inexpectatus*, meaning "unexpected".

Evans and Klembara (2005) described a second species, *L. dvoraki*, from the Lower Miocene of the Czech Republic. The holotype specimen is the left parietal region of the skull, with no other elements preserved. Evans and Klembara (2005) described several other fragmented specimens that clearly pertain to *Lazarussuchus* and were also assigned to *L. dvoraki* based on their stratigraphic position and locality. These specimens show that *L.*

Figure 1.4: Line drawing of *Lazarussuchus* sp. (BDL 1819; modified from Matsumoto et al., 2013).

dvoraki differs from *L. inexpectatus* in having smaller and more ovoid temporal fenestrae, where the postparietal processes are approximately one third the length of the 'parietal plate' (Evans and Klembara 2005:173).

Genus *Monjurosuchus* Endo, 1940

Type species – *Monjurosuchus splendens* Endo, 1940

Type locality and horizon – Late Jurassic-Early Cretaceous (Barremian–Aptian), Yixian Formation, Niuyingzi, Lingyuan, Liaoning, China.

Temporal and spatial distribution – Late Jurassic-Early Cretaceous (Barremian-Aptian), Liaoning, China (Gao et al., 2000); Early Cretaceous (Berriasian–Barremian), Japan (Matsumoto et al 2007).

Diagnosis – Matsumoto et al., (2007) used ten features to diagnose *Monjurosuchus*: (1) paired nasals that intervene posteriorly between anterior tips of prefrontals; (2) frontals fused, posterolaterally expanded, but markedly narrow and constricted between orbits; (3) prefrontal equal to frontal in length; (4) lacrimal facet on prefrontal longer than maxillary facet; (5) supratemporal fenestra roughly equal to orbital length; (6) postorbitofrontal fused; (7) squamosal square, laterally expanded; (8) infratemporal fenestra closed mainly by the enlarged jugal; (9) interclavicle "T" shaped with straight stem; (10) fore and hind feet webbed, with only the claws projecting. It must be noted that feature (10) of Matsumoto et al., (2007) is not an informative character because other choristoderan taxa do not have soft tissue preserved.

Remarks – As with many choristoderan taxa, *M. splendens* was initially described as a reptile of uncertain affinities (Endo 1940; Gao et al., 2000), and further description was complicated when the holotype specimen was lost during World War II. A description of new material by Gao et al. (2000) showed that this genus belongs to Choristodera. The initial descriptions of *M. splendens* involved material from Liaoning, China (Early Cretaceous); however, specimens attributed to *Monjurosuchus* were also found in central Japan (Early Cretaceous; Matsumoto et al., 2007). The description by Gao et al. (2000) included five new specimens from the Yixian Formation of Liaoning Province, China (Early Cretaceous), ranging in ontogeny from juvenile to adult stages. These specimens are in remarkable condition (Figure 1.5), including skin impressions, integument, and intestinal contents (see Discussion for description and biological implications). The specimens described by Gao et al. (2000) also possess impressions of webbing between the digits of the fore and hind feet, suggesting that *Monjurosuchus* was well adapted for an aquatic lifestyle.

Although Endo (1940) classified *M. splendens* as a basal archosaur, other researchers (von Huene, 1942; Kuhn, 1969; Ren et al., 1995) have attributed it to Rhynchocephalia due to apparent morphological similarities with the extant *Sphenodon*. Gao et al. (2000) showed that this relationship is impossible because rhynchocephalians possess an acrodont dentition and a single row of palatine teeth, as well as a suite of characters seen in lizards. *Monjurosuchus splendens* shows none of these features, and additionally possesses a sub-thecodont dentition with a battery of palatal teeth (Gao et al., 2000), and, therefore, cannot be attributed to Rhynchocephalia. Gao et al. (2000) suggested that *M. splendens* is a choristodere based on the dorsoventrally flattened skull, cordiform dorsal skull profile, palatal tooth battery, and the absence of a parietal foramen.

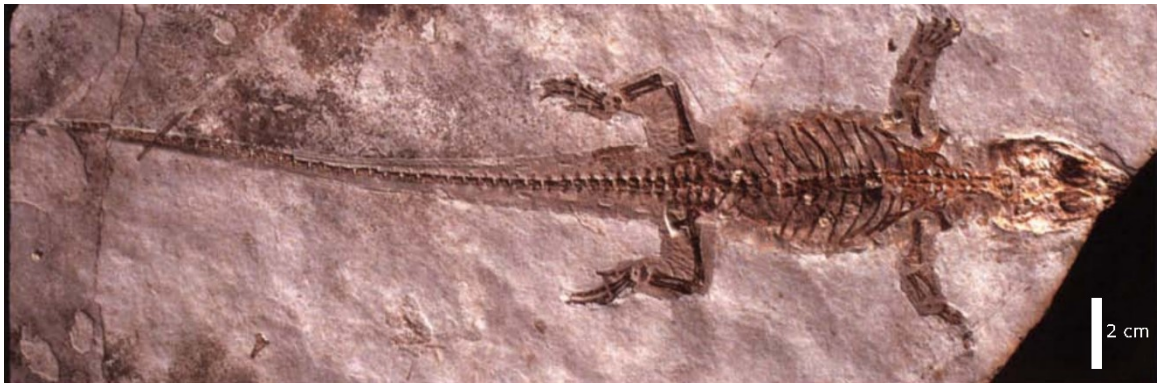

Figure 1.5: A nearly complete juvenile *Monjurosuchus splendens* (GMV 2135; from Gao et al., 2000).

Genus *Philydrosaurus* Gao and Fox, 2005

Type species – *Philydrosaurus proseilos* Gao and Fox, 2005.

Attributes species – Same as type species.

Type locality and horizon – Early Cretaceous (Aptian), Chiufotang Formation, Liaoning, China (Gao and Fox, 2005).

Temporal and spatial distribution – Same as for the type.

Diagnosis – Gao and Fox (2005) noted that *P. proseilos* closely resembles *M. splendens* in both size and morphology; however, they differ from one another in several ways, the most significant being an elongate skull in *P. proseilos*, with elongate narial openings and orbits and the presence of a spike-like posterior process of ischium.

Remarks – The similarity between *P. proseilos* to *M. splendens* led Gao and Fox (2005) to include *Philydrosaurus* in the monophyletic Monjurosuchidae (Endo 1940) along with *Monjurosuchus*. More recent phylogenies of Choristodera (e.g., Matsumoto et al., 2007; Skutschas 2008; Matsumoto et al., 2019) fail to retrieve Monjurosuchidae; instead *Monjurosuchus* and *Philydrosaurus* form a polytomy with other non-neochoristoderes.

Family Hyphalosauridae Gao and Fox, 2005

Type genus – *Hyphalosaurus* Gao et al., 1999.

Attributed genera – *Hyphalosaurus* and *Shokawa.*

Temporal and spatial distribution – Early Cretaceous (Barremian-Aptian), Yixian Formation, Liaoning, China (Gao et al., 1999); Early Cretaceous (Valanginian), Okurodani Formation, Shokawa, Japan.

Diagnosis – Choristoderes with elongate necks consisting of 16 or more cervical vertebrae (Gao and Ksepka 2008).

Remarks – It is likely that the elongated neck is an adaptation for a highly aquatic lifestyle, a hypothesis that is supported by the deep-water lacustrine sediments in which some hyphalosaurids are found (Gao and Ksepka 2008).

Genus *Hyphalosaurus* Gao et al., 1999

Type species – *Hyphalosaurus lingyuanensis* Gao et al., 1999.

Attributed species – *H. lingyuanensis, H. baitaigouensis.*

Type locality and horizon – Early Cretaceous (Barremian-Aptian), Yixian Formation, western Liaoning Province, China (Gao et al., 1999).

Temporal and spatial distribution – Same as for the type.

Diagnosis – Hyphalosaurids with elongate necks consisting of 19 or more cervical vertebrae (Gao and Ksepka 2008).

Remarks – Like other choristoderes, these animals were adapted for an aquatic lifestyle, but possess a unique morphology where their necks have become highly elongate (Figure 1.6). This morphology is also seen in several groups of sauropterygians, suggesting that an elongate neck is a specialization associated with piscivory. The type species of

Figure 1.6: A mature *Hyphalosaurus baitaigouensis* (CAGS-IG-06131; from Ji et al., 2010).

Hyphalosaurus is well represented, consisting of several specimens of different ontogenetic stages from the Lingyuan area (Western Liaoning). The second species is known from thousands of specimens from the upper Yixian Formation of Yizhou (approximately 150 km East of Lingyuan). Localities from Yizhou have also yielded several clutches of soft-shelled eggs that have been confirmed to have belonged to *H. baitaigouensis* (see Discussion for biological implications).

There are several morphological differences between *H. lingyuanensis and H. baitaigouensis*, but the most notable and significant difference is the number of cervical vertebrae (19 and 26, respectively; Ji et al., 2004; Gao and Ksepka 2008). Gao et al., (1999) provided the first description of the holotype of *Hyphalosaurus*, but were unable to describe the specimen in its entirety due to incomplete preparation. Gao and Ksepka (2008) revised the description of both *H. lingyuanensis* and *H. baitaigouensis*, and described the first complete material of *H. lingyuanensis*.

Genus *Shokawa* Evans and Manabe, 1999

Type species – *Shokawa ikoi* Evans and Manabe, 1999.

Type locality and horizon – Early Cretaceous (Valanginian), Okurodani Formation, Shokawa village, Gifu Prefecture, Japan.

Temporal and spatial distribution – Same as for the type.

Diagnosis – From Evans and Manabe (1999): (1) at least 16 cervical vertebrae, of which most or all bear small bicapitate ribs; (2) cylindrical vertebral centra persistently separated from the neural arches except in the neck; (3) caudal vertebrae with deep descending ventral

flanges; (4) anterior caudals with tall slender neural spines; (5) interclavicle rhomboid with clavicles meeting at a strong angle in the ventral midline; (6) strong quadrangular coracoids and reduced scapular blades; (7) humerus, forearm and hand relatively short and broad; (8) ilium with narrow vertical blade bearing strong vertical striations; (9) ribs, limb bones and gastralia pachyostotic.

Remarks – *Shokawa ikoi* is the only known species of hyphalosaurid choristodere from Japan, and is based on a partially complete postcranium (the holotype) and isolated fragments (Evans and Manabe 1999). The postcranial skeleton is well represented by these specimens, but the skull of *Shokawa* is unknown. The exact size of these animals is difficult to determine due to the fragmentary nature of the specimens, but Evans and Manabe (1999) believed that 37-40 cm was a reasonable length, given all the material that had been found, and known proportions of other choristodere species.

Genus *Khurendukhosaurus* Sigogneau-Russell and Efimov, 1984

Type species – *Khurendukhosaurus orlovi* Sigogneau-Russell and Efimov (1984).

Type locality and horizon – Early Cretaceous (Barremian-Albian), Khuren-Dukh, Mongolia.

Temporal and spatial distribution – Early Cretaceous (Barremian-Aptian), Mongolia and Russia.

Diagnosis – From Matsumoto et al., (2009): Medium-sized (approximately 1 m long) choristodere characterized by (1) closed neurocentral sutures in adults; (2) anteroposteriorly elongated neural spines with transversely expanded, rugose, spine tables on dorsal vertebrae;

(3) tall, narrow caudal vertebral neural spines; (4) a twisted ilium with an almost rectangular iliac blade patterned by coarse anteroposterior ridges.

Remarks – *Khurendukhosaurus* was assigned to Choristodera based on the similarity of its vertebral centra to those of *Champsosaurus* and *Simoedosaurus*, but a lack of well-preserved material made this assignment tentative. A second species, *K. bajkalensis,* was described by Efimov (1996); however, the distinction of this species from *K. orlovi* was based on features that vary through ontogeny, and it is no longer considered valid (Efimov and Storrs 2000; Matsumoto et al., 2009). New material from eastern Mongolia illuminates the morphology of the mandible in *Khurendukhosaurus* that provides strong evidence that these animals are, indeed, choristoderes (Skutschas 2008), a position supported by Matsumoto et al. (2009). Postcranial features suggest that *Khurendukhosaurus* is more derived than *Cteniogenys*, and basal to Neochoristodera, but its exact placement within Choristodera is uncertain (Matsumoto et al., 2009).

Skutschas and Vitenko (2017) ran a cladistic analysis of non-neochoristoderes with the inclusion of recently discovered fragmentary cranial material of *Khurendukhosaurus*, and an updated character matrix. They found that *Khurendukhosaurus* is possibly a sister-taxon to *Hyphalosaurus* and *Shokawa*, suggesting that *Khurendukhosaurus* may also be a long-necked, highly aquatic choristodere, but more complete material is needed to confirm this.

Suborder Neochoristodera Evans and Hecht 1993

Type genus – *Champsosaurus* Cope, 1876.

Attributed genera – *Champsosaurus, Simoedosaurus, Tchoiria,* and *Ikechosaurus.*

Temporal and spatial distribution – Late Cretaceous to late Paleogene of North America, Europe, and Asia (Gao and Fox 1998; Ksepka et al., 2005).

Diagnosis – Medium to large choristoderes (1-3 m long) with an elongated snout, posteriorly expanded temporal foramen, dorsally facing orbits, fused nasals, and confluent nares that open into the tip of the snout (Evans and Hecht 1993).

Remarks – Two families are included in Neochoristodera: Simoedosauridae (Lemoine 1884) and Champsosauridae (Cope 1884a). Evans (1990) found Simoedosauridae to contain *Simoedosaurus* and *Ikechosaurus*, and Champsosauridae to contain *Champsosaurus* and *Tchoiria* (Evans 1990), but some of these species have been reassigned within Neochoristodera in subsequent phylogenies (Gao and Fox 1998). Gao and Fox (1998) found *Ikechosaurus* is included in Simoedosauridae and *Champsosaurus* is the only genus within Champsosauridae. More recent phylogenies have not supported this conclusion, instead recovering all neochoristoderan genera together in a polytomy (Matsumoto et al., 2013; Matsumoto et al., 2019). Despite the uncertainty regarding Simoedosauridae and Champsosauridae, there has been no comment on the validity of these groups since Gao and Fox (1998). Therefore, Simoedosauridae and Champsosauridae are not included here due to the absence of recent support for their existence.

Genus *Simoedosaurus* Gervais, 1877

Type species – *Simoedosaurus lemoinei* Gervais, 1877.

Attributed species – *S. lemoinei*, *S. dakotensis.*

Type locality and horizon – Late Paleocene (Thanetian), Mouras Quarry, Berru, Marne, France.

Temporal and spatial distribution – Late Paleocene of France, and North Dakota (Erickson 1987); Late Paleocene-Early Eocene, Dzhylga, Kazakhstan (Averianov 2005).

Diagnosis – *Simoedosaurus* is a relatively large choristodere (2-3 m long) and is morphologically similar to the contemporaneous *Champsosaurus,* but is easily distinguished in having a proportionately shorter and much broader snout than other neochoristoderes, an interorbital table wider than the orbit, a reduced mandibular symphysis when compared to other simoedosaurids, and a splenial that does not enter the symphysis (Sigogneau-Russell and Baird 1978; Gao and Fox 1998).

Remarks – *Simoedosaurus* was first named by Gervais (1877) on the basis of three isolated vertebral centra found in the upper Paleocene deposits of France. He had initially identified these remains as an indeterminate simosaurian (Gervais 1873), but later assigned the material to a new genus in 1877. Sigogneau-Russell (1985) pointed out that this holotype material did not distinguish the genus from the European *Champsosaurus*, and so provided a neotype for the genus and holotype species. A neotype for this genus and species was needed regardless of the quality of the holotype, as the holotype specimen had apparently been lost by this time (Sigogneau-Russell, 1985).

The European species, *S. lemoinei* (late Paleocene, Europe; Sigogneau-Russell 1979), is known from a collection of partial skeletons that may belong to multiple species of *Simoedosaurus*, but sufficient diagnostic material needed to discern these differences has not been preserved (Erickson 1987). The North American species, *S. dakotensis* (early Paleocene-early Eocene, North America; Sigogneau Russell and Baird 1978), is known from

several well-preserved specimens, and differs most notably from the European species in possessing a proportionately shorter snout (one third the length of the skull in *S. dakotensis* versus two fifths in *S. lemoinei*; Figure 1.7; Erickson 1987).

Averianov (2005) described fragmentary material of *Simoedosaurus* from the upper Paleocene-lower Eocene deposits of Southern Kazakhstan, providing the first evidence of choristoderes in the Paleogene of Asia. His description included dozens of disarticulated and fragmented remains that had initially been described as crocodilian, but Averianov (2005) diagnosed them as choristoderan based on features such as sub-thecodont dentition, unfused neural arches, and pachyostosis of the ribs and long bones. Diagnosing the genus was difficult, as diagnostic features for choristoderan genera are in the skull, which was not preserved. Averianov (2005) concluded that they could have belonged to either *Champsosaurus* or *Simoedosaurus*, as these are the only known choristoderans from the Paleogene but are most morphologically similar to *Simoedosaurus*.

Genus *Tchoiria* Efimov, 1975

Type species – *Tchoiria namsarai* Efimov, 1975.

Attributed species – *T. namsarai*, and *T. klauseni.*

Type locality and horizon – Late Cretaceous (Albian), Khuren Duhk Formation, Dornogov, Mongolia.

Temporal and spatial distribution – Early Cretaceous (Aptian), Mongolia (Ksepka et al., 2005).

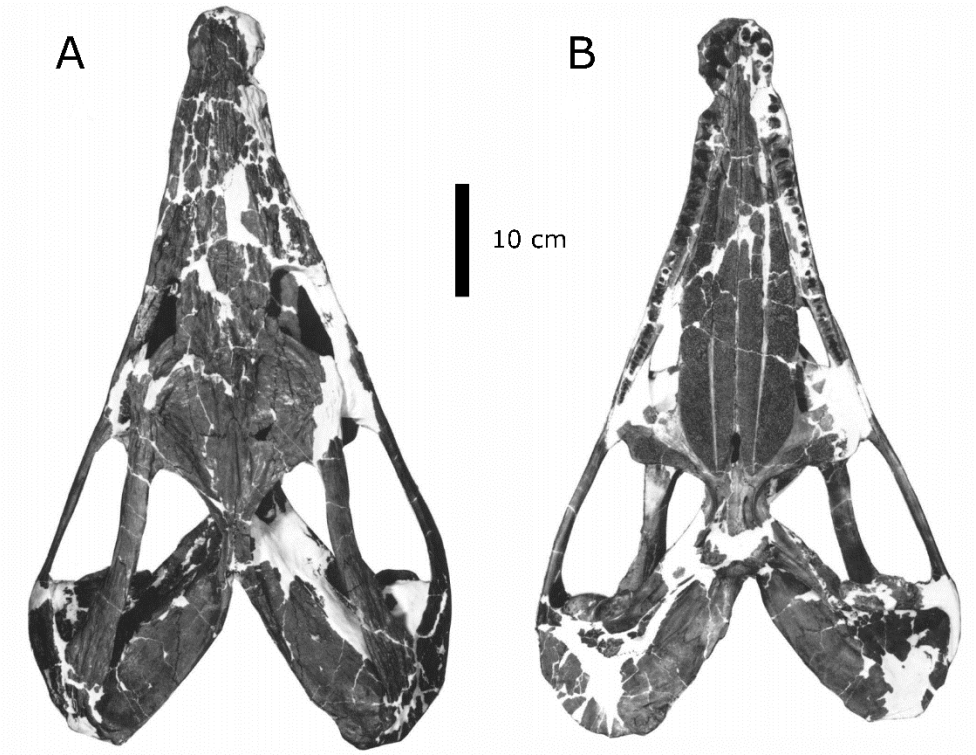

Figure 1.7: The skull of *Simoedosaurus dakotensis* (SMM P76.10.1) in: **A** dorsal view, and **B** ventral view (modified from Erickson 1987).

Diagnosis – A genus of medium-sized (1-1.5 m long; Efimov and Storrs 2000) neochoristodere from the Lower Cretaceous of Mongolia, noted for having a more triangular dorsal skull profile, and a shorter mandibular symphysis than what is seen in other neochoristoderes.

Remarks –Like other neochoristoderes, *Tchoiria* possessed an elongated snout and posteriorly expanded temporal fenestrae, which were likely adaptations for piscivory (Figure 1.8). The holotype species provided the first definitive example of an Asian choristodere, demonstrating that these animals ranged across the entirety of Laurasia during the Cretaceous. Two other species of *Tchoiria* were named by Efimov (1979, 1983), but have since been tentatively identified as pertaining to separate genera (*Irenosaurus egloni*; *Ikechosaurus magnus*; Efimov and Storrs 2000). A fourth (valid) species, *T. klauseni*, was named by Ksepka et al. (2005) based on a reduced number of maxillary teeth (34 maxillary teeth in *T. klauseni* vs. 60 maxillary teeth in *T. namsarai*). It seems possible that these differences vary through ontogeny, where younger, smaller individuals have fewer teeth, but this has yet to be assessed.

Genus *Ikechosaurus* Sigogneau-Russell, 1981b

Type species – *Ikechosaurus sunailinae* Sigogneau-Russell, 1981b.

Attributed species – *I. sunailinae, I. magnus, I. gaoi,* and *I. pijiagouensis.*

Type locality and horizon – Early Cretaceous (Aptian-Albian), Lauhongdong Formation, Chabu Sumu, Inner Mongolia, China.

Figure 1.8: Dorsal (left) and ventral (right) surfaces of the skull of *Tchoiria* (IGM 1/8). Scale bar represents 5 cm (from Ksepka et al., 2005).

Temporal and spatial distribution – Early Cretaceous (Aptian), Jiufotang Formation, Chifeng, Inner Mongolia, China; Early Cretaceous (Aptian-Albian), Lauhongdong Formation, Chabu Sumu, Inner Mongolia, China.

Diagnosis – (1) Snout long, broad and flat in front of the orbits; (2) gradually tapering to about the midpoint along the snout where it is subcircular in cross section; (3) interorbital bar narrow; (4) temporal openings largely placed above one another; (5) nasal with strong contact with prefrontal; jugal extends anteriorly as far as does the lacrimal; (6) parietal extends only about half way along the posterior edge of the upper temporal opening; (7) parasphenoid with narrow anterior end and expanded posterior end; (8) internal carotid foramen located in or near the suture between the parasphenoid and pterygoid; (9) interpterygoid vacuity small; (10) cultriform process of parasphenoid entering interpterygoid vacuity; (11) maxilla enters border of the suborbital fenestra; (12) tooth bases of marginal dentition closely packed and mediolaterally elongate; (13) splenial enters symphysis; (14) centra of posterior dorsal vertebrae dorsoventrally compressed, wider than high; (15) ilium with well-developed anterior process on the iliac blade, and without distinct neck region between the acetabulum and iliac blade (Brinkman and Dong 1993).

Remarks – The phylogenetic position of *Ikechosaurus* (Figure 1.9) within Neochoristodera has been debated, where it was initially placed close to *Champsosaurus* by Brinkman and Dong (1993), but more recent reconstructions place it closer to *Tchoiria* than to either *Champsosaurus* or *Simoedosaurus* (Liu 2004), a position that has been supported by subsequent analyses (Matsumoto et al., 2013).

The type species was originally identified as belonging to the crocodilian *Eotomistoma* (Young 1964; Brinkman and Dong 1993), but was allocated to *Ikechosaurus* by

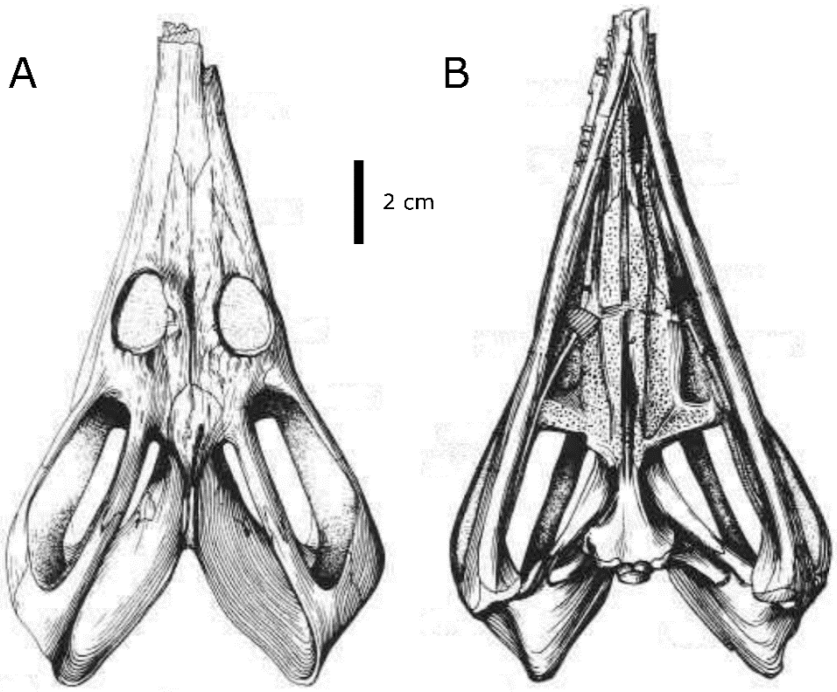

Figure 1.9: The skull of *Ikechosaurus sunailinae* (IVPP V9611-3) in: **A** dorsal, and **B** ventral view (modified from Brinkman and Dong 1993).

Sigogneau-Russell (1981b). This reassignment was based predominantly on the rectangular tooth base of the holotype specimen, which is a feature unique to *Ikechosaurus*, even among neochoristoderes (Brinkman and Dong 1993). A second species, *I. magnus*, was erected following the redescription of a specimen of *Tchoiria* (Efimov 1983), which was found to have a rectangular tooth base, and therefore pertained to *Ikechosaurus*. Two other species from the Jiufotang Formation (Lower Cretaceous) of China have since been described, *I. gaoi* (Lu et al., 1999b) and *I. pijiagouensis* (Liu 2004). *Ikechosaurus gaoi* is noted for having proportionately larger teeth, which are spaced farther apart, while *I. pijiagouensis* differs mainly in features of the pelvis, including a pronounced processes on the ilium.

Genus *Champsosaurus* Cope, 1876

Type species – *Champsosaurus annectens* Cope, 1876.

Attributed species – *C. ambulator*, *C. laramiensis*, *C. albertensis*, *C. natator*, *C. gigas*, *C. tenuis*, and *C. lindoei.*

Type locality and horizon – Late Cretaceous (Campanian), Judith River Formation, Montana, USA.

Temporal and spatial distribution – Late Cretaceous (Turonian) to earliest Eocene of North America and Europe.

Diagnosis – From Gao and Fox (1998): (1) great elongation of snout, exceeding half the length of the skull; (2) interorbital width narrower than maximum diameter of orbit; (3) lacrimal strongly reduced to small triangle; (4) postorbital excluded from formation of orbit; (5) premaxilla/vomer contact lost; (6) internarial present; (7) choanae located posteriorly, in

correspondence with elongation of vomer; (8) interpterygoid foramen small, enclosed both anteriorly and posteriorly by pterygoids and located near posterior border of suborbital fenestra; (9) suborbital fenestra shortened and kidney-shaped; (10) pterygoid/parasphenoid articulation fused; (11) craniomandibular joint anterior to level of occipital condyle; (12) neomorphic bone forming most of ventral border of posttemporal fenestra; (13) paroccipital process strongly deflected ventrally; (14) wing-like basal tubera of basisphenoid expanded posteroventrally; (15) elongation of mandibular symphysis to over half of the length of the tooth row; (16) splenial strongly intervening in mandibular symphysis.

Remarks – Sixteen species have been attributed to *Champsosaurus* (Figure 1.10); however, only seven are now considered valid (Table 1.1). The seven recognized species are all from North America (Figure 1.11), ranging temporally from the Late Cretaceous to the Early Paleogene. Gao and Fox (1998) provided the first description of *C. lindoei*, and redescribed *C. albertensis*, *C. gigas*, and *C. natator*, but did not provide a redescription of the remaining three species, instead stating that revisions of these taxa are still needed. As a result, the latest description of some of these species dates back to the early 20th century, which has hindered phylogenetic systematics of *Champsosaurus*, and at present, the evolutionary relationships of these species to one another is unknown (Gao and Fox 1998).

Only one European species of *Champsosaurus* has been described, *C. dolloi* (Sigogneau-Russell 1979); however, the validity of this species is debated. Evans and Hecht (1993), and later Gao and Fox (1998), concluded that the material is too fragmentary to be confidently attributed to a new species, while Matsumoto and Evans (2016) included it as a distinct species in their description of choristodere dentition. There is an absence of literature discussing the validity of this taxon, and as such, will not be discussed here.

Figure 1.10: The dorsal surface of the skull of *Champsosaurus lindoei* (CMN 8920). Scale bar represents 5 cm.

Table 1.1. Sixteen species of *Champsosaurus* and their current taxonomic status (Gao and Fox 1998). * indicates the genotype species (see Discussion).

Taxon	Status
C. profundus Cope, 1876	Synonym of *C. natator*
*C. annectens** Cope, 1876	*Nomen vanum*, undetermined neochoristodere
C. brevicollis Cope, 1876	Synonym of *C. natator*
C. vaccinsulensis Cope, 1876	*Nomen vanum*, undetermined pleisiosaur
C. australis Cope, 1881	Synonym of *C. laramiensis*
C. puercensis Cope, 1881	Synonym of *C. laramiensis*
C. saponensis Cope, 1881	Synonym of *C. laramiensis*
C. laramiensis Brown, 1905	Valid
C. ambulator Brown, 1905	Valid
C. albertensis Parks, 1927	Valid
C. natator Parks, 1933	Valid
C. inelegans Parks, 1933	Synonym of *C. natator*
C. inflatus Parks, 1933	Synonym of *C. natator*
C. gigas Erickson, 1972	Valid
C. tenuis Erickson, 1981	Valid
C. lindoei Gao and Fox, 1998	Valid

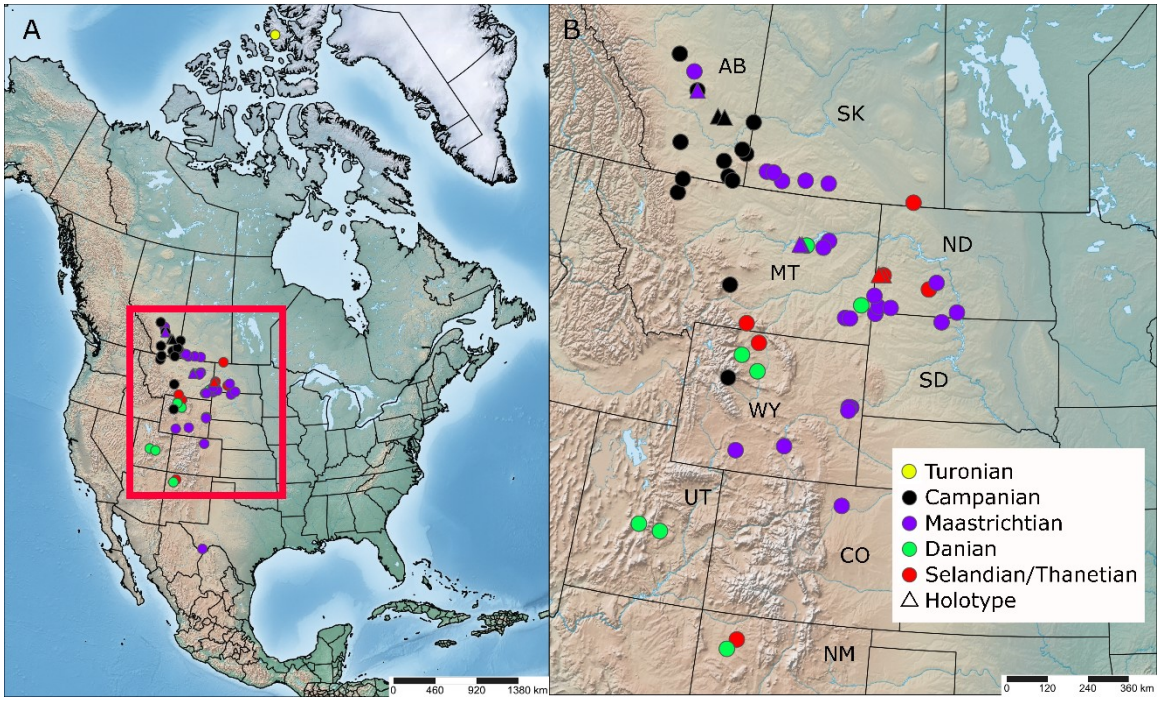

Figure 1.11: **A** Map of North America with reported occurrences of *Champsosaurus*. **B** Map of western Canada and USA with reported occurrences of *Champsosaurus*. Red box in map A indicates the location of map B. Data retrieved from Paleobiology Database (paleobiodb.org). Image created using SimpleMappr (simplemappr.net). *Abbreviations: AB, Alberta; CO, Colorado; MT, Montana; ND, North Dakota; NM, New Mexico; SD, South Dakota; SK, Saskatchewan; UT, Utah; WY, Wyoming.*

It must be stated that the genotype species, *C. annectens* (Cope, 1876), is also no longer recognized due to inadequate diagnostic features (Brown 1905; Gao and Fox 1998). The implications of this are examined in the Discussion.

Champsosaurus laramiensis **Brown, 1905**

Holotype – AMNH 982, a nearly complete skull and skeleton.

Paratype – AMNH 981, a partially complete skeleton lacking hind limbs and tail.

Type locality and horizon – Late Cretaceous (Maastrichtian), Hell Creek Formation, Hell Creek, Montana, USA.

Temporal and spatial distribution – Late Cretaceous (Maastrichtian), Hell Creek Formation, Montana, USA; Late Cretaceous (late Maastrichtian), Frenchman Formation, Saskatchewan, Canada; early Paleogene (early Paleocene), Tullock Formation, Montana, USA; early Paleogene (early Paleocene), Puerco Formation and Torrejonian Formation, New Mexico, USA.

Diagnosis – At present, *C. laramiensis* has not been formally diagnosed. Brown (1905) did not provide a diagnosis of the species, instead simply providing a description of the holotype and paratype. The best diagnosis of this species provided thus far is of a skeleton from the Hell Creek Formation (Laramie Beds of Brown 1905) that differs from the contemporaneous *C. ambulator* (see below) in having relatively gracile limb girdles and long bones (Brown 1905).

Champsosaurus ambulator Brown, 1905

Holotype – AMNH 983, a partially preserved skeleton with a fragmentary skull.

Type locality and horizon – Late Cretaceous (upper Maastrichtian), Hell Creek Formation, Hell Creek, Montana, USA.

Temporal and spatial distribution – Late Cretaceous (upper Maastrichtian), Hell Creek Formation, Montana, USA; early Paleogene (Paleocene), Tullock Formation, Montana, USA.

Diagnosis – From Brown (1905): Similar to *C. laramiensis*, differing in its possession of more robust limb girdles and long bones.

Remarks – *Champsosaurus ambulator* was based on a skeleton that was found along the banks of Hell Creek, about 100 m away from and about 2 m above the holotype of *C. laramiensis* (Brown 1905). The more robust limbs and limb girdles, and fused sacral vertebrae of *C. ambulator* may have facilitated a more terrestrial lifestyle (Brown 1905; Erickson 1972; Katsura 2007), although it is possible that this morphology varies due to ontogeny or sexual dimorphism (see Discussion).

Brown (1905) stated that the holotypes for *C. laramiensis* and *C. ambulator* come from the 'Laramie Cretaceous exposures' on the banks of Hell Creek and they are, therefore, Maastrichtian in age. Erickson (1972) suggested that this age was incorrect because the types were found in the 'lignite beds' (Brown 1905) that are more characteristic of the overlying Tullock (Paleocene) deposits. Neither of these species have been revised and there has been no additional comment on the age of these specimens. The American Museum of Natural History online database (research.amnh.org/paleontology/search.php) follows Brown (1905), listing the types as coming from the Hell Creek Formation.

Champsosaurus albertensis Parks, 1927

Holotype – ROM 806, a partial postcranium.

Type locality and horizon – Late Cretaceous (latest Campanian and earliest Maastrichtian), Horseshoe Canyon Formation, Alberta, Canada.

Temporal and spatial distribution – Late Cretaceous (latest Campanian and earliest Maastrichtian), Horseshoe Canyon Formation, Red Deer River, Alberta, Canada.

Diagnosis – *Champsosaurus* with proportionately short epipodials (Erickson 1972).

Remarks – *Champsosaurus albertensis* was named by Parks (1927) based on a partial postcranial skeleton, but the species was not properly diagnosed until 1972 by Erickson. Gao and Fox (1998) argue that the proportionately short epipodials of *C. albertensis* are only 5-10% shorter than other *Champsosaurus* species, and state that this difference may not be taxonomically significant. Based on this, Gao and Fox (1998) suggest that the holotype of *C. albertensis* is indistinct, and the name of the species may therefore be dubious. Despite this, they conclude that *C. albertensis* likely is a distinct species based on other specimens that have been found with a skull preserved. These skulls posses a distinctly broad base to the snout and anteroposteriorly elongate orbits that differentiate these individuals from all other known champsosaurs, but a formal amendment to the species diagnosis has yet to be made.

Champsosaurus natator Parks, 1933

Holotype – TMP 81.47.1, an incomplete skeleton with a fragmentary skull.

Type locality and horizon – Late Cretaceous (Campanian), Belly River Group, Red Deer River valley, Alberta, Canada.

Temporal and spatial distribution – Late Cretaceous (middle to late Campanian), Dinosaur Park Formation, Alberta.

Diagnosis – A relatively large *Champsosaurus* (approximately 2 m long) with: (1) a more robust skull than the contemporaneous *C. lindoei*; (2) laterally swollen lower temporal bar; (3) lower temporal fenestra expanded mediolaterally; (4) expansion of the postfrontal separating the postorbitals from the frontals (Gao and Fox 1998).

Remarks – The holotype was initially catalogued as ROM 5737, then ROM 857, before being sent to Texas as TMM 41269 (Gao and Fox 1998). The holotype currently resides at the Royal Tyrrell Museum as TMP 81.47.1. Parks (1933) used AMNH 5364 to supplement the description of the type. *Champsosaurus natator* was erected based on comparisons with some species that are no longer considered valid (e.g. *C. annectens*), and was based on variations in the vertebrae, femora, and humeri. Russell (1956) described the first complete skull of *C. natator*, and provided more concrete evidence to differentiate this species from other species of *Champsosaurus*. Parks (1933) stated that *C. natator* differs from other champsosaurs in having a long and slender snout with an expanded bulla at the tip, but this is a feature now known to be shared with the contemporaneous *C. lindoei* and is therefore non-diagnostic. It should be noted that feature (3) of the diagnosis by Gao and Fox (1998; above) is a product of the laterally swollen lower temporal bar (feature 2), and is therefore not an independent feature.

Champsosaurus gigas Erickson, 1972

Holotype – SMM P71.2.1, a partial skeleton and skull.

Type locality and horizon – Early Paleogene (Paleocene), Sentinal Butte Formation, Golden Valley County, North Dakota, USA.

Temporal and spatial distribution – Early Paleogene (Paleocene), Sentinel Butte Formation, North Dakota, USA; Early Paleogene (Paleocene), Ravenscrag Formation, Saskatchewan, Canada.

Diagnosis – A large *Champsosaurus* differing from other species in having (1) parietal table strongly projecting laterally at anterior margin of superior temporal fenestra; (2) posterior part of parietal table narrower than in other species of comparable size; (3) postorbital extending anteromedially to meet frontal and parietal, preventing postfrontal-parietal contact (Gao and Fox 1998).

Remarks – *Champsosaurus gigas* (Erickson 1972) is known from many Paleocene localities in North America, and is the largest known species (approximately 3 m long). Langston (1958) noted an isolated *Champsosaurus* vertebra and rib from the Ravenscrag Formation (Lower Paleocene), Saskatchewan, which he described as unusually large, but did not coin a new species due to the scarcity of material. Erickson (1972) described eight large specimens from the Paleocene of North America, and attributed them to *C. gigas*. Tokaryk (2009) referred to five partial skeletons of *Champsosaurus* from the Ravenscrag Formation of Saskatchewan that he believed pertain to *C. gigas* based on their size, and suggested that these specimens likely represent the earliest Cenozoic *Champsosaurus* found to date.

Champsosaurus tenuis Erickson, 1981

Holotype – SMM P79.14.1, a partial skeleton and cranium.

Type locality and horizon – Early Paleogene (Paleocene), Bullion Creek Formation, North Dakota, USA.

Temporal and spatial distribution – Same as for the type.

Diagnosis – (1) An extremely long and slender snout; (2) postcranial skeleton with narrow shoulder girdle; (3) clavicles short and deeply concave anteriorly; (4) limbs reduced in length (Erickson 1981).

Remarks – *C. tenuis* has received little attention since its initial description by Erickson, and the holotype specimen is the only individual referred to this species. Gao and Fox (1998) did not discuss the validity of *C. tenuis*, simply stating that the diagnosis of the species needs to be revised. The holotype specimen was found in fine sediments that Erickson interpreted as lacustrine deposits, making *C. tenuis* unique in that other Paleocene *Champsosaurus* (i.e., *C. gigas*) have been found in fluvial deposits. Erickson (1981) suggested that the slender and gracile anatomy of *C. tenuis* could have been an adaptation for deeper water habitats, but this conclusion was tentative due to the fragmentary nature of the holotype.

Champsosaurus lindoei Gao and Fox, 1998

Holotype – UALVP 931, a nearly complete skeleton with skull and mandibles.

Type locality and horizon – Late Cretaceous (mid-upper Campanian), Dinosaur Park Formation, Dinosaur Provincial Park and its vicinity, Alberta, Canada.

Temporal and spatial distribution – Same as for the type.

Diagnosis –A relatively small and gracile *Champsosaurus* with (1) snout significantly more slender in proportion to the skull size, and the bulla on the snout is proportionately larger; (2) the pterygoid flange is weekly developed with reduced number of teeth; (3) inferior temporal arch is nearly straight, and is not swollen laterally; (4) subtemporal fenestra is rectangular, not oval (Gao and Fox 1998).

Remarks – The holotype specimen was initially described as *Champsosaurus* sp. by Fox (1968) and was not attributed to any particular species until the description of *C. lindoei* by Gao and Fox (1998). Other specimens of *C. lindoei*, such as CMN 8920, were initially attributed to *C. natator* (Russell 1956), which lived contemporaneously with *C. lindoei*. It should be noted that feature (4) from Gao and Fox (1998) is dependant on feature (3).

Gao and Fox (1998:23) described the largest *C. lindoei* specimen (TMP 90.36.68) as "comparable in size to the mature skull in *C. natator*", and measures approximately 34.5 cm long (pers. obs., 2019). This is substantially smaller than some specimens of *C. natator* (e.g., UALVP 33929, approximately 42 cm long; CMN 8919, approximately 59 cm long), suggesting that there may actually be a significant size difference between *C. lindoei* and *C. natator*, contrary to what is suggested by Gao and Fox (1998). A rigorous comparison of *C. lindoei* and *C. natator* specimens is needed to properly quantify size differences between these species.

Discussion

The problem of *Champsosaurus*

Cope (1876, p. 348) erected the genus *Champsosaurus*, along with the order Choristodera, based on isolated vertebrae from the Judith River Formation along the Judith River, Fergus county, Montana (AMNH database). Although *C. profundus* was the first species Cope (1876, p. 350) named, he explicitly stated that *C. annectens* is the type species because of the greater number of vertebrae attributed to it. *Champsosaurus annectens* was based on nine isolated, unfigured vertebral centra (AMNH FR 5696); however, two of these vertebrae have been lost from the AMNH collections, or possibly were never taken from the field by Cope, and only seven vertebrae are attributed to AMNH FR 5696 (AMNH database; Figure 1.12).

Brown (1905) noted that the vertebrae Cope (1876; 1881) used to diagnose *Champsosaurus* species are often heavily worn, and the diagnostic features vary in morphology along the spinal column of a single animal, as well as throughout ontogeny; a conclusion later supported by Russell (1956). Brown (1905) noted that a species previously identified by Cope (1976), *C. vaccinsulensis*, was invalid because the type specimen actually pertains to an indeterminate plesiosaur. Brown (1905,) acknowledged that the vertebrae of *C. annectens* are weathered and lack diagnostic features, but did not explicitly state that the species was invalid. Instead, he stated that although the vertebrae provide good generic characters, the diagnosis of the species awaits better material from the Judith River beds (the type horizon).

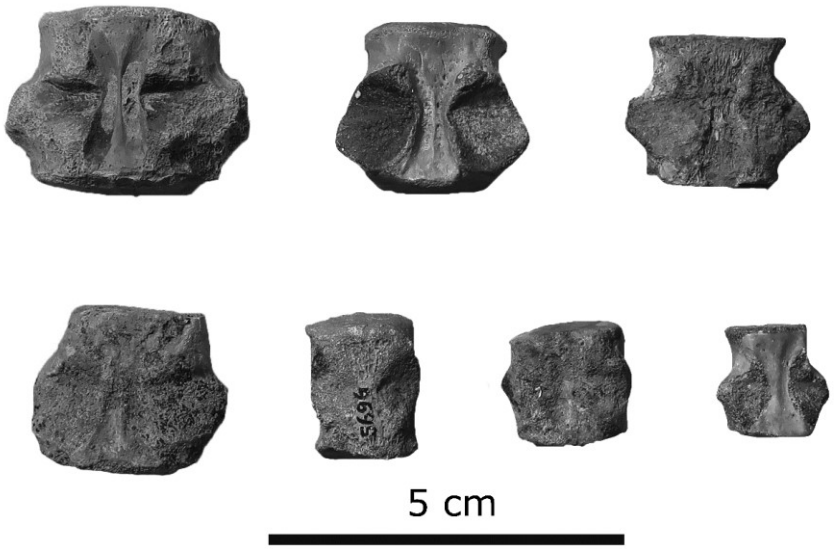

Figure 1.12: Dorsal view of the *Champsosaurus annectens* type specimen, AMNH FR 5696.

Parks (1933) acknowledged that *C. annectens* was invalid, and noted that researchers have continued to ascribe isolated vertebrae to the type species without justification (e.g., Lambe 1902; Bowen 1915; Matthew 1916). Parks (1933) noted that, as a result, many isolated vertebrae from the Judith River Formation of Montana and the Belly River Group of Alberta are attributed to this species. Parks (1933:134) later explicitly states that "Species of *Champsosaurus* cannot be identified with certainty from isolated vertebrae." Despite this, Parks (1933) referred three small dissociated vertebrae from the Belly River group of Alberta to "*C.* cf. *profundus* cf. *annectens*" due to the apparent similarity between the referred material and some of Cope's (1876) type vertebrae.

Russell (1956) acknowledged that the type specimen of *Champsosaurus* (AMNH 5696) cannot be confidently attributed to a single animal, and that the vertebrae of *Champsosaurus* are highly variable and lack specific identifiers. He reiterated Brown's (1905) conclusion that *C. annectens* may be "redefined if new material could be discovered" (Russell 1956:2).

Erickson (1972) recognized *C. annectens* as the type species, but also provisionally synonymized it with *C. natator* due solely to the stratigraphic agreement of the species. The provisional allocation of *C. annectens* as a senior synonym to *C. natator* has not been accepted, as later sources continue to refer to *C. annectens* as the type species of *Champsosaurus* (e.g., Gao and Fox 1998; Gao and Brinkman 2005). Gao and Fox (1998) stated that the invalidity of *C. annectens* does not change its nomenclatural status as the type species, seeing as the validity of the genus has never been questioned, but this does not address the issue that the type species is invalid. *Champsosaurus* is the nominal genus for Champsosauridae and the use of the family name hinges on the validity of the genus name

(ICZN, Article 35.3). Therefore, in order to secure both the genus name and family name, a valid type species for *Champsosaurus* must be established.

As established previously (Parks, 1933:134), the vertebrae of *Champsosaurus* do not provide specific characters, and possess poor diagnostic features. These features are so poor that Cope (1884a) misidentified the vertebrae of *Simoedosaurus* from France with those of *Champsosaurus*, leading him to incorrectly synonymize the genera under *Champsosaurus* (Brown 1905; Parks 1927; Gao and Fox 1998). This was later corrected by Lemoine (1884) who described new cranial and appendicular material of *Simoedosaurus* that adequately distinguished the genera from one another. Subsequent confusion between the genera has not occurred, but this is likely because recent diagnoses of *Champsosaurus* do not use vertebral characters, and instead use features from the skull and appendages to diagnose the genera. The most recent diagnosis of *Champsosaurus* comes from Gao and Fox (1998), who used 16 characters in their diagnosis, none of which pertain to the vertebral centra. The holotype of *C. annectens* (AMNH 5696) therefore lacks all characters used to diagnose the genus and does not reflect the modern understanding of *Champsosaurus*.

It would be logical to designate a neotype for *C. annectens* to maintain the validity of the species, but this would fail to address the issue, as all other material referred to *C. annectens* is of poor diagnostic value and cannot be identified to species. Isolated remains of *Champsosaurus* (i.e., vertebrae and limb bones) are easily identified and frequently cited across much of the Cretaceous and Paleocene deposits of western North America (Parks 1933; Russell 1956; Brinkman 1990; Gao and Fox 1998; Gao and Brinkman 2005), and several highly diagnostic specimens are known from other species that are attributed to the same genus as AMNH 5696.

According to Article 23.3.5 of the International Code of Zoological Nomenclature, "The Principle of Priority requires that if a name in use for a taxon is found to be unavailable or invalid it must be replaced by the next oldest available name from among its synonyms, including the names of the contained taxa of the same group (e.g. subgenera within genera), providing that that name is not itself invalid. If the rejected name has no potentially valid synonyms a new substitute name (see Article 60.3) must be established in its place." Erickson (1972) tentatively synonymized *C. annectens* with *C. natator* solely due to their stratigraphic agreement, but emphasized that this allocation was provisional, likely until more complete material is recovered from the Judith River beds (the type locality). At present, no diagnostic material is forthcoming from the Judith River Formation, and Erickson's (1972) allocation of *C. annectens* as a senior synonym of *C. natator* was overlooked in subsequent studies (e.g., Gao and Fox 1998; Gao and Brinkman 2005). *Champsosaurus annectens* has therefore not yet been formally synonymized with another species. According to Article 23.3.5, a new name must be established for *Champsosaurus*; however, this would cause considerable confusion in the literature because *Champsosaurus* is a well-known genus due to their common vertebral centra in Late Cretaceous and Paleocene beds of western North America. Therefore, establishing a new name for the genus should be avoided, and the case should go to the Commission for ruling to establish a new type species, maintaining stability and avoiding confusion.

The elected type species should be well represented, have characters that adequately describe the genus and the higher groups to which it belongs, and will ideally come from the same beds as the original holotype (AMNH 5696). As stated previously, no specifically diagnostic material is forthcoming from the Judith River beds of Montana, so all other

species should be considered for replacement as the type. *Champsosaurus albertensis* and *C. tenuis* were erected on fragmentary material and are in need of revision (Gao and Fox 1998) and, therefore, should not act as type species. *Champsosaurus laramiensis* and *C. ambulator* are also poorly known, having not been diagnosed since their initial description by Brown (1905) and are in need of revision (Gao and Fox 1998). *Champsosaurus gigas* is represented from the Paleocene deposits of Saskatchewan and North Dakota by isolated remains and a few partial skeletons (Erickson 1972; Tokaryk 2009), and is recently diagnosed (Gao and Fox 1998), but its earliest occurrence (early Paleocene) is approximately 10 million years younger than the Judith River Formation (Gao and Fox 1998).

Champsosaurus natator and *C. lindoei* are well represented, and recently diagnosed (Gao and Fox 1998), and are good candidates for the type species. *Champsosaurus natator* is known from several well-preserved specimens that adequately reflect the autapomorphies of *Champsosaurus*, although the holotype specimen is fragmentary and does not represent all of the generic characters. The holotype of *C. lindoei* is a nearly complete skeleton with skull and mandibles, and possesses all synapomorphies of the genus (Gao and Fox 1998). It may therefore be tempting to suggest that *C. lindoei* be named the type species; however, *C. natator* is represented by many well-preserved specimens and is the best represented *Champsosaurus* species (Gao and Fox 1998; Gao and Brinkman 2005). Additionally, given that *C. natator* and *C. lindoei* are contemporaneous, in the event that these species are found to be synonyms, electing *C. lindoei* as the type species over *C. natator* could result in future confusion as the new type species will then be invalid. As such, to preserve stability and universality, it would presently be best to erect *C. natator* as the type species of *Champsosaurus*, preserving both the genus and family.

The absence of definitions within Choristodera

At present, Choristodera has never been given a phylogenetic definition. Brown (1905) provided the first taxonomic definition of the group, saying that Choristodera includes *Champsosaurus*, and *Simoedosaurus*. Gao and Fox (1998) provided the most recent taxonomic definition, stating that Choristodera "included *Cteniogenys*, Champsosauridae, and Simoedosauridae"; however, taxonomic definitions do not consider common ancestry, nor do they take into account subsequently discovered taxa. Defining a group based on ancestry, and not simply on character states in a diagnosis, is necessary to consolidate the membership of the group (Rowe 1987), and define the boundaries of the group in a phylogenetic context (Padian and May 1993), preventing the continuous inclusion of more basal taxa. Once a phylogenetic definition has been established, it allows the diagnosis of the group to be properly evaluated based solely on the included taxa (Fraser et al., 2002).

The absence of a phylogenetic definition for Choristodera has already posed an issue when *Cteniogenys*, a basal choristodere from the Middle and Late Jurassic, was assigned to Choristodera by Evans (1989). Prior to the recognition of *Cteniogenys* as a choristodere, only four highly derived neochoristoderes from the Late Cretaceous and Paleocene were known. The inclusion of *Cteniogenys* was based on a few shared synapomorphies with neochoristoderes (see Systematic Palaeontology section for synapomorphies), but resulted in some features becoming non-diagnostic of Choristodera (e.g., long, gavial-like snout; a single, fused narial element; medium to large body size). All subsequently discovered choristoderes have been more derived than *Cteniogenys*, so this issue has not reoccurred, but a definition must still be established to solidify the group in a phylogenetic framework.

Three main types of clade definitions are used in the literature: apomorphy-based, stem-based, and node-based (Sereno 1999). Apomorphy-based definitions define a group as the first taxon to possess a trait, and all descendants of that taxon that inherited said trait. Apomorphy-based definitions are often problematic because defining a group based on characters does not allow for the inclusion of forms yet to be found, or for the rearrangement of known forms in a phylogeny (Fraser et al., 2002). Apomorphy-based definitions therefore tend to be avoided (Sereno 1999) in favour of ancestry-based definitions (i.e., stem-based or node-based; Fraser et al., 2002). Stem-based definitions define a group as all taxa more closely related to taxon X than to some other taxon Y (e.g., Ornithischia can be defined as all taxa more closely related to *Triceratops* than to modern birds; Padian and May 1993). Stem-based definitions are often used due to their simplicity and their ability to encompass a whole clade, but the position of the lineage being defined must be well known within a larger group. A stem-based definition, therefore, cannot be used for Choristodera because the relationship of this group to the rest of Diapsida is uncertain (Matsumoto and Evans 2010). A node-based definition would therefore be the most appropriate, which would include the most recent common ancestor of taxon X and taxon Y, and all other taxa descended from that common ancestor (e.g., Dinosauria is defined as the most recent common ancestor between modern birds and *Triceratops*, and all descendants from that common ancestor; Padian and May 1993). *Cteniogenys* was considered the basal-most choristodere at the time of its assignment to Choristodera (Evans 1989), and has remained as such following the discovery of subsequent choristoderes (Gao and Fox 1998; Matsumoto et al., 2013; Matsumoto et al., 2019). Neochoristoderes are the most derived choristoderes, and *Champsosaurus* is considered the most derived of the neochoristoderes (Gao and Fox 1998; Matsumoto et al.,

2013). Therefore, Choristodera should be defined as the most recent common ancestor of *Champsosaurus* and *Cteniogenys*, and all descendants of that common ancestor. Taxa discovered in the future that are basal to *Cteniogenys*, but are more closely related to choristoderes than other neodiapsids could be included in a newly erected group, e.g., 'Choristoderomorpha'.

A definition for Neochoristodera has also not yet been established. This group includes four choristoderes from the Late Cretaceous and Paleocene: *Champsosaurus*, *Simoedosaurus*, *Tchoiria*, and *Ikechosaurus* (Evans and Hecht 1993), but the relationship of these species to one another is ambiguous (Matsumoto et al., 2013; Matsumoto et al., 2019). An apomorphy-based definition would be problematic because synapomorphies for Neochoristodera have not been updated since the initial description the group (Hecht and Evans 1993), and are therefore out of date. A stem-based definition seems more appropriate, but this would also be problematic because the relationship of non-neochoristoderes to one another is uncertain (Matsumoto et al., 2013) and it is, therefore, difficult to determine which non-neochoristodere to use as an out-group. Therefore, a node-based definition for Neochoristodera would be the most suitable.

Although the relationship of neochoristoderan taxa to one another is uncertain (Matsumoto et al., 2013), *Champsosaurus* and *Simoedosaurus* are reliably separated from one another and are the most morphologically distinct neochoristoderes (Evans 1990; Gao and Fox 1998; Matsumoto and Evans 2010). Neochoristodera should therefore be defined as the most recent common ancestor between *Champsosaurus* and *Simoedosaurus*, and all descendants from that common ancestor. All taxa that are basal to this common ancestor should be included in the informal group, non-neochoristoderes.

Palaeobiology of Choristodera

After their initial discovery by Cope (1876), choristoderes were described as highly aquatic reptiles with a suite of relevant adaptations. Further evidence for this has come from the sediments in which some of these animals were found, which indicate deep-water and shallow-water lacustrine and fluvial environments, and shallow swamps. *Hyphalosaurus* and *Philydrosaurus* from the Upper Cretaceous of Liaoning, China, have been found in close proximity to one another, but appear to be adapted to different environments. Gao and Ksepka (2008) noted that *Hyphalosaurus* is found in sediments that pertain to deep-water lacustrine environments, suggesting that these animals spent most of their time in deep, freshwater bodies. Interestingly, *Hyphalosaurus* is entirely absent from the nearby Jiufotang Formation (overlies the Yixian Formation; approximately 120 Ma), and instead the short-necked brevirostrine choristodere, *Philydrosaurus proseilos* (Gao and Fox, 2005; Gao et al., 2007) is found there. The Jiufotang Formation represents an ancient shallow, swampy environment, suggesting that the short-necked brevirostrine morphology was better adapted for shallow water environments. Indeterminate neochoristodere elements (LPMC R00070, 00071) were also found in the Jiufotang Formation, but the taxonomic status of these elements is in question because they have yet to be published.

Further evidence for a highly aquatic, deep-water lifestyle of *Hyphalosaurus* comes from the discovery of an adult animal with two eggs in the abdominal cavity, and several eggs in close proximity that have been confirmed to have belonged to *H. baitaigouensis*, based on the number of cervical vertebrae in the neonates (24; Ji et al., 2006). Ji et al. (2006) noted that the embryos in these eggs are of a similar developmental stage, and are likely from the same clutch of the associated adult. They also noted that the embryos are at a late stage

and likely were close to birth, which is unusual because oviparous reptiles oviposit when the embryos are early in development. This lead Ji et al. (2006) to suggest that *Hyphalosaurus* may have been viviparous, like what is seen in other aquatic reptiles, and some of the eggs simply escaped the mother's body post-mortem, but they could not conclude this definitively. Later, Hou et al. (2010) used scanning electron microscopy to describe the egg shell structure of two *Hyphalosaurus* eggs that were found separate from an adult, and showed that these were soft-shelled, similar to what is seen in some extant marine turtles. Hou et al. (2010) appear to have assumed that *Hyphalosaurus* was oviparous, and did not provide a discussion on reproductive mode in these animals. As such, it remains possible that the eggs were expelled from their mother pre, or post-mortem, and *Hyphalosaurus* was actually ovoviviparous.

Ji et al. (2010) described a new specimen of *H. baitaigouensis* that appears to support the hypothesis of vivipary in these animals. This specimen consists of an adult female with at least 18 embryos within the body cavity. These embryos were at a very late stage of development and were likely close to birth at the time of death. Additionally, the embryos in the posterior region of the abdominal cavity were in an extended position, similar to what is seen in extinct aquatic viviparous reptiles such as ichthyosaurs and pachypleurosaurs (Böttcher 1990; Deeming et al., 1993; Cheng et al., 2004). Interestingly, one embryo that is in an extended posture near the posterior abdominal cavity faces anteriorly, similar to the birthing posture of extant cetaceans (Deeming et al., 1993; Cheng et al., 2004), while a second embryo beside the previous faces posteriorly with its head passing between the pelves. This may suggest that the mother died due to complications during parturition. The distribution of viviparity among choristoderes is not known, as eggs and embryos are only

known from *Hyphalosaurus*. It is therefore possible that other, less aquatic species of choristoderes expressed oviparity, but Ji et al. (2010) suggested that the presence of viviparity across Choristodera could explain the complete absence of egg preservation in the other species.

Remarkably, a *Hyphalosaurus* embryo was found in Northeastern China (Yixian Formation) that expresses axial bifurcation (Buffetaut et al., 2007). This individual possessed two heads and two necks that connect at the base to a single torso, and represents the earliest known example of axial bifurcation.

Matsumoto et al. (2013) described new material pertaining to *Lazarussuchus* from upper Paleocene deposits of France, providing the oldest known example of *Lazarussuchus*, and extending the temporal range of this genus to over 30 Ma. This specimen is remarkably well-preserved, and the caudal region shows clear indications that *Lazarussuchus* possessed keratinous caudal crests over the neural spines, similar to what is seen in some extant crocodiles and lizards. Soft tissue outlines on the hind foot show that the digits lacked webbing, but this feature was not discernable on the forefoot. This could suggest that *Lazarussuchus* was adapted to a more terrestrial lifestyle, contrary to what is seen in the soft tissue of other choristoderes such as *Monjurosuchus* (see below; Matsumoto et al., 2013).

A juvenile *Monjurosuchus* specimen (GMV 2135) shows remarkable preservation of soft tissues and integument, providing important information on the biology of these animals. Gao et al. (2000) described the integumentary scales as fine, with slightly larger scales over the dorsal surface of the hindlimbs. Two rows of large scales run axially along the dorsal surface of the trunk, with an unorganized pattern of smaller scales surrounding them. Both the fore and hind-feet show webbing up to the ends of the digits, with only the claws

protruding, providing strong support for the hypothesis that these animals were aquatic. Gao et al. (2000) noted that this specimen shows morphological similarity to the extant Chinese crocodile lizard (*Shinisaurus crocodilurus*), and suggested that they may have had a similar lifestyle. The abdominal cavity contains a dark mass composed of fine sediments and fragmented arthropod cuticles, supporting previous hypotheses that early choristoderes preyed on invertebrates (Evans 1990; Matsumoto and Evans 2010).

The first reported skin impressions of *Champsosaurus* come from Brown (1905), who reported possible skin impressions on the left humerus of AMNH 982. He did not provide a detailed description or illustration of these impressions, but stated that the impressions were fine, and were larger on the lower surface than on the upper surface.

Erickson (1985) reported the most extensive known *Champsosaurus* skin impressions from six locations across the torso, limbs, and tail of SMM P77.33.24 (*C. gigas*). Erickson's (1985) observations support those of Brown (1905); the scales are all small, pustulate or rhomboid (0.1 – 0.3 mm wide, and 0.2 – 0.6 mm long for rhomboid), and lack osteoderms, a conclusion supported by the absence of osteoderms preserved with other *Champsosaurus* specimens. The largest scales are located laterally on the body while the smallest are located dorsally, supporting Brown's (1905) observation that the scales appear to decrease in size dorsally. A well-preserved specimen of *Champsosaurus* sp. on display at the Royal Ontario Museum (ROM 50000) shows what appears to be a skin impression on the ventral surface near the left shoulder (pers. obs., 2019). The scale impressions preserved there appear similar to what Erickson (1985) described on SMM P77.33.24, but because a formal description of ROM 50000 has not been provided, the detailed nature of these impressions remains illusive. Additionally, there is a small lump (approximately 1 cm wide) of material near the pelvis of

this animal which may be gut contents, but again, a description of the specimen is be required to confirm this. Behavioural and ecological implications of scale morphology in choristoderes has not been explored at present, and may serve as a future line of inquiry into the lifestyle of these enigmatic animals.

Cranial anatomy of choristoderes and its biological implications

Cranial Bones and the Neomorphic Bone

Choristoderes are remarkable due to their unique cranial anatomy, possessing posteriorly expanded temporal fenestrae, a proportionately long and slender snout, and possibly a neomorphic bone in the lateral wall of the braincase (Gao and Fox, 1998). Additionally, all neochoristoderes and some non-neochoristoderes possess anteriorly oriented narial openings, an unusual condition for aquatic animals where the nares typically open dorsally. The external sutures of choristodere crania are well described, but little is known about the internal cranial anatomy of these animals due to the fragile nature of their skulls, which hinders preservation (Erickson, 1985).

The putative choristoderan neomorphic bone was first reported by Fox (1968) as a small triangular element in the lateral walls of the *Champsosaurus* braincase. It was later suggested that there is no evidence for the presence of the neomorphic bone, and that this element is actually part of the parietal (Erickson 1972). The most recent interpretation (Gao and Fox (1998) suggests that the neomorph is distinct, but elongate, contrary to the original observations of Fox (1968). This element has since been inferred in all other neochoristodere species (Sigogneau-Russell and Russell 1978; Brinkman and Dong 1993; Ksepka et al.,

2005), as well as some non-neochoristoderes (Gao and Ksepka 2008; Matsumoto et al., 2007; Gao and Fox 2005; Matsumoto et al., 2019), but the neomorphic bone has yet to be properly described. Based on Fox's (1968) description of the neomorph in *C. natator*, it appears that the bone does not contact the brain endocast, but, the 3D morphology of this element and its relation to other cranial features remains unknown. Skepticism regarding the presence of a neomorphic bone in the braincase is warranted because this region of the skull has remained relatively stable across Tetrapoda (Knoll et al., 2012). It is possible that the neomorphic bone developed due to the modification of internal soft tissue structures, such as the brain and inner ear, to provide structural support for the expanded temporal arches, or through random drift, but, at present these hypotheses remain untested.

Neurosensory anatomy of Champsosaurus

Fox (1968) attempted a cursory description of the brain endocast and cranial nerves of *Champsosaurus* with reference to UALVP 930. By viewing the fragmentary surface of this skull, he identified the location of the exits for cranial nerves V through XII; however, he did not provide a description of their path through the skull. Fox (1968) was also unable to identify exits for cranial nerves I through IV due to poor ossification of the anterior portion of the braincase. He noted that the canal connecting the endocast with the auditory capsule, which would have conveyed cranial nerve VIII, was unusually large, suggesting that it would have been partially enclosed by cartilage in life. His study, as well as others (Russell, 1956; Fox, 1968; Erickson, 1985), relied on direct observation of a few fragmentary remains, and were, therefore, unable to describe these structures in their entirety.

These gaps were first identified by Russell (1956) as the external auditory meatuses, but have been subsequently interpreted as unossified gaps in the otic capsule that may have enclosed the stapes (Fox, 1968). If so, this would be an unusual arrangement as a ventral orientation of the fenestrae ovales is rare amongst tetrapods, but is seen in some urodeles (e.g., Capshaw and Soares 2016), some plesiosaurs (Sato et al., 2011) and some aistopods (Anderson et al., 2003). These gaps have received no attention since their descriptions by Russell (1956) and Fox (1968), and the auditory system remains undescribed across Choristodera.

The morphology of the *Champsosaurus* cranium led Erickson (1987) to suggest that these animals likely preyed on smaller, fast-moving fish, where the long, slender snout and large temporal fenestrae were adaptations for quick movements of the head and jaws while submerged. The unique position of the nares in *Champsosaurus* lead Erickson (1985) to conclude that these animals stayed fully submerged when in the water, and when they needed to breathe, they would tilt their head dorsally so that the tip of the snout broke the surface in a "snorkeling" posture. A description of the neurosensory equipment associated with equilibrium could shed light on the behaviour of these animals, but a comprehensive description of these structures has not been done at present.

Turbinates and thermoregulation

Lu et al. (1999a) used CT scanning to describe the interior anatomy of the nasal passage of *Ikechosaurus sunailinae*. They found that *Ikechosaurus*, like modern reptiles, possessed a main respiratory tract with an olfactory chamber that extended posteriorly from the dorsal surface to communicate with the olfactory stalk of the brain. Lu et al. (1999a) also

found a series of grooves and ridges along the walls of the olfactory chamber that they believed were the attachments for cartilaginous conchae that acted to increase the surface area of the olfactory epithelium for enhanced olfaction, a feature also seen in many extant animals. Interestingly, these ridges appeared to extend anterior into the nasal tract, where they would no longer have had an olfactory function (Tattersall et al., 2006). This led Lu et al. (1999a) to conclude that these conchae would likely have been used to increase the surface area of the nasal epithelium to facilitate thermoregulation.

Oxygen isotope analyses of material from Asian vertebrate fossil assemblages suggest the Early Cretaceous would have had a relatively cool climate, with fluctuating temperatures (10 ± 4 °C; Amiot et al., 2011). The aquatic lifestyle of choristoderes meant that their body temperature would have remained fairly constant relative to the fluctuating air temperature; however, an ability to adjust the temperature of inspired air would have allowed these animals to remain active even when air temperatures dropped (Erickson 1985). During the Cretaceous, central Alberta (an area rich in *Champsosaurus* fossils; Figure 1.11) would have been located between 30˚ and 45˚ north of the equator, where air temperatures would have likely fluctuated by several degrees throughout the year (Erickson 1985). It is therefore possible that North American choristoderes, such as *Champsosaurus,* also possessed conchae for thermoregulation, but no studies have tested this hypothesis.

Vandermark et al. (2007) described an assemblage of vertebrate material from the Kanguk Formation (Upper Cretaceous) of Axel Heiburg Island in the high Arctic of Canada. The assemblage was found to contain many fluvial vertebrates including turtles, freshwater fishes, and large bodied neochoristoderes that Vandermark et al. (2007) tentatively referred to *Champsosaurus*. This *Champsosaurus* material is extensive, consisting mainly of isolated

bones ranging across ontogeny. These remains are mainly from the postcrania, but some fragmentary mandibles were preserved that diagnose these animals as neochoristoderes. Paleomagnetic data indicate that this locality would have been located at approximately 71˚N during the Cretaceous (Tarduno et al., 1997), and that the area would likely have been a temperate environment where temperatures fluctuated by several degrees throughout the year. Interestingly, no crocodilian material has been found from this locality, likely because these animals are restricted to lower latitudes with more constant annual temperatures. The presence of a large population of neochoristoderes with sub-adults suggests that these animals were living there year-round, and they would, therefore, have had some adaptations to deal with the dramatically fluctuating temperatures. It is therefore possible that neochoristoderes other than *Ikechosaurus* possessed conchae to facilitate thermoregulation; however, evidence for this has not been found.

Conclusions

The diversity and biology of Choristodera was reviewed based on information available in the literature, with particular emphasis on the most abundant and well known choristodere, *Champsosaurus*. Nomenclatural problems within Choristodera were addressed, such as the invalidity of the type species of *Champsosaurus*, and the absence of phylogenetic definitions within Choristodera.

To address the invalidity of the type species of *Champsosaurus*, *C. annectens*, and to secure both the genus name *Champsosaurus* and family name Champsosauridae, all valid species of *Champsosaurus* were reviewed for consideration as the new type species. *Champsosaurus natator* was chosen as the best replacement type species because it is coeval

to *C. annectens*, and is the best represented *Champsosaurus* species. The International Commission on Zoological Nomenclature must be petitioned to formally establish *C. natator* as the type species, stabilizing both the genus and family names.

To address the absence of definitions within Choristodera, and consolidate the group in a phylogenetic context, a node-based definition was proposed, where Choristodera was defined as the most recent common ancestor of *Champsosaurus* and *Cteniogenys*, and all descendants of that common ancestor. Taxa discovered in the future that are basal to *Cteniogenys*, but are more closely related to choristoderes than other neodiapsids should be included in a newly erected group, e.g., 'Choristoderomorpha'.

To consolidate Neochoristodera in a phylogenetic context, a node-based definition was also proposed for this group, where Neochoristodera was defined as the most recent common ancestor between *Champsosaurus* and *Simoedosaurus*, and all descendants from that common ancestor. All taxa that are basal to this common ancestor should be included in the informal group, non-neochoristoderes.

Palaeobiological evidence was also discussed in this chapter, providing a review of the current understanding of choristoderan anatomy and biology. Major gaps in the understanding of choristodere cranial anatomy were reviewed, specifically highlighting: (1) the lack of understanding regarding the presence and morphology of the choristoderan neomorphic bone; (2) the presently undescribed neuroanatomy of choristoderes; and (3) the possible presence of turbinates in the nasal passages of these taxa. These major gaps in the understanding of choristoderan cranial anatomy are avenues for further research, and will form the remainder of this thesis.

Research Objectives

The objectives of this thesis are as follows:

1. Provide a detailed description of the cranial elements of *Champsosaurus* in three dimensions, comment on the validity of the putative neomorphic bone and describe how it relates to the brain endocast.

2. Conduct a description of the brain endocast of an intact skull to describe the size and shape of the different regions of the brain, with reference to the previous work conducted by Russell (1956), Fox (1968), and Erickson (1985).

3. Describe the previously undescribed internal pathways of the cranial nerves.

4. Describe the previously undescribed choristodere endosseous labyrinth of the inner ear. Since the inner ear is the organ responsible for sensing orientation relative to Earth's gravity, and is responsible for sensing angular acceleration of the head during fast movement (Rabbit et al., 2004), knowledge of the inner ear is important for making inferences about the ecology of fossil taxa (Dickson et al., 2017). Additionally, cochlear length is strongly correlated with hearing capability, vocalization, and sociality (Walsh et al., 2009), and a description of this organ in *Champsosaurus* will provide important behavioural information.

5. Provide a description of the nasal passages of *Champsosaurus* to comment on the possible presence of turbinates in choristoderes.

Chapter 2: Computed tomography (CT) analysis of the cranium of *Champsosaurus lindoei* and implications for the choristoderan neomorphic ossification

This chapter was accepted for publication in the *Journal of Anatomy* on June 18th, 2019.

Introduction

Choristoderes were small to medium sized (30 cm – 3 m long) neodiapsid reptiles that lived from the Middle Jurassic (Bathonian) to the Miocene (Eggenburgian) of Laurasia (Matsumoto and Evans, 2010; Evans and Klembara, 2005). These animals are known for their unusual cranial morphology, characterized by an elongated preorbital region and posteriorly expanded temporal arches (Gao and Fox, 1998). *Champsosaurus* exhibits the most extreme condition of these features, where the snout has become particularly elongated and slender, comprising half the length of the skull. The temporal arches are also dramatically expanded posterolaterally, giving the skull a cordiform dorsal profile. Other unusual features of the skull of *Champsosaurus* include the presence of paired gaps on the ventral surface of the skull that border the parasphenoid laterally. These gaps were first identified by Russell (1956) as the external auditory meatuses, but have been subsequently interpreted as unossified gaps in the otic capsule that may have enclosed the stapes (Fox, 1968). These gaps have received no attention since their descriptions by Russell (1956) and Fox (1968), and the auditory system is undescribed among Choristodera.

Another peculiarity of the choristodere skull is the putative presence of a neomorphic bone in the lateral wall of the braincase. This bone was first identified by Fox (1968) as a

small triangular element, having previously been identified as part of the squamosal (Brown, 1905) or prootic (Fox, 1968). Erickson (1972) later suggested that there was no evidence for the neomorphic bone in *C. gigas*, and that this element was simply a misidentified extension of the parietal. More recent interpretations (Gao and Fox, 1998) have again suggested that the neomorph is indeed a distinct, elongate element, extending posteriorly to the pterygoquadrate foramen. Despite the previous uncertainty in the literature, subsequent descriptions of choristoderes follow the conclusions of Gao and Fox (1998) and refer to the neomorphic bone as a distinct ossification (e.g., Gao and Fox, 2005; Matsumoto et al., 2007; Gao and Ksepka, 2008; Matsumoto et al., 2019), but the neomorphic bone has yet to be properly described. Skepticism regarding its presence in the braincase region is well justified, as the morphology of the neomorph has been previously debated, and the braincase is considered to have remained relatively conserved throughout tetrapod evolution (Cardini and Elton, 2008; Goswami and Polly, 2010; Knoll et al., 2012; Maddin et al., 2012).

Fox (1968) stated that the neomorphic bone does not contact the endocranial cavity, but the relationship of this element to the brain cavity, endosseous labyrinth, and cranial nerve tracts has not been re-evaluated following its description as a larger element by Gao and Fox (1998). As such, the neomorphic bone requires an exhaustive 3D description to determine its validity, and its relationship to the other cranial elements and endocranial structures.

The objectives of this paper are as four-fold. Using high-resolution micro-computed tomography: (1) Describe the cranial elements of a well-preserved specimen of *Champsosaurus lindoei* (CMN 8920) in three dimensions; (2) Provide a description of the paired gaps reported on the ventral surface of the skull and investigate the hypothesis that

these relate to the fenestrae ovales; (3) Illustrate the morphology of the putative neomorphic bone and discuss how it relates to other cranial elements and the internal structures of the skull (e.g., brain cavity, and endosseous labyrinth, cranial nerves); (4) Consider the possible developmental and functional origins of the neomorph.

Definitions

The putative choristoderan neomorphic bone has often been described as a component of the braincase (e.g. Fox, 1968; Brinkman and Dong, 1993; Gao and Fox, 2005; James 2010), but in order to determine whether the putative neomorph is indeed a braincase element, the definition of a braincase bone needs to be established. There are three recurring definitions of braincase bones in the literature: (1) only bones of the chondrocranium (Romer, 1956); (2) all bones of the chondrocranium plus the dermatocranial parasphenoid (Romer and Parsons, 1977; Atkins and Franz-Odendaal, 2016); (3) all bones that enclose the brain cavity (Specht et al., 2007). The reason for the inclusion of the dermatocranial parasphenoid (definition 2) is well justified, as most lineages of amniotes fuse the parasphenoid with the basisphenoid (Atkins and Franz-Odendaal, 2016), and the paraphenoid plays a role in supporting the brain ventrally. Definition (3) is common in human and mammalian anatomy more generally (Hopson and Rougier, 1993; Specht et al., 2007), as the chondrocranial elements play a significantly smaller role in the mammalian cranium than they do in other lineages (Romer and Parsons, 1977). The issue with definition (3) is that it includes several bones of either dermatocranial origin, or of mixed dermatocranial and chondrochranial origin, such as the mammalian temporal bone and sphenoid respectively, making broad comparisons across lineages difficult (Porto et al., 2009).

The braincase is therefore defined here using definition (2), which includes all bones of the chondrocranium, plus the parasphenoid. This definition is often used when discussing the braincase of reptiles (Romer, 1956; Romer and Parsons, 1977) and is therefore effective for comparisons across many lineages. As such, if the neomorphic bone is found to be a distinct ossification, it will only be considered here as a braincase bone if it could have ossified from the chondrocranium, or is tightly integrated or fused with other chondrocranial bones.

Institutional abbreviations

CMN, Canadian Museum of Nature, Ottawa, Ontario; IVPP, Institute of Vertebrate Paleontology and Paleoanthropology, Beijing, China; ROM, Royal Ontario Museum, Toronto, Ontario; SMM, Science Museum of Minnesota, St. Paul, Minnesota; TMP, Tyrrell Museum of Palaeontology; UALVP, Laboratory for Vertebrate Palaeontology, University of Alberta, Edmonton, Alberta; UTCT, University of Texas High-Resolution X-ray Computed Tomography Facility, Austin, Texas.

Anatomical abbreviations

Bone abbreviations in brackets indicate suture surfaces.

ac, passage for the anterior semicircular canal; **art,** articular surface for the jaws; **bo,** basioccipital; **bs**, basisphenoid; **bt**, basal tubera; **ca,** impression of the internal carotid artery; **cc**, canal for the crus communis; **ch**, choana; **CN I,** passage for CN I; **CN IX,** exit for CN IX; **CN V**, opening for CN V; **CN V_2f,** foramena for CN V2; **CNV_2n,** passage for CN V2 and nasolacrimal duct; **CN VI**, canal for CN VI; **mf**, metotic foramen (canal for CN X and CN

XI); **CN XII**, canal for CN XII; **cp**, clinoid process; **d,** midline depression; **dc,** dorsal concavity; **dcp,** dorsal concavity for pineal body; **den**, dentine; **dr,** dorsal ridge; dv, foramina for diploic veins; **ect**, ectopterygoid; **en**, enamel; **ex,** exoccipital; **flan**, flange for articulation with the first cervical vertebra; **fm,** foramen magnum; **fr,** frontal; **fo,** fenestra ovalis; **gv,** groove; **hvnt,** lateral head vein trough; **hvnw**, wall of lateral head vein; **inc,** incisive foramen; **int,** internarial; **ita,** inferior temporal arch; **itf,** infratemporal fenestra; **itfw,** wall of the infratemporal fenestra; **ju,** jugal; **k**, dorsal keel; **lac,** lacrimal; **lat frk,** lateral fork; **lc**, passage for the lateral semicircular canal; **lshf**, lacrimal shelf; **max,** maxilla**; max alv,** maxillary alveoli; **med frk**, medial fork; **mpr**, median pharyngeal recess; **na**, nasal; **no**, narial opening; **ne**, neomorph; **npt**, nasopalatal trough; **nv**, nasal vestibule; **oc**, occipital condyle; **ocf,** olfactory chamber floor; **olf,** dorsal impression of olfactory stalk; **och**, olfactory chamber; **op**; opisthotic; **orb,** orbit; **orn**, ornamentation; **otc,** otic capsule; **pa**, parietal; **pal**, palatine; **pal alv**, palatine alveoli; pc, passage for the posterior semicircular canal; **pit**, pituitary fossa; **plc,** plicidentine infolding; **pm**, premaxilla; **pm alv**, premaxillary alveoli; **pof**, postfrontal; **pop,** paroccipital process; **por**, postorbital; **pr**, prootic; **prf**, prefrontal; **ps**, parasphenoid; **pt**, pterygoid; **pta,** post-temporal arch; **ptf,** pterygoid flange; **ptf**, post-temporal fenestra; **ptq,** pterygoquadrate foramen; **ptv,** interpretygoid vacuity; **pt alv,** pterygoid alveoli; **pul,** pulp cavity; **q**, quadrate; **qj**, quadratojugal; **qr,** quadrate ramus; **rid,** ridges; **sf**, suborbital fenestra; **sfw**, wall of suborbital fenestra; **shf,** dorsal shelf extending ventral to the parietal; **so**, supraoccipital; **sof**, subolfactory flange**; sq**, squamosal**; sta,** superior temporal arch; **stf,** supratemporal fenestra; **stfw,** wall of the supratemporal fenestra; **t**, teeth; **tf**, temporal fossa; **U,** U-shaped groove; **vfm**, ventral rim of the foramen magnum;

vo, vomer; **vom alv**, vomerine alveoli; **vpn,** ventral projection of the nasal**; vpq,** ventral projection of the quadrate; **vs**, vomerine septum; **(i-max)**, intermaxillary contact.

Materials and Methods

CMN 8920 was collected by H.L. Shearman on July 13th, 1953 from what is now defined as the Dinosaur Park Formation of the east branch of Sand Creek, Alberta (NAD83; 12U 460541.290, 5619553.359). The specimen was found approximately 100 ft (approximately 30 m) above river level in a clear sandstone (1953 field notes, CMN archives). CMN 8920 was first described by Russell (1956) as pertaining to *C. natator* Parks, 1933, but was reassigned to the newly erected *C. lindoei* Gao and Fox, 1998, based on its relatively small size (approximately 24.3 cm basioccipital length), gracile snout, expanded narial bulla, weak pterygoid flange, and strait inferior temporal arch.

CMN 8920 was scanned at UTCT with a voxel size of 60.5 μm, at 200 kV, and 0.3 mA. This produced 4579 slices, which were converted to 8-bit tiff files for segmenting. The dataset was divided into five subunits, where every other tiff file within each subunit was selected for loading into Amira 5.4.3 to perform visualization and segmentation using the LabelFields module. Elements of the cranium were segmented individually and rendered using the SurfaceView module. The surface models of each subunit were then recombined, creating a colour coded model of the complete skull for manipulation and description. The 3D models generated from this study will be made freely available online via MorphoSource.

Results

Overall skull morphology

CMN 8920 is a remarkably complete skull, lacking jaws, that suffers only slight post-mortem and taphonomic modifications (Figure 2.1; Figure 2.2; Figure 2.3). These include crushing of the right squamosal and quadratojugal; the posterior tips of the opisthotics and parasphenoid have broken away; the premaxillae, maxillae, nasal, internarial, and prefrontals are fractured and have been infilled with matrix; and the tip of the rostrum is twisted counter-clockwise when the skull is viewed anteriorly.

The length of CMN 8920 is typical for an adult-sized skull of *C. lindoei* (Table 2.1; Figure 2.4) and is similar in overall morphology to other specimens reported by Gao and Fox (1998). As is characteristic for choristoderes, the skull is dorsoventrally flattened, with prominent temporal arches that expand posterolaterally and give the skull a cordiform dorsal profile. The nares are confluent and open anteriorly on the snout, as is seen in many choristoderes (Gao and Fox, 1998).

Dermatocranium

Premaxilla – Both premaxillae are preserved (Figure 2.5A), although they have both undergone slight fragmentation. When viewed dorsally, the paired premaxillae form a rounded nasal bulla that is wider than the anteriormost extent of the maxillae. The premaxillae are prevented from contacting one another posterodorsally by an invasion of the nasal. This condition is mirrored ventrally, where the premaxillae are separated from one another by the internarial posterior to the incisive foramina. The premaxilla contacts the

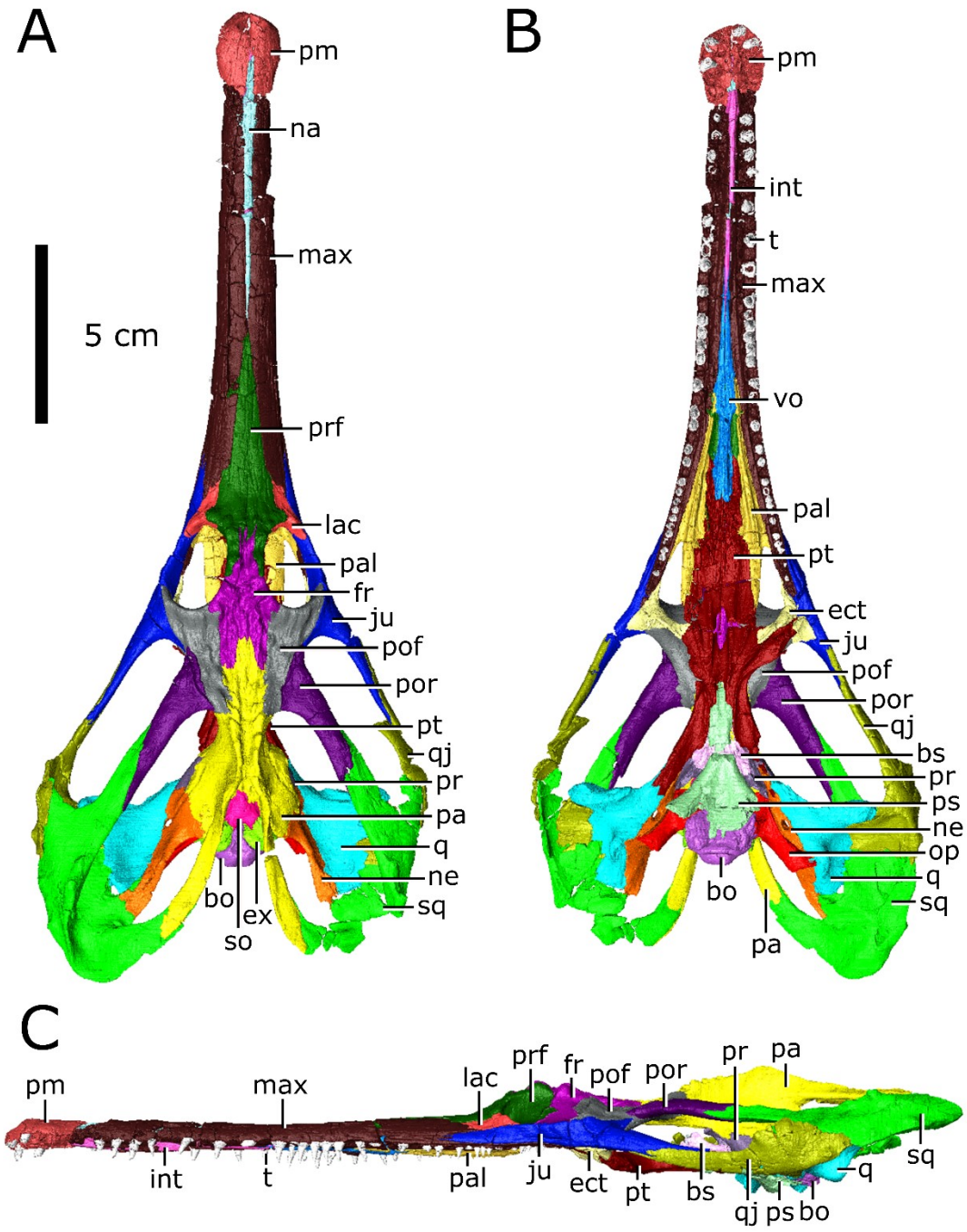

Figure 2.1: Articulated skull of *Champsosaurus lindoei* (CMN 8920). **A** dorsal view; **B** ventral view; **C** lateral view.

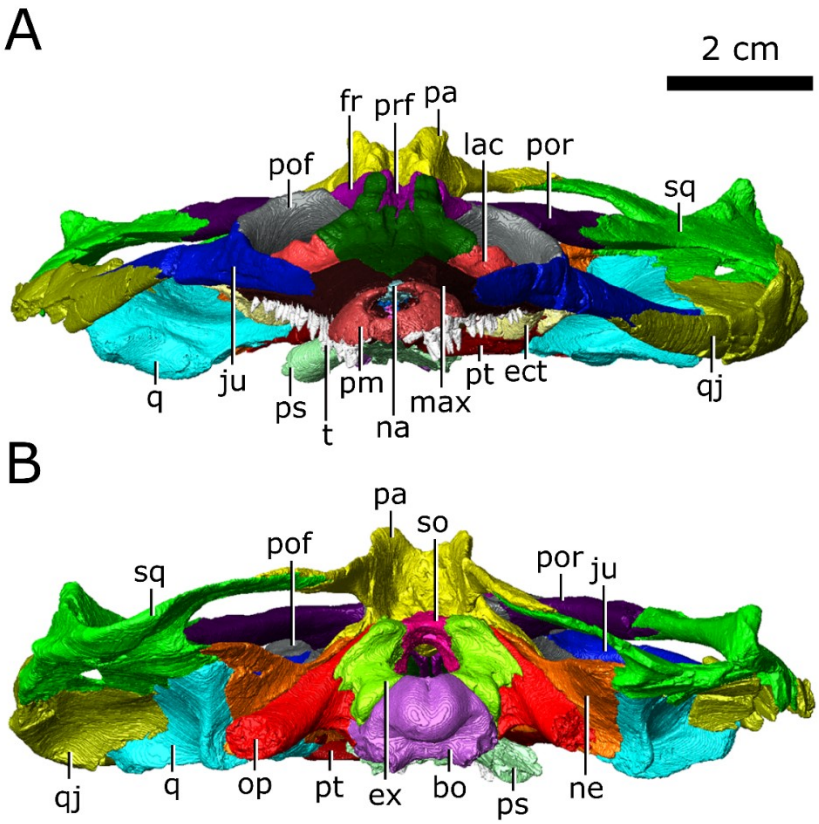

Figure 2.2: Articulated skull of *Champsosaurus lindoei* (CMN 8920). **A** anterior view; **B** posterior view.

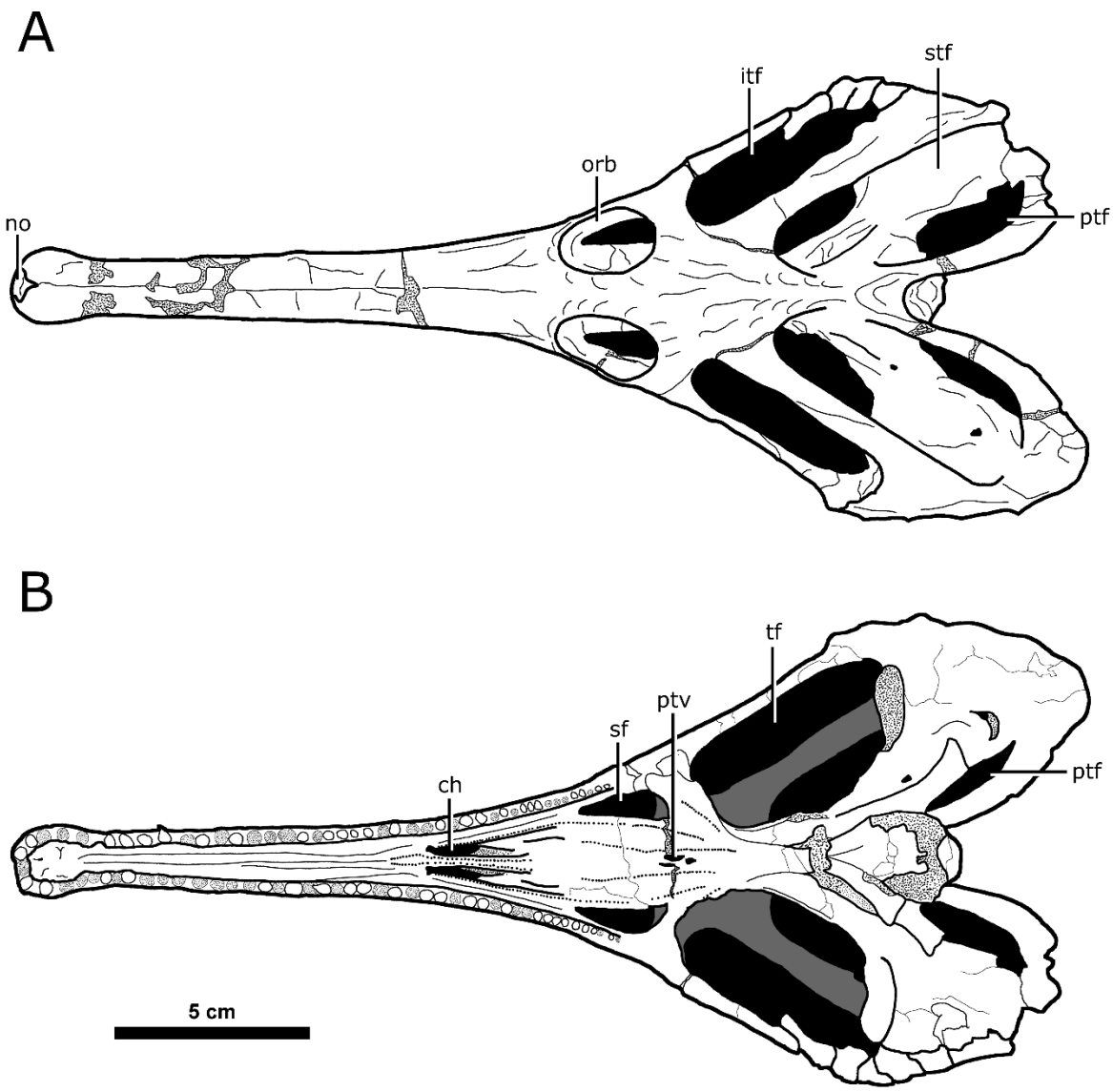

Figure 2.3: Major skull openings of *Champsosaurus lindoei* (CMN 8920). **A** dorsal view; **B** ventral view.

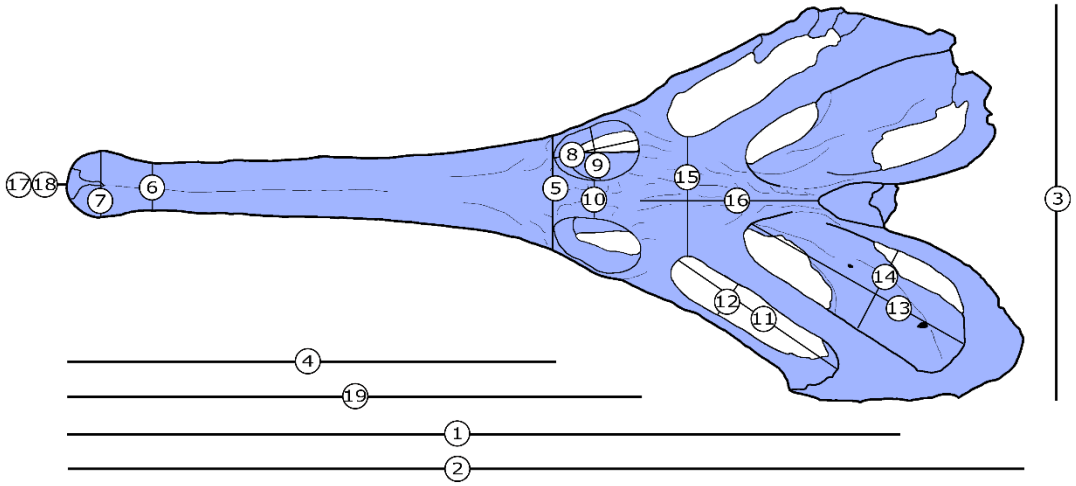

Figure 2.4: Skull measurements for *Champsosaurus lindoei* (CMN 8920). See Table 2.1 for corresponding measurement descriptions and values.

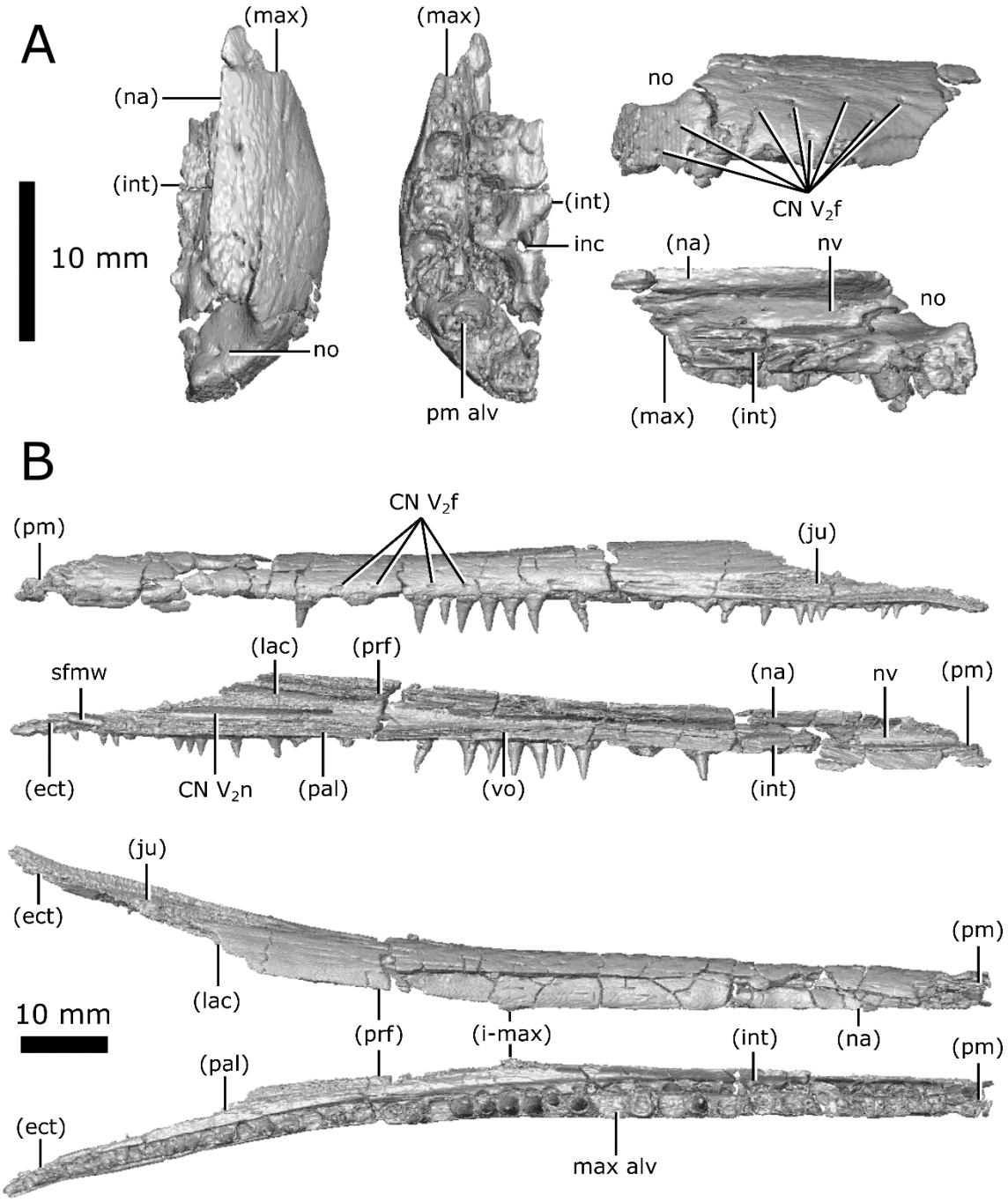

Figure 2.5: Isolated premaxilla and maxilla of *Champsosaurus lindoei* (CMN 8920). **A** left premaxilla in dorsal view (left), ventral view (middle), lateral view (top right), medial view (bottom right); **B** left maxilla in lateral view (top), medial view (second from top), dorsal view (second from bottom), ventral view (bottom).

Table 2.1: Measurements for the skull of *Champsosaurus lindoei* (CMN 8920).

	Measurement	Value(s) (mm; left/right)
1	Basal skull length	243
2	Maximum skull length	278
3	Skull width at quadratojugals	113
4	Snout length (anterior of orbits)	14.7
5	Width of snout base	3.3
6	Width of distal snout posterior to bulla	1.4
7	Width of bulla	2.0
8	Maximum orbital length	2.5/2/4
9	Maximum orbital width	1.7/1.7
10	Interorbital width	1.1
11	Maximum infratemporal fenestra length	5.5/5.4
12	Maximum infratemporal fenestra width	1.6/1.6
13	Maximum supratemporal fenestra length	6.6/6.6
14	Maximum supratemporal fenestra width	2.6/2.6
15	Width of parietal table	3.4
16	Length of parietal table (posterior to orbits)	4.9
17	Nares length (anteroposterior)	0.5
18	Nares width	0.7
19	Anteroposterior length of maxillary tooth row	16.4

maxilla immediately posterior to the seventh tooth position with a suture that runs relatively perpendicular to the long axis of the snout. Together, the premaxillae nearly completely surround the narial opening, which opens onto the anterior surface of the snout. The dorsal rim of the narial opening does not extend as far forward as the ventral rim, causing the narial opening to face slightly dorsally.

Internally these elements possess a network of canals that run from foramina on the external surface (Figure 2.5A; CN V_2f) into a large tract that runs the entire length of the snout. This canal likely carried the maxillary branch of the trigeminal nerve (CN V_2), and these foramina, therefore, would have held sensory nerves that innervated the snout. The medial surface of the premaxilla indicates that the anterior region of the nasal vestibule was smooth, lacking any evidence of conchae.

Maxilla – Both maxillae are preserved (Figure 2.5B), but are highly fragmented anteriorly. In lateral view, the maxilla is elongate and dorsoventrally thin, extending from the seventh tooth position to the ectopterygoids (Figure 2.1B). The maxillae only briefly contact one another at the midpoint of the dorsal surface of the snout, where the nasal and prefrontals taper towards one another. On the dorsal surface, the maxillae are separated by the nasal anteriorly and the prefrontals posteriorly, and vanish from external view posteriorly at the suture with the lacrimal. On the ventral surface, the maxillae are separated anteriorly by the internarial and vomers. Ventromedially, the maxilla contacts the palatine for the entire length of the latter, extending from the anterior margin of the choana to the midpoint of the suborbital fenestra, terminating anterior to the ectopterygoid.

Like the premaxilla, the maxilla is smooth externally, but punctured by dozens of foramina scattered across its surface (Figure 2.5B; CN V_2f). These foramina penetrate the

maxilla and commune with the canal for CN V_2 that extends the entire length of the maxilla. However, the maxilla only surrounds the canal completely for the anterior half of its length; the posterior half of the maxilla comprises only the dorsolateral wall of the CN V_2 canal. The maxilla surrounds the nasal vestibule for the anterior half of its length, before diverging laterally away from the nasal passage.

Nasal – The nasals are elongate and fused with no identifiable suture, and will therefore be treated as a single element (Figure 2.6A). In dorsal view, the nasal is slender and elongate, narrowing as it extends posteriorly. The anteriormost portion is fragmented and poorly preserved, and as a result, this element does not contact the narial opening; however, it is likely that the nasal would contact the narial opening when intact, as indicated by the medial suture of the premaxillae, and the condition seen in other more complete specimens (Erickson, 1972). The nasal extends anteriorly between the premaxillae and terminates between the anterior projections of the prefrontals posteriorly, ventral to the outer surface of the maxillae. A thin projection (approximately 1 mm high; Figure 2.6A; vpn) extends ventrally along the entire length of the nasal towards the internarial, suggesting a cartilaginous wall may have separated the nasal passages for at least the anterior portion of the nasal passage.

Lacrimal – Both lacrimals are perfectly preserved (Figure 2.6B). The lacrimal is a relatively small element on the dorsal surface of the snout that composes the anteriormost margin of the orbits. It is triangular when viewed dorsally and is bordered by the maxilla anteriorly, the prefrontal medially, the jugal laterally, and the palatine ventrally. The CT data reveal a triangular, striated shelf (Figure 2.6B; lshf) that projects deep to the maxilla anteriorly, making the extent of this element nearly twice as large as what is seen on the surface. The

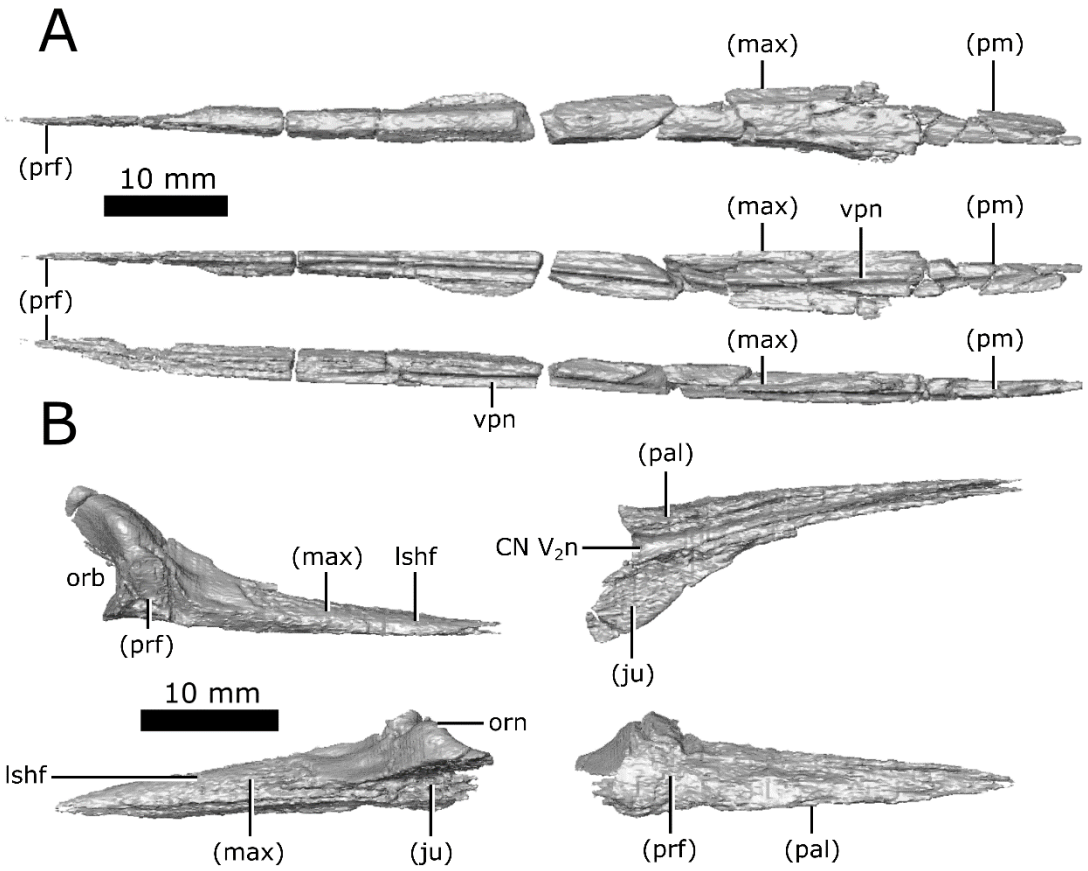

Figure 2.6: Isolated nasal and lacrimal of *Champsosaurus lindoei* (CMN 8920). **A** nasal in dorsal view (top), ventral view (middle), right lateral view (bottom); **B** left lacrimal in dorsal view (top left), ventral view (top right), lateral view (bottom left), medial view (bottom right).

surface of the lacrimal becomes rugose anterior to the orbit, resembling the ornamentation seen on the prefrontal, frontal, and parietal.

The ventral surface of the lacrimal forms the dorsomedial wall of the nasolacrimal canal that opens posteriorly into the orbit. The CT data show that this canal opens anteriorly into the nasal passage through a small gap (0.8 mm high by 4 mm long) between the maxilla and palatine, supporting the interpretation of Russell (1956). Interestingly, the canal continues anterior to this gap and extends through the maxilla and premaxilla to the very tip of the snout, with branches towards the outer surface of the skull, as is typical of CN V_2. This morphology suggests that the nasolacrimal canal was confluent with CN V_2 in *Champsosaurus*, a feature that is also observed in other species of *Champsosaurus* (e.g., *C. natator*; Russell, 1956) and possibly other neochoristoderes (e.g., *Tchoiria namsarai*; Ksepka et al., 2005). There is no other duct connecting the orbit to the nasal passage in *Champsosaurus*, and this is therefore the only canal that could have possibly carried the nasolacrimal duct.

Prefrontal – Both prefrontals are well-preserved with little fracturing and distortion (Figure 2.7A). Anteriorly, the prefrontal sits medial to the lacrimal and maxilla, where the prefrontal forms a large triangular projection when viewed dorsally. This projection penetrates the maxilla before terminating near the midpoint of the snout, at the posterior extent of the nasal. The prefrontals contact for approximately 80% of their length, forking laterally around the frontals posteriorly, and form the rugose anteromedial rim of the orbit. The elongate and highly interdigitated prefrontal-frontal suture is obscured on the surface by ornamentation, but is clearly visible on the CT data. On the ventral surface, the anterior portion of the prefrontal forms the roof of the nasal vestibule that expands posteriorly to form the body of

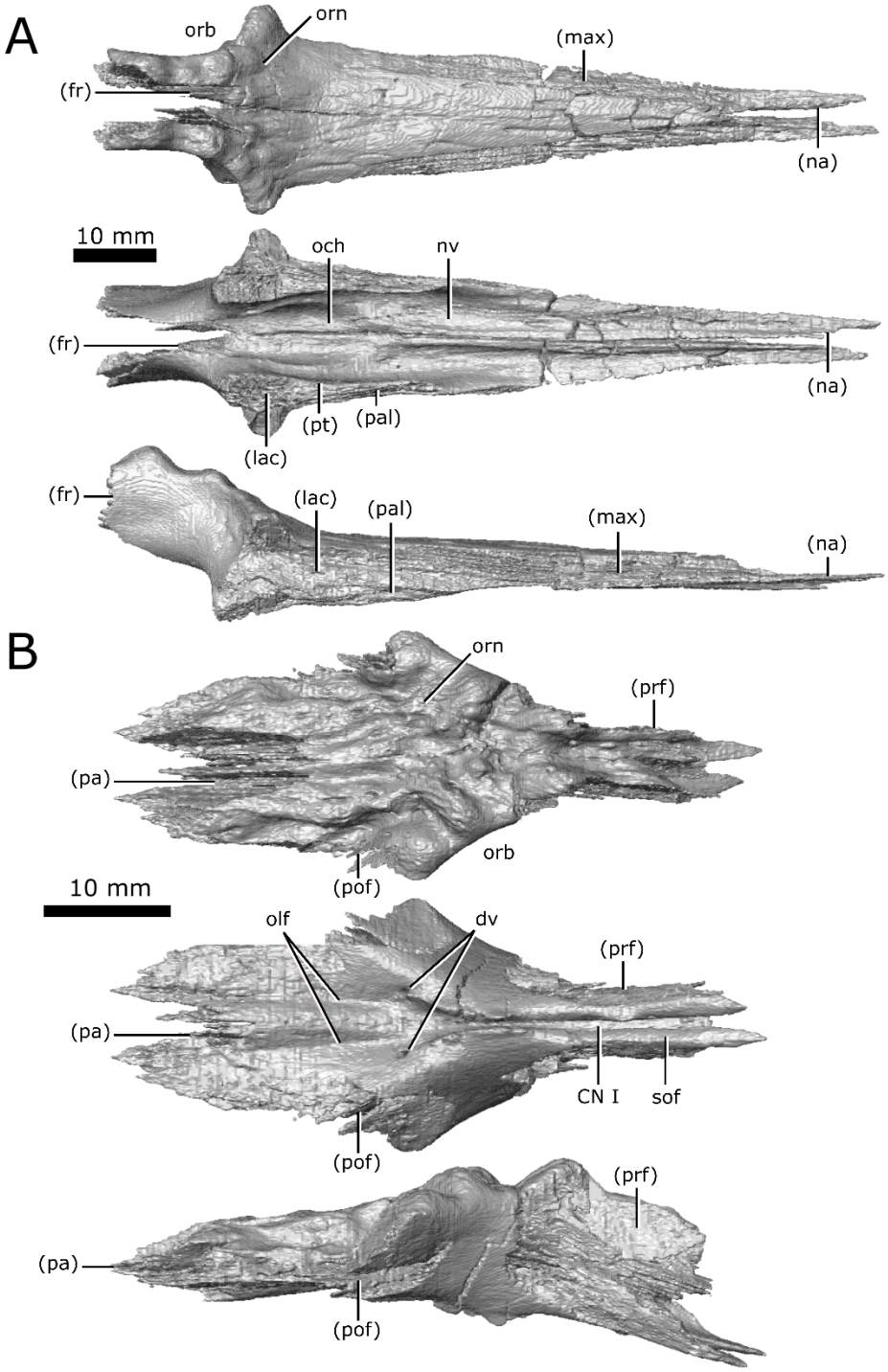

Figure 2.7: Isolated prefrontals and frontals of *Champsosaurus lindoei* (CMN 8920). **A** prefrontals in dorsal view (top), ventral view (middle), right lateral view (bottom); **B** frontals in dorsal view (top), ventral view (middle), right lateral view (bottom).

the olfactory chamber (Figure 2.7A; och). The chamber narrows posteriorly to commune with the olfactory duct (CN I) housed by the frontals. Ventrolaterally, the prefrontal contacts the palatine with a suture that extends from the choana to the orbit. The prefrontal contacts the pterygoid along the ventralmost portion of the walls of the olfactory chamber, although it cannot be determined if this contact is genuine or due to crushing of the pterygoid.

Frontal – Both frontals are well-preserved and complete, and together are roughly rhomboid when viewed dorsally (Figure 2.7B). The dorsal surface of the frontal is rugose, possessing the most prominent cranial ornamentation on the skull, and composes the posteromedial portion of the orbits. The frontal is bordered anteriorly by the prefrontals, laterally by the postfrontal, and posteriorly by the parietal, which penetrates the frontals in a wide V-shaped suture when viewed dorsally. The CT data show that the frontoparietal suture has a complex internal structure, with a high degree of interdigitation. The subolfactory flanges (Figure 2.7B; sof) on the ventral surface of the frontals wrap around the olfactory duct (CN I) but do not completely enclose it, and the duct remains open ventrally. This duct extends from the frontal-prefrontal suture to the midline of the posterior rim of the orbits. At this point, the duct opens and communicates with the olfactory stalk of the brain, represented by two shallow, parallel troughs extending from the posterior opening of the olfactory duct, along the ventral surface of the frontals and parietals to the midbrain. Two foramina can be seen leading into the ventral surface of the frontals in the impression left by the anterior-most extent of the olfactory stalks. The CT data reveal that these foramina fork and dissipate into the cortical bone of the frontals, suggesting that they are vascular and carried diploic veins (Witmer and Ridgely, 2009).

Postfrontal – Both postfrontals are preserved with only slight fragmentation, and are triangular in dorsal view (Figure 2.8A). The dorsal surface of the postfrontal has slight pitting, although it is modest compared to the ornamentation of the frontal, prefrontal, or parietal. The anterior margin of the postfrontal forms the posterior rim of the orbit and is separated from its counterpart by the frontals anteromedially, and the parietals posteromedially. The postfrontal borders the jugal laterally and the postorbital posterolaterally, and forms a portion of the anterior border of both the supratemporal and infratemporal fenestrae.

Postorbital – The postorbitals are well-preserved (Figure 2.8B), with a slight amount of fragmentation, particularly on the right element. In dorsal view, the postorbital is roughly cylindrical and forms the anterior portion of the superior temporal arch. The right postorbital shares a small suture with the right jugal at its anteriormost extent. Anteriorly, it contacts the postfrontal, but the postorbitals have no contact with the orbits. The postorbital usually contacts the orbits in other tetrapods, but the arrangement seen in CMN 8920 is typical for *Champsosaurus* (Gao and Fox, 1998). The suture with the postfrontal is badly damaged on both sides, having cracked along the length of the suture and infilled with sediment. Posteriorly, the postorbital contacts the squamosal via a suture along the length of the superior temporal arch.

Parietal – Both parietals are well-preserved (Figure 2.9), with significant fragmentation only occurring along the post-temporal arch. When viewed dorsally, the parietal is elongate, covering the majority of the length of the brain cavity. The parietal shares a complex suture with the frontal anteriorly and is bordered by the postfrontal anterolaterally. The suture between the parietals lies along the midline of the skull in a depression on the dorsal surface

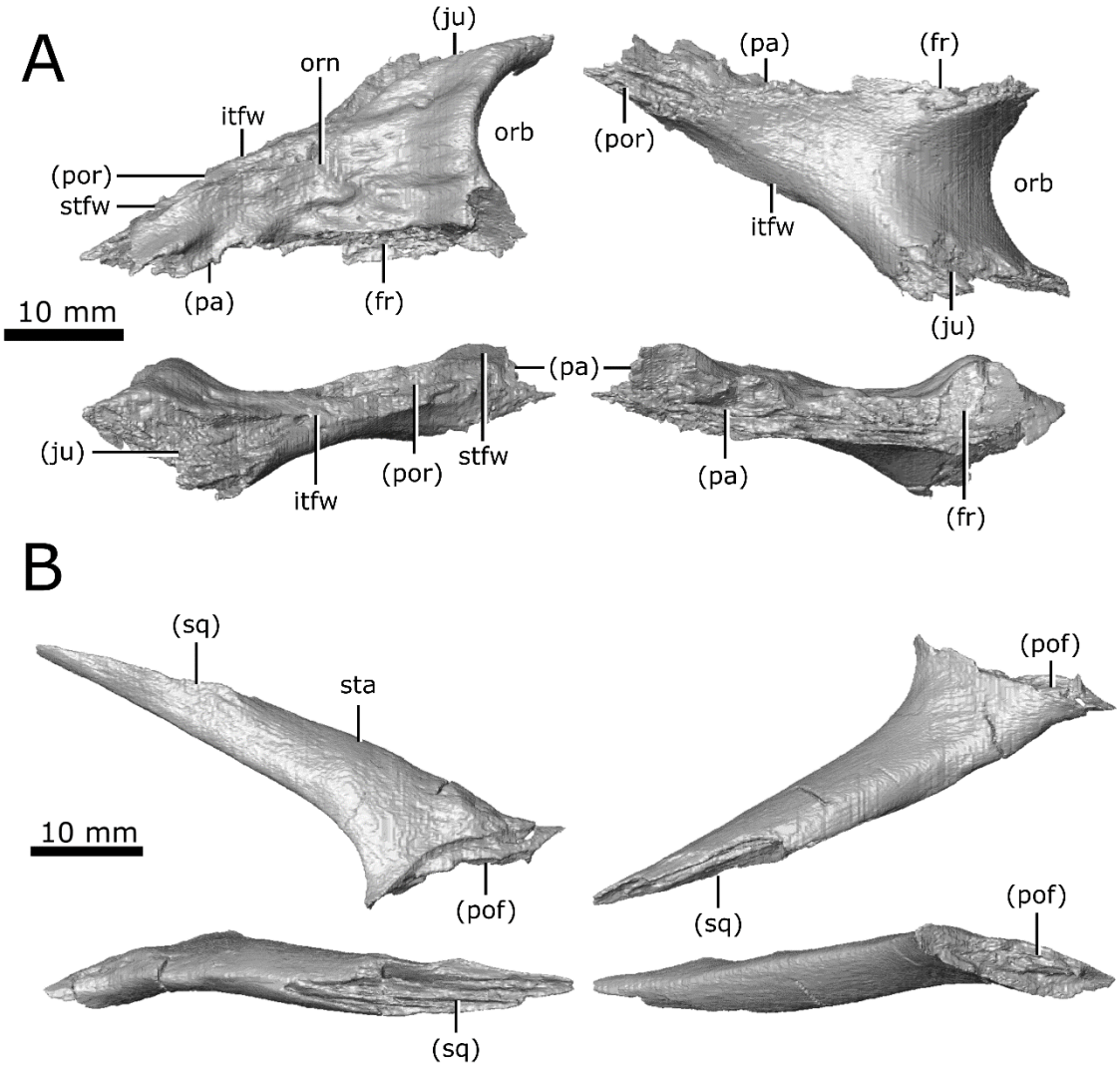

Figure 2.8: Isolated postfrontal and postorbital of *Champsosaurus lindoei* (CMN 8920). **A** left postfrontal in dorsal view (top left), ventral view (top right), lateral view (bottom left), medial view (bottom right); **B** left postorbital in dorsal view (top left), ventral view (top right), lateral view (bottom left), medial view (bottom right).

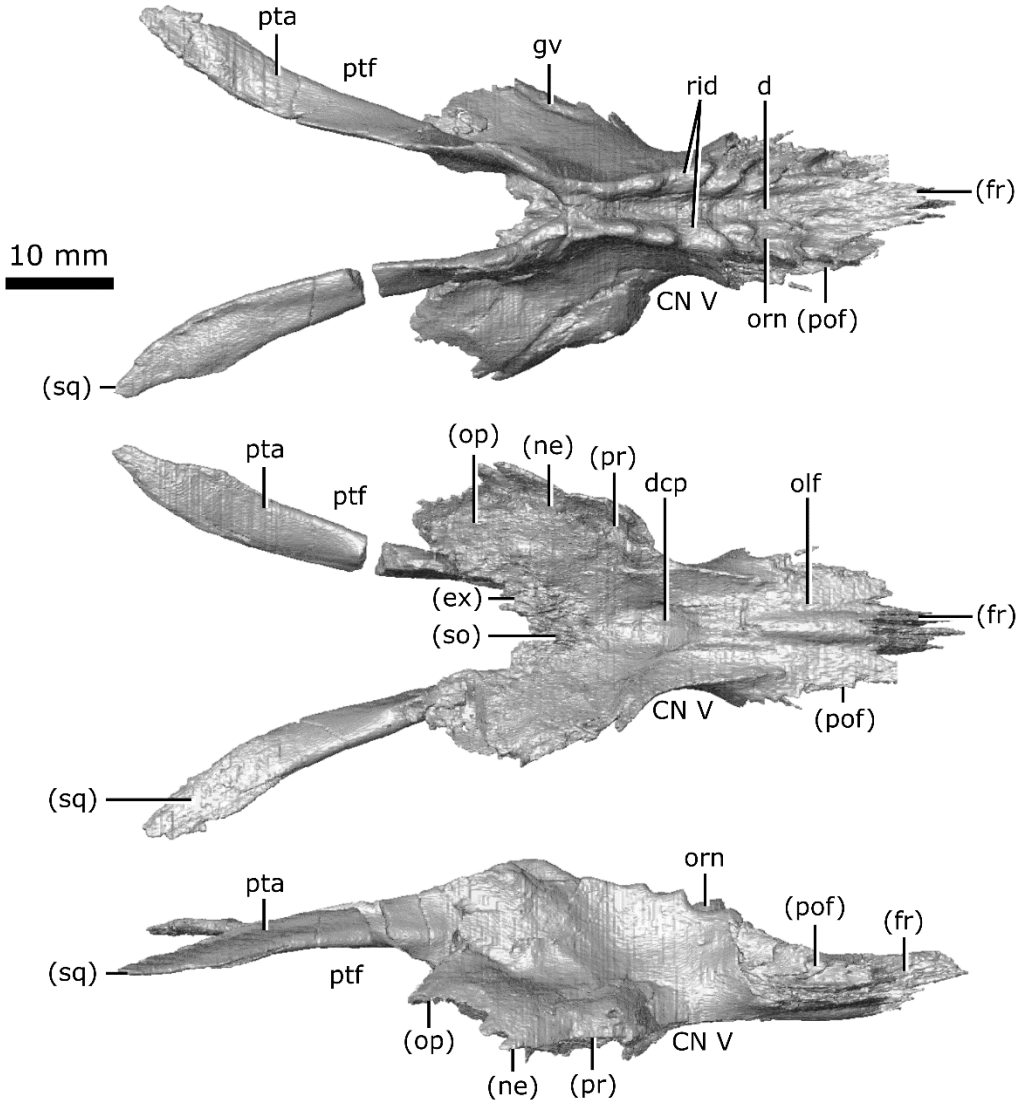

Figure 2.9: Isolated parietals of *Champsosaurus lindoei* (CMN 8920) in dorsal view (top), ventral view (middle), right lateral view (bottom).

that is bordered laterally by an ornamented ridge. The parietals extend laterally over the dorsal portion of the neomorph, as well as the body of the opisthotic and the posterior portion of the prootic. Posteriorly, the parietals extend along the post-temporal arch (Figure 2.9; pta) to contact the squamosal. The parietal forms approximately half of the post-temporal arch, and forms the dorsal rim of the post-temporal fenestra.

A distinct groove is seen on the lateral surface of the parietal (Figure 2.9; gv) that extends from the opening for CN V, onto the lateral surface of the neomorph, and terminates at the rim of the pterygoquadrate foramen. Russell (1956:11) described a "low but distinct ridge" extending anteroventrally along the lateral surface of the parietal that presumably represented the demarcation between the small anterior and large posterior portions of the temporal muscles. This ridge is absent on CMN 8920, consistent with previous observations (Gao and Fox, 1998) that this ridge tends to be less prominent in smaller *Champsosaurus* such as *C. lindoei*. The ventral surface of the parietal over the braincase is concave (Figure 2.9; dcp) , and housed the large dorsal expansion of the pineal body, although there is no evidence for a pineal opening in *C. lindoei*. The ventral surface of the parietal anterior to the concavity for the pineal body is striated with vascular sulci, suggesting that the dura matter pressed close to the bone in life. Anterolateral to the dorsal concavity of the parietal, the lateral edge of the parietal forms the dorsal rim of the exit for CN V. The concave ventral surface of the parietal continues posteriorly for the rest of its length, where it roofs the opisthotic and exoccipital laterally, and the supraoccipital medially.

Neomorph – The neomorphic bone was first identified by Fox (1968) as a small triangular bone when viewed laterally, having previously been identified as part of the squamosal (Brown, 1905) or prootic (Fox, 1968). The exact extent of this element was poorly

understood, and was simply described as bordering the prootic, parietal, and pterygoquadrate foramen (Fox 1968). In the first description of *C. gigas*, Erickson (1972) stated that there was no evidence for a neomorphic element, and that this bone was simply an extension of the parietal. This interpretation was refuted by Gao and Fox (1998), who described the neomorph as an elongate element extending posterior to the pterygoquadrate foramen that appears to share an extensive dorsal suture with the parietal. The data presented here support Fox's (1968) hypothesis that the neomorphic element is a distinct ossification and follows a morphology similar to that proposed by Gao and Fox (1998).

Both left and right neomorphic elements are well-preserved in CMN 8920, with fracturing only occurring in the dorsal region near the juncture with the parietals.
The neomorph is an elongate ossification when viewed laterally, extending along the entire medial surface of the quadrate, and sits lateral to the braincase without contacting the brain cavity or endosseous labyrinth (Figure 2.10). At its anterior extent, a projection of the neomorph penetrates the quadrate ramus of the pterygoid. The neomorph extends posteriorly, ventral to the parietal and dorsolateral to the prootic and opisthotic. The CT data reveal for the first time a short tapering shelf (Figure 2.10; shf) that extends dorsally underneath the parietal for the entirety of its shared suture with the neomorph. A distinct groove (Figure 2.10; gv) extends along the dorsal surface of the neomorph from the parietal to the pterygoquadrate foramen (Figure 2.10; ptq). This groove has been illustrated in *C. gigas* (Erickson, 1972) and *C. natator* (Fox, 1968), and is presumed to be common to *Champsosaurus*. The neormorph contacts the quadrate laterally, extending posterodorsally in a long and slender projection to meet the squamosal. The neomorph forms almost the entire ventral rim of the post-temporal fenestra. Contrary to previous interpretations (e.g., Gao and

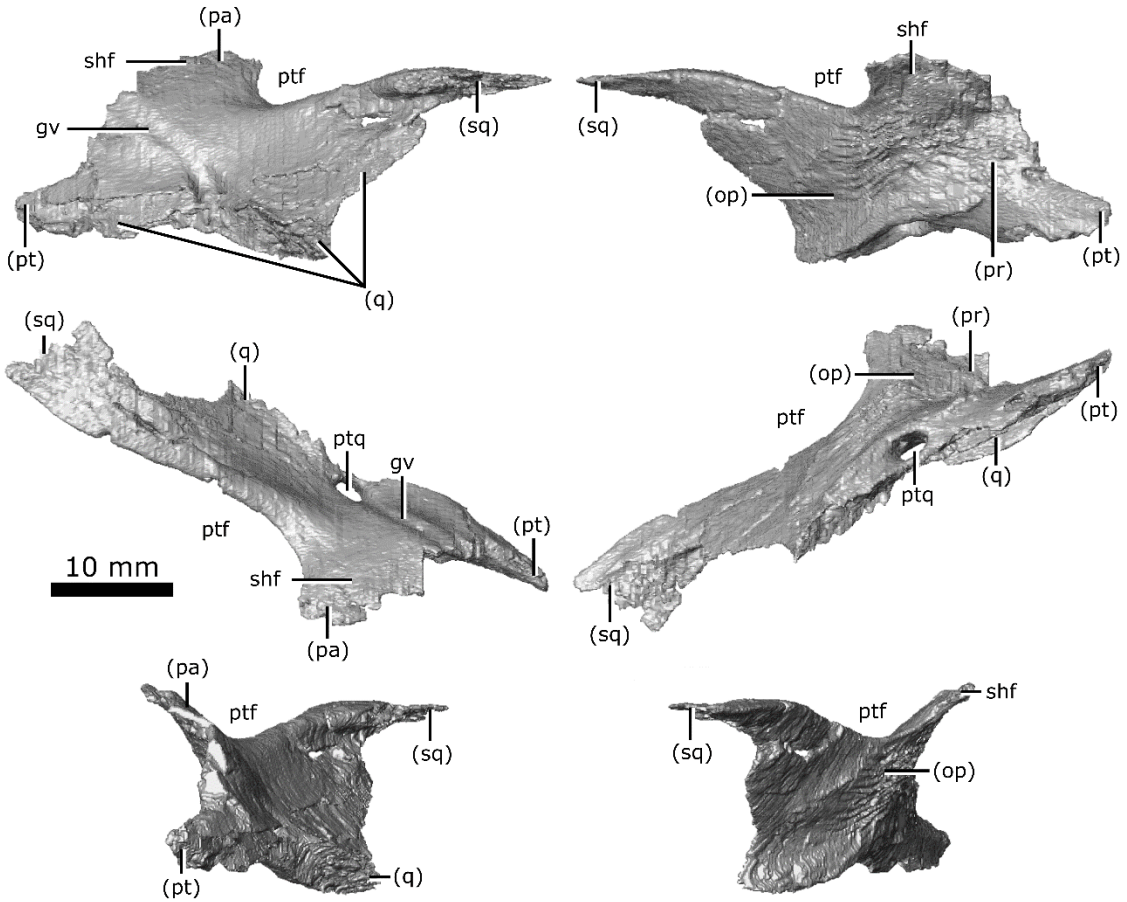

Figure 2.10: Isolated left neomorphic bone of *Champsosaurus lindoei* (CMN 8920) in lateral view (top left), medial view (top right), dorsal view (middle left), ventral view (middle right), anterior view (bottom left), posterior view (bottom right).

Fox 1998), the pterygoquadrate foramen is completely encompassed by the neomorphic bone.

Jugal – Both jugals are preserved with some fragmentation around the orbits and along the inferior temporal arch (Figure 2.11A). The jugal is long and slender when viewed laterally. It contacts the maxilla anteriorly by a long, thin projection, and contacts the lacrimal dorsally along the length of this projection. The jugals share a short suture with the palatine near the opening for the CN V_2 canal and the nasolacrimal duct. The jugal composes the most lateral portion of the orbits, posterior to its contact with the lacrimal. The jugal shares a suture with the postfrontal, which extends from the posterolateral portion of the orbit to the anteromedial portion of the infratemporal fenestra. The right jugal has a small contact with the right postorbital (approximatley 1 mm long), but the left jugal terminates immediately anterior to the postorbital. The jugal extends posterolaterally to form the gracile inferior temporal arch, along with the anterior portion of the quadratojugal. The jugal-quadratojugal suture is long, extending for the majority of the length of the inferior temporal arch (Figure 2.11A; ita). This arch is straight, giving the infratemporal fenestra a rectangular profile, as is typical for *C. lindoei* (Gao and Fox, 1998). This differentiates the species from the contemporaneous *C. natator*, which has an inferior temporal arch that is bowed outwards (Gao and Fox, 1998).

Quadratojugal – Both quadratojugals are preserved; the right one is heavily fragmented but the left one remains intact (Figure 2.11B). When viewed laterally, the quadratojugal is elongate and widens posterior to the inferior temporal arch. The quadratojugal forms the lateralmost portion of the temporal region, with only minimal ornamentation on the lateral surface. It contacts the jugal anteriorly via a long suture and expands posteroventrally to form the anteroventral portion of the temporal region. Here, the quadratojugal contacts the

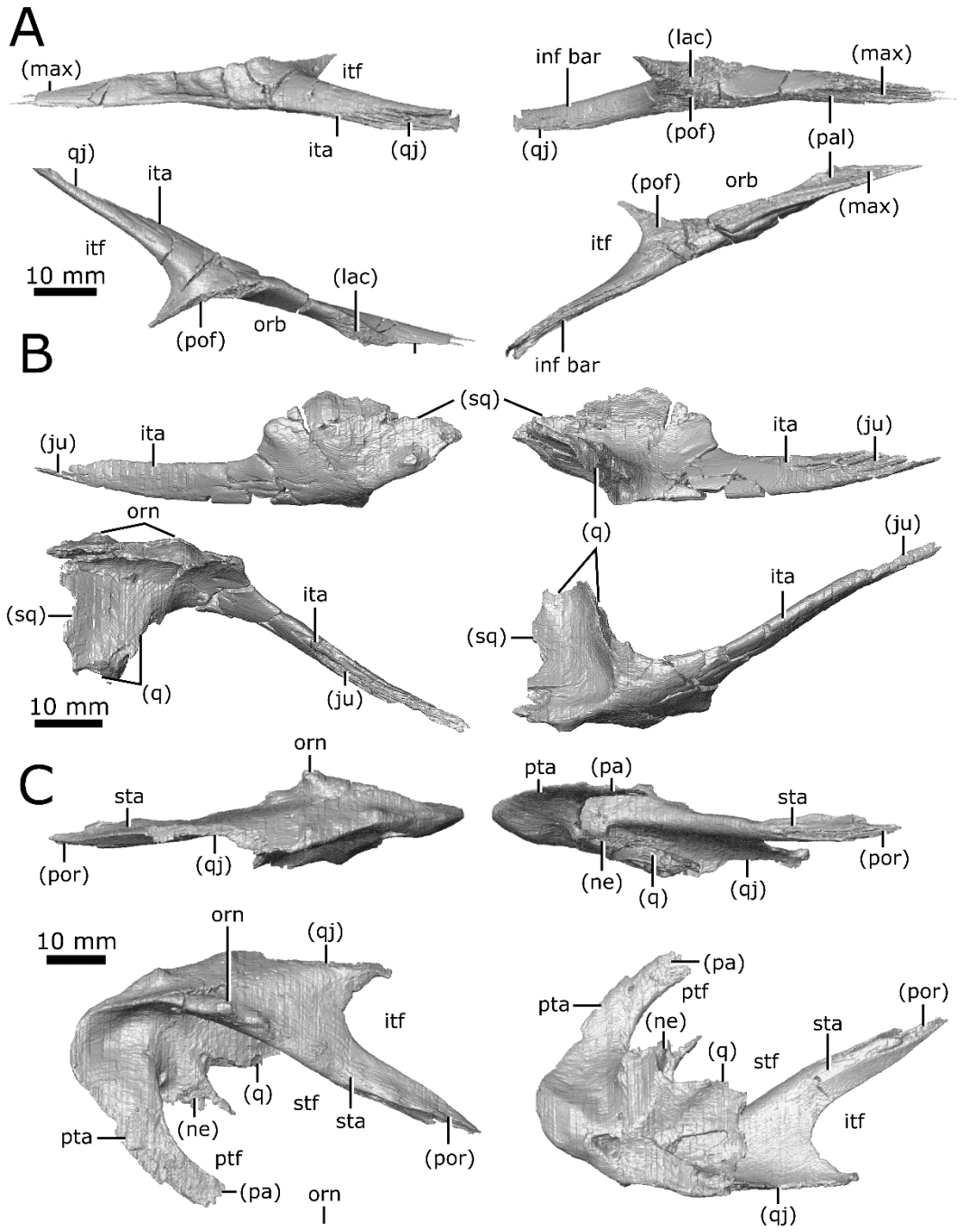

Figure 2.11: Isolated jugal, quadratojugal, and squamosal of *Champsosaurus lindoei* (CMN 8920). **A** left jugal in lateral view (top left), medial view (top right), dorsal view (bottom left), ventral view (bottom right); **B** left quadratojugal in lateral view (top left), medial view (top right), dorsal view (bottom left), ventral view (bottom right); **C** left squamosal in lateral view (top left), medial view (top right), dorsal view (bottom left), ventral view (bottom right).

squamosal dorsolaterally and posteriorly via a long, thin suture. The quadratojugal also contacts the quadrate medially, immediately lateral to the articular surface for the jaws.

Squamosal – Both squamosals are preserved in CMN 8920, but the right is fragmented such that morphological interpretation must be based entirely on the left element. The squamosal is large in relation to the other cranial elements (Figure 2.11C), with ornamentation on the posterolateral, lateral, and dorsal surfaces. When viewed laterally, the squamosal is long and dorsoventrally flat. This element forms the posterior margin of the supratemporal fenestrae and gives the skull its stereotypical cordiform profile. Anterolaterally, the squamosal shares a suture with the quadratojugal, beginning posterior to the inferior temporal arch and extending posterior to the ventral truncation of the superior temporal arch. The squamosal extends anteromedially along the superior temporal arch (Figure 2.11C; sta) where it contacts the postorbital in an elongated suture. Ventromedially it contacts the quadrate, and the posterolateral projection of the neomorph. The squamosal forms the dorsolateral rim of the post-temporal fenestra, and contacts the parietal along the post-temporal arch (Figure 2.11C; pta).

Vomer – Both vomers are present and have experienced significant fracturing throughout (Figure 2.12A). In ventral view, the vomer is triangular in profile. The vomer originates anteriorly as a slender projection within the internarial, but expands posteriorly, becoming exposed on the ventral surface. As it extends posteriorly, it widens laterally and contacts the maxilla and the anterior projection of the palatine laterally, before separating from them to form the medial wall of the choana. At its posterior extent, it contacts the pterygoid laterally, before terminating with a short, wedge-shaped projection that extends ventral to the pterygoid. A single row of vomerine teeth are present that run the length of the ventral

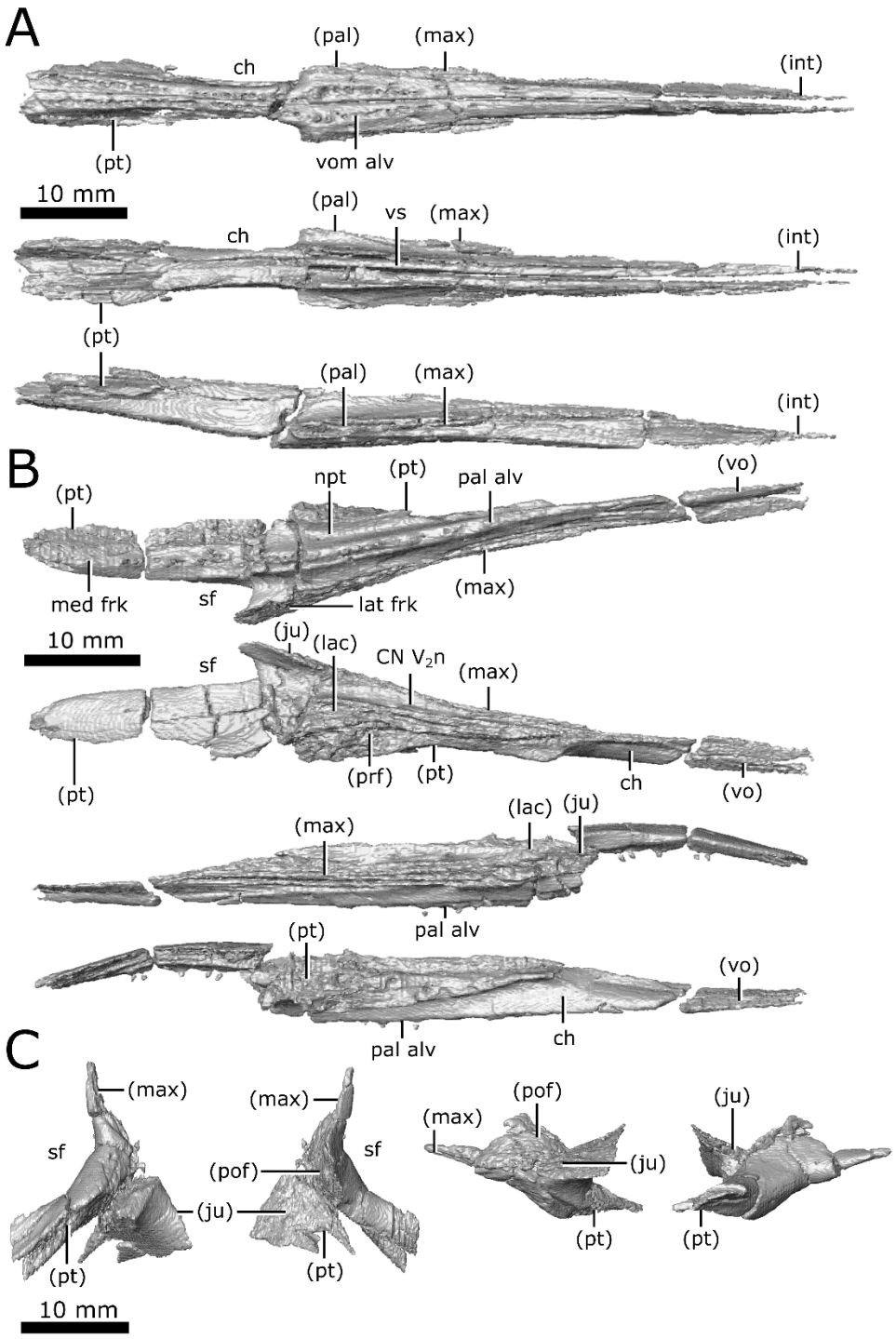

Figure 2.12: Isolated vomers, palatine, and ectopterygoid of *Champsosaurus lindoei* (CMN 8920). **A** vomers in ventral view (top), dorsal view (middle), right lateral view (bottom); **B** left palatine in ventral view (top), dorsal view (second from top), lateral view (second from bottom), medial view (bottom); **C** left ectopterygoid in ventral view (left), dorsal view (second from left), lateral view (second from right), medial view (right).

surface and enlarge posteriorly (Figure 2.12A; vom alv). The CT data show a distinct ridge (approximately 1 mm high) that extends dorsally from each vomer into the nasal passage, and likely represents the paired vomerine septum (Figure 2.12A; vs). These projections become enlarged posteriorly (approximately 1.8 mm high), curling medially, although some of this curling may be due to breakage post-mortem.

Palatine – Both palatines are well-preserved (Figure 2.12B), with fracturing only occurring on the posterior process that borders the suborbital fenestra. In ventral view, the palatine is triangular, elongate, and thin, comprising the lateral portion of the palate posteriorly and the anteromedial wall of the suborbital fenestra. A single row of palatine teeth (Figure 2.12B; pal alv) runs the entire length of this element along a ridge that continues posteriorly onto the pterygoid. The nasopalatal trough (Figure 2.12B; npt) extends the length of the palatine on the ventral surface and continues posteriorly onto the pterygoids. This trough is shallow in CMN 8920 compared with those of other *Champsosaurus* specimens (e.g., TMP 87.36.41, TMP 94.163.01, TMP 86.12.11, CMN 8919; Matsumoto and Evans, 2016), likely due to crushing of the palatal region.

The palatine originates anteriorly between the vomer medially and the maxilla laterally, before separating from the vomer to form the lateral rim of the choana. Posterior to the choana, the palatine contacts the pterygoid medially, and remains wedged between this element and the maxilla for the majority of its length. Extending posteriorly, it forks around the suborbital fenestra, where the shorter lateral fork contacts the maxilla laterally and a small portion of the jugal dorsally, and the longer medial fork contacts the pterygoid. Posterior to the choana, the palatine contacts the prefrontal and lacrimal dorsally, and these bones remain in contact with one another until the anterior rim of the orbit, where they

separate. The dorsal surface of the palatine forms the floor of the common canal for CN V_2 (laterally) and the nasolacrimal duct (medially; Figure 2.12B; CN V_2n).

Ectopterygoid – Both ectopterygoids are well-preserved with little to no fracturing or distortion (Figure 2.12C). When viewed ventrally, the ectopteygoids are short and pillar-like and articulate with the lateralmost extent of the pterygoid flange, as reported previously by Erickson (1972), and Gao and Fox (1998). This element forms the posterior wall of the suborbital fenestra and separates it from the temporal fossa. The suture between the ectopterygoid and the pterygoid is well ossified and indistinct on the external surface. The suture is only visible intermittently along its length in the CT scan, and the remainder of the suture had to be interpreted. The well-fused suture has been reported before by Erickson (1972) who described it as heavily ankylosed, and by Gao and Fox (1998) who were able to identify the suture on the right side of TMP 87.36.41, but not the left. The ectopterygoid contacts the pterygoid posteromedially, the jugal laterally, the postfrontal dorsolaterally, and the posterior tip of the maxilla anterolaterally. Erickson (1972) described a ridge on the ventral surface of the pterygoid flange that extends onto the ectopterygoid, but these CT data reveal that the ridge is only present on the pterygoid flange, adjacent to the suture between the pterygoid and the ectopterygoid.

Pterygoid – Both pterygoids are preserved and complete, but they have experienced heavy fragmentation in the anterior palatal region (Figure 2.13). In ventral view, the pterygoids form a large plate of bone that comprises the majority of the surface of the palate. It contacts the vomer anteromedially and the palatine anterolaterally, and forms the posteromedial wall of the suborbital foramen. It expands posteriorly to form the floor of the olfactory chamber where it appears to share a slender contact with the prefrontals laterally, although it cannot be

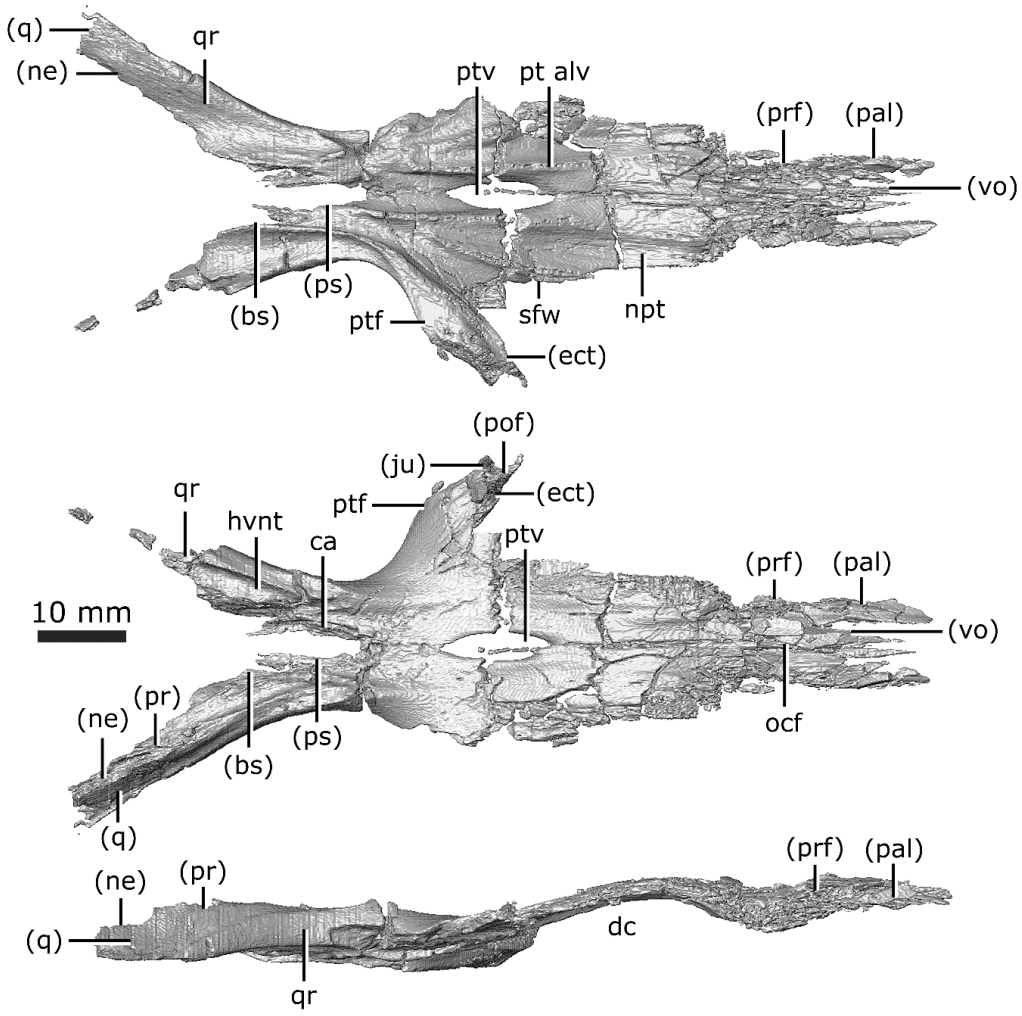

Figure 2.13: Isolated pterygoids of *Champsosaurus lindoei* (CMN 8920) in ventral view (top), dorsal view (middle), right lateral view (bottom).

determined if this contact is genuine or due to displacement of the element by crushing. The pterygoid usually forms a dorsal concavity in the palate of *Champsosaurus* (Erickson, 1985), but this feature is exacerbated in CMN 8920 by crushing (Figure 2.13; dc). The nasopalatal troughs run along the anterior half of the ventral surface of the pterygoid (Figure 2.13; npt), and are bordered on each side by rows of palatal teeth (Figure 2.13; pt alv). These troughs are indistinct across their anterior halves, possibly due to crushing of the palatal region.

A distinct flange extends laterally from the pterygoid along the anterior wall of the temporal fossa and posterior surface of the ectopterygoid (Figure 2.13; ptf). Previously (Erickson, 1972), this flange, along with the ectopterygoid, have been identified together as the pterygoid flange due to the high degree of ossification between these elements, but it can be seen here that the true pterygoid flange is actually much more gracile than previously described. The flange has a small contact with the jugal and postfrontal at its distal dorsal margin. Medial to the pterygoid flange, the pterygoids briefly separate from one another to form the interpterygoid vacuity (Figure 2.13; ptv), which has small struts of bone extending across it. Russell (1956) interpreted the interpterygoid vacuity as resulting from incomplete ossification, but the presence of this feature in other, larger specimens suggests that this vacuity does not ossify in *Champsosaurus*. Russell (1956) suggested the struts of bone across the interpterygoid vacuity in CMN 8920 were evidence of incomplete ossification, but the CT data reveal they are due to breakage of the pterygoid.

The pterygoid narrows as it extends posteriorly, forming the medial portion of the temporal fossa. At their narrowest points, the pterygoids are separated from one another by the anterior projection of the parasphenoid. Each pterygoid forks laterally around the parasphenoid, with the carotid artery canal projecting dorsally between them. These lateral

forks are the quadrate rami (posterior branches of Russell, 1956; lateral branches of Erickson, 1972; Figure 2.13; qr). The quadrate rami extend posteriorly on either side of the basisphenoid, forming a trough on each side of the braincase that housed the lateral head vein. The quadrate ramus forms the ventral and lateral walls of the lateral head vein trough (Figure 2.13; hvnt), and the basisphenoid forms the medial wall. The ramus extends posteriorly to briefly contact the prootic dorsally and the anteriormost portion of the quadrate. The ramus becomes wedged between the quadrate dorsolaterally and the neomorph dorsomedially, only being exposed on the ventral surface. The quadrate ramus envelopes the anterior projection of the neomorph, obscuring the projection from external view. The quadrate ramus terminates posteriorly at the mid-length of the fenestra ovalis.

Dentition – A single row of marginal teeth runs along the premaxilla and maxilla, posteriorly terminating ventral to the mid-length of the orbit (Figure 2.1C). There are six alveoli on the premaxilla, and 41 on the maxilla, resulting in a total of 94 alveoli, of which 62 have teeth at least partially preserved. No replacement teeth were identified in this individual. The marginal teeth are sub-thecodont and conical (Figure 2.14). Previous descriptions of *Champsosaurus* (Matsumoto and Evans, 2016) described the marginal teeth as having plicidentine, with visible longitudinal striations in the enamel. These striations are not apparent on the maxillary teeth of CMN 8920, but the CT data show internal plicidentine infolding. This infolding is only present near the base of the tooth and vanishes apically. No premaxillary teeth are completely preserved in CMN 8920, but plicidentine infolding is seen internally near the base of the fragmentary premaxillary teeth. Overall, the marginal teeth show a trend of decreasing size posteriorly (6 mm at 21st alveoli, 2 mm at 47th alveoli), a

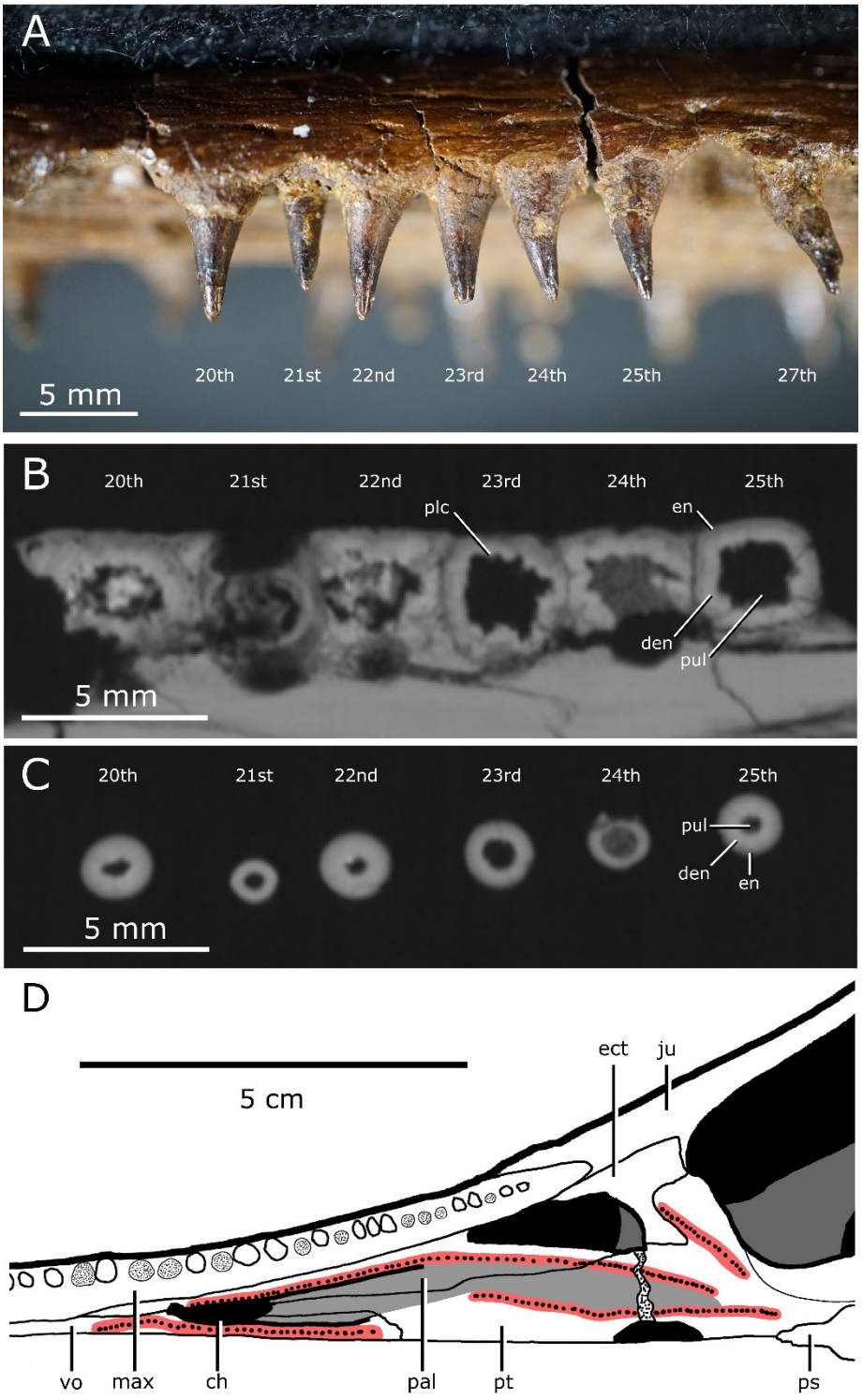

Figure 2.14: Tooth morphology of *Champsosaurus lindoei* (CMN 8920). **A** Labial view of left maxillary tooth row; **B** Basal transverse cross section of the maxillary teeth; **C** Apical transverse cross section of the maxillary teeth; **D** Left palatal dentition. Red coloured areas mark the palatal teeth, light-grey coloured area marks the nasopalatal trough.

trend that is consistent with previous descriptions of *Champsosaurus* and other neochoristoderes (Matsumoto and Evans, 2016).

Distinct rows of fine palatal teeth are seen on the pterygoids, palatines, and vomers, giving these elements a sandpaper-like texture ventrally (Figure 2.14D; red areas). Rows of palatal teeth on the palatine, vomer, and pterygoid border the nasopalatal trough as it extends posteriorly from the choana. All palatal teeth were either broken or had fallen out, but have been described as conical and unstriated in other specimens of *C. lindoei* (Matsumoto and Evans, 2016). Like the marginal teeth, the palatal teeth are also sub-thecodont, but differ in that they lack plicidentine infolding.

Splanchnocranium

Quadrate – Both quadrates (Figure 2.15) are preserved, but the right has lost the cortical surface on the joint with the articular element of the jaw (Figure 2.15; art). When viewed ventrally, the quadrate is large and dorsoventrally flat, forming a broad table ventral to the temporal arches. The quadrate contacts the quadratojugal and squamosal laterally, and the pterygoid, prootic, opisthotic, and neomorph medially. Fox (1968) states that the quadrate is firmly bound to both the prootic and opisthotic, but the CT data show that the quadrate is separated from the prootic for the majority of its length by the neomorph. Additionally, the quadrate is separated from the opisthotic by the neomorph, only briefly contacting one another between a small ventral projection (approximately 5 mm long) on the quadrate and the paroccipital process of the opisthotic. The quadrate has a small suture with the pterygoid at its anteromedialmost corner. This suture has been damaged on the left quadrate, but is

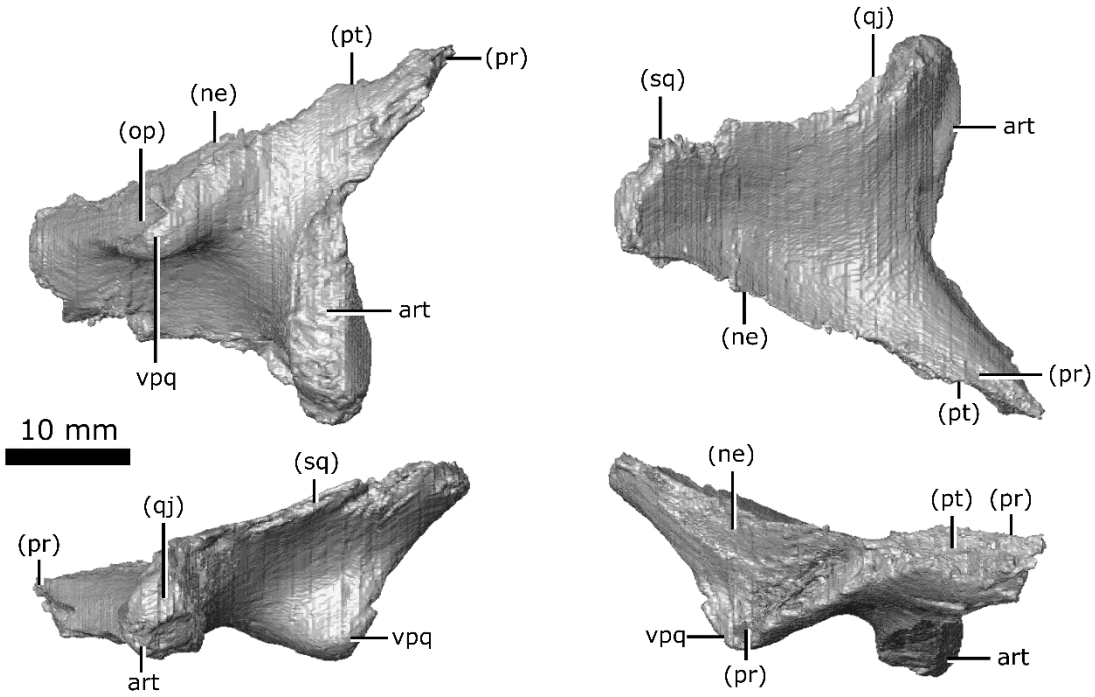

Figure 2.15: Isolated left quadrate of *Champsosaurus lindoei* (CMN 8920) in ventral view (top left), dorsal view (top right), lateral view (bottom left), medial view (bottom right).

well-preserved on the right. The right quadrate forms a small portion of the lateral rim of the pterygoquadrate foramen dorsally, but the left quadrate does not contact this opening.

Epipterygoid and Stapes – These elements were not preserved in CMN 8920. Previous descriptions of the epipterygoid in other specimens are reviewed in the Discussion. No known stapes has been preserved in any choristodere and cannot be commented on at present (but see Discussion for comment on possible choristodere stapes).

Chondrocranium

Internarial – Brown (1905) initially reported this element as the ethmoid and stated that "the homology of this bone is somewhat questionable". Russell (1956) and Erickson (1972) reported it as the internarial and described it as a neomorphic ossification that likely derived from the cartilaginous internarial septum. The internarial septum is a component of the anterior chondrocranium (Bellairs and Kamal, 1981) and the internarial is therefore tentatively included here as a chondrocranial ossification. When viewed ventrally, the internarial is an elongate, midline element that extends along the anterior portion of the mouth roof, separating the paired maxillae and premaxillae (Figure 2.1B, Figure 2.16A). It is slightly shorter than the overlying nasal. It originates anteriorly between the paired incisive foramina of the premaxilla and extends posteriorly to terminate between the anterior tips of the vomers. The internarial is not visible anterior to the premaxilla/maxilla suture because the premaxilla wraps ventrally around the internarial, obscuring it from ventral view. The internarial has a gentle U-shape on the anterior two-thirds of its dorsal surface, forming the floor of the nasal passage (Figure 2.16A; U). The posterior third has an elongated ridge

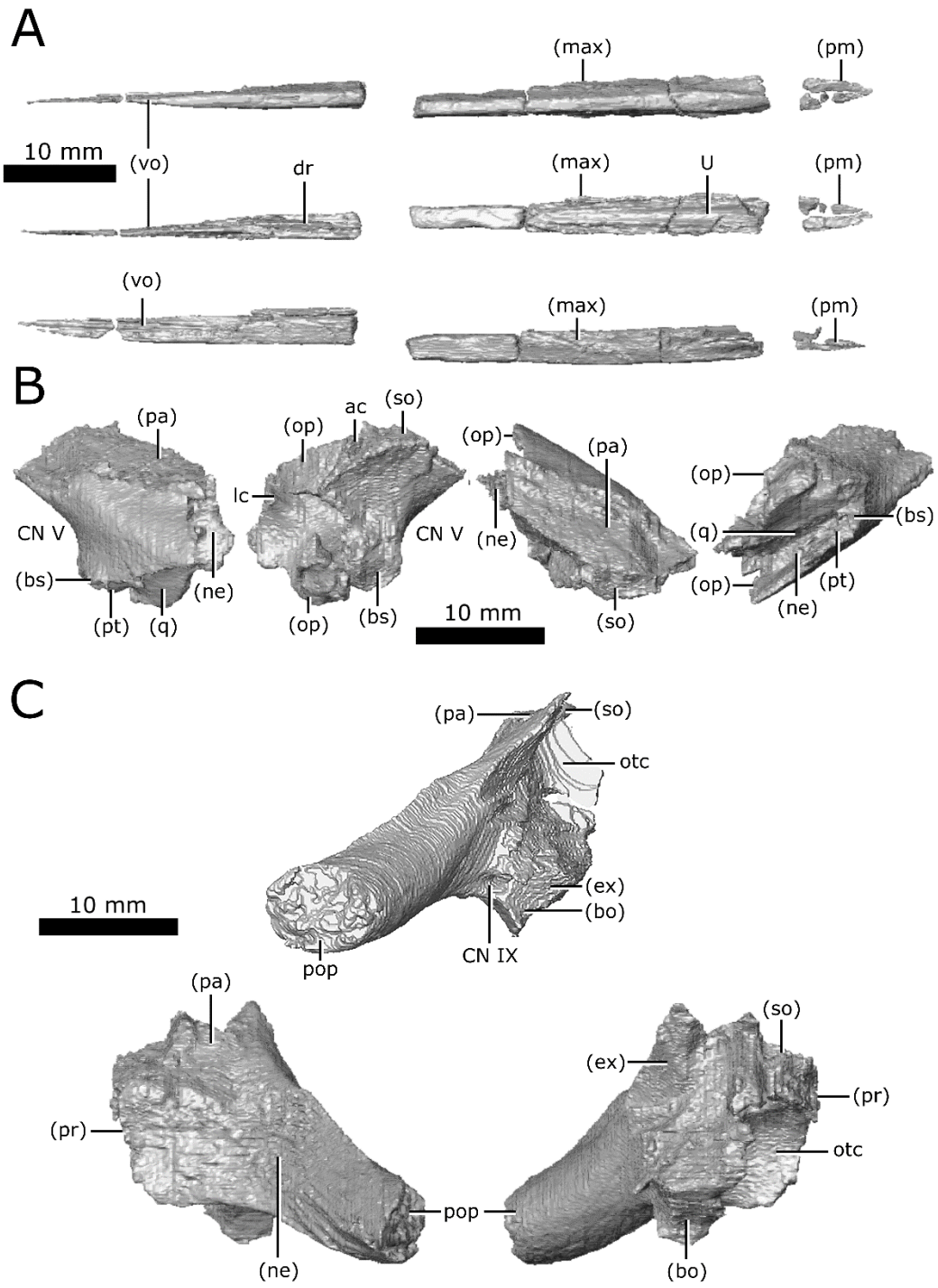

Figure 2.16: Isolated internarial, prootic, and opisthotic of *Champsosaurus lindoei* (CMN 8920). **A** internarial in ventral view (top), dorsal view (middle), right lateral view (bottom); **B** left prootic in lateral view (left), medial view (second from left), dorsal view (second from right), lateral view (right); **C** left opisthotic in posterior view (top), lateral view (bottom left), medial view (bottom right).

(approximately 0.8 mm high; Figure 2.16A; dr) extending dorsally into the nasal passage, which is mirrored by a ridge on the ventral surface of the nasal bone above. Together, these elements may have supported the cartilaginous wall that bifurcated the nasal passage, as in extant reptiles (Romer, 1956).

Prootic – Both prootics are preserved and are slightly fractured (Figure 2.16B). Internally, trabecular bone continues to the otic capsule with no surface of cortical bone. The prootic is relatively small (approximately 1.7 cm long) and roughly rhomboid when viewed laterally, forming the anterolateral wall of the fenestra ovalis and otic capsule. It houses the anterior half of the lateral semicircular canal and the anterior portion of the anterior semicircular canal. The prootic forms the posterodorsal rim of the opening for CN V, contacts the parietal posterodorsally, and extends ventrally to contact the basisphenoid, neomorph, pterygoid, and quadrate. As it extends posteriorly, it is obscured from external view by the neomorph before terminating at an abrupt, vertically oriented suture with the opisthotic. The facial nerve (CN VII) is interpreted to pass between the basisphenoid and the prootic on the left side, but this nerve exits directly through the prootic on the right, barely contacting the basisphenoid as it exits the skull.

Opisthotic – Both opisthotics are preserved in CMN 8920 (Figure 2.16C), which form the posterior portion of the otic capsule, and extend posteriorly to form the paroccipital process (Russell, 1956), giving the opisthotic a cylindrical shape when viewed posteriorly (Figure 2.16C; pop). This element originates anteriorly at a vertical suture with the prootic, and borders the neomorph laterally and parietal dorsally. Posteriorly, it expands medially to contact the supraoccipital. The opisthotic forms the posterior wall of the otic capsule, and houses the posterior portions of both the lateral and posterior semicircular canals. A canal

extends through the opisthotic from the posterior wall of the otic capsule to the external posteroventral surface of the opisthotic that is interpreted here as the pathway for the glossopharyngeal nerve (Figure 2.16C; CN IX). Among diapsids, the pathway for CN IX is highly variable, but is often in close association with the otic capsule due to its location within the metotic fissure in development (Bellairs and Kamal, 1981; Rieppel, 1985), and is known to exit through the posterior margin of the otic capsule in other reptiles (Romer, 1956). As the opisthotic continues posteriorly, it becomes separated from the brain cavity by the exoccipital medially, and is bordered by the basioccipital ventrally, the neomorph laterally, and the parietal dorsally. The suture with the exoccipital is obscured internally due to fracturing and partial fusion between these two elements in this area, but all external sutures are clearly visible. The left opisthotic contacts a small portion of the quadrate laterally, but the right does not due to asymmetrical breakage of the paroccipital processes.

Supraoccipital – The supraoccipital is well-preserved with little to no fragmentation or distortion and forms the posterior roof of the brain cavity (Figure 2.17A). This element roofs the posterior region of the brain cavity, giving it a concave-down profile when viewed posteriorly. The supraoccipital is roofed by the parietals along an interdigitated suture for the majority of its length. The supraocciptial becomes exposed dorsally as the parietals fork laterally to commune with the squamosals. The posterior edge of the supraoccipital forms the dorsal rim of the foramen magnum and is concave when viewed dorsally (Figure 2.17A; fm). The supraoccipital contacts the paired prootic, opisthotic, and exoccipital laterally. The supraoccipital houses the posterior portion of the anterior semicircular canal (Figure 2.17A; ac), the crus communis (Figure 2.17A; cc), and the anterior portion of the posterior semicircular canal (Figure 2.17A; pc). The supraoccipital, opisthotic, and prootic fail to

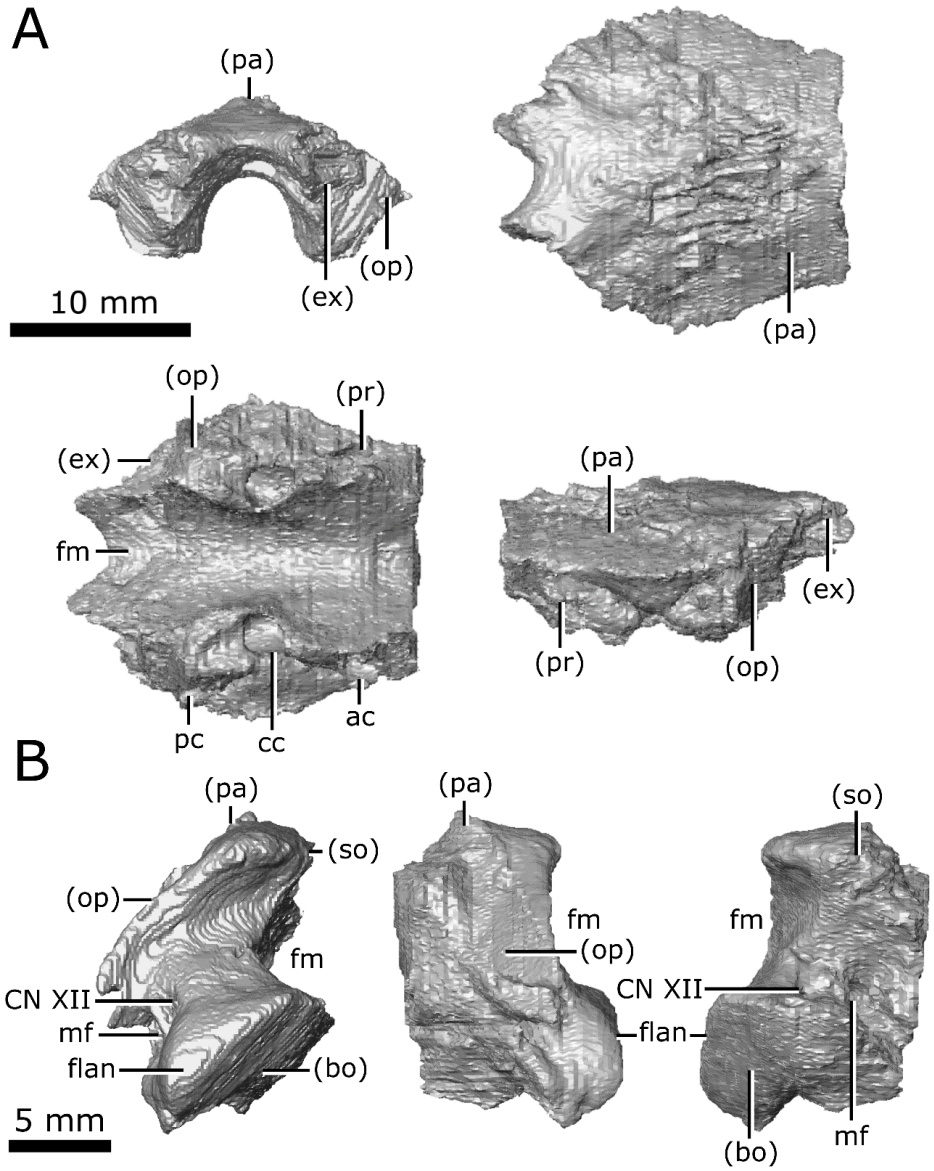

Figure 2.17: Isolated supraoccipital and exoccipital of *Champsosaurus lindoei* (CMN 8920). **A** supraoccipital in posterior view (top left), dorsal view (top right), ventral view (bottom left), left lateral view (bottom right); **B** left exoccipital in posterior view (left), lateral view (middle), medial view (right).

contact one another dorsal to the endossoues labyrinth, forming a cavity that projects dorsally from the pars inferior of the inner ear to reach the ventral surface of the parietal. The presence of this cavity is the basal condition in Diapsida and is a product of the lack of ossification in the otic region (Evans 2008).

Exoccipital – Both exoccipitals are preserved in CMN 8920 and are only slightly fractured (Figure 2.17B). The exoccipital is a column-like element when viewed posteriorly that forms the lateral wall of the posterior portion of the brain cavity and the lateral margin of the foramen magnum. It originates anteriorly about level with the crus communis, separating the supraoccipital from the opisthotic, contacting the parietal dorsally, and the brain cavity ventrally. The suture with the opisthotic is internally obscured due to fracturing and partial fusion between these two elements, but the external suture is clearly visible. The exoccipital expands posteroventrally to contact the basioccipital. In posterior view, a flange occurs on the ventral portion of the posterior surface (Figure 2.17B; flan), likely to articulate with the first cervical vertebra, as reported by Brown (1905). The metotic foramen passes through the exoccipital for the majority of its length, exiting the skull posteriorly between the exoccipital and opisthotic (Figure 2.17B; mf). This foramen likely carried the vagus nerve (CN X) and accessory (CN XI) nerves, which usually exit the skull together through the metotic foramen between the opisthotic and exoccipital (Romer, 1956; Bellairs and Kamal, 1981; Rieppell 1985). The passage of the metotic foramen through the exoccipital internally seems unusual, but is likely due to the partial fusion of the exoccipital and opisthotic. Posterior to the metotic foramen, two paired canals pass through the exoccipital that likely housed branches of the hypoglossal nerve (Figure 2.17B; CN XII), which often exit the skull through the exoccipital (Romer 1956; Bellairs and Kamal, 1981). The ventralmost canal is narrow (less than 1 mm

across) and was not identified by Fox (1968), who described CN XII as exiting as a single root through the exoccipital.

Parasphenoid – Although the parasphenoid is technically a dermatocranial ossification, it is defined here as part of the chondrocranium due to its frequent fusion with the chondrocranial basisphenoid across Amniota (see Discussion for details). Russell (1956) identified this element as having completely fused with the basisphenoid in *C. natator*, but the CT data show that it is a distinct ossification in *C. lindoei*, and the two elements only show fusion in a small section at the center of their shared suture. The parasphenoid has undergone slight fragmentation along its length, but otherwise remains undistorted (Figure 2.18). This element is triangular when viewed ventrally, but is fractured in CMN 8920, where the posterior tips and a portion in the middle has not preserved. The ventral surface of the parasphenoid possesses a depression that represents the median pharyngeal recess (Figure 2.18; mpr). The parasphenoid originates anteriorly, medial to the quadrate rami of the pterygoids, just anterior to the anteriormost point of the basisphenoid. The canals for the carotid arteries can be seen on the ventral surface of the parasphenoid where the basisphenoid originates. Anteriorly, the parasphenoid is covered dorsally by the basisphenoid. As the parasphenoid extends posteriorly, it forms the ventral surface of the axially symmetrical basal tubera (Figure 2.18; bt), and a prominent dorsal keel forms medial to the otic capsules (Figure 2.18; k). The dorsal keel remains prominent until the parasphenoid meets the basioccipital dorsally, where the keel terminates and the bone becomes flat and thin. Fox (1968) described the keel as a low ridge that extends from the parasphenoid posterior onto the dorsal surface of the basioccipital, but the CT data clearly show the keel is prominent and only occurs on the parasphenoid. The basal tubera of the parasphenoid extend posterolaterally, but are

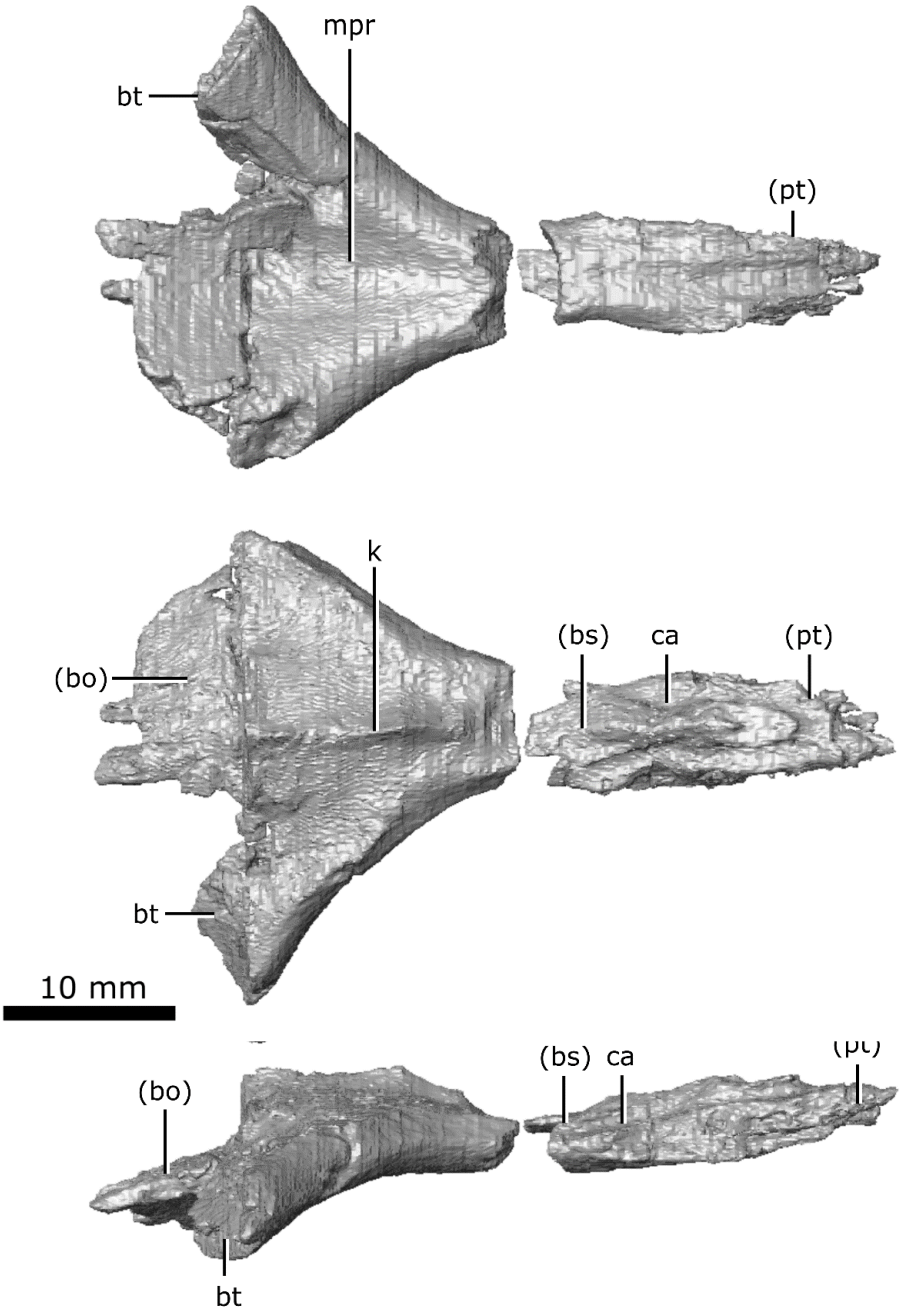

Figure 2.18: Isolated parasphenoid of *Champsosaurus lindoei* (CMN 8920) in ventral view (top), dorsal view (middle), right lateral view (bottom).

terminated by breakage. Intact specimens of *C. gigas* (Erickson, 1972) suggest that the parasphenoid would not have continued much farther than that seen in CMN 8920 and would naturally truncate in a smooth rounded projection. The parasphenoid partially forms the posterior floor of the endocranial cavity, as well as the medial rim of the fenestra ovalis.

Basisphenoid – The basisphenoid is well-preserved in CMN 8920 with little fracturing (Figure 2.19A). When viewed laterally, the basisphenoid is roughly triangular in outline due to the dorsally expanded clinoid processes. These clinoid processes (Figure 2.19A; cp) form a distinct concave-up trough when viewed anteriorly to house the midbrain. The base of this trough forms the posterior margin of the pituitary fossa and the ventral rim of the CN V opening. A long and slender canal that held CN VI extends anteriorly from the ventral surface of the cavity to the lateral wall of the clinoid process. The basisphenoid contacts the parasphenoid ventrally for its entire length, and the quadrate rami of the pterygoids ventrolaterally. Together, the basisphenoid and the pterygoid form a trough lateral to the brain cavity that housed the lateral head vein. The basisphenoid contacts the prootic laterally and becomes dorsoventrally compressed and flattened. The canals for the internal carotid arteries enter the skull between the pterygoid laterally and parasphenoid medially, and are roofed by the basisphenoid.

Basioccipital – The basioccipital is well-preserved in CMN 8920, with the exception of the basal tubera, which have fractured away at the base (Figure 2.19B; bt). The basioccipital is located dorsal to the parasphenoid and forms the posteriormost floor of the endocranial cavity. The occipital condyle is symmetrical, and has a shallow groove situated medially on the dorsal surface giving it a reniform shape in posterior view (Figure 2.19B; oc). As the brain cavity reduces in volume and diameter towards the foramen magnum, the exoccipital

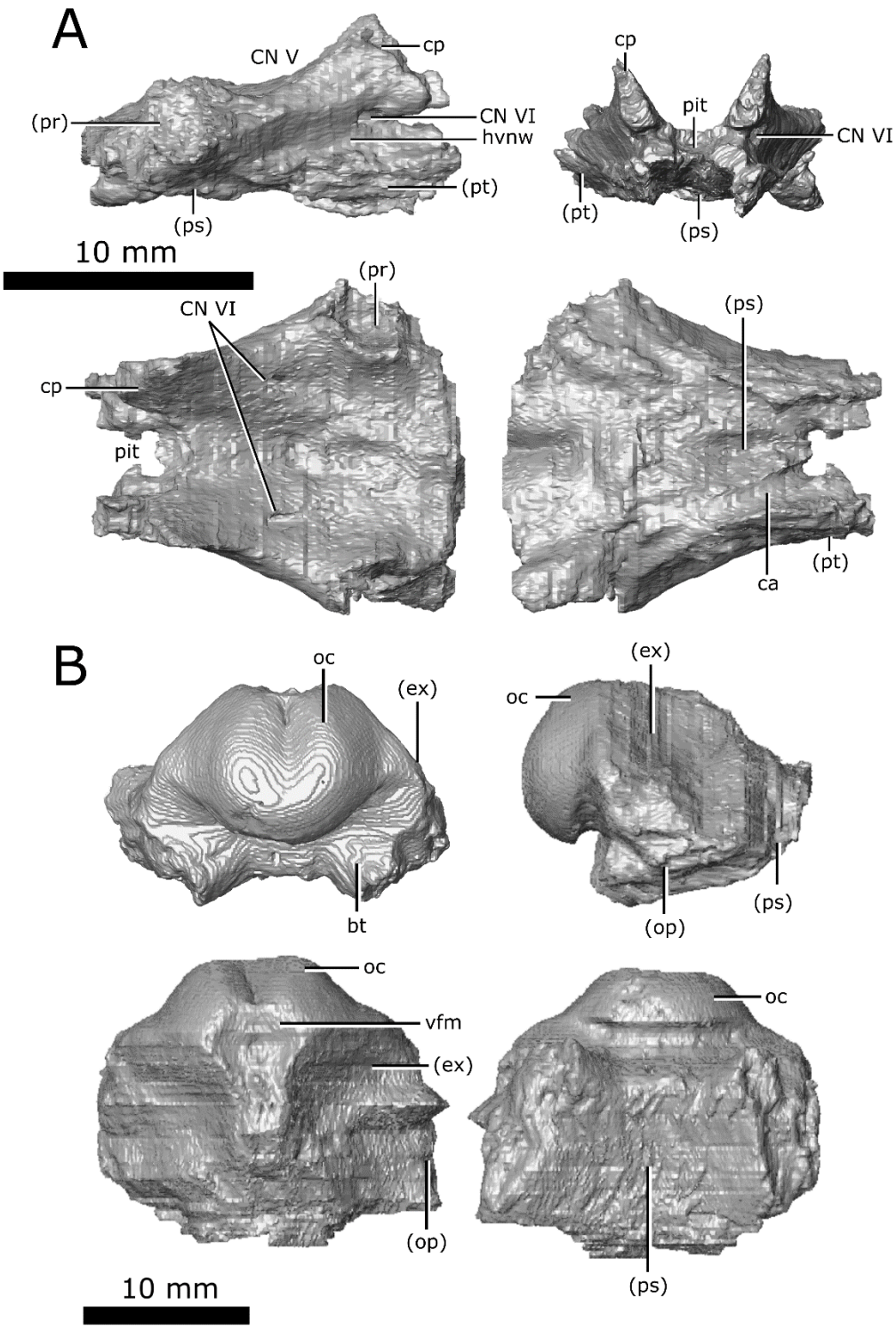

Figure 2.19: Isolated basisphenoid and basioccipital of *Champsosaurus lindoei* (CMN 8920). **A** basisphenoid in right lateral view (top left), anterior view (top right), dorsal view (bottom left), ventral view (bottom right); **B** basioccipital in posterior view (top left), right lateral view (top right), dorsal view (bottom left), ventral view (bottom right).

and the opisthotic contact the basisphenoid laterally, and the parasphenoid terminates, allowing the basisphenoid to be exposed on the ventral surface. Posteriorly, the opisthotics diverge laterally, leaving only a portion of the exoccipital in contact with the basioccipital. The exoccipital and basisphenoid diminish and terminate at the foramen magnum, where the basioccipital forms the occipital condyle.

Discussion

This study provides the first exhaustive description of the skull of a choristodere using micro-CT data, and has allowed the cranial bones of *Champsosaurus* to be imaged and described in three dimensions for the first time. The data presented here confirm that the neomorphic ossification is distinct, and is not an extension of one of the neighboring bones. Despite this confirmation, I choose not to give the neomorph a unique name because renaming an element that has been consistently referred to as the 'choristoderan neomorph' for over 50 years would likely cause unnecessary confusion in the literature. The neomorphic ossification has previously been reported in all neochoristoderes (Fox, 1968; Erickson, 1987; Brinkman and Dong, 1993; Ksepka et al., 2005), but the sutures surrounding the bone were often obscured by breakage or matrix. Although the neomorph was interpreted as elongate in these taxa, the presence and morphology of this element was ambiguous. Confirmation of the neomorph as elongate in *Champsosaurus* supports previous interpretations of an elongate neomorph in all other neochoristoderes.

A recent publication describing a non-neochoristodere from the Upper Jurassic (Oxfordian) of China, *Coeruleodraco jurassicus* (IVPP V 23318; Matsumoto et al., 2019), suggests that the neomorphic bone is present in this taxon; however, the validity of the

neomorphic bone was not discussed, nor the wider implications of its presence in *Coeruleodraco*. The data presented here support the observations of Matsumoto et al. (2019), suggesting that the neomorph is present in all choristoderes more derived than *Coeruleodraco* (i.e., all choristoderes other than *Cteniogenys*; Matsumoto et al., 2019). Evans (1990) inferred the presence of the neomorph in *Cteniogenys* based on facets in the neighboring bones, a conclusion that is now supported by the presence of this element in other choristoderes. It therefore seems probable that the neomorphic ossification is a synapomorphy of Choristodera, but a thorough description of the element in other non-neochoristoderes is needed to confirm this.

The groove on the lateral surface of the parietal and neomorph is not well understood, but it has been suggested to correlate with the stapedial branch of the carotid artery (Fox, 1968). Given that this groove extends from the opening for CN V to the pterygoquadrate foramen, it seems possible that this groove carried the mandibular branch of the trigeminal nerve (CN V_3), which would have extended ventrally through the pterygoquadrate foramen and entered the jaw.

Lu et al. (1999a) described an enlarged pineal system in *Ikechosaurus* that extends dorsally and is roofed by the parietals. The concavity on the ventral surface of the parietals of CMN 8920 suggest that *C. lindoei* also possessed an enlarged pineal system, a feature that may therefore be common to Neochoristodera. Lu et al. (1999a) also reported a short and simple series of tubes extending dorsally from the pineal body into the parietal that they interpreted as a remnant of the pineal eye, but no such structures were seen in CMN 8920. This suggests that the pineal eye has been completely lost in *C. lindoei*, and there is no internal evidence to indicate its presence within the cranium.

Lu et al. (1999a) also reported a small paired gap between the vomer and palatine of *Ikechosaurus* that may have housed the vomeronasal organ; however, no such structure is seen in CMN 8920, nor has it been reported in other choristoderes. This leads to the conclusion that *C. lindoei*, and choristoderes more broadly, reduced or lost the vomeronasal organ.

The nasopalatal trough (narial trench of Brown, 1905; narial groove of Russell, 1956; palatonasal trough of Erickson, 1985), unique to choristoderes, is shallow but distinct in CMN 8920. The function of this trough is not well understood, but it may have supported a soft tissue extension of the nasal passage posterior to the choana, creating a secondary palate (Erickson, 1985). The nasopalatal trough was once considered to be a synapomorphy of Neochoristodera (Gao and Fox, 1998) but may also be present in some non-neochoristoderes (e.g., *Monjurosuchus*; Gao et al., 2007).

Although some splanchnocranial elements are not preserved in CMN 8920 (e.g., epipterygoid), this element has been reported in other specimens. The epipterygoid was reported in *Champsosaurus* by Fox (1968) as a paired, slender element that projects anterodorsally over the pterygoid from the basisphenoid trough. This element is only reported in a few specimens of *Champsosaurus* (Gao and Fox, 1998), likely due to its gracile shape and fragility.

As is typical for stem-diapsids (Romer, 1956), the ossified chondrocranium does not fully enclose the brain cavity in *C. lindoei*, where the anterior portions of the chondrocranium would remain cartilaginous in life and would also be supplemented anterodorsally by several dermatocranial elements (e.g., parietals and frontals). The parasphenoid and basisphenoid often fuse completely in amniotes to form the parabasisphenoid; however, complete fusion of

these elements does not occur in *C. lindoei*. These elements only undergo fusion over a small portion of their shared surface internally, a feature that is evident from the CT data as the suture vanishes internally and the two bones become confluent. A similar condition is seen between the exoccipital and the opisthotic. These elements often fuse completely in diapsids to form the otoccipital, but this is not seen in *C. lindoei*. An external suture between the exoccipital and opisthotic is clearly visible in CMN 8920, other specimens of *C. lindoei*, and other species of *Champsosaurus* (Fox, 1968; Gao and Fox, 1998). Internally, these bones remain separate for the majority of their shared surfaces, only becoming fused for a small portion near the endocranial cavity.

The CT data from CMN 8920 indicate that the paired, ventrally oriented gaps lateral to the parasphenoid enclosed the fenestrae ovales (Figure 2.20), supporting Fox's (1968) interpretation. Supporting this conclusion is the fact that there is no other opening to the inner ear through which the stapes could have articulated. Fox (1968) states that these openings commune to the otic capsule laterally, but the CT data show that these openings actually commune to it ventrally. Based on images and illustrations in the literature, these gaps also occur in *Simoedosaurus dakotensis* (SMM P76.10.1; Erickson, 1987) and *Ikechosaurus sunailinae* (IVPP V9611-3; Brinkman and Dong, 1993), suggesting that a ventrally oriented fenestra ovalis is synapomorphic to Neochoristodera. This arrangement cannot be determined at present in non-neochoristoderes because few specimens are preserved with the ventral surface exposed, and those that are tend to be heavily fractured, obscuring the braincase. A ventrally oriented fenestra ovalis is unusual among tetrapods, but it has been reported in other aquatic taxa, such as some plesiosaurs (e.g., *Dolichorhynchops*; Sato et al., 2011), some aistopods (e.g., Phlegethontiidae; Clack and Anderson 2016; Pardo et al., 2019), and some

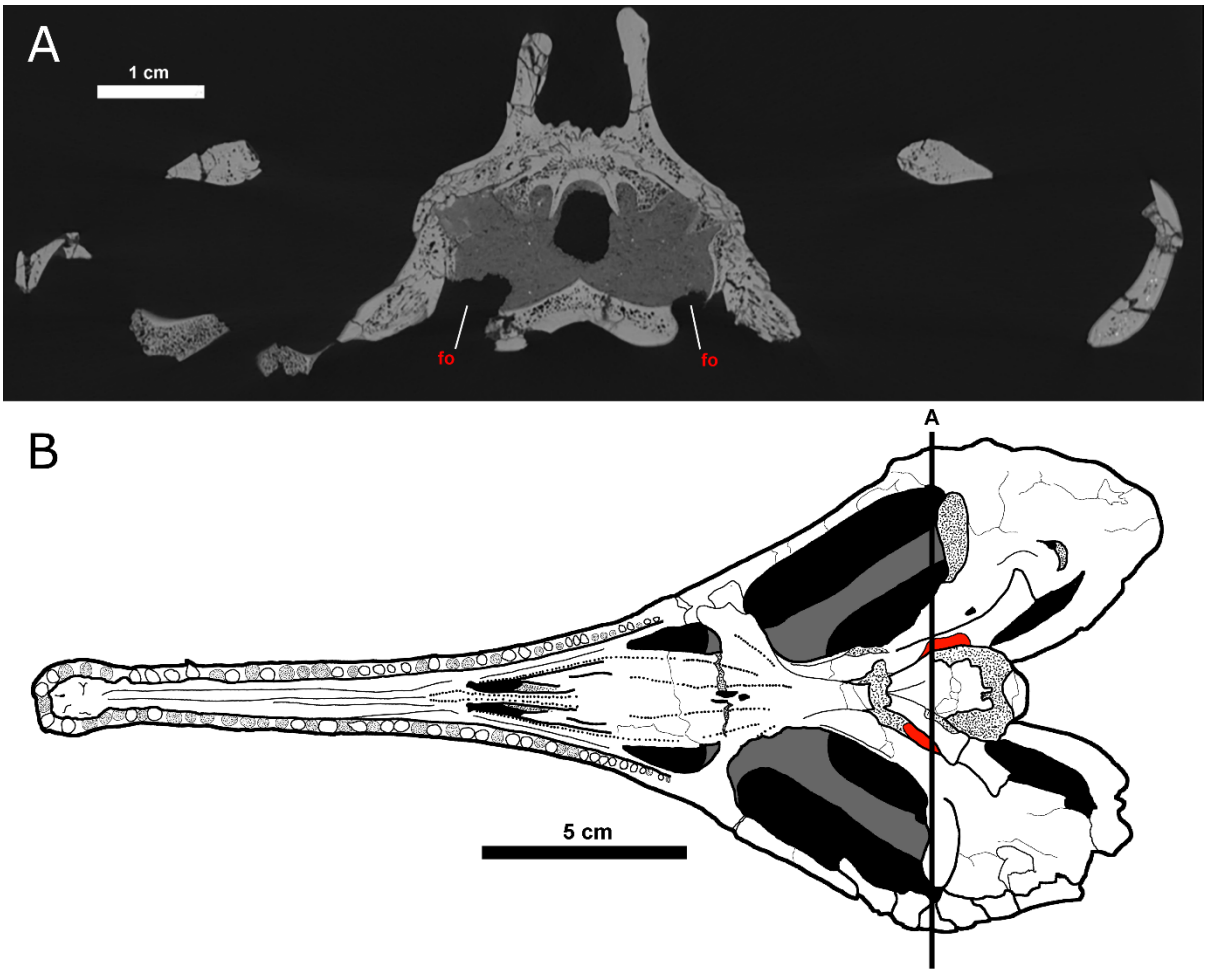

Figure 2.20: The fenestrae ovales of *Champsosaurus lindoei*. **A** coronal cross section of the braincase of CMN 8920; **B** ventral view of CMN 8920 with the fenestrae ovales coloured red. Black line labelled 'A' indicates the position of cross section A. Fine stippling indicates fractured surfaces exposing cancellous bone.

urodeles (e.g., *Siren*; Hilton, 1949; Hetherington and Lombard, 1983; Mason, 2007; Capshaw and Soares, 2016). The functional implications of this morphology in *Champsosaurus* will be discussed in Chapter 3.

Conservation of the braincase among amniotes and its implications for the choristoderan neomorphic ossification

The choristoderan neomorphic bone has previously been described as a component of the braincase (Fox, 1968; Brinkman and Dong, 1993; Gao and Fox, 2005; James, 2010), likely due to its external location on the lateral wall of the braincase, but the internal connections of the element remained poorly understood. Now that the existence of the neomorph has been confirmed, and its morphology described, it should be determined whether this element should be properly defined as a braincase bone. As stated in the Introduction, the braincase is defined here as all bones of the chondrocranium, plus the parasphenoid, which often fuses with chondrocranial elements (Atkins and Franz-Odendaal, 2016). Since it has been shown here that the neomorphic bone is not fused with any chondrocranial element, in order to classify the neomorph as a braincase bone, it must be determined whether it is chondrocranial in origin. Although the developmental path of a structure in an extinct taxon cannot be absolutely determined (Romer, 1956), possible developmental paths can be hypothesized based on the variation seen in the development of cranial bones in living amniotes. If it is found that the complement of bones in the chondrocranium tends to be conserved, it can be concluded that an element peripheral to this conserved complement is unlikely to be chondrocranial, and the neomorphic bone will therefore not be classified here as a braincase bone.

Based on the condition seen in early reptiles, the ancestral braincase of Amniota is inferred to consist of the supraoccipital, exoccipital, basioccipital, basisphenoid, opisthotic, prootic, and parasphenoid (Romer and Parsons, 1977). With the exception of the parasphenoid, these elements form as ossifications of the chondrocranium around the posterior portion of the braincase, where the anterior portion remains enclosed by cartilage into maturity (Romer, 1956). More derived amniotes, such as diapsids (Romer and Parsons, 1977), enclose the anterior portion of the braincase with dermal bones (e.g., frontals and parietals; Romer and Parsons, 1977), but the development of new ossifications of the chondrocranium is considered exceedingly rare (Cardini and Elton, 2008; Goswami and Polly, 2010; Knoll et al., 2012; Maddin et al., 2012). To illustrate this, ossifications from the braincase in several lineages of amniotes have been tabulated for a broad comparison (Table 2.2).

Based on the data derived from Table 2.2, there are apparently three novel bones that originate from the chondrocranium; the laterosphenoid, orbitosphenoid, and internarial. In archosaurs, the laterosphenoid forms as an ossification of the anterior chondrocranium (more specifically, from the cartilaginous pila antotica) between the exits for CN III, CN IV, and CN V, and ventrally supports the anterior portion of the brain (Evans, 2008; Sobral et al., 2016). The laterosphenoid is also known to occur in fossilized stem turtles and may suggest that turtles are a sister-group to archosaurs (Bhuller and Bever, 2009). The laterosphenoid has subsequently been obliterated in modern turtles by down-growths of the parietal and they cannot be seen in modern forms (Bhuller and Bever, 2009). The homology of the laterosphenoid between archosaurs and lepidosaurs is not well understood as it appears that

Table 2.2: A comparison of braincase bones across Amniota. 'X' indicates the bone is present. Superscripts: (1) Elements have fused to form the parabasisphenoid; (2) fused to form the otoccipital; (3) may be dermatocranial.

	Prootic	Supraoccipital	Opisthotic	Exoccipital	Basioccipital	Basisphenoid	Parasphenoid	Laterosphenoid	Orbitosphenoid	Internarial
Anthracosauria										
Palaeoherpeton sp.	X	X	X	X	X	X	X			
Seymouriamorpha										
Seymouria sp.	X	X	X	X	X	X	X			
Stem-Neodiapsida										
Youngina capensis	X	X	X	X	X	X	X			
Neodiapsida *incertae sedis*										
Champsosaurus lindoei	X	X	X	X	X	X	X			X[3]
Sauropterygia										
Nothosaurus sp.	X	X	X	X	X	X[1]	X[1]			
Pantestudines										
Proganochelys quenstedti	X	X	X	X	X	X[1]	X[1]	X		
Meiolania platyceps	X	X	X	X	X	X[1]	X[1]			
Pseudemys texana	X	X	X	X	X	X[1]	X[1]			
Sternotherus oderatus	X	X	X	X	X	X[1]	X[1]			
Archosauria										
Erythrosuchus africanus	X	X	X[2]	X[2]	X	X[1]	X[1]	X		
Euparkeria capensis	X	X	X	X	X	X[1]	X[1]	X	X	
Stenonychosaurus inequalis	X	X	X[2]	X[2]	X	X[1]	X[1]	X	X	
Spinophorosaurus nigerensis	X	X	X[2]	X[2]	X	X[1]	X[1]	X	X	
Lesothosaurus diagnosticus	X	X[3]	X	X	X	X[1]	X[1]	X		
Alligator mississippiensis	X	X	X	X	X	X[1]	X[1]	X		
Rhynchocephalia										
Sphenodon punctatus	X	X	X	X	X	X[1]	X[1]			
Squamata										
Trachylepis laevis	X	X	X[2]	X[2]	X	X[1]	X[1]		X	
Shinisaurus crocodilurus	X	X	X[2]	X[2]	X	X[1]	X[1]		X	
Iguana iguana	X	X	X[2]	X[2]	X	X[1]	X[1]		X	
Diplometopon zarudnyi	X	X	X	X	X	X[1]	X[1]	X	X	
Varanus varanus	X	X	X[2]	X[2]	X	X[1]	X[1]			
Varanus prisca	X	X	X[2]	X[2]	X	X[1]	X[1]			
Tupinambis nigropunctatus	X	X	X[2]	X[2]	X	X[1]	X[1]		X	
Pogona vitticeps	X	X	X[2]	X[2]	X	X[1]	X[1]		X	

Alligator mississippiensis – Rowe et al., 1999; *Diplometopon zarudnyi* – Abo-Eleneen et al., 2017; *Erythrosuchus africanus* – Gower 1997; *Euparkeria capensis* – Gower and Weber 1998; *Iguana iguana* – Lima et al., 2014; *Lesothosaurus diagnosticus* – Sereno 1991; *Meiolania platyceps* – Gaffney 1983; *Nothosaurus* sp. – Rieppel 1994; *Palaeoherpeton* (*Palaeogyrinus* of Romer 1956) – Romer 1956; *Pogona vitticeps* – Ollonen et al., 2018; *Proganochelys quenstedti* – Gaffney 1990; Bhuller and Bever 2009; *Pseudemys texana* – Bever 2009; *Seymoria* – Romer 1956; *Spinophorosaurus nigerensis* – Knoll et al., 2012; *Shinisaurus crocodilurus* – Bever et al., 2005; *Sphenodon punctatus* – Romer 1956; Sobral et al., 2016; *Stenonychosaurus inequalis* – Currie 1985; *Sternotherus oderatus* – Bever 2009; *Trachylepis laevis* – Paluh and Bauer 2017; *Tupinambis nigropunctatus* – Jollie 1960; *Youngina capensis* – Gardner et al., 2010; *Varanus Prisca* – Head et al., 2009; *Varanus varanus* – Rieppel and Zaher 2000.

the element ossifies independently from the pila antotica in snakes and some skinks, and therefore may have evolved independently in squamates (Rieppel, 1976).

The orbitosphenoid is represented by cartilage in basal amniotes (de Beer, 1937), but can ossify in some lineages of archosaurs, lepidosaurs, and mammals (Hernandez-Jaimes et al., 2012; Benoit et al., 2017). When present, this element is found anterior to the laterosphenoid, located between the exits for CN II, CN III, and CN IV, and usually forms as an ossification from the pila metoptica (Evans, 2008) and the taenia medialis (de Beer, 1937; Benoit et al., 2017). The ossification of this region of the chondrocranium is highly variable between species and appears to have evolved several times independently. The variability in the ossification of this region is not well understood, but it is possible that it correlates with bite force, and the distribution of that force across the chondrocranium (Evans, 2008; Jones et al., 2017).

The internarial element is unique to *Champsosaurus* and is a diagnostic feature of the genus (Gao and Fox 1998; Matsumoto et al., 2013). The internarial was described as a neomorphic ossification by Russell (1956), Romer (1956), and Erickson (1972) and is possibly derived from the cartilaginous internarial septum (Russell, 1956). The CT data presented here indicate that the internarial possesses a ridge on the dorsal surface that extends into the nasal cavity and may have supported the cartilaginous internarial septum. This evidence could support the previous hypothesis that the internarial is derived from the cartilaginous internarial septum due to their close association to one another in the skull. Alternatively, the internarial bone may have ossified from the dermatocranium, given that the septum does not ossify other than on the palatal surface. At present, there is insufficient evidence to determine whether the internarial is of dermal or chondrocranial origin, but it is

tentatively designated here as a chondrocranial ossification, due to its previous description as an ossification from the internarial septum (Russell, 1956). The exact function of this element is difficult to explain, but it is possible that the extra ossification running the length of the snout provided additional support for the snout when under load.

What is clear from the comparison of braincase bones across Amniota (Table 2.2) is that, although the anterior chondrocranium shows some variation in ossification between taxa, there are no new ossifications, nor re-ossifications, in the posterior region across Amniota. The posterior braincase shows an overall trend towards reduction in the number of discrete elements through fusion, i.e., the basisphenoid and parasphenoid often fuse to form the parabasisphenoid, and the exoccipital and the opisthotic often fuse to form the otoccipital (Knoll et al., 2012). This trend in the reduction of discrete elements is also reported in Lissamphibia (Atkins et al., 2019), suggesting that braincase simplification may be common in tetrapods. Therefore, the appearance of a novel ossification in the posterior chondrocranium of choristoderes is highly unlikely. Additionally, the neomorph does not fuse with chondrocranial elements, as does the dermatocranial parasphenoid, and so it fails to meet the parameters of inclusion to the chondrocranium that are applied to the parasphenoid in this study. Although the exact developmental path of a structure cannot be determined in extinct taxa (Romer, 1956), the choristoderan neomorphic bone is probably not chondrocranial in origin. Based on these facts, I posit that the choristoderan neomorphic bone should not be considered as a braincase element, but instead as an element that occurs lateral, but attached, to the braincase. Further to this suggestion, even when using a less conservative definition of a braincase bone (definition 3: any bone that contacts the brain

cavity), the neomorphic bone still fails to meet this definition as it is clearly separated from the endocranial cavity by the underlying prootic and opisthotic (Figure 2.21).

Although the neomorph is unlikely to be chondrocranial in origin, there are two other possibilities regarding its origin: it is splanchnocranial and developed from the embryonic gill arches, or it is dermatocranial and developed as an intramembranous ossification. It seems highly unlikely that the neomorph developed from the splanchnocranium, as a novel development from the embryonic gill arches has not occurred since the evolution of ossified jaws (e,g,, the articular element of osteichthians; DeLaurier, 2018). This does not entirely rule out the splanchnocranium as a source of origin for the neomorph, but instead suggests that the development of a neomorphic ossification from the splanchnocranium is unlikely. Additionally, it is impossible for the neomorph to have developed as a modification of a pre-existing splanchnocranial element in the jaw (as seen in the inner ear bones of mammals) as all the typical reptilian jaw bones are found in the *Champsosaurus* mandible (Brown, 1905). The stapes is the only undescribed splanchnocranial element in choristoderes and may be homologous with the neomorph. The possible homology of the neomorph and stapes is supported by: (1) the ancestral role of the stapes as a structural element in the diapsid skull (and in amniotes and tetrapods more generally; Carroll, 1980; Carroll, 1982; Gardner et al., 2010), (2) the medial articulation of the neomorph with the prootic and opisthotic of the otic capsule, (3) the lateral articulation of the neomorph with the quadrate, (4) the presence of a foramen (the pterygoquadrate foramen) penetrating the neomorph that may be homologous with the stapedial foramen. Matsumoto et al. (2019) found that the early non-neochoristodere, *Coeruleodraco*, may posses both the stapes and the neomorphic bone, suggesting that these elements are not homologous; however, they acknowledged that the

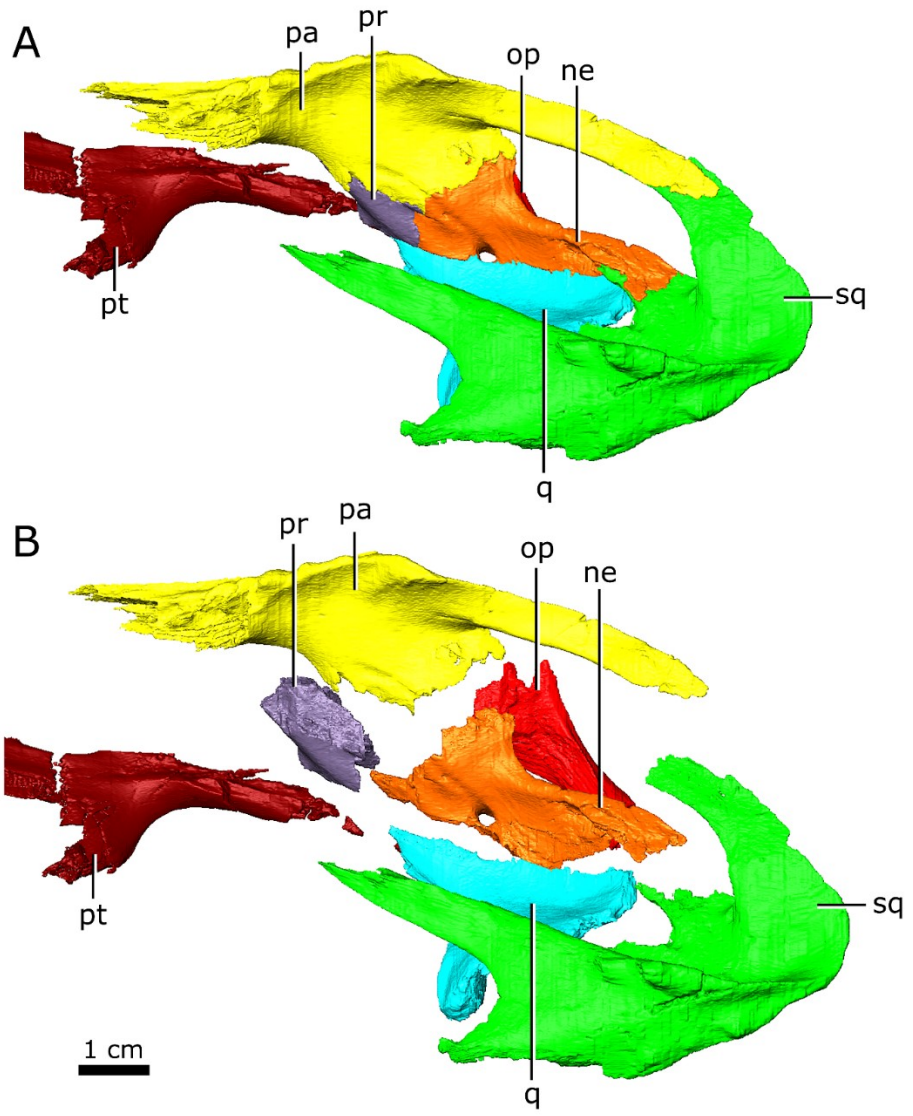

Figure 2.21: Left neomorphic bone and adjoining bones of *Champsosaurus lindoei* (CMN 8920) in left dorsolateral view with the elements **A** articulated, and **B** exploded.

identification of the stapes was hindered by low scanning resolution, and is therefore inconclusive. As such, the data presented here indicate that the neomorph may be homologous with the stapes, and a more precise description of the putative stapes in *Coeruleodraco* is needed to comment on the presence and morphology of the bone in that taxon.

If the neomorphic bone is not homologous with the stapes, the only other possible origin of the neomorphic bone is as a novel ossification from the dermatocranium. These bones form through intramembranous ossification, where the bones arise directly from the cranial dermis, and lack cartilaginous precursors (Romer and Parsons, 1977). Although cranial anatomy shows a trend towards fewer discrete elements over time (Sidor, 2001; Table 2.2), the known instances of neomorphic ossifications (e.g., the palpebral found in some lacertoids, cordyloids, scincoids, and anguimorphs, the supraorbital found in pythonid snakes, and the parafrontal of some gekkos; Estes et al., 1988; Conrad, 2008; Daza and Bauer, 2010) have developed from the dermatocranium, making it a good candidate for the origin of the choristoderan neomorph.

What remains elusive is how neomorphic ossifications are instigated in the developing cranium. Sidor (2001) reviewed possible developmental origins of dermatocranial neomorphic ossifications in synapsid skulls and noted three mechanisms by which these bones could appear. One mechanism involves gene duplication, where the duplication of a gene responsible for inducing ossification of a tissue causes an element to be duplicated. Although gene duplication leading to duplicated structures has been observed in invertebrates and vertebrates (Patel, 1994; Shubin et al., 1997), this has only been known to occur in the duplication of body segments, and not in the duplication of cranial bones. The misexpression

of hox genes, however, is known to cause the duplication of pharyngeal arch derivatives of the skull (e.g., the bones of the inner ear and jaw), but these mutations usually result in the addition of multiple cranial elements of the ear and jaw, and the mutant individuals are usually nonviable (e.g., Gendron-Maguire et al., 1993; Helms and Schneider, 2003). Therefore, it is unlikely that the choristoderan neomorphic bone developed from a misexpression of hox genes because there are no additional neomorphic bones in the jaw region of *Champsosaurus*, and the presence of the neomorphic bone throughout choristodere evolution suggests that it was not deleterious.

The second mechanism involves epigenetic factors, where new ossification sites are created through heritable, but non-genetic characters. Epigenetic ossifications are well documented in human development where novel ossifications develop between cranial sutures. These elements are called supernumerary, or Wormian bones, and in humans are most frequently seen between the parietals, frontals, temporals, and occipital (Sanchez-Lara et al., 2007). These bones can occur without any negative health effects or obvious external deformities, and their cause is not well understood (Cremin et al., 1982). Wormian bones are known to occur with increased frequency among patients with hydrocephalus and ossify from the dermis to occupy the space between the cranial bones that is created by the expanded brain cavity (Bellary et al., 2013). Interestingly, Wormian bones also occur at a higher frequency when human skulls are artificially deformed by binding, and these ossifications tend to occur more frequently in the posterior skull along the sutural boundaries (O'Laughlin, 2004). O'Laughlin (2004) concluded that environmental stressors on the skull can increase the number of Wormian ossifications, a conclusion that has implications for Choristodera.

At least 53% of human children have at least one Wormian bone, and up to 10% have at least four, suggesting these elements are common, even in healthy individuals (Marti et al., 2013). It may be tempting to say that the choristoderan neomorphic ossification developed as a Wormian bone to occupy the space created as the temporal arches expanded away from the braincase over evolutionary time, but this conclusion is hindered by the lack of evidence for the heritability of Wormian bones. At present, there is no evidence for heritability in the number, shape, size, or location of Wormian bones and the formation of these bones seems to be random in healthy individuals (Bennett, 1965; Marti et al., 2013). Additionally, when present, Wormian bones are highly variable in number, size and shape (Marti et al., 2013). As such, it seems unlikely that the choristoderan neomorph developed as a Wormian bone because it is suggested to occur in every neochoristodere (and some non-neochoristoderes), and appears to be morphologically similar in size, shape, and location across Neochoristodera.

The third mechanism for neomorphic bone formation involves subdividing a pre-existing element into multiple components, such as the jointed premaxilla of bolyerine snakes (Frazzetta, 1970). Subdivision can occur through the incomplete fusion of multiple ossification sites of a single element (Romer, 1956), and is known to produce the neomorphic echidna pterygoid (de Beer, 1937), which forms three bones instead of two.

Based on the three mechanisms discussed here, if the choristoderan neomorphic bone developed from the dermatocranium, it is most probable that it developed via the subdivision of a pre-existing element, as this mechanism is most prominent in the formation of dermatocranial neomorphic bones in amniotes. If this is true, it means the neomorph developed from one of the surrounding bones in the skull, but determining conclusively

which bone it could have developed from is difficult. The simplest way to determine possible origins of the neomorph, other than finding embryonic choristoderans with the neomorphic bone preserved, would be to observe the bones in contact with this element and determine the likelihood of the neomorph originating from these elements.

In CMN 8920, the neomorphic bone is in contact with the prootic, opisthotic, pterygoid, squamosal, quadrate, and parietal (Figure 2.21). In the early choristodere *Coeruleodraco*, the neomorph appears to only contact the parietal, opisthotic, and a small portion of the squamosal (Matsumoto et al., 2019). Although the neomorphic bone is more accurately described here in *Champsosaurus*, the morphology of the neomorph in the more basal *Coeruleodraco* (Figure 2.22) is more likely to resemble the ancestral condition, and can therefore provide more accurate information regarding its origin.

In *Coeruleodraco*, the neomorph appears to only briefly contact the squamosal at its posteriormost extent (Figure 2.22). This suture is very short, where the neomorph is mostly separated from the squamosal by the adjacent opisthotic and parietal and it is therefore unlikely that the neomorph developed from this element. The neomorph shares extensive sutures with both the opisthotic and parietal, but based on the rarity of neomorphic bones developing from chondrocranial elements (Table 2.2) and the abundance of neomorphic bones developing from the dermatocranium (Estes et al., 1988; Conrad, 2008; Daza and Bauer, 2010) it can be concluded that the neomorphic bone most likely developed from the parietal, although this is entirely speculative at present.

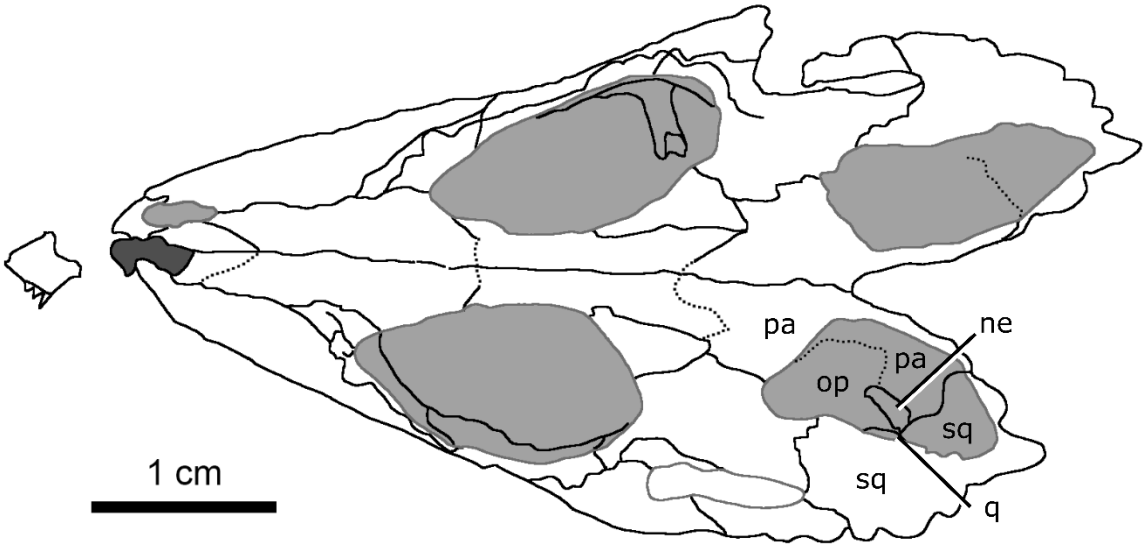

Figure 2.22: Line drawing of the skull of *Coeruleodraco jurassicus* (IVPP V 23318) in dorsal view. Modified from Matsumoto et al. (2019).

Functionality of the choristoderan neomorphic ossification

The functionality of the neomorphic bone in the early choristodere *Coeruleodraco* is hard to determine, given that this element is interpreted as quite small and does not appear to be structural. Prior to the discovery of this genus, the neomorph has always been found in conjunction with the pterygoquadrate foramen (pterygoid foramen of Matsumoto et al., 2019), and it is therefore possible that those two structures were related. The discovery of *Coeruleodraco* refutes this, where the neomorphic bone appears to occur in the absence of the pterygoquadrate foramen, suggesting that this foramen may be a synapomorphy of Neochoristodera. This conclusion is supported by the apparent absence of the pterygoquadrate foramen in all known non-neochoristoderes, but these specimens were too damaged to definitively determine if the pterygoquadrate foramen and neomorphic bone were present (Evans, 1990; Gao and Fox, 2005; Gao and Ksepka, 2008).

Fox (1968) suggested that the neomorph developed to strengthen the connection between the braincase and the pterygoquadrate region, but the small size of the neomorph reported in *Coeruleodraco* (Matsumoto et al., 2019) makes this unlikely. As such, it is possible that the neomorphic ossification did not develop due to some driving selection pressure, but developed randomly and became fixed in the population because it had no deleterious effects. Such traits could develop by chance through genetic drift or as an evolutionary spandrel (Lande, 1976; Gould and Lewontin, 1979; Dieckmann and Doebeli, 1999).

Regardless of its origin, once instigated, the morphology and function of this element was free to change. Given the size and location of the neomorph at the base of the temporal arches in *Champsosaurus*, a possible function of this element in neochoristoderes is to

strengthen the connection between the large temporal arches and the braincase and palatal region (Fox 1968). A potential advantage to enlarging the neomorph is the expansion of the surrounding sutures. The primary role of sutures in the mature skull is for stress transfer and dampening (Pritchard et al., 1956; Curtis et al., 2013), where the sutures reduce the stress gradient between bones and distribute the bite force evenly across the skull (Mao, 2002, Kopher and Mao, 2003, Curtis et al., 2013). Increasing the length of sutures at the base of the temporal arches could be beneficial, as they would help absorb and distribute the mechanical stress from biting.

James (2010) described the feeding mechanics of *Champsosaurus*, and he calculated that these animals could generate bite forces that are equal to and potentially greater than those of similarly sized modern crocodilians. Alligators are known to increase the width of their cranial sutures through ontogeny to better absorb the stress on the skull when biting (Erickson et al., 2003; Bailleul et al., 2016). However, if a suture becomes too wide it can allow the skull to flex and become kinetic, which dampens bite force (Iordansky, 1990). As such, a neomorphic ossification in *Champsosaurus* could provide an optimal state, increasing the number of sutures to better distribute stress while maintaining the strength and rigidity of the skull.

A second possible function of the neomorph in *Champsosaurus* is to increase the size of the attachment sites for the jaw adductors. Given the long and slender profile of the neomorph, and its location at the base of the temporal arches, the only muscle that may have partially attached to the neomorph was the *M. pseudotemporalis profundus*, which acts to adduct the jaw (James, 2010). It therefore seems unlikely that the neomorph developed to allow larger attachment surfaces for the jaw adductors because it likely played a very small

role, if any, in supporting the jaw musculature. Additionally, even if the neomorph was a major attachment site for jaw muscles, it is difficult to explain how the muscles could not be supported by the pre-existing bones of the skull.

It is also possible that the enlargement of the neomorphic ossification over evolutionary time is simply due to the expansion of the temporal region in neochoristoderes. The other bones of the temporal region (i.e., parietal, squamosal, postorbital, quadratojugal) are all elongated in neochoristoderes when compared to non-neochoristoderes, and the neomorphic bone could therefore have simply been modified in congruence with the other elements in the expanded temporal region.

Conclusions

This study describes the cranial bones of *Champsosaurus lindoei* in 3D using CT scanning. The data reveal that the fenestra ovalis of *C. lindoei* is located ventrally on the skull, an unusual feature that may be synapomorphic to Neochoristodera. *Champsosaurus lindoei* was also found to have a large pineal body, like the previously reconstructed *Ikechosaurus* (Lu et al., 1999a), but lacked all evidence for a pineal eye and the vomeronasal organ. These data also allowed for the confirmation of the neomorphic element, and revealed the nature of its morphology and relationship to other cranial bones.

I provided the first review of the variation seen in amniote chondrocranial ossifications, which illustrates how this region of the skull tends to be evolutionarily conserved, showing a trend towards simplicity over time. As such, it is concluded that the neomorphic bone is unlikely to have developed from the chondrocranium and therefore should not be described as a braincase bone. The stapes is a pre-existing cranial element that

may be homologous with the neomorphic bone, and a more precise description of the putative stapes in *Coeruleodraco* is needed to comment on the presence of the bone in that taxon. If the neomorph is not homologous with the stapes, the most likely developmental membership of the neomorphic bone is as a component of the dermatocranium. The exact developmental mechanism for the origin of the neomorph cannot be determined conclusively, but it is most probable that it developed through the incomplete fusion of ossification centers from a pre-existing cranial bone, possibly the parietal. Given the relatively small size of the neomorph in *Coeruleodraco*, it may not have had a structural role in the skull of early choristoderes and arose through non-adaptive means. In the more derived *Champsosaurus*, the additional sutures surrounding the neomorph may have provided greater stress absorption during biting while maintaining rigidity of the skull; however, it is also probable that the neomorph elongated following the expansion of the temporal region in neochoristoderes.

Chapter 3: The internal anatomy of the skull of *Champsosaurus* and implications for neurosensory function

Introduction

Palaeoneurology, the study of the brain in the fossil record and how it has changed through time (Witmer et al., 2008), provides some of the best evidence for how extinct animals behaved and interacted with their environment. The behaviour and sensory abilities of extinct taxa are inferred based on the morphology of the neural structures of the brain that are directly responsible for processing sensory information and forming behaviour. Other neural structures are often included in palaeoneurological studies, such as the cranial nerves and membranous labyrinth that transmit sensory and motor information to and from the brain, and facilitate the sensation of movement and orientation, respectively. Estimations of sensory ability and behaviour based on the morphology of the brain are made possible by the principle of proper mass, which states that the size of a brain region dedicated to a specific function is directly correlated with the amount of processing power required to complete that function (Jerison, 1973). Therefore, regions of the brain that require more processing power tend to be larger to accommodate a greater number of neurons. This correlation allows hypotheses to be made about the sensory ability of extinct animals based on the morphology of the brain.

The morphology of the membranous labyrinth is also known to correlate with equilibrioception (Spoor and Zonneveld, 1998) and auditory capabilities (Walsh et al., 2009), and is therefore a good proxy for estimating these abilities (Witmer et al., 2003). Recent studies have also found a correlation between the morphology of the semicircular canals, and locomotor strategy and ecology, where phylogenetically distant lineages have convergent ear

morphologies due to similar forms of locomotion and ecology (e.g., Dickson et al., 2017). Therefore, describing the morphology of the labyrinth in extinct taxa is likewise useful in inferring their locomotor strategies or ecologies.

Description of the brain, cranial nerves, and membranous labyrinth cannot be made directly in fossil taxa because these soft-tissue structures do not preserve; however, as they are usually encased within the osseous portion of the skull, which is frequently fossilized, their morphologies can be determined from their preserved molds within the skull. The brain cavity that holds the brain is often referred to as the endocranial cavity, and is encased by the osseous chondrocranium and elements of the dermatocranium. Digital segmentation of this cavity can be used to produce a 3D structure (brain endocast) that reflects the morphology of the endocranial cavity.

The brain endocast is not a perfect reflection of the brain in life, as it also represents other soft structures housed within the endocranial cavity that did not fossilize, such as the dura matter, cartilage, and vascular tissue. Despite this, a description of the brain endocast of an extinct animal provides data that can be used to infer its neurosensory capabilities by comparison to closely related extant taxa, which allows for the formation of hypotheses as to its behaviour and ecology (Witmer et al., 2008). The membranous labyrinth of the inner ear is encapsulated by the bony labyrinth, and the cavity in which the membranous labyrinth is housed is called the endosseous labyrinth. Like the endocranial cavity, the endosseous labyrinth holds other soft tissue structures, such as the lagenar macula (Wever, 1978; Gleich et al., 2005), and is therefore not a perfect representation of the membranous labyrinth within. In general, however, the bone sits quite close to the membranous semicircular canals

and the morphology of the canals is therefore well represented in the morphology of the surrounding bone.

Historically, description of neurosensory structures relied on fragmentary material, or destructive sampling methods such as thin sectioning, but computerized tomography (CT) scanning now allows for the 3D visualization of internal structures in intact specimens without causing damage to the specimen (Witmer et al., 2008).

The braincase of the Late Cretaceous-aged reptile *Champsosaurus* is enigmatic due to the fragile nature of their skulls, hindering preservation. Fox (1968) provided a cursory description of the brain endocast, auditory chamber, and cranial nerve passages of *Champsosaurus* based on fragmentary material, but was unable to provide an illustration of an intact endocast, comment on the relative size of lobes of the brain, the shapes of the semicircular canals, or the paths of cranial nerve passages through the skull. There has been little discussion on the endocranial anatomy of *Champsosaurus* since Fox (1968), and the 3D morphology of these structures remains elusive, despite the valuable behavioural and ecological information that it could yield. The occurrence of specimens in fluviolacustrine deposits suggests that *Champsosaurus* was highly aquatic, and its morphological similarity to the modern *Gavialis gangeticus* has led researchers to propose that *Champsosaurus* likely had a similar lifestyle (Erickson 1985), but neurological evidence has yet to be considered.

Lu et al. (1999a) described the endocranial anatomy of the Asian neochoristodere, *Ikechosaurus*, and commented on the possible presence of osteological correlates for turbinates in the nasal passage that may have facilitated thermoregulation. Choristodere thermoregulation was first proposed in *Champsosaurus* by Erickson (1985) simply due to the large surface area of the olfactory chambers of the nasal passages, but his description focused

on fragmentary specimens and did not comment on the presence of turbinates. Turbinates in the neochoristodere nasal passage have not been reported since Lu et al. (1999a), and it is not known whether this is a widespread feature of Neochoristodera. *Champsosaurus* is known to have occupied a wide latitudinal range, extending well into the polar region of the Canadian high arctic (Vandermark et al., 2007) where contemporaneous reptiles, such as crocodilians, were absent (Lehman and Barnes, 2010). This suggests that *Champsosaurus* was able to tolerate the dramatic fluctuation in temperatures between seasons when other reptiles could not, and *Champsosaurus* therefore may have had some form of thermoregulation.

Here, the internal cranial anatomy of two *Champsosaurus* specimens, CMN 8920 (*C. lindoei*; Figure 3.1) and CMN 8919 (*C. natator*), is described using CT scanning to provide data that can be used to make hypotheses about their sensory ability, behaviour, and ecology. A description of the endocranial anatomy using CT data, and comparisons with extant taxa, will provide novel data to either support or refute these previous hypotheses on the behaviour of *Champsosaurus*. Additionally, a description of the nasal passage of *Champsosaurus* will provide insight into the presence of turbinates, and allow for comment on the possible thermoregulatory ability of these animals.

Materials and Methods

Materials

CMN 8920 is a nearly complete skull, lacking jaws, with slight crushing of the right temporal arch. The specimen was found in 1953 in the Dinosaur Park Formation of the east branch of Sand Creek, Alberta, in what is now Dinosaur Provincial Park. It was first

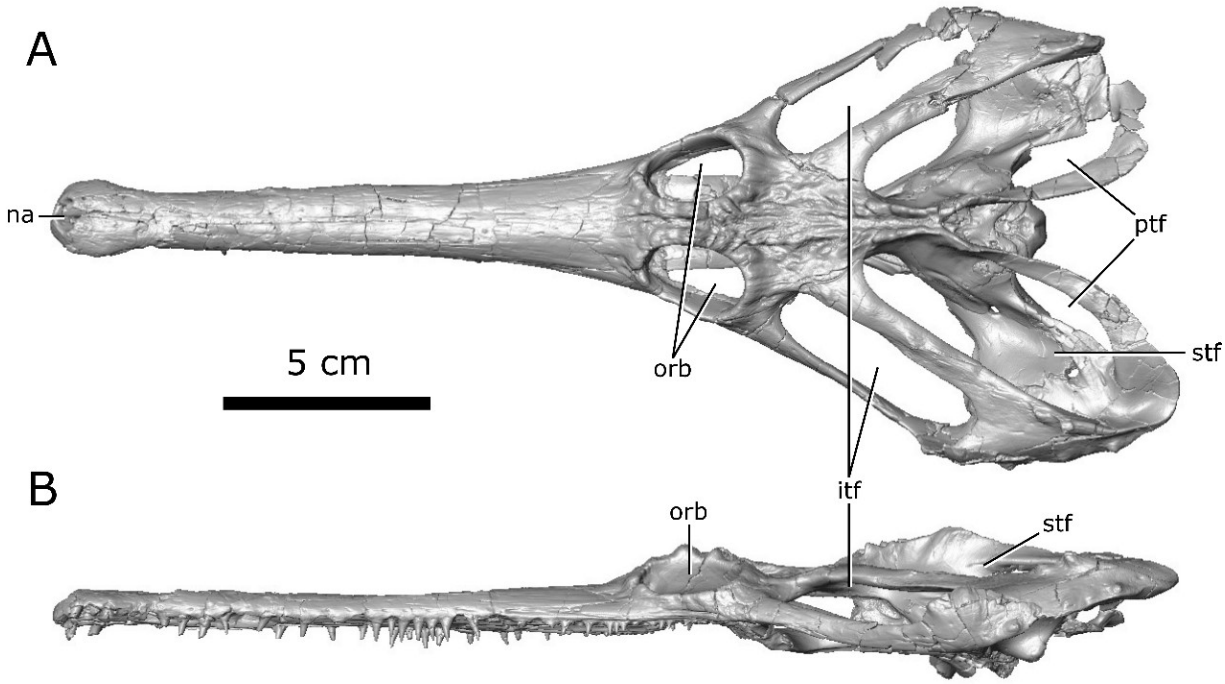

Figure 3.1: Digitized model of the skull of *Champsosaurus lindoei* (CMN 8920) based on micro-computed tomography scanning. **A** dorsal view; **B** left lateral view. *Abbreviations: itf, infratemporal fenestra; na, narial opening; orb, orbit; ptf, post-temporal fenestra; stf, supratemporal fenestra.*

described by Russell (1956) as *C. natator*, but was later shown by Gao and Fox (1998) to belong to *C. lindoei* based on its relatively small size (approximately 24.3 cm in basioccipital length; Dudgeon et al., In Revision), gracile snout, expanded narial bulla, and strait lower temporal bar.

CMN 8919 was found in 1917 in the Dinosaur Park Formation, near the same locality as CMN 8920, and approximately 10 m below the Bearpaw Formation (1917 field notes, CMN archives; Russell, 1956). This specimen consists of a well-preserved skull and mandible, and the anterior half of the vertebral column, and both forelimbs. This specimen was formally described by Russell (1956), who attributed it to *C. natator*.

Scanning and segmentation

CMN 8920 was scanned at the University of Texas CT facility. The specimen was scanned with a voxel size of 60.5 μm at 200 kV and 0.3 mA. This produced 4579 jpeg files. Images were converted into tiff files and every other image was selected for segmentation. CMN 8919 was scanned at the Alta Vista Veterinary Hospital (Ottawa) using a 16-slice medical CT scanner with a voxel size of 0.5 mm at 135 kV and 75 mA. This produced 2542 jpeg images, but only every other image was selected for segmentation. These data sets were loaded separately into Amira 5.4.3 (Visage Imaging GmbH, Berlin, Germany) for visualization and segmentation using the LabelFields module. Internal structures such as the brain endocast, endosseous labyrinth, cranial nerve passages, vasculature passages, and nasal passage, were segmented individually and rendered using the SurfaceView module, creating a colour coded model of the internal cavities for description and manipulation. The 3D

models generated from this study will be made freely available online via MorphoSource upon publication of this chapter in the peer-reviewed literature.

Estimation of auditory perception

To estimate the mean best hearing frequency and best hearing frequency range of *Champsosaurus*, the length of the ventral portion of the membranous labyrinth (the pars inferior), which is composed of the sacculus, utriculus, and cochlea (lagena of some authors; e.g., Gower and Weber, 1998) of the endosseous labyrinth (Figure 3.2) was compared to the extant dataset from Walsh et al. (2009). The dataset of Walsh et al. (2009) primarily used endocochlear duct length in their analysis, but for taxa that did not have a defined endocochlear duct (such as *Champsosaurus*), Walsh et al. (2009) used the maximum length of the pars inferior (i.e., ventral to the lateral semicircular canal) in its place. This measurement for CMN 8920 was scaled to the length of the basicranium to account for skull size, and log transformed to normalize the data (Walsh et al., 2009). The length of the basicranium was measured from the posteriormost extent of the occipital condyle to the anteriormost edge of the basisphenoid, excluding the length of the cultriform process and the basipterygoid process (Figure 3.2; Walsh et al., 2009). *Gerrhonotus multicarinatus* was excluded from this analysis because endocochlear duct length information was not available for that species. The dataset was subjected to ordinary least squares linear regression in RStudio 1.1.456 (RStudio Inc.) and the scaled and transformed endocochlear length for CMN 8920 was inserted into the resulting equations to estimate hearing capability.

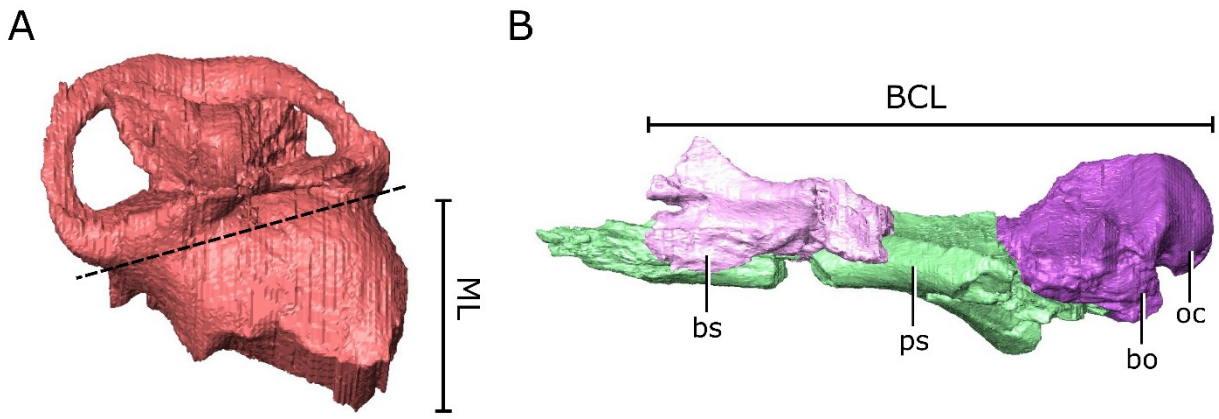

Figure 3.2: Measurements used for the estimation of auditory capabilities. **A** maximum endocochlear duct length (ML); **B** basicranial length (BCL). *Abbreviations: bo, basioccipital; bs, basisphenoid; oc, occipital condyle; ps, parasphenoid.*

Inferring ecology from the endosseous labyrinth

The following methods for inferring the ecology of *Champsosaurus*, based on the morphology of the semicircular canals, were modified from Dickson et al. (2017). The morphology of the semicircular canals of CMN 8920 and CMN 8919 were compared to 35 species of Lepidosauria and Archosauromorpha (see Appendices A-C for lists of taxa). Turtles were included in this analysis due to the growing body of evidence suggesting that Pantestudines share a close evolutionary history with early diapsids (Joyce et al., 2004; Bhullar and Bever, 2009; Wang et al., 2013; Crawford et al., 2015).

Many studies have landmarked the centerline of the semicircular canals (e.g., Boistel et al., 2011; Dickson et al., 2017); however, Mennecart and Costeur (2016) noted that landmarking the centerline does not take canal thickness into account, and that landmarks should instead be placed on the inner- and outer-most surfaces of the canals. This, unfortunately, cannot be done in this study because some taxa (including *Champsosaurus*) have some canals that are confluent with the pars inferior, and there is therefore no inner surface on which to place landmarks. Instead, the semicircular canals of the endosseous labyrinths were landmarked along the centerline using MorphoDig 1.2 (Lebrun, 2018). Left endosseous labyrinths were chosen because this side was best preserved in CMN 8920 and CMN 8919. When left endosseous labyrinths were not available for the comparative taxa, the right labyrinth was mirrored and used in place of the left. Curve handles and curve nodes were used to draw curves through the centerline of the three semicircular canals of each labyrinth. The first curve started at the center of the ampulla of the anterior canal, and ended at the junction of the anterior canal and the crus communis. The second curve started at the junction of the posterior canal with the crus communis, and ended at the center of the

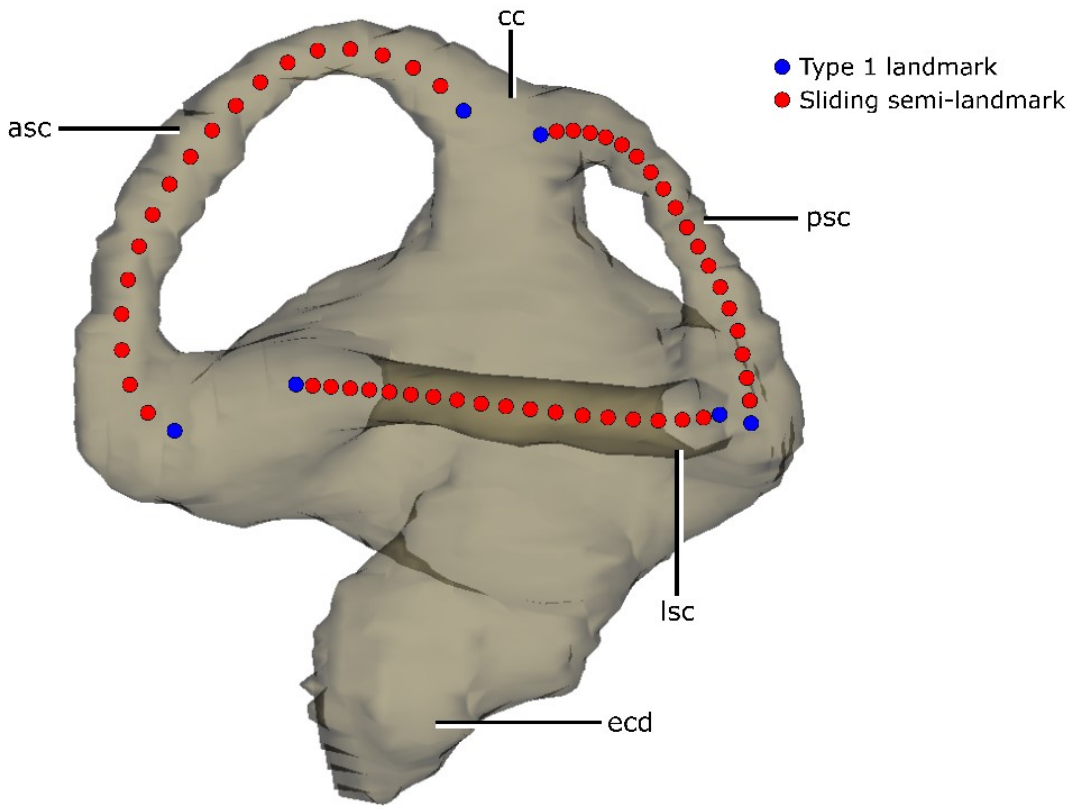

Figure 3.3: Landmark locations for the three semicircular canals of *Tomistoma schegelii*. *Abbreviations: asc, anterior semicircular canal; cc, crus communis; ecd, endocochlear duct; lsc, lateral semicircular canal; psc, posterior semicircular canal.*

ampulla for the posterior canal. The third curve started at the center of the ampulla for the lateral canal and ended where the lateral canal could no longer be differentiated from the pars inferior. Twenty evenly spaced landmarks were then projected onto each of these curves (total of 60 landmarks per labyrinth; Figure 3.3) and exported in landmark file (*.lmk) format.

The landmark files from the 36 included taxa were imported into RStudio 1.1.456 for analysis. The start and end landmarks of each curve were designated as type 1 landmarks (Bookstein, 1991), and the remaining landmarks were designated as sliding semi-landmarks that were allowed to slide along the curve of the semicircular canal (Figure 3.3). All landmarks and semi-landmarks were then rotated and scaled using General Procrustes Alignment in the R package geomorph 3.0.7 (Adams et al., 2019). The aligned landmarks were then projected into morphospace via a Principal Component Analysis (PCA) using the 'plotTangentSpace' function in geomorph to compare the morphology of the semicircular canals.

A phylogenetic tree was constructed based on the inferred relationships (Oaks 2011; Jetz et al., 2012; Lautenschlager et al., 2012; Tonini et al., 2016; Benson et al., 2018; Simões, et al., 2018) of these taxa to one another to evaluate phylogenetic signaling in the morphology of the semicircular canals. The occurrence data for these taxa were taken from the Paleobiology Database (paleobiodb.org). Some extant species did not have known first occurrence dates (i.e., they do not have a known fossil record), so occurrence data of the genus were used in its place. Some extant genera did not have a known first occurrence date, so these taxa were entered with a first occurrence date of zero million years before present. The tree was calibrated using the 'cal3TimePaleoPhy' tool in the R package *paleotree* 3.1.3

(Bapst, 2012). Unsampled evolutionary history was estimated using the instantaneous per-capita sampling rate and instantaneous per-capita extinction rate using the 'durationFreq' function in *paleotree*. Instantaneous per-capita speciation rates were assumed to equal the instantaneous per-capita extinction rate (Sepkoski, 1998). The time calibrated phylogeny was projected onto the PCA using the 'plotGMPhyloMorphoSpace' function in *geomorph* to visualize the change in canal shape across evolutionary time.

Bloomberg's multivariate K statistic (Adams, 2014) was calculated for centroid size and landmark coordinates using the time calibrated phylogeny and the *geomorph* function 'physignal' with 1000 permutations to evaluate phylogenetic signal on centroid size and canal morphology. Bloomberg et al. (2003) surveyed published datasets and determined that phylogenetic signal could be detected ($p < 0.05$) using the K statistic in 92% of studies that involved 20 or more taxa. This suggests that the number of taxa used here (35) is adequate to assess phylogenetic signal.

The included taxa were divided into five major ecological groups based on the medium that they interact with during locomotion: aerial taxa that fly; aquatic taxa that spend the majority of their time in water; arboreal taxa that live predominantly in trees; fossorial taxa that dig through soil; and terrestrial taxa that predominantly live on land. For fossil taxa (e.g., non-avian dinosaurs) the ecological groups were assigned based on inferred ecology in the published literature. Analysis of Covariance (ANCOVA) and phylogenetic generalized least squares (PGLS) were performed using the 'procD.lm' and 'procD.pgls' functions in *geomorph*, respectively, to determine whether taxa separate in the morphospace based on ecology. These two tests were used in tandem because, together, they illustrate the

relationship between ecology and canal morphology when phylogenetic lineages are considered as either independent (ANCOVA) or dependent (PGLS; Dickson et al., 2017).

A canonical variates analysis (CVA) was then run on the first 13 PC scores of all taxa except *Champsosaurus*, and the *Champsosaurus* specimens were then projected onto the CVA to predict their ecology. Only the first 13 PC scores were included in the CVA because this is the minimum number of PC scores needed to describe 95% of the total variation in canal morphology, and because removing the smaller PC scores eliminates subtle variances in canal morphology that may be due to error (Dickson et al., 2017). The CVA was run using the 'CVA' function in the R package *morpho*. Ninety-five percent confidence ellipses were visualized around the ecological groups within the CVA morphospace. A 95% confidence ellipse was not visualized for the aerial group because of small sample size. *Typhlops hypometheus* was removed from the dataset prior to the CVA because it was the only fossorial taxon included in the analysis, and the function 'CVA' cannot accept a group of n = 1. The posterior probability of group membership was calculated for both *Champsosaurus* specimens by calculating the Mahalanobis distances of the specimens from each group mean, and comparing those distances to within-group distances, with 10 000 resampling permutations. Specimens that plotted farther away from a group mean than 95% of within-group distances were considered significantly different from that ecological group. Log-likelihood estimations were calculated to determine ecological group assignment for *Champsosaurus*.

Results

Champsosaurus brain endocast

CMN 8920 (*Champsosaurus lindoei*) was scanned at a higher resolution than CMN 8919 (*C. natator*), and therefore more accurately illustrates the endocranial anatomy of *Champsosaurus*. As such, CMN 8920 forms the basis of this description, and only notable differences with CMN 8919 will be discussed. Taphonomic deformation of the braincases is minimal, so I infer that the reconstructed endocasts accurately reflect the living brain endocast morphology.

The brain endocast of CMN 8920 is narrow both mediolaterally and dorsoventrally, and does not show flexure (Figure 3.4). In contrast, the brain endocast of CMN 8919 shows a distinct cerebral and pontine flexure, an observation that is corroborated by fragmentary specimens of *C. natator* (ROM 688). The walls around the midbrain and hindbrain are well-ossified and provide good detail, but the lateral and ventral walls around the olfactory stalks did not ossify, and the exact shape of the olfactory stalks therefore cannot be determined. The ossified braincase of CMN 8920 is approximatley 32 mm long, but impressions of the olfactory stalks on the ventral surface of the parietals and frontals show that the entire brain cavity is 67 mm long (Figure 3.5). The olfactory stalks are substantial (approximately 37 mm long) and occupied approximately 55% of the length of the brain endocast.

The segmented braincase of CMN 8919 is approximately 66 mm long and the entire brain cavity is approximately 126 mm long (Figure 3.5). The olfactory stalks of CMN 8919 are also elongate, measuring approximatley 65 mm long, and occupy approximatley 51% of the length of the brain endocast. Two foramina lead into the ventral surface of the frontals in

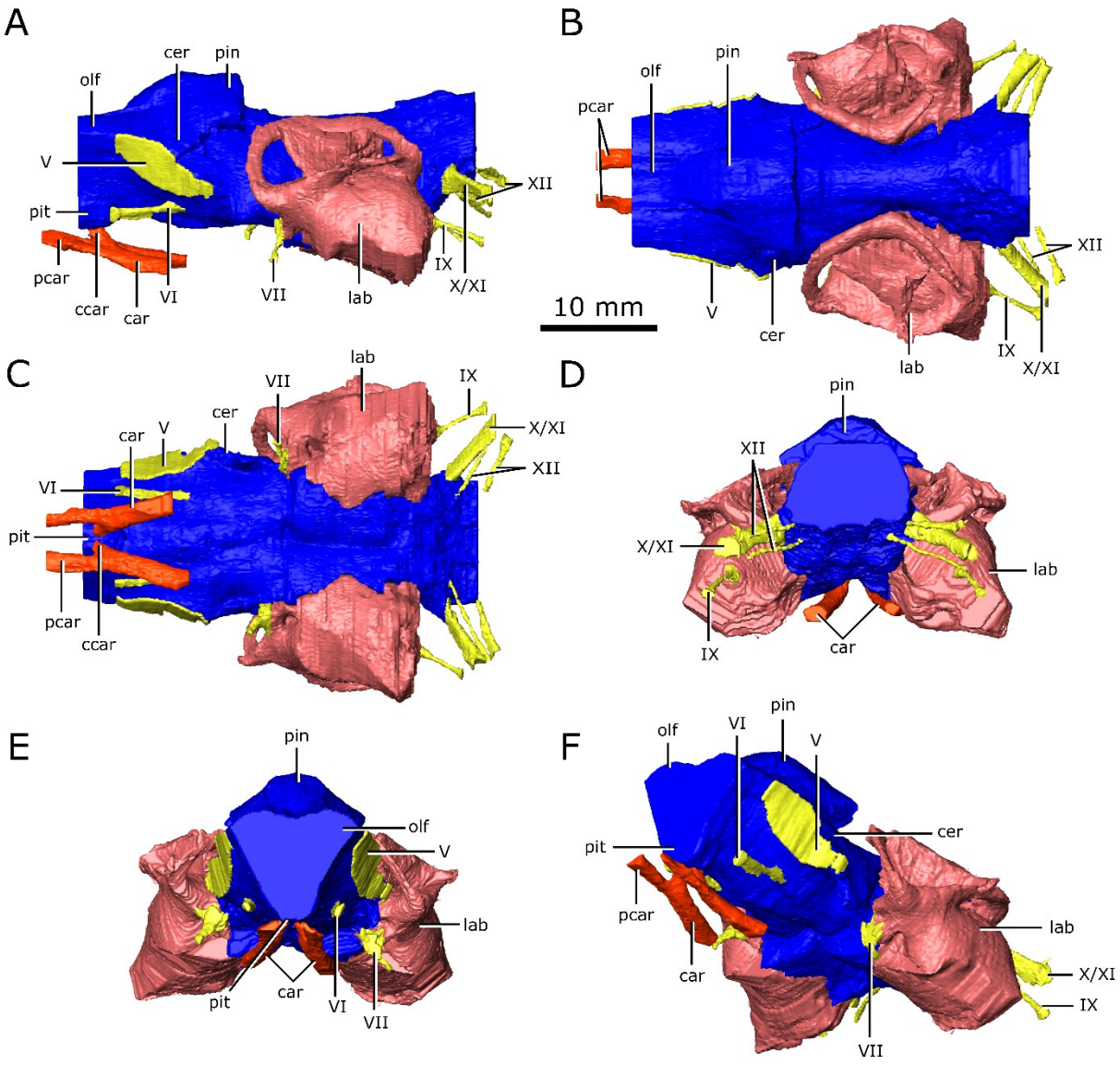

Figure 3.4: Reconstruction of the endocranial anatomy of *Champsosaurus lindoei* (CMN 8920). **A** left lateral view; **B** dorsal view; **C** ventral view; **D** posterior view; **E** anterior view; **F** left anterolateroventral view. The brain endocast is illustrated in blue, endosseous labyrinth in pink, cranial nerves in yellow, and carotid artery in red. *Abbreviations: car, carotid arteries; ccar, cerebral branch of the carotid arteries; cer, cerebrum; IX, canal for cranial nerve IX; lab, endosseous labyrinth; olf, base of the olfactory lobes; pcar, palatine branch of the carotid arteries; pin, pineal body; pit, pituitary fossa; X/XI, canal for cranial nerves X and XI; XII, canal for cranial nerve XII; V, opening for cranial nerve V; VI, canal for cranial nerve VI; VII, canal for cranial nerve VII.*

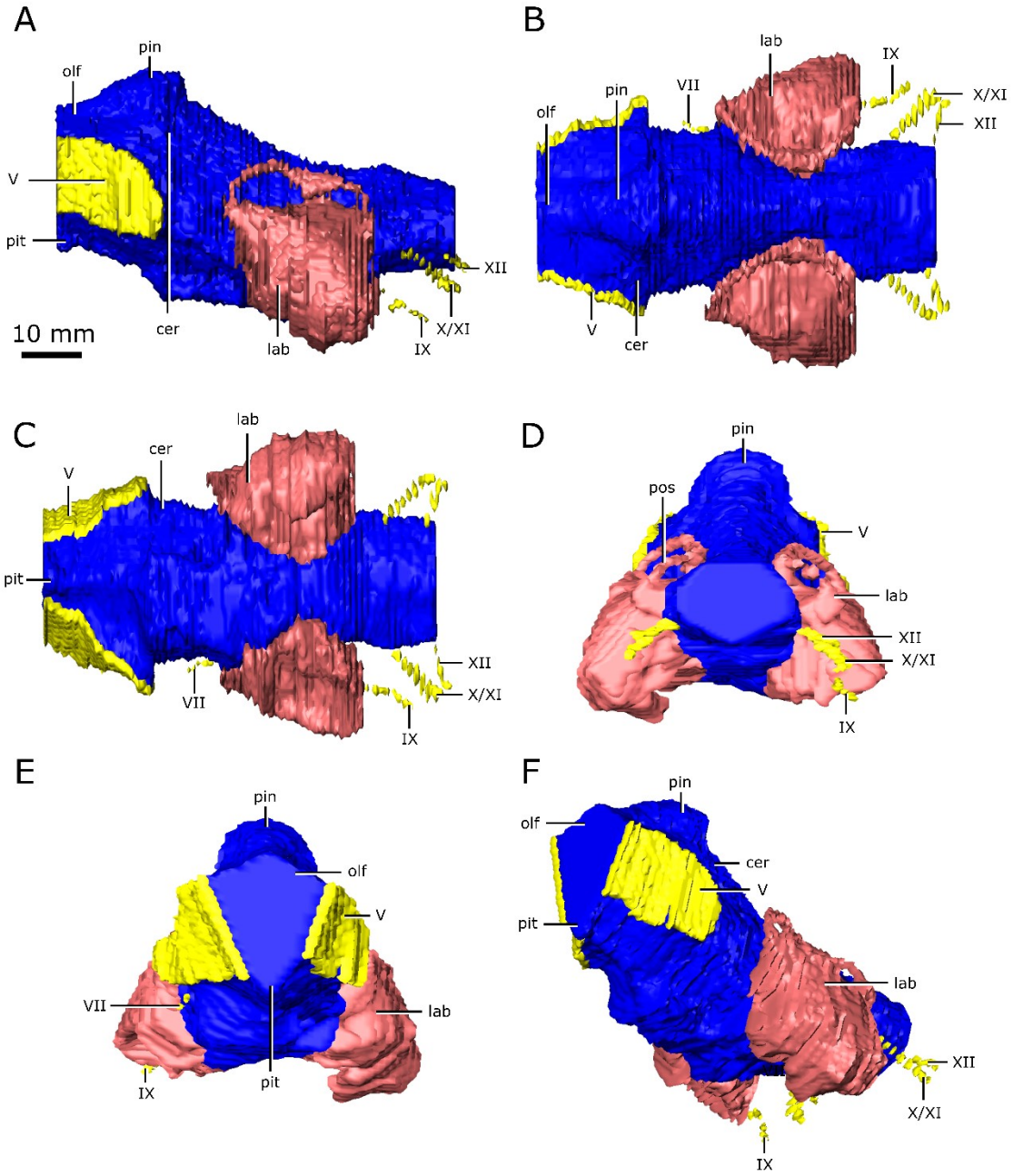

Figure 3.5: Reconstruction of the endocranial anatomy of *Champsosaurus natator* (CMN 8919). **A** left lateral view; **B** dorsal view; **C** ventral view; **D** posterior view; **E** anterior view; **F** left anterolateroventral view. The brain endocast is illustrated in blue, endosseous labyrinth in pink, cranial nerves in yellow, and carotid artery in red. *Abbreviations: cer, cerebrum; IX, canal for cranial nerve IX; lab, endosseous labyrinth; olf, base of the olfactory lobes; pin, pineal body; pit, pituitary fossa; X/XI, canal for cranial nerves X and XI; XII, canal for cranial nerve XII; V, opening for cranial nerve V; VII, canal for cranial nerve VII.*

the impression left by the anterior-most extent of the olfactory stalks of CMN 8920. CT data reveal that these foramina fork and dissipate into the cortical bone of the frontals, suggesting that they are vascular and carried diploic veins (Witmer and Ridgely, 2009; Figure 3.6). The brain endocasts of both specimens are fully enclosed by bone posterior to the olfactory stalks, preserving the morphology of the midbrain and hindbrain. The lateral, posterior, and ventral walls of the pituitary fossa are formed by the basisphenoid, but the anterior wall did not ossify. The pituitary fossa of both specimens is shallow, wide, and lacking details such as sulci, suggesting the pituitary gland would not have occupied the entirety of this space, and was supported by a thick layer of dura matter.

Posterior to the pituitary fossa, the endocast expands dorsally into a large concavity in the ventral surface of the parietals. Russell (1956) interpreted this expanson as a portion of the cerebellum, but based on its position in the midbrain, it appears to be the pineal expansion that is also present in other early reptiles (Holloway et al., 2013). The CT data of CMN 8920 show that the dorsal surface of the brain endocast anterior to the pineal expansion possesses sulci, suggesting that the brain pressed close to the skull in this region. The CT data of CMN 8919 are of too low resolution to capture these fine details; however, these sulci are also present on fragmentary specimens of *C. natator* (CMN 8921; CMN 8922; CMN 32579; ROM 688), suggesting that sulci in this region are widely present in *Champsosaurus*.

Posterior to the pineal expansion, the brain endocast narrows both dorsoventrally and mediolaterally, and is flanked on either side by the endosseous labyrinths. The optic lobes, cerebellum, and flocculus are not evident in the brain endocast of either CMN 8920 or CMN 8919, and were likely small and covered by thick dura matter.

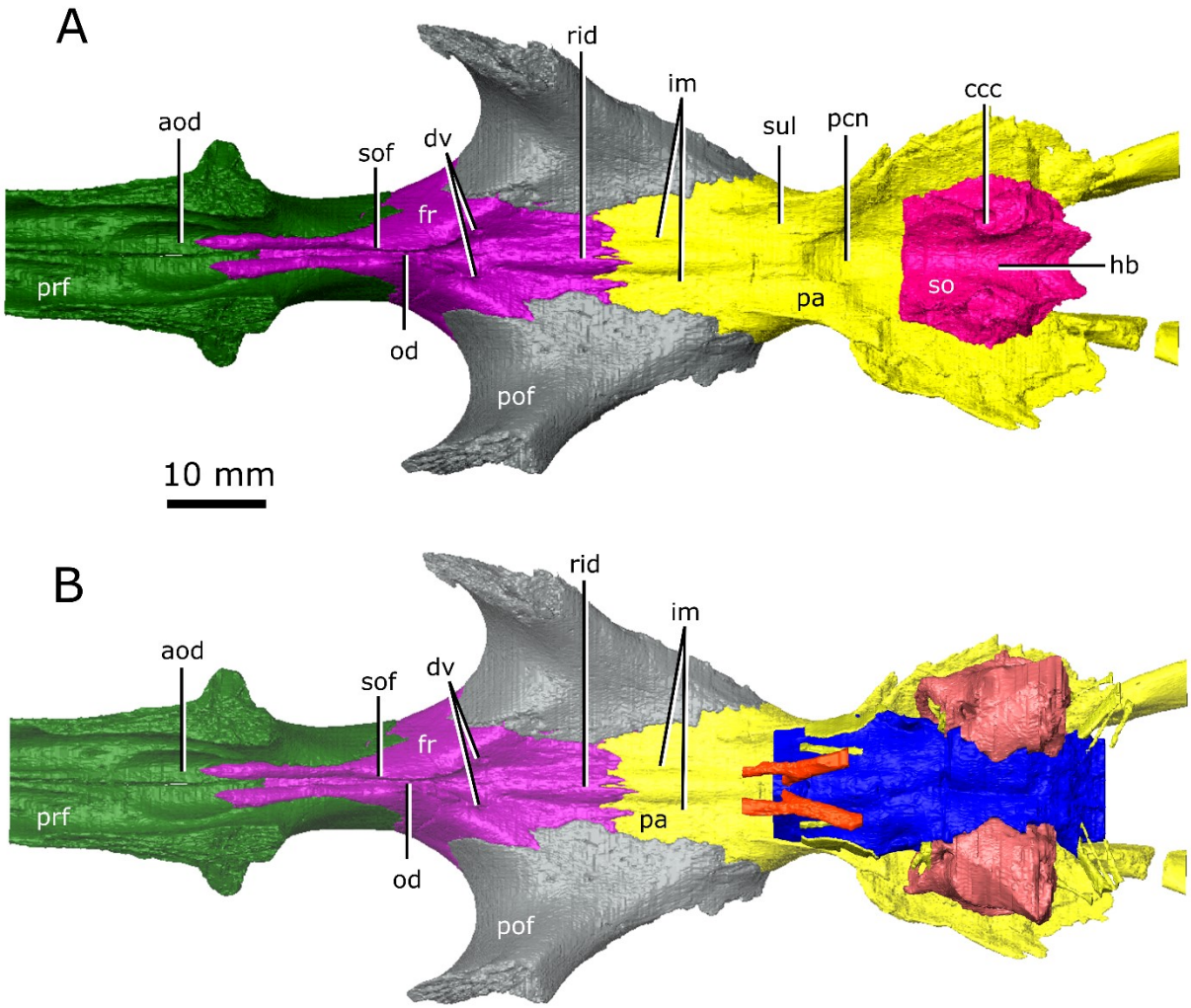

Figure 3.6: The isolated braincase roof (prefrontals, frontals, postfrontals, parietals, supraoccipital) of CMN 8920. **A** Ventral view of the isolated braincase roof; **B** Ventral view of the braincase roof with the segmented brain endocast (blue), endosseous labyrinth (pink), cranial nerves (yellow), and carotid arteries (red) in position. The braincase roof is slightly faded. *Abbreviations: aod, anterior of olfactory duct; ccc, canal for the crus communis; dv, diploic vein foramen; fr, frontal; hb, roof of the hindbrain; im, impressions of the olfactory tracks; od, olfactory duct; pcn, parietal concavity for the pineal body; pa, parietal; prf, prefrontal; pof,rid, ridge seperating the paired olfactory tracts; so, supraoccipital; sof, subolfactory flange; sul, area inundated with sulci.*

The parasphenoid forms the floor of the braincase medial to the endosseous labyrinths (Figure 3.7). A strong sagital keel is present on the dorsal surface of the parasphenoid that axially bisects the ventral portion of the endocranial cavity that housed the brain stem. The keel is evident in the CT data for CMN 8920 and is also present in fragmentary specimens (CMN 8922; ROM 688), but it is not seen in the CT data for CMN 8919, likely due to a combination of low scan resolution and damage during preperation. Fox (1968) described this region of the endocast as a deep basin, but did not comment on the presence of a dorsal keel on the parasphenoid. Posterior to the parasphenoid, the brain endocast is floored by the basioccipital and expands dorsally and mediolaterally, but does not reach the same width or height as it does anterior to the auditory system. The brain endocast extends posteriorly and opens to the foramen magnum.

Cranial nerves

The cranial nerve passages of CMN 8919 could not be observed due to low scanning resolution, but were clearly visable in CMN 8920. The following description is based predominantly on the cranial nerve passages of CMN 8920 (Figure 3.8).

The olfactory duct is preserved between the subolfactory flanges on the ventral surface of the frontals, extending from the posteriormost portion of the olfactory chambers of the nasal passages to the region occupied by the olfactory bulbs of the brain. As mentioned previously, the anterior braincase did not ossify in *Champsosaurus*, and the pathways for cranial nerves II-IV were not preserved. Dorsal to the pituitary fossa, there are large openings in the walls of the braincase that are bordered by the parietal dorsally, and the basisphenoid ventrally. This opening likely carried the trigeminal nerve (CN V) as it exited the endocast, but does not show evidence for the divergence of CN V into its three rami, CN V_1

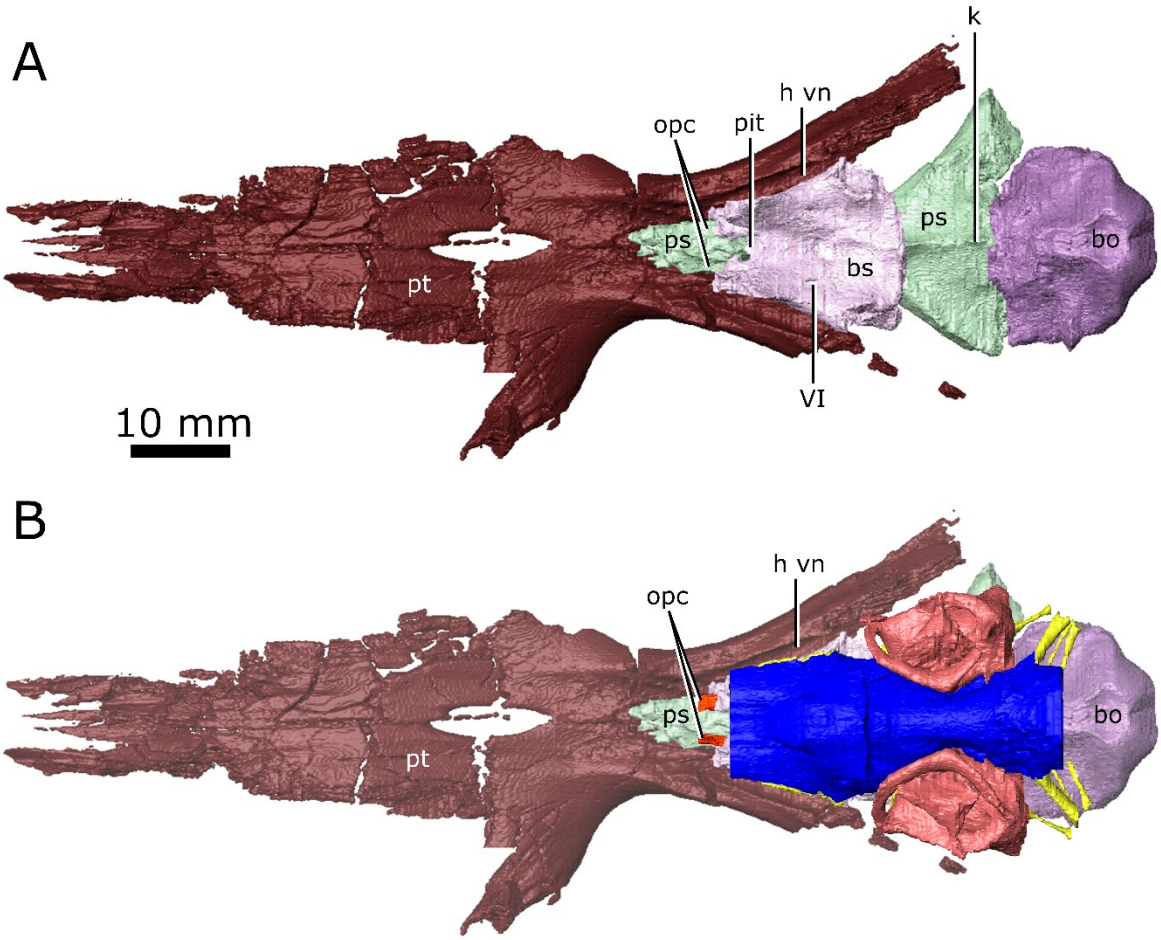

Figure 3.7: The isolated braincase floor (pterygoids, basisphenoid, parasphenoid, and basioccipital) of CMN 8920. **A** Dorsal view of the isolated braincase floor; **B** Dorsal view of the braincase floor with the segmented brain endocast (blue), endosseous labyrinth (pink), cranial nerves (yellow), and carotid arteries (red) in position. The braincase floor is slightly faded. *Abbreviations: bo, basioccipital; bs, basisphenoid; hvn, trough for the lateral head vein; k, parasphenoid keel; opc, opening for the palatine branch of the carotid artieries; pit, pituitary fossa; ps, parasphenoid; pt, pterygoid; VI, exit for cranial nerve VI.*

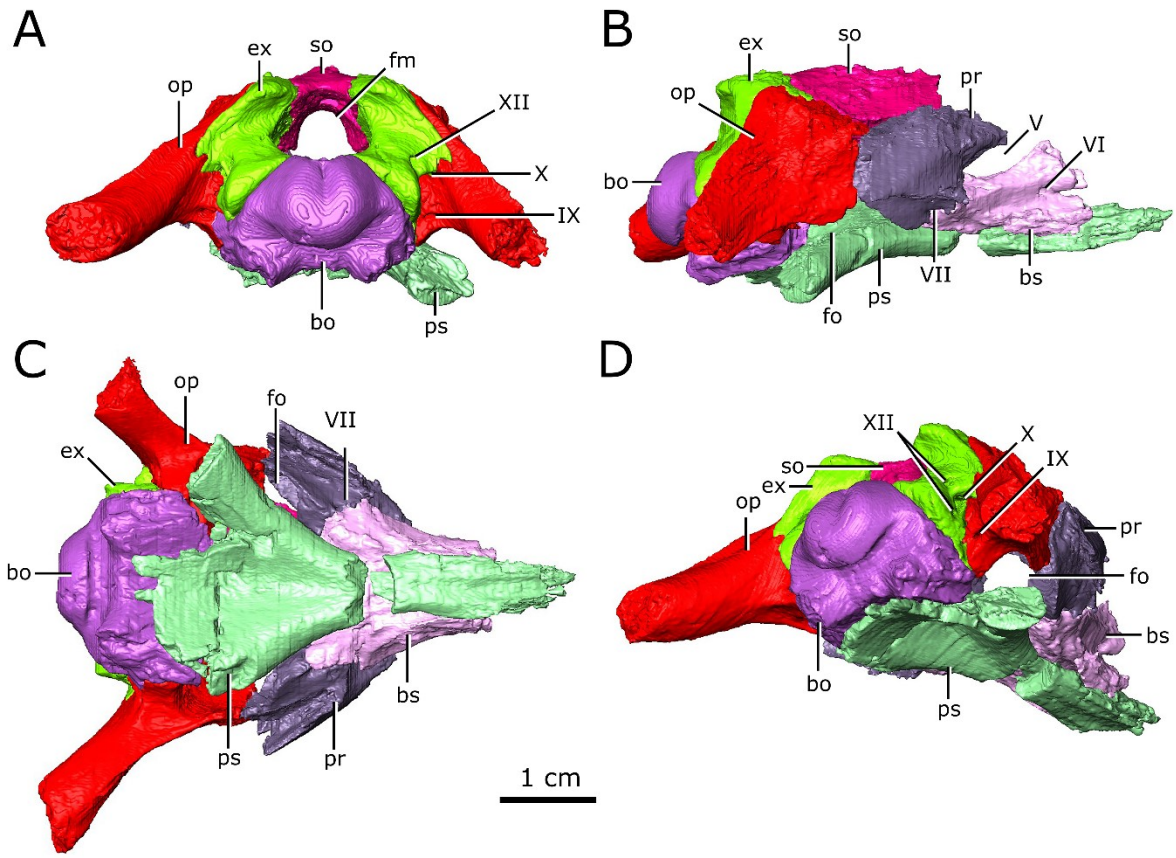

Figure 3.8: Cranial nerve exits of CMN 8920. **A** posterior view; **B** right lateral view; **C** ventral view; **D** posterolateroventral view. *Abbreviations: bo, basioccipital; bs basisphenoid; ex, exoccipital; fm, foramen magnum; fo, fenestra ovalis; op, opisthotic; pr, prootic; ps, parasphenoid; so, supraoccipital; V, exit for cranial nerve V; VI, exit for cranial nerve VI; VII, exit for cranial nerve VII; IX, exit for cranial nerve IX; X, exit for cranial nerve X; XI exit for cranial nerve XI; XII, exit for cranial nerve XII.*

(ophthalmic), CN V_2 (maxillary), and CN V_3 (mandibular), suggesting that this divergence would have occurred outside of the boney braincase. The only portion of the pathway of CN V_2 that preserved is in the snout, originating in the ventral rim of the orbit and extending anteriorly through the maxilla and premaxilla to the tip of the snout. The canal branches repeatedly along its length, where the branches lead to the outer surface of the skull and likely carried sensory nerves to innervate the snout. CN V_1 would have extended anterodorsally to inervate the orbit and integument of the snout (Romer and Parsons, 1977), but was supported by soft tissue and its pathway was not preserved. CN V_3 would have extended ventrally to inervate the lower jaw and jaw adductor muscles (Romer and Parsons 1977), but its pathway was not preserved in the skull.

Posterior to the pituitary fossa, a paired canal, which likely carried the abducens nerve (CN VI), extends anteriorly from the floor of the brain endocast and exits the lateral wall of the basisphenoid. The opening for the vestibulocochlear nerve (CN VIII) is wide in CMN 8920, a morphology that is also seen in other specimens of *Champsosaurus* (Fox, 1968). It is unlikely that the auditory nerve occupied the entirety of this space, and that the opening almost certainly would have been narrowed by cartilage in life. At the anteroventral edge of this opening, a paired canal which likely carried the facial nerve (CN VII) extends ventrolaterally from the floor of the endocast.

Interestingly, a canal originates at the posterior wall of the otic capsule and extends posteriorly through the opisthotic, and may have carried the glossopharyngeal nerve (CN IX). Among diapsids, the pathway for CN IX is highly variable, but is often in close association with the otic capsule due to its location within the metotic fissure in development (Bellairs and Kamal, 1981; Rieppel, 1985), and is known to exit through the posterior margin of the

otic capsule in other reptiles (Romer, 1956). This morphology is also reported in Dipnoi (de Beer, 1933), and suggests that the inner ear of *Champsosaurus* may have had cartilagenous divisions, and the nerve therefore would not have actually passed through the membranous labyrinth but would have been seperated from it by cartilage. A paired canal extends ventromedially from the endocast and exits between the opisthotics and exoccipitals. The relatively large diameter, and the position of the canals between the opithotics and exoccipitals, suggests that they are the metotic foramina, and would have carried the vagus nerve (CN X) and the accessory nerve (CN XI) (Romer, 1956; Bellairs and Kamal, 1981; Rieppell 1985). Posterior to the metotic foramina, two paired, narrow canals that carried branches of hypoglossal nerve (CN XII) exit ventromedially at the opening for the foramen magnum and extend posterolaterally through the exoccipitals.

Endosseous labyrinth

Dorsally, the anterior and posterior semicircular canals appear as distinct, tubular structures (Figure 3.9); however, the entire lateral canal of CMN 8919 is confluent with the dorsolateral surface of the pars inferior, as is the anterior half of the lateral canal of CMN 8920. This suggests that the endosseous labyrinth was poorly ossified in *Champsosaurus*, and that regions of the labyrinth, like the lateral canal, would have been supported by soft tissue and cartilage within the otic capsule in life. Additionally, the prootic, opisthotic, and supraoccipital fail to contact each other lateral to the labyrinth in CMN 8920, creating a cavity that projects dorsolaterally from the pars inferior. This cavity is absent in CMN 8919, suggesting that the otic region was better ossified in larger animals, although the lateral canal is no better preserved in CMN 8919 than it is in CMN 8920. The angle of the lateral canal

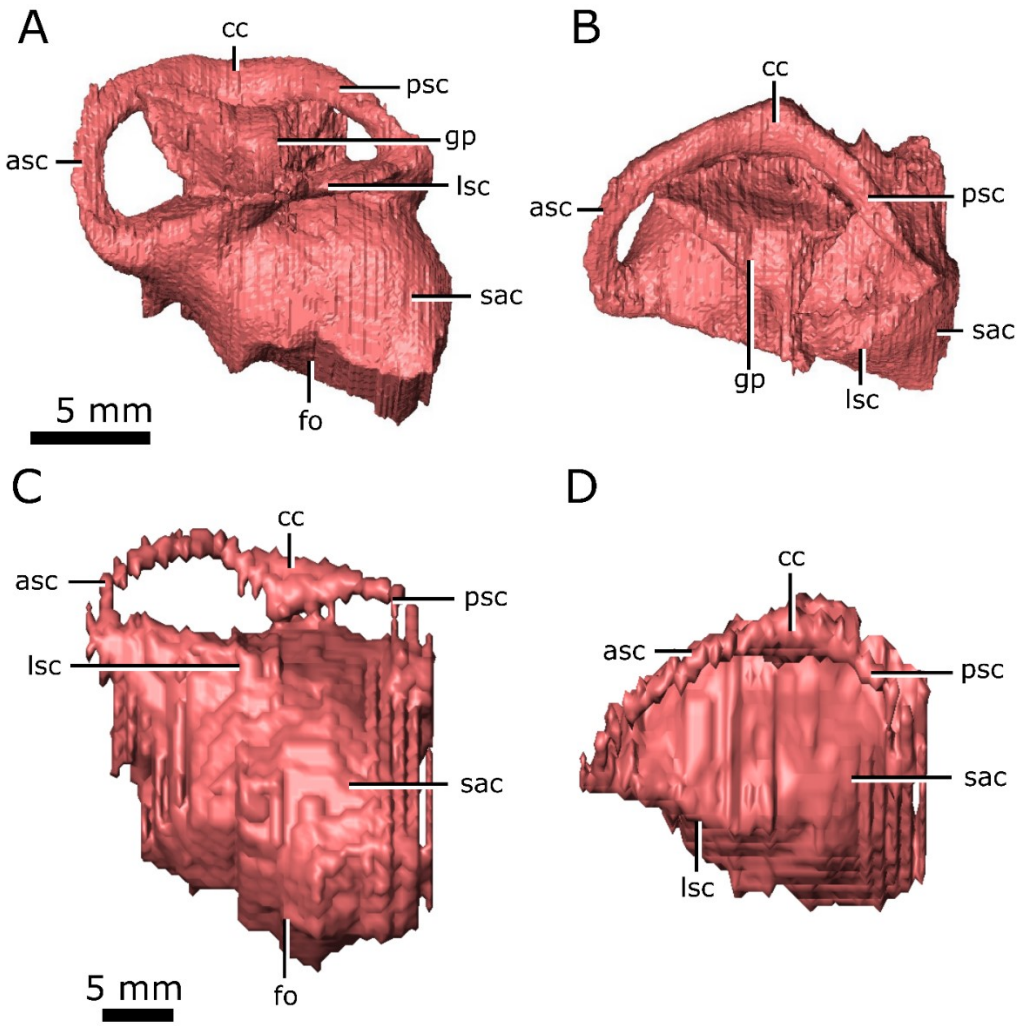

Figure 3.9: Left endosseous labyrinth of *Champsosaurus lindoei* (CMN 8920) in: **A** lateral view; and **B** dorsal view, and *Champsosaurus natator* (CMN 8919) in: **C** lateral view; and **D** dorsal view. *Abbreviations: asc, anterior semicircular canal; cc, crus communis, fo, fenestra ovalis; gp, unossified gap between the prootic, opisthotic, and supraoccipital; lsc, lateral semicircular canal; psc, posterior semicircular canal; sac, sacculus.*

from the long axis of the skull varies considerably between CMN 8920 and CMN 8919, where the lateral canal is oriented approximately 15.8° anteroventrally from the long axis of the skull in CMN 8920, and approximately 13.3° anterodorsally from the long axis of the skull in CMN 8919.

The ampullae of the anterior and lateral canals are small, but can be distinguished as an enlargement of the canals at their anteriormost extent. The ampulla of the posterior canal is not evident in the endosseous labyrinth, but would have been located at the posteriormost extent of the posterior canal. CMN 8920 and CMN 8919 lack distinct cochlear ducts, and the pars inferior forms a bulbous cavity ventral to the semicircular canals. The fenestra ovalis is located on the ventral surface of the pars inferior, with no portion of the endosseous labyrinth extending ventral to it. This is in contrast to the morphology of most reptiles, where the fenestra ovalis is located on the lateral surface of the pars inferior and the cochlear duct extends ventral to it.

Vasculature

The passages for the internal carotids are not visible in the CT data for CMN 8919, and the morphology of these arteries is based entirley on CMN 8920. The internal carotids entered the skull through passages on the ventral surface of the skull that passed between the contact of the parasphenoid and pterygoid, and extended anterodorsally towards the pituitary fossa. Ventral to the pituitary fossa, the canals fork, where the dorsal fork carried the cerebral artery that opened into the pituitary fossa, and the ventral fork carried the palatine artery and continued anteriorly until it opened on the dorsal surface of the pterygoid, anterior to the

basisphenoid. The path of the palatine artery anterior to the basisphenoid cannot be determined due to incomplete ossification of this region.

The lateral head vein sits in a deep trough formed by the quadrate ramus of the pterygoid, and the lateral wall of the basisphenoid. Fox (1968) stated that a channel is imprinted on the lateral wall of the clinoid process of the basisphenoid that drained the orbital sinus into the lateral head vein, but this channel is not present in CMN 8920. Additionally, Fox (1968) described a foramen penetrating the quadrate ramus of the pterygoid that carried the lateral head vein, but no such foramen is seen in either CMN 8920 or CMN 8919. Instead, the lateral head vein appears to have extended posteriorly along the trough formed by the pterygoid and basisphenoid and exited the skull lateral to the fenestrae ovales. Presumably, the vein would have been supported by soft tissue as it extended posteriorly towards the neck.

Fox (1968) also suggested that the groove imprinted into the lateral wall of the parietal and neomorph leading from the exit for CN V to the pterygoquadrate foramen is an impression of the stapedial artery; however, it seems more likely that this groove carried CN V_3, given its placement relative to the opening for CN V in the braincase.

Nasal cavity

Like the snout of *Champsosaurus*, the nasal passage of CMN 8920 is highly elongate, measuring approximately 14 cm from the anteriormost extent of the narial opening to the posteriormost extent of the olfactory chambers (Figure 3.10). An ossified internarial septum is absent, but longitudinal ridges at the confluence of the left and right vomers, and the midline of the internarial and nasal, suggest it would have been present as cartilage in life.

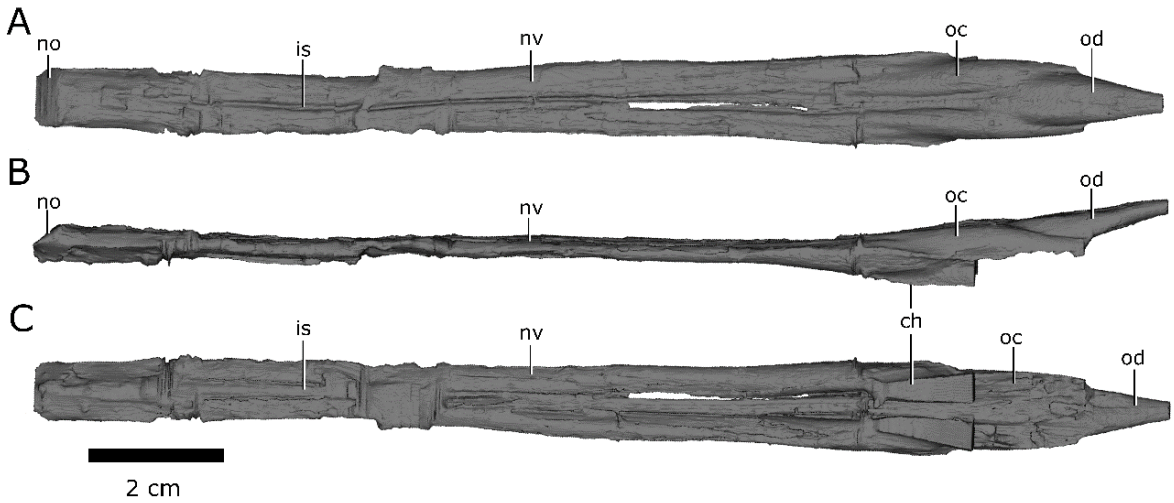

Figure 3.10: Left and right nasal passages of *Champsosaurus lindoei* (CMN 8920), in **A** dorsal view; **B** left lateral view; and **C** ventral view. *Abbreviations: ch, choana; is, ridge indicating the internarial septum; no, narial opening; nv, nasal vestibule; oc, olfactory chamber; od, olfactory duct.*

The nasal passages are ovoid in cross-section, each measuring approximately 0.8 cm in width, and 0.45 cm in height. The floor of the nasal passage is severely damaged, and several fragments of bone have been displaced dorsally into the nasal passage. The fragmentation is most prominent midway along the nasal passage, and along the posteriormost extent of the olfactory chambers. The dorsolateral walls of the olfactory chambers are well-preserved, revealing that the olfactory chambers are also elongate, measuring approximately 2.9 cm in length. The choanae open ventrally from the anterior floor of the olfactory chambers between the palatine laterally and the vomer medially. The single olfactory duct extends posterodorsally from the olfactory chambers towards the brain endocast, between the paired subolfactory flanges of the frontals (Figure 3.6), and narrows posteriorly to form the passage for the olfactory nerve (CN I). With the exception of fragmentation of the floor of the nasal passage, the osseous walls of the nasal passage are smooth, and there are no ridges present that are suggestive of turbinates.

Auditory capabilities

The mean best hearing frequency and best hearing range were plotted against the endocochlear duct length for the extant taxa from the data provided by Walsh et al. (2009). The length of the scaled and transformed pars inferior for CMN 8920 (-0.6887) was inserted into the derived equations of the regression lines (Figure 3.11), resulting in a best hearing frequency of 1691.3 Hz, and a best hearing range of 2740.4 Hz (overall best hearing range: 321.1 – 3061.5 Hz).

Geometric morphometrics of the semicircular canals

The PCA produced 34 PC axes, but only axes 1 through 3 will be discussed here (cumulative variation = 77.36%) because the remaining PC axes account for relatively little variance (less than 5% each). Plotting PC1 against PC2 (Figure 3.12) shows that PC1 (46.77% of variation) mostly represents curvature of the anterior semicircular canal and angling of the lateral canal relative to the rest of the labyrinth. Positive PC values represent a more elongated and curved anterior semicircular canal and an anteroventrally angled lateral canal, while negative PC values represent a shorter, less curved canal and an anterodorsally angled lateral canal. Birds, which plot towards PC1 positive, have the most extreme condition, with an anterior semicircular canal that arcs over the posterior semicircular canal and enters the crus comunis posteriorly, and have a steep anteroventrally angled canal relative to the rest of the labyrinth. PC2 (22.61% of variation) mostly represents torsion (out of plane curvature) of the lateral semicircular canal, where positive PC values represent less torion in the lateral canal, and negative PC values represent more torsion in the lateral canal. PC3 (7.98% of variation; Figure 3.13) represents a combination of variation in the out-of-plane curvature of the posterior canal, and the dorsoventral placement of the lateral canal, where positive PC values indicate a dorsally placed lateral canal, and negative PC values indicate a ventrally placed lateral canal.

When visualizing PC1 vs PC2 (Figure 3.12), three distinct groups are formed that appear separated by phylogeny: Aves (right), Lepidosauria (top left), and non-avian archosauromorphs (bottom left). Projecting a phylogeny (Appendix D) onto PC1 vs PC2 (Figure 3.14) clearly illustrates these groups, suggesting that phylogeny strongly influences grouping in this PCA. It should be noted that projecting the phylogeny onto PC1 vs PC2

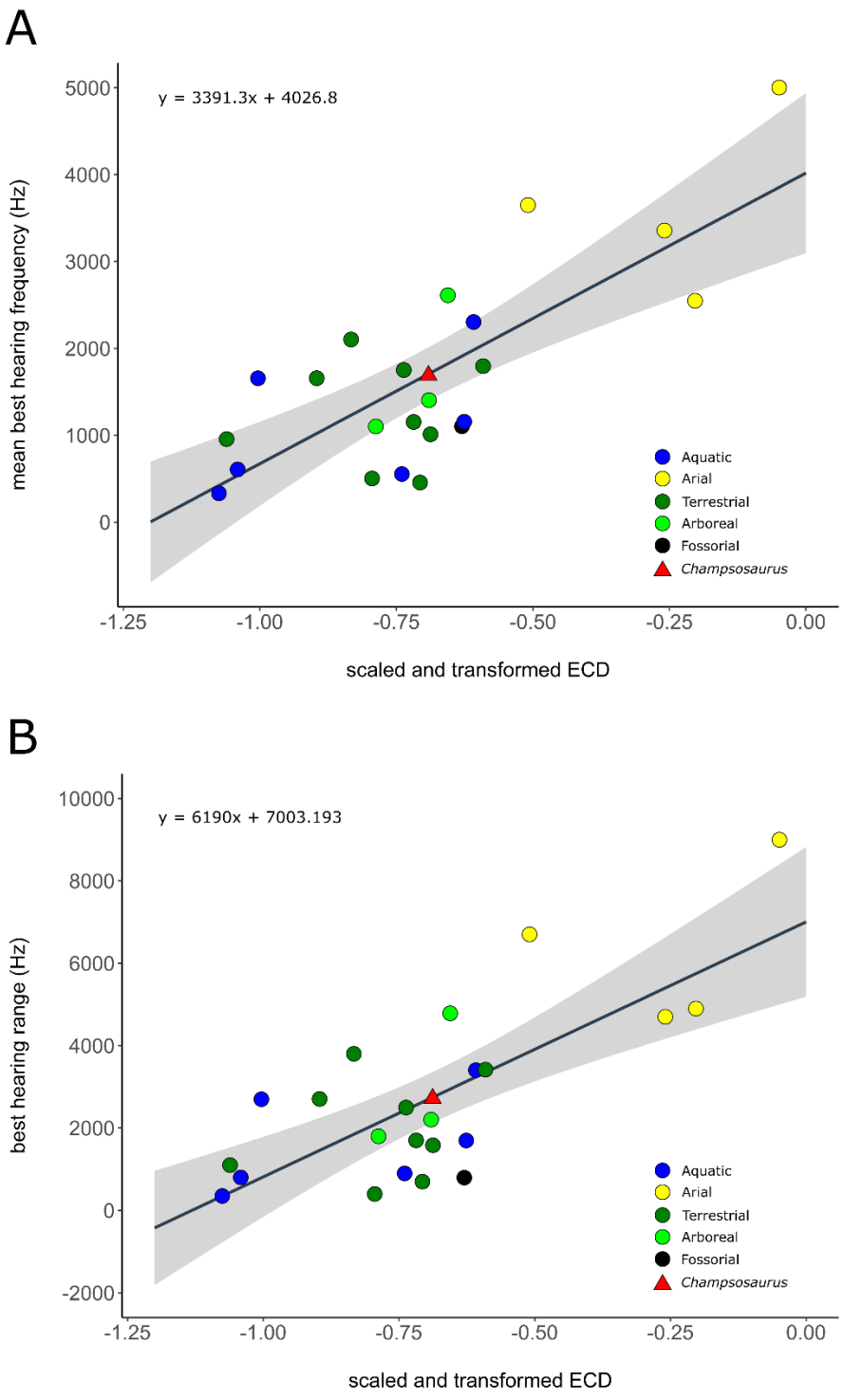

Figure 3.11: Correlation between scaled and transformed endocochlear duct length (ECD) and **A** mean best hearing frequency (y = 3391.3x + 4026.8; r^2 = 0.5825; *p* = 2.28e-05); **B** best hearing range (y = 6190x + 7003.193; r^2 = 0.5521; *p* = 4.875e-05) with ecologies coloured separately. Grey area indicates the 95% confidence interval of the regression line. Extant data from Walsh et al. (2009). Red triangle indicates the predicted value for *Champsosaurus lindoei* (CMN 8920).

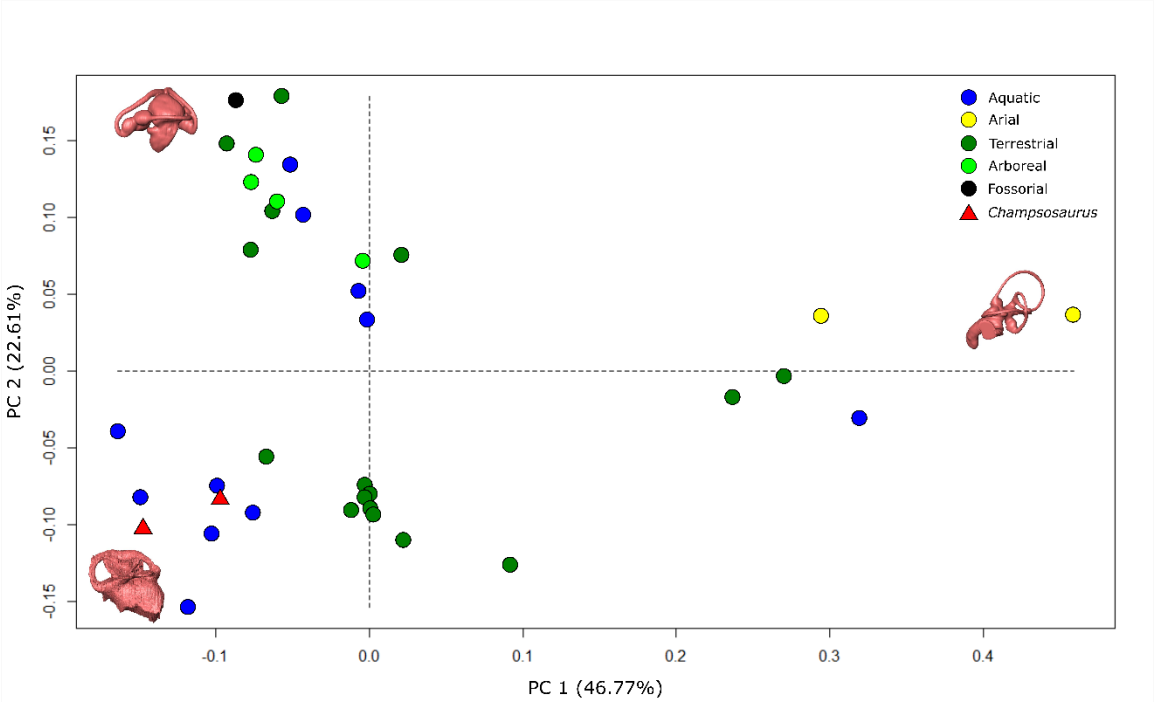

Figure 3.12: PC 1 vs PC 2, representing 69.38% of the total variation. Taxa are colour coded based on ecology. End-point morphologies: bottom left, *Champsosaurus lindoei*; top left, *Trachylepis laevis*; right, *Passer domesticus*.

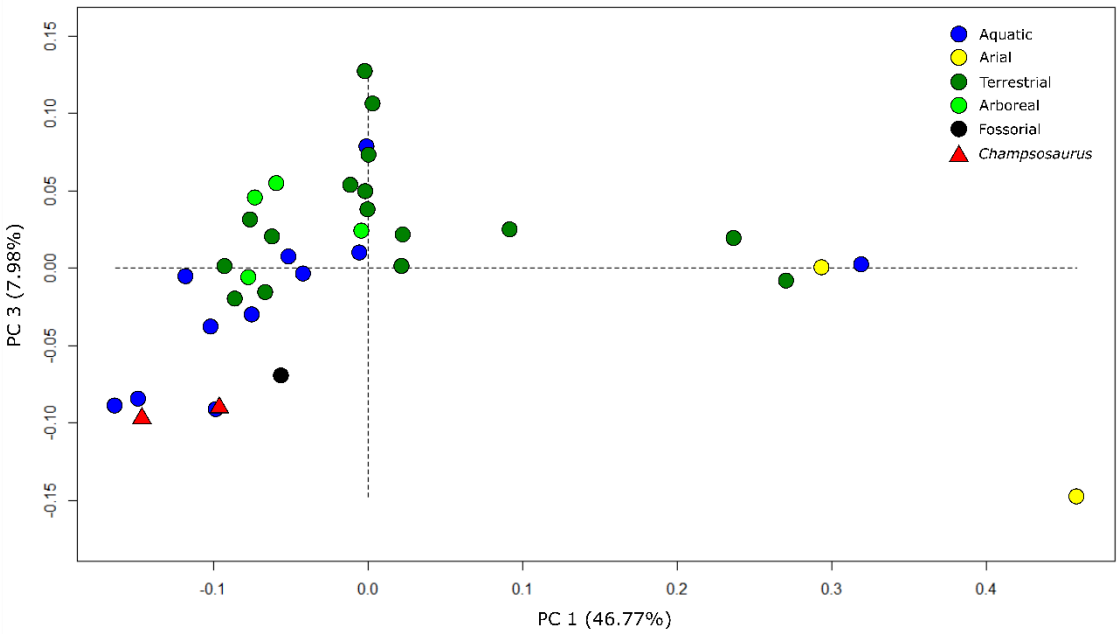

Figure 3.13: PC 1 vs PC 3 representing 54.75% of the total variation. Taxa are colour coded based on ecology.

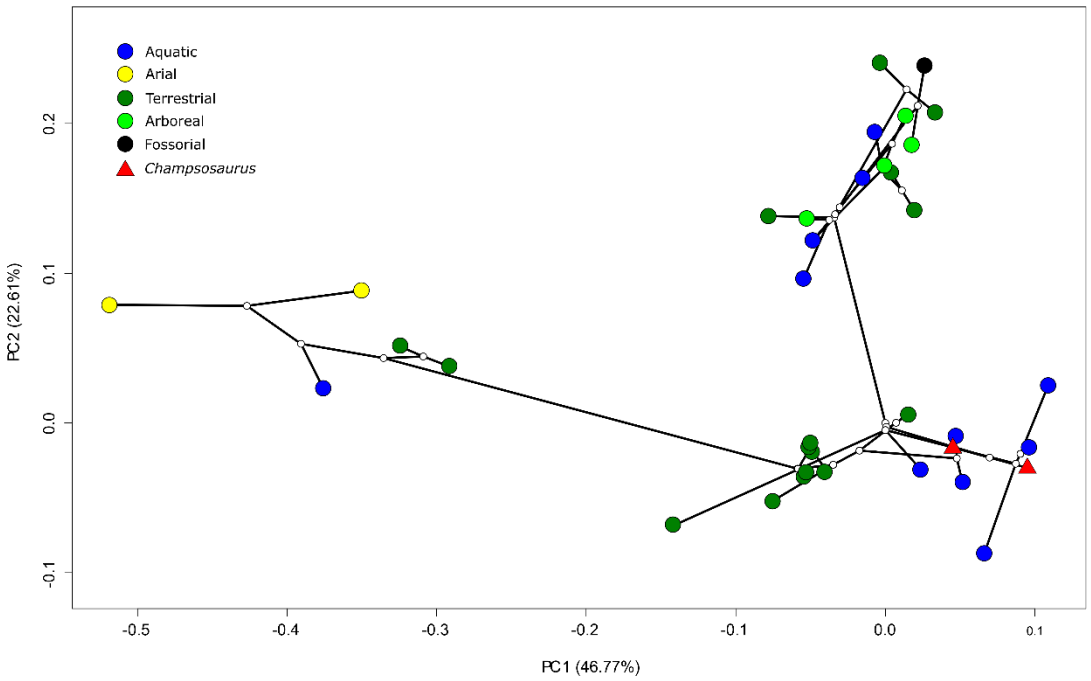

Figure 3.14: Time calibrated phylogeny (Appendix D) of included taxa projected into the morphospace of PC1 and PC2. Taxa are colour coded based on ecology.

(Figure 3.14) resulted in the PC scores being flipped along PC1; however, this PCA was created solely for visualization of the phylogeny in morphospace and the resulting PC scores were not used in the subsequent analyses. Therefore, the flipping of the PC scores along PC1 in Figure 3.14 does not influence the results of this study.

Both specimens of *Champsosaurus* plot close to the non-avian archosauromorphs, suggesting that *Champsosaurus* may share a close evolutionary history with this group. Within the non-avian archosauromorph group, the *Champsosaurus* specimens plot closest to the aquatic taxa (Figure 3.14; e.g., crocodilians and turtles), suggesting that the semicircular canals of *Champsosaurus* are most similar in morphology to aquatic archosauromorphs.

Phylogenetic signal was less than expected under Brownian motion ($K < 1$; Table 3.1) in both centroid size and canal morphology. The phylogenetic signalling in both centroid size and canal morphology was statistically significant ($p = 0.037$, and $p = 0.001$, respectively), suggesting that closely related species tend to have similarly sized labyrinths and similar canal morphologies.

ANCOVA (Table 3.2) indicates a moderate and significant relationship between ecology and canal shape ($R^2 = 0.39175$, $p = 0.0001$), and a weak, but significant, relationship between centroid size and canal shape ($R^2 = 0.09116$, $p = 0.0001$). The interaction between ecology and centroid size was also found to have a weak, but significant relationship with canal shape ($R^2 = 0.05988$, $p = 0.0128$).

PGLS (Table 3.3) indicates similar relationships to the ANCOVA, with a moderate and significant relationship between ecology and canal shape ($R^2 = 0.24871$, $p = 0.0007$), and a weak, but significant relationship between centroid size and canal shape ($R^2 = 0.06186$, $p = 0.0015$). The interaction between ecology and centroid size was also found to have a

Table 3.1: Bloomberg's K value and associated p-value for both centroid size and landmark coordinates of the endosseous labyrinths. Bloomberg's multivariate K statistic calculated using 1000 permutations. Bold indicates significance (alpha = 0.05).

	K_{mult} statistic	p-value
Centroid Size	0.0671	**0.037**
Coordinates (shape)	0.0833	**0.001**

Table 3.2: ANCOVA of ecology, centroid size, and the interaction between ecology and centroid size against canal shape. Bold indicates significance (alpha = 0.05). *Abbreviations: d.f., degrees of freedom; F, F statistic; MS; mean square; R^2, coefficient of determination; SS, sum of squares; Z, Z score.*

	d.f.	SS	MS	R^2	F	Z	p-value
Ecology	4	0.59945	0.149863	0.39175	5.7835	4.2934	**0.0001**
Centroid	1	0.13949	0.139485	0.09116	5.3830	4.1262	**0.0001**
Ecology: Centroid	3	0.09163	0.030542	0.05988	1.1787	2.2586	**0.0128**
Residuals	27	0.69963	0.025912	0.45722			
Total	35	1.53019					

Table 3.3: Phylogenetic generalized least squares of semicircular canal shape against ecology, and semicircular canal centroid size. Bold indicates significance (alpha = 0.05). *Abbreviations: d.f., degrees of freedom; F, F statistic; MS; mean square; R^2, coefficient of determination; SS, sum of squares; Z, Z score.*

	d.f.	SS	MS	R^2	F	Z	p-value
Ecology	4	0.027546	0.0068864	0.24871	4.0851	2.8319	**0.0007**
Centroid	1	0.006851	0.0068512	0.06186	04.0642	2.8702	**0.0015**
Ecology: Centroid	3	0.030843	0.0102811	0.27848	6.0989	3.7227	**0.0002**
Residuals	27	0.045515	0.0016857	0.41095			
Total	35	0.110755					

moderate and significant relationship with ecology ($R^2 = 0.27848$, $p = 0.0002$). It is interesting to note that the correlation coefficient for ecology and canal shape was lower in the PGLS than in the ANCOVA, and the correlation coefficient for the interaction of ecology and centroid size with canal shape was higher in the PGLS than in the ANCOVA. This is most likely because there is an interaction between ecology, centroid size, and phylogeny, and ecology and centroid size are not totally independent of phylogeny (Dickson et al., 2017). This is supported by the Bloomberg's K value for centroid size ($K = 0.0671$, $p = 0.037$), suggesting that centroid size is significantly influenced by phylogeny.

Visualization of the CVA (Figure 3.15; Figure 3.16) and posterior probabilities (Table 3.4) show that the ecological groups occupy significantly different regions of morphospace, except for the arboreal group. The arboreal group was significantly different from the aerial group, but was insignificantly different from both the aquatic and terrestrial groups, which may be due to the small sample size of arboreal taxa (n=4). The classification accuracy of the CVA was approximately 90.9%.

CV1 is mostly separated by PC1, where negative CV1 values represent greater curvature of the anterior canal and a dorsoventrally angled lateral canal. Aerial taxa plot towards CV1 negative, while arboreal, aquatic, and terrestrial taxa plot towards CV1 positive. Both *Champsosaurus* specimens plot towards CV1 positive, and *C. natator* plots farther towards CV1 positive than all other taxa (Figure 3.14). CV2 is mostly influenced by PC3, where positive CV2 values represent greater out-of-plane curvature of the posterior canal and a more dorsally placed lateral canal. Aquatic taxa plot towards CV2 negative, while arboreal, terrestrial, and aerial taxa plot towards CV2 positive. *Champsosaurus lindoei* and *C. natator* plot towards CV2 negative, and overlap with the

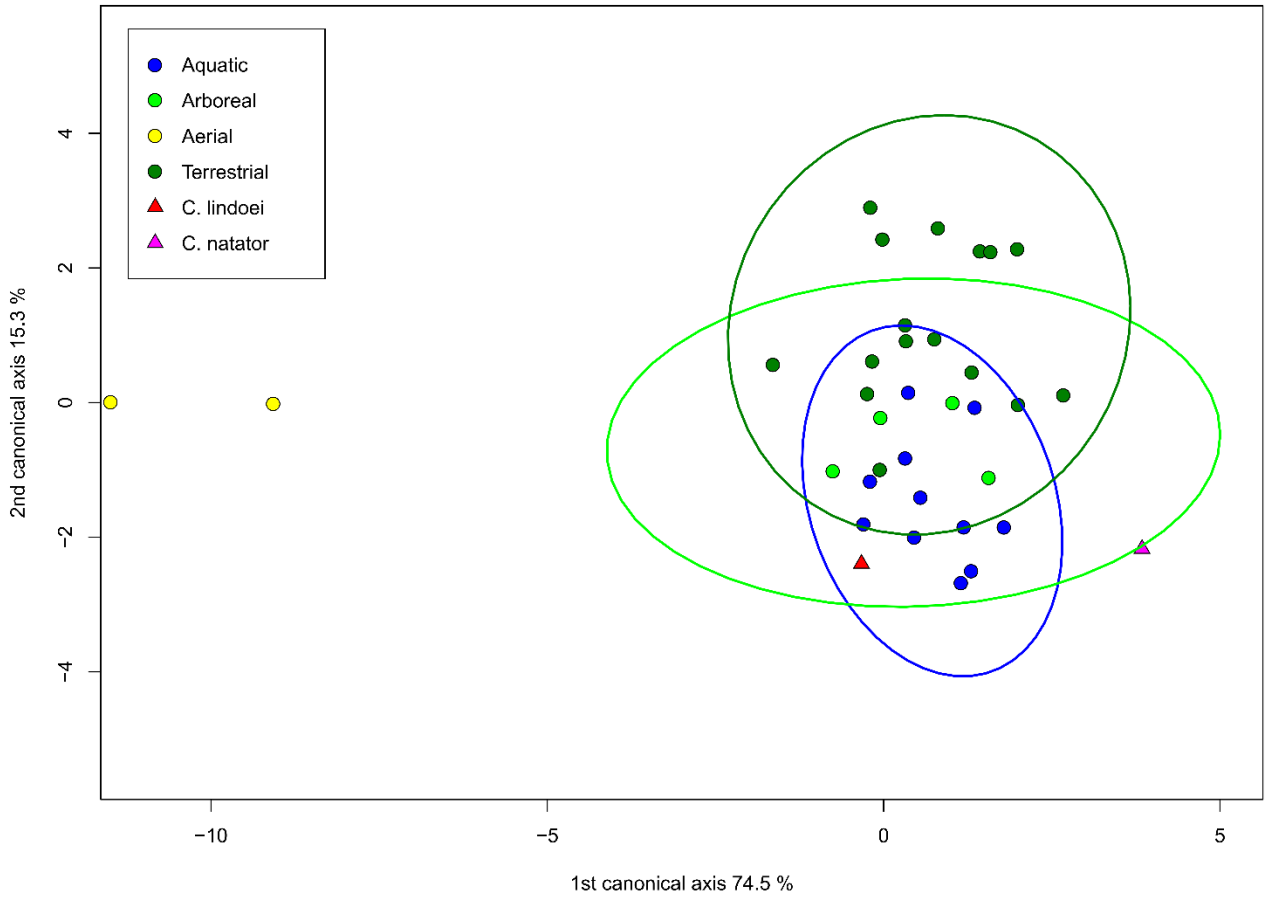

Figure 3.15: CV1 vs CV2 representing 89.8% of the total between-group variation. 95% confidence ellipses of each ecological group are plotted, except for the aerial group (due to low sample size).

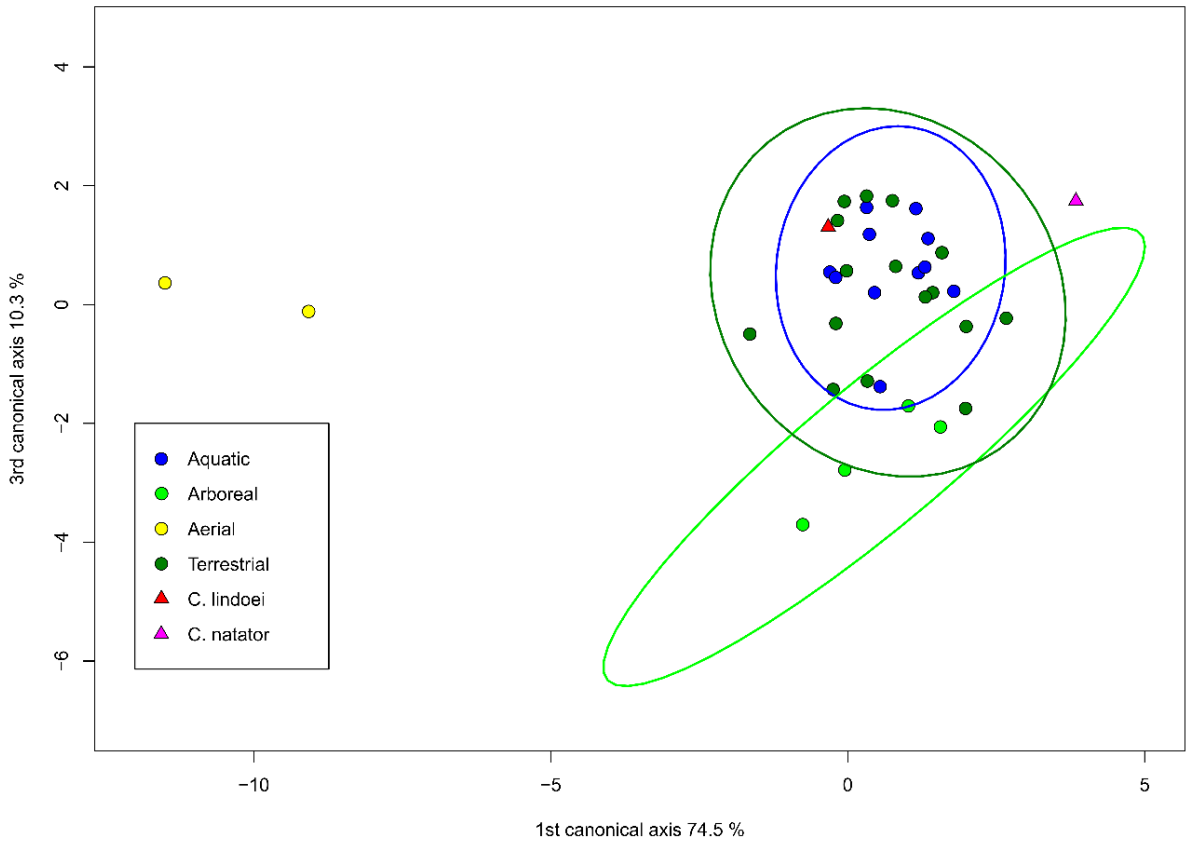

Figure 3.16: CV1 vs CV3 representing 84.8% of the total between-group variation. 95% confidence ellipses of each ecological group are plotted, except for the aerial group (due to low sample size).

Table 3.4: Posterior probabilities (10 000 permutations) of significant differences between the ecological groups based on Mahalanobis distances. $\alpha = 0.05$.

	Aquatic	Aerial	Arboreal	Terrestrial
Aquatic	-	0.0004	0.1355	0.0267
Aerial	0.0004	-	0.0009	0.0006
Arboreal	0.1355	0.0009	-	0.1077
Terrestrial	0.0267	0.0006	0.1077	-

aquatic group along CV2 (Figure 3.14). CV3 is mostly influenced by PC2, where negative CV3 values represent greater torsion of the lateral canal, and CV3 positive represents less torsion. Arboreal taxa plot towards CV3 negative, and aquatic, terrestrial, and aerial taxa plot towards CV3 positive. Both *Champsosaurus* species plot towards CV3 positive, and plot among the aquatic and terrestrial groups.

Posterior probabilities of Mahalanobis distances found that both *Champsosaurus* specimens occupy a significantly different region of morphospace from the arboreal, aerial, and terrestrial ecological groups, but do not occupy a significantly different region from the aquatic group (Table 3.5). *Champsosaurus lindoei* plots well within the 95% confidence ellipse for the aquatic group, and *C. natator* plots outside of the ellipse, but log-likelihood estimations assign both *Champsosaurus* specimens to the aquatic group (0.999).

Discussion

The brain endocast

Overall, the brain endocasts of CMN 8920 and CMN 8919 are typical of other early diapsids, such as some phytosaurs (e.g., *Pseudoplatus*; Holloway et al., 2013), and early turtles (e.g., *Proganochelys*; Lautenschlager et al., 2018) possessing large olfactory lobes, a large pineal body, and small optic lobes and flocculi. A major difference between the brain endocast of *C. lindoei* and *C. natator* is the variation in brain endocast flexure. *Champsosaurus lindoei* does not exhibit any flexure, while *C. natator* exhibits strong cerebral and pontine flexures. The cerebral and pontine flexures of CMN 8919 are both approximatley 22°, resulting in parallel cerebral and medullar axes that is typical of reptiles

Table 3.5: Posterior probabilities (10 000 permutations) and log-likelihood estimations of *Champsosaurus* species belonging to separate ecological groups. $\alpha = 0.05$. Posterior probabilities less than alpha suggest that *Champsosaurus* is significantly different from that ecological group.

	Log-likelihood	Posterior probability			
		Aquatic	Aerial	Arboreal	Terrestrial
Champsosaurus lindoei	Aquatic (0.999)	0.333	< 0.0001	< 0.0001	< 0.0001
Champsosaurus natator	Aquatic (0.999)	0.090	< 0.0001	< 0.0001	< 0.0001

(Griffin, 1989). Brain endocast flexure is known to vary substantially across taxa (e.g., nearly 0° in *Iguanodon*; Lauters et al., 2012; approximatley 55° in *Caiman crocodilus*; Hopson, 1979), but there is an overall trend towards greater flexure in smaller animals and less flexure in larger animals (Griffin, 1989). This is due to the negative allometric scaling of the brain, where smaller animals tend to have a proportionatley larger brain that is more restricted by the size limits of the skull and spacial limits from other cranial structures, such as the orbits (Platel, 1979; Hopson, 1979). As a result, smaller animals tend to have increased flexure of the brain endocast to accommodate the spacial restrictions of the skull anteroposteriorly (Hopson, 1979). This trend also holds true through ontogeny, where young animals tend to have greater flexure of the brain endocast that decreases as the animal grows (Hopson, 1979).

Champsosaurus violates this trend, where the smaller *C. lindoei* possesses no flexure, and the larger *C. gigas* possesses prominent flexure. This may also be due to spacial constraints in the skull, but is likely due to the dorsoventral compression of the skull, as opposed to anteroposterior constraint from the orbits. This is because the skull of *Champsosaurus* is quite long, but dorsoventrally flat, and the brain is more constricted dorsoventrally than it is anteroposteriorly. Therefore, smaller specimens of *Champsosaurus* likely lack flexure due to the limited space dorsoventrally, but the flexure becomes evident in larger individuals where the dorsoventral spacial limitations of the skull are less restricting. This should be explicitly tested in the future by comparing the ratio of braincase length to depth with the degree of brain endocast flexure in multiple specimens of *C. lindoei* and *C. natator*.

An unusual structure in the braincase of *Champsosaurus* is the dorsal keel on the midline of the parasphenoid. Fox (1968) suggested that this region of the endocast was

occupied by the 4th ventricle of the brain, but this is unlikely, given that the ventricles of the brain sit deep within the nervous tissue and do not press against bone (Gignac and Kley, 2014). The neurological structure that comprises the ventral portion of the brain stem is the medulla oblongata (Gignac and Kley, 2014), but this structure is typically small in reptiles and is not known to correlate with a ventral midline keel (e.g., *Anniella*, *Sceloporus*, and *Gerrhonotus*; Larsell, 1929; *Erythrosuchus*; Gower and Sennikov, 1996). Given the close proximity of the parasphenoid keel to the pars inferior of the endosseous labyrinths, it is possible that the enlarged pars inferior would have occupied part of this space, where the parasphenoid keel would have projected medially between the pars inferior, further expanding its size medially. This hypothesis is supported by the fact that the keel is only present in the region between the otic capsules. It is also possible that the dorsal keel represents a suture surface with a posterior cartilagenous extension of the overlying basisphenoid (Figure 3.7), which did not fossilize, similar to the cartilagenous basisphenoid observed in lissamphibians (Atkins et al., 2019).

Olfaction

Evaluation of olfactory capabilities in extinct taxa relies on measurements of the olfactory bulb (Zelenitsky et al., 2011), the region of the brain that detects and processes scent information. The walls and floor of the olfactory bulbs did not ossify in *Champsosaurus* and the size of these structures is therefore unknown. Olfactory capabilities in *Champsosaurus*, therefore, cannot be commented upon quantitatively, but basic comparisons can still be made. The olfactory stalks (comprised of the anterior olfactory bulbs that process olfactory information, the posterior olfactory peduncles that transmitted sensory

information from the olfactory bulbs to the cerebrum; Kuhlenbeck, 1977; Zelenitsky et al., 2011) of *Champsosaurus* comprise half of the length of the entire brain endocast, suggesting that olfaction was a powerful sense for this animal. This is similar to extinct phytosaurs, and early turtles, which also possessed large and elongated olfactory stalks and a powerful sense of smell (Lautenschlager and Butler, 2016; Lautenschlager et al., 2018), suggesting that powerful olfaction was an ancestral trait to reptiles.

McGowan (1973) and Kirton (1983) noted that ichthyosaurs lack a secondary palate, and that the nasal cavities open into the buccal cavity (Marek et al., 2015). This possibly allowed the fleshy nostrils to remain open when the ichthyosaur was submerged, enabling water to enter the nasal passages for the detection of waterborne odours (Marek et al., 2015). In contrast, it has been suggested that *Champsosaurus* possessed narial tubes on the ventral surface of the secondary palate that extended the nasal passages posterior to the choanae (Erickson, 1985). The nasal passages of *Champsosaurus* therefore were unlikely to have opened into the buccal cavity, and *Champsosaurus* would not have been capable of allowing water to enter the nasal passages through the nostrils. Therefore, it is unlikely that *Champsosaurus* was capable of detecting waterborne odours, and olfaction would have been restricted solely to airborne odours.

Erickson (1985) noted that *Champsosaurus* may have possessed a well-developed sense of smell due to the pronounced olfactory chambers of the nasal passages, a conclusion supported here by the prominent olfactory chambers and olfactory duct of CMN 8920 (Figure 3.10) that appear comparable to those of modern crocodilians (Witmer and Ridgely, 2008). He also stated that a well-developed sense of smell in *Champsosaurus* would be inconsistent with its aquatic habits, because detecting airborne odours would have had little

importance for detecting food, but Erickson (1985) did not consider other advantages of high olfactory acuity. Within Mammalia, aquatic taxa tend to have a weaker sense of smell than terrestrial taxa (Gittleman, 1991), but the influence of ecology on olfactory acuity has not been studied in reptiles. Modern crocodilians have a well-developed sense of smell that is used for detecting airborne odours for locating food (Scott and Weldon, 1990) and mates (Cummins and Bowie, 2012). Although *Champsosaurus* was likely piscivorous (Erickson, 1985) and detecting airborne odours would not have provided an advantage for locating aquatic prey, *Champsosaurus* may still have used a developed sense of smell for identifying other nearby animals. It is also possible that the developed sense of smell of *Champsosaurus* allowed it to hunt terrestrial prey in nearshore environments. If so, this hunting behaviour must have been restricted to small terrestrial prey items because the gracile skull of *Champsosaurus* was inadequate for acquiring large bodied animals (James, 2010).

Lu et al. (1999a) suggested that the neochoristodere *Ikechosaurus* may have possessed turbinates to better facilitate olfaction or thermoregulation, but there is no evidence of turbinates in the nasal passage of the *Champsosaurus* specimens examined here. It is still possible that *Champsosaurus* possessed nasal turbinates, or turbinate-like structures, but these would have been cartilaginous because they left no osteological correlate on the walls of the nasal passage.

Vision

There is no evidence for prominent optic lobes in the *Champsosaurus* endocast. Additionally, there is no evidence of the flocculus on the *Champsosaurus* endocast, suggesting that this brain structure was also small, and/or obscured by dura matter. A small

flocculus is typical of early diapsids (Holloway et al., 2013), suggesting that *Champsosaurus* had, at best, average visual acuity for a basal reptile.

Some effort has been made to estimate diel activity and colour perception in extinct taxa (Schmitz and Motani, 2011), but these estimates rely on dimensions of the scleral ring, which *Champsosaurus* lacked. Erickson (1985) suggested that *Champsosaurus* possessed good binocular vision based on the raised position of the orbits on the dorsal surface of the skull and their close spacing, but estimates of the degree of overlap between the visual fields of the two eyes is hindered because there is no way to determine the exact size, position, and orientation of the eyes within the orbits.

Hearing

Based on the length of the pars inferior, the estimated best hearing frequency of *Champsosaurus* is 1691.3 Hz, and the best hearing range is 2740.4 Hz (overall best hearing range: 321.1 – 3061.5 Hz). Among the extant taxa examined by Walsh et al. (2009), this is most comparable to the American crocodile (*Crocodylus acutus*; best hearing frequency: 1650 Hz; best hearing range: 2700 Hz; overall best hearing range: 300 – 3000 Hz) and the Indian spiny-tailed lizard (*Uromastyx hardwickii*; best hearing frequency: 1650 Hz; best hearing range: 2700 Hz; overall best hearing range: 300 – 3000 Hz). It should be noted that the estimated hearing capabilities of *Champsosaurus* are higher than those of most other aquatic reptiles included in this dataset, such as the spectacled caiman (*Caiman crocodylus*; best hearing frequency: 1150 Hz; best hearing range: 1700 Hz: overall best hearing range: 300 – 2000 Hz), American alligator (*Alligator mississippiensis*; best hearing frequency: 550 Hz; best hearing range: 900 Hz; overall best hearing range: 100 – 1000 Hz), common

snapping turtle (*Chelydra serpentina*; best hearing frequency: 600 Hz: best hearing range: 800 Hz; overall best hearing range: 200 – 1000 Hz), and the green sea turtle (*Chelonia mydas*; best hearing frequency: 325 Hz; best hearing range: 350 Hz; overall best hearing range: 150 – 500 Hz). This may be because the pars inferior of tetrapods also contains soft tissue structures around the cochlea, such as the lagenar macula (Wever, 1978; Gleich et al., 2005), and the length of the pars inferior is therefore an overestimate of the length of the cochlea. This would bring the estimated hearing capabilities of *Champsosaurus* closer to that of most modern crocodiles and turtles.

A striking feature of the endosseous labyrinth of *Champsosaurus* is the absence of a distinct cochlear duct, and the apparently large size of the sacculus in the pars inferior. Ancestrally, fully aquatic vertebrates (such as fish) detected sound vibrations through the water via the saccular otolith (Popper and Lu, 2000), where sound vibrations pass directly through the body to the inner ear due to the similar density of animal tissues to water (Ketten, 2008). The saccular otolith is much denser than the water and surrounding soft tissues, and vibrates out of sync with the body and surrounding water when stimulated by sound waves, allowing sound vibrations to be detected by ciliary hair cells (Ladich and Winkler, 2017). Many fish, therefore, possess an enlarged saccular otolith to better detect these waterborne vibrations (Popper and Lu, 2000). In air, sound detection via the sacculus is ineffective because the body is far denser than the surrounding air, and most air vibrations are not able to conduct through the skull to reach the inner ear (Christensen et al., 2015). As a result, several lineages of tetrapods (e.g., Lepidosauria, Archosauria, Testudines, Synapsida, and some parareptiles such as *Bashkyroleter*, *Macroleter*, and Millerettidae; Gow 1972; Müller and Tsuji, 2007; Sterli and Joyce, 2007; Müller et al., 2018) have independently evolved a

tympanum, an air-filled middle ear, and specialized middle ear ossicles (e.g., the stapes), which convert sound pressure from the air to vibrational motion of fluid within the specialized lagena (cochlea) for detection (Christensen et al., 2015). In water, this tympanic system is redundant because sound vibrations are able to conduct directly through the body to reach the ear. Consequently, some secondarily aquatic tetrapods, such as cetaceans, eliminated the tympanum and encased the inner ear within the bony tympanic bulla, which is only connected to the skull by cartilage and connective tissue (Mooney et al., 2012). It is assumed that waterborne vibrations easily penetrate the body due to their similar density, and are conducted to the tympanic bulla through the fatty canal of the lower jaw (Ladich and Winkler, 2017). The reason for the differences in ear morphology between fully aquatic vertebrates, such as fish and cetaceans, is because cetaceans descend from ancestors that detected sound via the cochlea, and the pre-existing structures of the ear in cetaceans were simply modified to facilitate sound detection in water (Ladich and Winkler, 2017).

Sea turtles use a combination of both the cochlea and saccular otolith to enable sound detection in water and air. This is facilitated by stapedosaccular strands, unique to turtles, that connect the stapes and fenestra ovalis to the sacculus (Piniak et al., 2012). It is thought that the stapedosaccular strands facilitate the transmission of vibrations between the sacculus and cochlea for better aquatic sound detection (Lenhardt et al., 1985), but the performance of these strands is poorly understood. Interestingly, sea turtles also posses an enlarged sacculus and reduced cochlear duct relative to other reptiles, but it is not known whether the sacculus tends to be larger in sea turtles than in tortoises. Freshwater turtles also possess a large, circular sacculus that is best adapted for detecting low frequency vibrations (300 – 500 Hz)

underwater, although the tympanum and cochlea still play a major role in sound detection (Christensen-Dalsgaard et al., 2012).

Given the inferred highly aquatic lifestyle of *Champsosaurus*, the question arises as to whether they relied solely on sound detection via the sacculus in water, or if they also possessed a tympanum to increase sensitivity to airborne sounds. In all tympanic amnitoes, there is a distinct otic notch (conch in lepidosaurs; Evans, 2008) in the posterior margin of the skull that correlates with the location of the tympanum on the lateral surface of the skull (Clack and Allin, 2004; Müller et al., 2018). In crown-group diapsids, such as lepidosaurs, archosaurs, and turtles, the otic notch is formed by the posterior margin of the quadrate, but in parareptiles, the otic notch is formed by the posterior margin of the squamosal and quadratojugal (Müller et al., 2018). The quadrate of *Champsosaurus* is broad and dorsoventrally flat, forming the floor of the temporal region, but is not a component of the lateral surface of the skull. Instead, the quadratojugal and squamosal comprise the majority of the lateral surface of the skull. Although the posteroventral margin of these elements is slightly concave when viewed laterally, the concavity does not approach the prominent otic notch used to infer the presence of a tympanum in extinct lineages (Gow 1972; Müller and Tsuji, 2007; Müller et al., 2018). The absence of a prominent otic notch suggests that *Champsosaurus* lacked a tympanum, likely a retention of the basal amniote condition (Gardner et al., 2010).

Sobral and Müller (2019) used osteological correlates established in Crocodyliformes (Montefeltro et al., 2016) to infer the presence of a tympanum in the rhynchosaur *Mesosuchus*, which lacks a distinct otic notch in the quadrate; however, they emphasized that this was done with caution due to the specialization of the crocodyliform outer ear (e.g.,

presence of an osseous meatal chamber and fleshy ‘ear lid’), from basal archosauromorphs. These correlates proposed by Montefeltro et al. (2016) will not be used here, because they relate primarily to the lateral surface of the quadrate (which does not form the lateral surface of the skull of *Champsosaurus*, as it does in Crocodyliformes), and the usefulness of these correlates outside of Crocodyliformes has not been established.

Since *Champsosaurus* lacks a prominant otic notch, and therefore likely lacked a tympanum, *Champsosaurus* also likely did not possess a stapes specialized for transmitting sound vibrations to the inner ear. Currently, no stapes has been described in *Champsosaurus*, and its relationship to other cranial elements remains unknown, but it likely would have articulated with the quadrate (and possibly the hyoid elements, as in *Sphenodon*) and acted primarily to support the skull. Among amniotes (and tetrapods more generally), the function of the stapes as a structural element is the basal condition (Carroll, 1980), and is also present in early diapsids, such as *Youngina* (Gardner et al., 2010). The role of the stapes as a supporting element in the skull of basal diapsids supports the hypothesis proposed in Chapter 2 that the choristoderan neomorph may be homologous with the stapes, given the location of the neomorph lateral to the otic capsule and medial to the quadrate, and the presence of a foramen (the pterygoquadrate foramen) penetrating the bone; however, the holotype specimen of the early choristodere, *Coeruleodraco*, may have both the neomorphic bone and stapes preserved, but the authors emphasized that the identification of the stapes was hindered due to low CT scan resolution (Matsumoto et al., 2019), and the identification of the element is therefore uncertain.

Regardless of the exact morphology of the stapes in *Champsosaurus*, it can be concluded that the stapes was unlikely to have played a major role in sound detection due to

the absence of a tympanum. In modern atympanic taxa, such as *Sphenodon* and Serpentes, the stapes articulates with the quadrate, and sound detection is limited to low frequency vibrations (Gans and Wever, 1976; Christensen et al., 2012) that are better able to conduct through the skull and transmit to the inner ear (Christensen et al., 2012). This has led researchers to suggest that extinct atympanic reptiles likely would have had similar low frequency hearing capabilities to *Sphenodon* (e.g., Gardner et al., 2010). In *Champsosaurus*, the absence of a tympanum, the possible presence of a stapes that was not specialized for detecting sound, and the reduction of the cochlea, suggest that the inner ear would have been ineffective at detecting airborne sounds, although they still may have been able to detect some low frequency sounds through vibrations of the skull.

In some aquatic amniotes, thickening of ossifications in and around the middle ear better facilitates the transmission of sound vibrations to the inner ear (Mooney et al., 2012; Ladich and Winkler, 2017). Sobral and Müller (2019) inferred good auditory capabilities in the rhynchosaur *Mesosuchus* based partially on the location of the fenestra ovalis deep within the bone of the lateral wall of the otic capsule, which may have facilitated the transmission of sound vibrations. In *Champsosaurus*, the fenestra ovalis is not located deep within the bone of the otic capsule, and it is therefore unlikely that the bone of the otic capsule facilitated the detection of sound vibrations. However, many secondarily aquatic amniotes (e.g., cetaceans, sea turtles, and sea birds) possess adipose tissue within the middle ear, thought to have evolved convergently to better transmit waterborne vibrations through the skull to the inner ear (Kitten, 2008; Willis et al., 2013). Adipose tissue is also present in the middle ear of the terrestrial *Sphenodon*, and may reflect the ancestral diapsid condition (Clack, 1997; Tucker, 2016). *Champsosaurus*, therefore, may also have possessed adipose tissue around the otic

region to better transmit waterborne sound vibrations to the inner ear, although these tissues were not preserved and their presence cannot be proven quantitatively.

Given the inferred highly aquatic lifestyle of *Champsosaurus*, it is probable that they did not have a need for detecting airborne sounds, and so reduced the size of the cochlea and enlarged the sacculus to better detect waterborne vibrations, similar to the inner ear morphology of modern sea turtles, although the latter are tympanic (Lenhardt et al., 1985; Christensen-Dalsgaard et al., 2012). The sacculus is best able to detect low frequency vibrations, and as a result, animals that use the sacculus to detect sound information, such as fish, are only able to detect low frequency sounds, and usually have a narrow range of hearing. This also holds true for turtles, which have an enlarged sacculus and reduced cochlea, and are only able to detect low frequency sounds (Walsh et al., 2009). It therefore stands to reason that the estimated hearing capability of *Champsosaurus* based on the equations derived from Walsh et al. (2009) is overestimated, and these animals would have been adapted to detecting low frequency water borne vibrations, similar to modern sea turtles.

An interesting similarity also exists between the inner ear of *Champsosaurus* and many fossorial tetrapods. An enlarged sacculus in fossorial taxa better facilitates the detection of substrate vibrations (Olori, 2010; Maddin and Sherratt, 2014; Yi and Norell, 2015). This seems unusual for *Champsosaurus*, given the inferred highly aquatic lifestyle of these animals, but the large sacculus of *Champsosaurus* may have also facilitated the detection of substrate vibrations. It is possible that *Champsosaurus* spent a great deal of time at the bottom of slow-moving bodies of water, such as rivers and lakes, and detected sound vibrations via the substrate, similar to some modern urodeles (Hilton, 1949; Mason, 2007).

The ventral orientation of the fenestra ovalis may have facilitated this activity, increasing the sensitivity of the sacculus to vibrations received ventrally from the substrate; however, the highly aquatic plesiosaur *Dolichorhynchops* also possessed a ventrally oriented fenestra ovalis (Sato et al., 2011), but presumably did not detect substrate vibrations due to its habitat in the pelagic waters of the Western Interior Seaway. The plesiosaur endosseous labyrinth has not been formally described, so the morphology of the cochlea and sacculus cannot be properly compared with *Champsosaurus*, but figures illustrated by Neenan et al. (2017) suggest that plesiosaurs may have possessed a short cochlea and large sacculus, similar to *Champsosaurus* and sea turtles. This suggests that a short cochlea and large sacculus (and possibly a ventrally oriented fenestra ovalis) are typical for an aquatic reptile, and that the inner ear of *Champsosaurus* is well adapted for hearing in an aquatic environment.

Since most species that vocalize produce sound within the range of their own hearing (Walsh et al., 2009; and references therein), if *Champsosaurus* produced vocalizations, they were likely restricted to low frequency sounds. Crocodilians are well known for their vocalizations, consisting of grunts, bellows, and/or hisses, but these vocalizations tend to be restricted to above water behaviour (Verne et al., 2009), although infrasonic body vibrations that travel predominantly through water are known to occur during courtship (Young et al., 2014). Aquatic turtles, however, vocalize extensively underwater, producing a wide variety of sounds, such as clicks, hoots, chirps, and grunts, that can range from low frequency (approximately 100 Hz) to high frequency (approximately 2500 Hz; Giles et al., 2009; Ferrera et al., 2013). These vocalizations are most common during the breeding months, suggesting that aquatic turtles may use vocalizations as a mating display (Giles et al., 2009).

Giles et al. (2009) proposed that these vocalizations may be particularly important to aquatic turtles due to limited line-of-sight from turbid water and habitat complexity.

Although the exact sounds produced by *Champsosaurus* cannot be determined, the inner ear suggests that if they vocalized, these animals likely produced low frequency vocalizations when submerged, similar to some modern turtles. These vocalizations may have been used in a similar manner to modern freshwater turtles, and aided in locating individuals in a turbid fluvial system with a limited line-of-sight. Vocalizations above water are also possible, but the ability of *Champsosaurus* to detect airborne vibrations was likely poorer than waterborne vibrations due to the absence of a tympanum, and the reduction of the cochlea.

Phylogeny and the endosseous labyrinth

Bloomberg et al. (2003) determined that most traits other than body size tend to show less phylogenetic signal than expected under Brownian motion ($K < 1$), an observation that is supported here by the low K value associated with canal morphology. Despite the low K value, the data presented in figures 3.11 and 3.13, and Table 3.1 demonstrate that there is a strong phylogenetic signal in the morphology of diapsid semicircular canals. Three distinct groups are apparent when plotting PC1 vs PC2: Aves, Lepidosauromorpha, and Archosauromorpha (Figure 3.12; Figure 3.14). Both *Champsosaurus* specimens plot among the non-avian archosauromorphs, supporting some phylogenetic assessments that place Choristodera as a stem-group of early archosauromorphs (e.g., Evans, 1990; Lee, 2013). Given the strength of the phylogenetic signal on semicircular canal shape over large phylogenetic scales, inner ear morphology may provide a good method for discerning

evolutionary history in phylogenetically ambiguous taxa. This has significant implications for choristodere phylogeny because the early evolution of the group is poorly understood, and recent phylogenies have failed to resolve their position within Neodiapsida (Ezcurra, 2016; Simoes et al., 2018).

Ideally, a larger sample size would be used in the PCA, but this is hindered by relatively low variation in some extant groups (e.g., modern archosaurs are solely Aves and Crocodylia), and the limited abundance of fossil CT data. Despite this, the data presented here provide novel evidence supporting an archosauromorph origin for Choristodera, but their position within Archosauromorpha remains uncertain. The morphology of the inner ear may be used as a character in future phylogenies to evaluate the systematics of Choristodera, but is beyond the scope of this study. Additionally, turtles plot among the non-avian archosauromorphs, supporting a growing body of morphological (Bhullar and Bever 2009) and molecular (Wang et al. 2013) evidence for an archosauromorph origin of Pantestudines (Crawford et al., 2015).

Unfortunately, the position of the ancestral diapsid canal morphology in morphospace is unknown because CT data for basal diapsids are lacking, and the morphology of the inner ear is often unpreserved; however, the ancestral amniote semicircular canal morphology is inferred as short and simple (Müller et al., 2018), based on the morphology of *Youngina* (Gardner et al., 2010), and some early synapsids (Laaß, 2016; Araujo et al., 2017). CT data of the inner ear of the stem-diapsid *Youngina* could not be acquired, and therefore, were not included in this analysis.

Significant phylogenetic signal ($p = 0.037$) was also observed in centroid size, but was less than expected under Brownian motion ($K = 0.0671$), consistent with previous

studies that have found significant phylogenetic signal in centroid size (e.g., Dickson et al., 2017). This phenomenon is possibly due to the significant correlation between centroid size, ecology, and canal shape (Table 3.2; Table 3.3). Several studies have found that semicircular canals with a larger radius of curvature, and therefore a greater centroid size (Dickson et al., 2017), tend to be more sensitive to angular movement (Spoor et al., 2002; Witmer et al., 2003). Agile species therefore tend to have canals with a greater radius of curvature than sedentary species (Spoor et al., 2007; Billet et al., 2012). Both ecology and canal shape are also known to be strongly influenced by phylogeny (Losos, 2008; Dickson et al., 2017), and the close relationship of centroid size with ecology and canal shape makes the strength of phylogenetic signaling unsurprising. The close correlation between centroid size and ecology is also evident in the PGLS, where the interaction effect of centroid size and ecology (R^2 = 0.27848) is greater than the effects of centroid size (R^2 = 0.06186) or ecology (R^2 = 0.24871) alone. Although beyond the scope of this study, future analyses should compare centroid sizes between distinct ecological groups to describe possible patterns in the variation of centroid size.

Ecology and the endosseous labyrinth

It has repeatedly been suggested that canal morphology is closely associated with ecology (e.g., Boistel et al., 2011; Billet et al., 2012; Pfaff et al., 2015; Neenen et al., 2017; Palci et al., 2018), but as discussed above, the morphology of the canals also carries a strong phylogenetic signal (Dickson et al., 2017). Shape analyses have repeatedly been conducted on reptiles, but have focused on relatively closely related groups, such as snakes (Yi and Norell, 2015) or squamates as a whole (Boistel et al., 2011). Previous studies have also

demonstrated that semicircular canal morphology may converge between separate lineages when they have similar ecologies, but within reptiles, these studies have also focused on relatively closely related taxa (e.g., anolis lizards; Dickson et al., 2017; Serpentes; Palci et al., 2018) and have not investigated the influence of ecology on larger evolutionary scales. The data presented here suggest that, despite the strength of phylogenetic signaling on such large scales, the morphology of the semicircular canals is additionally influenced by ecology (Table 3.2; Table 3.3).

Some studies (e.g., Malinzak et al., 2012; Berlin et al., 2013) have suggested that the orthogonality of mammal semicircular canals is more closely associated with canal sensitivity than canal shape, where species that move dynamically tend to have canals oriented closer to 90 degrees from one another than species with less dynamic movements. Along the PCAs there is no obvious difference in orthogonality from PC maxima to minima, suggesting that orthogonality is not a major component of the morphological variation in diapsid semicircular canals. In the future, canal angle could be tested separately by measuring the angles between the semicircular canals and testing for differences via PGLS, following the methods of Malinzak et al. (2012).

Among non-avian archosauromorphs included in this analysis, the aquatic taxa plot negatively along PC1, unlike the terrestrial taxa, suggesting that the former possess less curved anterior semicircular canals and a lateral canal that is angled more anterodorsally than the latter. This seems unusual, given that aquatic taxa are able to move in three spatial dimensions, whereas terrestrial animals typically move within only two dimensions, and thus all three canals should be more curved to increase sensitivity in all dimensions in aquatic taxa (Georgi and Sipla, 2008). In contrast, the majority of terrestrial non-avian archosauromorphs

(e.g., dinosaurs and *Triopticus*) included in this study possess a larger anterior canal; however, this may be due to an enlarged flocculus.

Among the lepidosauromorphs, ecological groups do not separate as cleanly in the PCA as they do among the non-avian archosauromorphs, probably due to the strength of phylogenetic signalling (Figure 3.14), but subtle trends are still apparent. Aquatic lepidosaurs tend to plot positively along PC1 and negatively along PC2 compared to terrestrial, arboreal, and fossorial taxa, suggesting that the aquatic lepidosaurs exhibit a more curved anterior canal, and a lateral canal that is angled more anteroventrally. This coincides with the notion that aquatic taxa require greater sensitivity to angular movement than terrestrial taxa due to differences in movement in water than on land, but this does not explain why the arboreal taxa do not also exhibit such curvature. The arboreal lepidosauromorphs mostly plot with the terrestrial taxa, which is unusual, given that they too move through their environment in three dimensions. The lack of difference between the terrestrial, arboreal, and fossorial ecological groups within Lepidosauromorpha may be because animals with similar ecologies can interact with their environment in different ways (Maddin and Sherratt, 2014). Within arboreality, taxa may occupy regions high in the canopy, along trunks, within low shrubs, or on branches, and interact with the environment differently due to these more subtle differences in ecology (Dickson et al., 2017). Within anolis lizards, these different arboreal ecological groups are known to have subtly different canal morphologies (Dickson et al., 2017), and this may explain the variation seen in canal shape within ecological groups in this study. Additionally, some arboreal and aquatic reptiles may not have the same dynamic behaviour of aerial taxa (or even the fast-moving behaviour of some arboreal mammals such as sciurids), and instead may have a similarly sedentary, slow moving lifestyle to their

terrestrial counterparts. Speed of movement is known to correlate with canal shape in other lineages (Spoor et al., 2007; Malinzak et al., 2012), and therefore may also influence the morphology of diapsid semicircular canals. Unfortunately, no study thus far has investigated differences between the dynamics or speed of movement of similarly sedentary (or dynamic) arboreal, aquatic, and terrestrial reptiles, so this similarity is speculative at present. This possible similarity of movement, however, may explain the insignificant difference of the arboreal group from the terrestrial and aquatic groups. Future studies could include more precise ecological bins than what was used here to incorporate the speed of movement (e.g., the arboreal group could be split into 'dynamic arboreal' and 'sedentary arboreal') to investigate how it is correlated with canal shape in diapsids.

Among Aves, taxa are clearly separated along PC1 by ecology, where aerial taxa plot the farthest towards PC1 positive, terrestrial taxa plot towards PC1 negative, and aquatic taxa plot in between those two groups. This suggests that aerial birds possess more curved anterior canals and a lateral canal that is angled more anteroventrally relative to the rest of the labyrinth than aquatic birds, whereas aquatic birds possess more curved anterior canals and a lateral canal that is angled more anteroventrally relative to the rest of the labyrinth than terrestrial birds. This supports the hypothesis that animals living in three dimensional environments, such as the air or water, require higher sensitivity to movement than terrestrial animals. It should be noted that this phylogenetic group is the smallest included in this analysis (n = 5), and a greater sample size is needed to properly determine ecological patterns in canal morphology in these taxa.

The lack of difference between the arboreal group and other groups in the CVA (Figure 3.4) may simply be due to the small sample size of arboreal taxa (n = 4). Aerial taxa

clearly differ from other ecological groups along CV1, and tend to have greater curvature of the anterior canal, and a lateral canal that is angled more anteroventrally than other taxa. The aquatic, terrestrial, and arboreal groups overlap significantly along CV1, suggesting that these groups have similar curvature of the anterior canal, and angle of the lateral canal. Aquatic taxa are most separated from the other groups along CV2, and tend to have less out-of-plane curvature of the lateral canal and a more ventrally placed lateral canal than the other ecological groups. Terrestrial taxa are also most separated from the groups along CV2, but show the opposite trend to aquatic taxa, and tend to have more out-of-plane curvature of the lateral canal and a more dorsally placed lateral canal than the other ecological groups. Aerial and arboreal taxa show no difference from one another along CV2, and are intermediate between the aquatic and terrestrial groups. Arboreal taxa are most separated from the other groups along CV3, and tend to have greater torsion of the lateral canal than the other groups, which strongly overlap with one another along CV3.

The similarities in the semicircular canal morphology within each ecological group may suggest some convergence in the morphology of the canals; however, this seems unlikely given that the birds, non-avian archosauromorphs, and lepidosaurs that have similar ecologies occupy separate regions of PCA morphospace, suggesting that there is no convergence in canal morphology on large evolutionary scales. This should be explicitly tested in the future to quantitatively determine if this is true (e.g., by fitting Hansen models using Akaike Information Criterion (AIC); Ingram, 2014).

Within the PCA, both *Champsosaurus* species plot among the aquatic non-avian archosauromorphs, suggesting that semicircular canal morphology of *Champsosaurus* was adapted to an aquatic lifestyle; a canal morphology characterized by shorter, less curved

canals, less out-of-plane curvature of the posterior canal, a more ventrally placed lateral canal, and less torsion of the lateral canal. This conclusion is further corroborated by the CVA, which plots both *Champsosaurus* species closest to the aquatic group.

A notable difference in morphology between the labyrinths of *C. lindoei* and *C. natator* is the angle of the lateral semicircular canal relative to the long axis of the skull (Figure 3.9). The lateral canal of *C. lindoei* is angled approximately 15.8° anteroventrally to the long axis of the skull, and the lateral canal of *C. natator* is angled approximately 13.3° anterodorsally to the long axis of the skull, a difference of approximately 29°. Previously, the angle of the lateral canal relative to the long axis of the skull has been used to reconstruct head posture in extinct taxa (e.g., Taylor et al., 2009), but some evidence suggests that the angle of the lateral canal is highly variable and does not accurately reflect head posture (Marugán-Lobón et al., 2013). The variation in the lateral canal of *Champsosaurus* supports the growing body of evidence suggesting that the angle of the lateral canal is highly variable, as *Champsosaurus* species are thought to have had similar ecologies and behaviour to one another (Erickson 1972) and are therefore unlikely to have had significantly different habitual head postures.

The relationship between semicircular canal morphology and ontogeny is poorly understood, and there is not enough information to comment on whether the variation in canal morphology between CMN 8920 and CMN 8919 is ontogenetic. Slow moving taxa, such as sloths, have greater variation in canal morphology than most animals due to their slow-moving lifestyle that has lessened selective pressures on the morphology of the semicircular canals (Billet et al., 2012). It is possible that the variation in canal shape in *Champsosaurus* is due to a sedentary lifestyle, but a much larger sample size is needed to

determine if the variation in *Champsosaurus* canal morphology is atypical for reptiles. A study describing the semicircular canals of several individuals within each species of *Champsosaurus* would also describe whether the variation in morphology between CMN 8920 and CMN 8919 is typical for the genus, or is due to interspecific variation between *C. lindoei* and *C. natator* (Cerio and Witmer, 2019).

Posterior probabilities of Mahalanobis distances demonstrate that the *Champsosaurus* species occupy significantly different regions of the CVA morphospace from the arboreal, terrestrial, and aerial groups, but are insignificantly different from the aquatic group (Table 5). Additionally, log-likelihood estimates strongly support the inclusion of the *Champsosaurus* specimens within the aquatic group (log likelihood = 0.999; Table 5). This supports previous notions based on skeletal and sedimentological evidence (Erickson, 1985) that *Champsosaurus* was adapted for an aquatic lifestyle.

Conclusions

The detailed analysis of the braincase of two specimens of *Champsosaurus* revealed it was a poorly ossified structure. The morphology of the brain endocast is similar to that of other basal archosauromorphs, possessing an enlarged pineal body and olfactory bulbs, and reduced optic lobes and flocculi. Although the olfactory ability of *Champsosaurus* cannot be estimated quantitatively due to lack of ossification, the olfactory stalks of the brain endocast and olfactory chambers of the nasal passages are quite large, and likely facilitated good olfaction. There is no evidence of turbinates in the nasal passage of *Champsosaurus*, and if *Champsosaurus* did possess these structures, they were likely entirely cartilaginous and left no osteological correlate. The small size of the optic lobes and flocculi suggest that

Champsosaurus had, at best, average sight for a basal archosauromorph. Based on the length of the pars inferior, the hearing capabilities of *Champsosaurus* were typical for a reptile, but this is likely an overestimate of the hearing capabilities due to lack of constraint on cochlear length presented in the endosseous labyrinth reconstruction. An expansion of the sacculus within the pars inferior of *Champsosaurus* is interpreted as conferring sensitivity to low frequency sounds and vibrations, similar to modern turtles. Posterior probabilities demonstrate that the morphology of the semicircular canals of *Champsosaurus* are most similar to other aquatic reptiles, suggesting that the semicircular canals of *Champsosaurus* was adapted for an aquatic lifestyle.

At present, this is the first study to analyse the morphology of reptile semicircular canals across Diapsida. The PCA suggests that non-avian archosauromorphs possess significantly different canal morphologies in comparison to lepidosauromorphs due to high phylogenetic signalling in the morphology of the semicircular canals. The *Champsosaurus* species and turtles plot among the non-avian archosauromorphs, supporting previous hypotheses that these groups share a close relationship with basal archosauromorphs.

A larger dataset should be used in the future to include more arboreal taxa to determine if this ecological group is significantly different from the aquatic and terrestrial groups. Convergence in the morphology of the semicircular canals was not evident here, but this should be explicitly tested to determine if this is true. Future studies should use more precise binning than what was used here (e.g., the arboreal group could be divided into ‘dynamic arboreal’ and ‘sedentary arboreal’) to more accurately describe the animals’ behaviour in relation to the morphology of the semicircular canals, and investigate how the morphology of the canals relates to movement. Finally, an avenue for further research would

be to conduct a more thorough analysis of amniote semicircular canal morphology. This would be done by expanding beyond Diapsida, and involving both extant and extinct taxa from other lineages (e.g., synapsids) to elucidate evolutionary trends of the semicircular canals across Amniota.

Chapter 4: Conclusions and future work

The current study sought to address aspects of the evolution and morphology of the choristoderan reptile, *Champsosaurus*. The diversity and systematics of Choristodera were reviewed, with particular emphasis on the systematics of *Champsosaurus*, to illustrate the diversity of choristoderan taxa, and to identify gaps in our knowledge of *Champsosaurus*. Two specimens of *Champsosaurus* were analyzed by means of micro-computed tomography scanning to: elucidate the morphology of the cranial elements in three dimensions, comment on the presence and morphology of the putative neomorphic bone, and illustrate the neurocranial anatomy of *Champsosaurus* to infer the behaviour and sensory ability of these animals.

Choristodere taxonomy and systematics

There are several issues within choristodere systematics that must be resolved to stabilize the taxonomy of the group. Possible solutions to these issues were proposed here, but they deserve further attention in the future to adequately address them. Firstly, the type species of *Champsosaurus*, *C. annectens*, is invalid, and *Champsosaurus* is therefore unavailable for use as the genus name, or for use as the root of the family name, Champsosauridae (Article 10.6-10.7, International Code of Zoological Nomenclature [ICZN]). The principle of priority (Article 23.3.5, ICZN) states that if a name is invalid, the next oldest synonym is to be used in its place. If there are no valid synonyms, a new name must be established instead (Article 23.3.5, ICZN). *Champsosaurus annectens* does not have a valid synonym, and according to the Code, a new name must be established for

Champsosaurus. This would cause considerable confusion in the literature, as *Champsosaurus* is a well-known taxon found throughout the Upper Cretaceous and Paleocene deposits of North America. Instead, the Commission should be petitioned to establish a new type species, maintaining the validity of *Champsosaurus*. The best replacement species to act as type would be *C. natator*, because it is well represented, possesses all features that are encompassed by the modern understanding of the genus, and is contemporaneous with *C. annectens* (Erickson 1972).

Secondly, the systematics of the genus and the higher group, Choristodera, need revision. Although there are many phylogenies describing the interrelationships of choristoderan genera (e.g., Matsumoto et al., 2013; Matsumoto et al., 2019), the evolutionary relationships of *Champsosaurus* species to one another are unknown (Gao and Fox 1998). This is likely because some of these species have not been revised in over 100 years (e.g., *C. laramiensis* and *C. ambulator*; Brown 1905) and the currently established diagnostic features are not adequate to use in a character matrix. Gao and Fox (1998) established the species *C. lindoei*, and revised the diagnosis for *C. natator* and *C. gigas*. They suggested that the type specimen for *C. albertensis* does not possess diagnostic features, but other specimens from the Horseshoe Canyon Formation (TMP 86.12.11; UALVP 930; TMP 95.11.1) appear similar to the type specimen, and may possess features that differentiate *C. albertensis* from other species of *Champsosaurus*. They did not comment on the validity of the remaining species, *C. laramiensis*, *C. ambulator*, and *C. tenuis*, simply stating that these taxa need revision. To properly assess the interrelationships of *Champsosaurus* species, *C. laramiensis*, *C. ambulator*, and *C. tenuis* need to be revised. The three specimens mentioned by Gao and Fox (1998) that may pertain to *C. albertensis* should be described in detail, and their features

compared with other species to determine if the features proposed by Gao and Fox (1998) are indeed diagnostic of the species. Once diagnostic features have been established for all *Champsosaurus* species, a character matrix should then be formed to facilitate cladistic analyses to describe the relationships of these species to one another.

Several of the features used to differentiate *C. lindoei* from *C. natator* (e.g., snout length and width, lower temporal bar curvature, skull ornamentation) are known to vary with skull size (Russell 1956), raising the possibility that these traits vary due to ontogeny. Gao and Fox (1998) stated that the supposed size similarity between the sympatric species *C. lindoei* and *C. natator* was strong evidence against these species being ontogenetic variants of a single species, but an exhaustive comparison of these species has yet to be made. To address this possibility, histological sections could be taken from limb bones of *C. lindoei* and *C. natator* specimens to compare the age of the individuals at the time of death. If it is found that *C. lindoei* specimens are typically younger than *C. natator* specimens, this would support the hypothesis that these species are actually ontogenetic variants of the same species.

Finally, both Choristodera and Neochoristodera lack phylogenetic definitions. Gao and Fox (1998) provided a rudimentary definition, but this does not adequately describe the evolutionary history of the group, nor the subsequently discovered taxa. A node-based definition would be most appropriate for both Choristodera and Neochoristodera due to the uncertainty regarding their position within Neodiapsida (e.g., Ezcurra, 2016). Choristodera would then be defined as the most recent common ancestor of *Cteniogenys* and *Champsosaurus*, and all descendants of that common ancestor. Neochoristodera would be

defined as the most recent common ancestor of *Champsosaurus* and *Simoedosaurus*, and all descendants of that common ancestor.

Cranial anatomy and the choristoderan neomorphic bone

The cranial elements of *Champsosaurus* were described here in 3D for the first time, illustrating the internal morphology of these elements, and their relationship to structures such as the braincase, inner ear, and cranial nerves. It was shown that the choristoderan neomorphic ossification is indeed a distinct element, and possesses an anterodorsally elongate morphology, similar to that proposed by Gao and Fox (1998). Internally, the neomorphic bone does not contact the endocranial cavity, endosseous labyrinth, or cranial nerve tracts.

The neomorphic bone may be homologous with the stapes, which has never been conclusively identified in choristoderes. Further study of the putative stapes in *Coeruleodraco* is needed to comment on the morphology of the bone in that taxon. If the neomorphic bone is not homologous with the stapes, it is most likely to constitute an element of the dermatocranium, given the greater variation seen in elements of the dermatocranium in comparison to those of the chondrocranium and splanchnocranium. The developmental origin of the choristoderan neomorphic bone from the dermatocranium cannot be stated with certainty, but it is most likely that the element developed as an unfused ossification center of a pre-existing element, and was retained simply because it was not deleterious. The parietal is most likely to be the element the neomorph originated from, given the large contact surface between the neomorph and the parietal in *Champsosaurus*, and the early non-neochoristodere *Coeruleodraco* (Matsumoto et al., 2019).

The functional origin of the neomorphic bone is also hard to determine, but given the relatively small size of the element in the early choristodere *Coeruleodraco*, the instigation of this element may have been random, as the bone does not appear to have any significant structural role. However, the neomorphic bone in *Champsosaurus* is far larger than that seen in *Coeruleodraco*, and it is possible that the bone developed to increase the size of sutures to absorb stress in the temporal region. This could be tested by conducting a finite element analysis of the *Champsosaurus* skull with and without the sutures surrounding the neomorphic bone to determine if it had any effect on stress distribution. It is also possible that the expansion of the neomorphic bone in neochoristoderes is not functional, but simply a by-product of the expanded temporal region in neochoristoderes. Future analyses should describe the morphology of the neomorphic bone across Choristodera to determine the morphology of the bone in other non-neochoristoderes, and to document change in the neomorphic bone over time. This analysis could help elucidate the possible function, if any, of the neomorphic bone in the choristodere skull.

Neuroanatomy, behaviour, and ecology

Like other basal diapsids (e.g., *Youngina*), *Champsosaurus* did not ossify the anterior region of the braincase. In CMN 8920, the braincase only ossified posterior to the base of the olfactory stalks, and only the tracts for cranial nerves V through XII are preserved; a morphology consistent across *Champsosaurus* (Fox 1968). Impressions of the olfactory stalks on the roof of the braincase (frontals and parietals) show that the olfactory stalks were substantial, comprising over 50% of the length of the brain endocast. The size and dimensions of the olfactory bulbs could not be determined, so olfactory capabilities cannot be

evaluated for *Champsosaurus*. However, the large size of the olfactory bulbs of the brain and the olfactory chambers of the nasal passages suggest that *Champsosaurus* had good olfactory acuity. Contrary to the results of Lu et al. (1999a), there is no evidence for turbinates in the nasal passage of *Champsosaurus*, suggesting that if these structures were present, they were entirely cartilaginous and left no osteological correlate.

Champsosaurus possessed an enlarged pineal body that protruded dorsally from the brain, and small optic lobes and flocculi, which are consistent with endocasts of other basal diapsids (Romer 1956). The small optic lobes and flocculi of *Champsosaurus* suggest that it had, at best, average vision for a basal diapsid. The osseous labyrinth of *Champsosaurus* is poorly ossified, as is evident from the incomplete ossification between the prootic, opisthotic, and supraoccipital, incomplete ossification around the lateral semicircular canal, large size of the pars inferior, absence of a defined cochlear duct, and exit of CN IX through the posterior wall of the pars inferior. Despite the absence of a defined cochlear duct, the length of the pars inferior suggests that *Champsosaurus*' best hearing frequency was 1691.3 Hz, the best hearing range was 2740.4 Hz, and overall best hearing range was 321.1 – 3061.5 Hz, which are fairly typical for living reptiles (Walsh et al., 2009). However, these are most definitely overestimates because the structures of the inner ear would have been smaller, being housed in soft tissues, and therefore would not have taken up the entirety of this space. Additionally, the absence of a cochlear duct and bulbous pars inferior of *Champsosaurus* suggests a large sacculus was present. This indicates potentially specialized sensitivity to low frequency sounds that are pervasive in the aquatic environment, convergently similar to the ear and sensitivity range present in living turtles.

The morphology of the semicircular canals among diapsids is strongly influenced by phylogeny, where included taxa plot into one of three groups retrieved in a principle components analysis: avians, lepidosaurs, and non-avian archosauromorphs. *Champsosaurus lindoei* (CMN 8920) and *Champsosaurus natator* (CMN 8919) both plot among the non-avian archosauromorph group, supporting previous hypotheses that *Champsosaurus* is a stem archosauromorph (Evans 1990). Interestingly, turtles also plot with the non-avian archosauromorph group, supporting recent evidence that turtles are stem archosauromorphs (Bhullar and Bever 2009; Wang et al., 2013).

Despite the strong phylogenetic signal in the morphology of the semicircular canals, different ecological groups (i.e., arboreal, terrestrial, aquatic, aerial) possess significantly different canal shapes, as shown by CVA, ANCOVA, and PGLS. Based on log-likelihood estimations, and posterior probabilities of Mahalanobis distances, *C. lindoei* and *C. natator* have significantly different canal morphologies from the aerial, arboreal, and terrestrial groups, but show no significant difference from the aquatic group. These results suggest that the inner ear of *Champsosaurus* was adapted for a highly aquatic lifestyle, consistent with previous hypotheses based on morphological and sedimentological evidence (Erickson 1985). Future analyses should describe the morphology of the semicircular canals using a wider phylogenetic sample than what was studied here to better describe evolutionary changes of the inner ear over time.

Based on the data collected here, evolutionarily distant lineages do not evolve convergent ear morphologies, despite possessing similar ecologies. This is indicative of the strength of phylogenetic signalling on the morphology of the semicircular canals, where closely related species tend to have similar canal morphologies, regardless of ecology.

Previous studies have found that skull size is a major driver of canal morphology (Georgi et al., 2013), and this may be a factor influencing variation in the morphology of the semicircular canals across evolutionary lineages. Comparisons of the shape of the semicircular canals with physical traits of the skull should be made across Amniota to determine if the major differences in shape between evolutionary lineages are driven by skull morphology.

Final remarks

In summary, the presence of the choristoderan neomorphic bone has been confirmed in *Champsosaurus*, and is likely present throughout Choristodera. The neuroanatomy of *Champsosaurus* suggests that they were well-adapted for an aquatic lifestyle, supporting previous hypotheses based on their skeletal morphology. Although the research presented here elucidates the cranial anatomy and behaviour of these understudied animals, further work is needed to better understand the evolution of these unique reptiles.

Appendices

Appendix A: Taxa included in the analysis that were acquired via Morphosource, with their specimen ID, specimen institution, and Morphosource media number .

Group	Species	Specimen	Specimen Institution	Media number
Archosauromorpha	*Apalone spinifera*	FMNH:22178	Field Museum of Natural History	M22038
	Dermochelys coriacea	UMZC:R:3031	University Museum of Zoology	M22024
	Casuarius casuarius	NHMUK:zoo:1939.12.9.964	Natural History Museum	M17005
	Gavia immer	NCSM-herp-93545	National Museum of Scotland	M17717
	Gavialis gangeticus	uf:herp:118998	Florida Museum of Natural History	M20938
	Passer domesticus	NMS:Passer_unreg	National Museum of Scotland	M17720
	Spheniscus magellanicus	USNM:birds:347603	National Museum of Natural History	M15987
	Stegoceras validum	UALVP-2	University of Alberta Laboratory for Vertebrate Paleontology	M22180
	Sternotherus minor	FMNH:211696	Field Museum of Natural History	M22123
	Triopticus primus	TMM:31100-1030	University of Texas Vertebrate Paleontology Collections	M7293
	Wannia scurriensis	TTU P:00539	University of Texas Vertebrate Paleontology Collections	M12518
Lepidosauria	*Amblyrhynchus cristatus*	uf-herp-41558	Florida Museum of Natural History	M20753
	Anolis carolinensis	NCSM:herp:93545	North Carolina Museum of Natural Sciences	M20838
	Anolis cristitellus	UF:Herp:47686	Florida Museum of Natural History	M12744
	Gekko gecko	SHSVM:H:0001-2014	Sam Houston State Vertebrate Museum	M13432
	Shinisaurus	UF-H-60925	Florida Museum of Natural History	M12414
	Sphenodon	UF:Herp:11978	Florida Museum of Natural History	M8675
	Trachylepis laevis	cas:herp:254838	California Academy of Science	M15846

Appendix B: Taxa included in the analysis that were acquired via Digimorph (University of Texas High-Resolution X-ray CT Facility), with their specimen ID, specimen institution, and NSF grant number.

Group	Species	Specimen	Specimen Institution	NSF grant num.
Archosauromorpha	*Tomistoma schlegelli**	TMM M-6342	Texas Memorial Museum	IIS-0208675
	Rhea Americana	TMM M-6721	Texas Memorial Museum	IIS-9874781
Lepidosauria	*Lanthanotus borneensis*	FMNH 148589	Field Museum of Natural History	IIS-0208675 and EF-0334961
	Varanus exanthematicus	FMNH 58299	Field Museum of Natural History	IIS-0208675 and EF-0334961

*Additional credit to Chris Brochu

Appendix C: Taxa included in this analysis that were acquired via personal contact with researchers, with their specimen ID, source, and specimen institution.

Group	Species	Specimen	Source	Specimen Institution
Choristodera	*Champsosaurus lindoei*	CMN FV 8920	This study	Canadian Museum of Nature
	Champsosaurus natator	CMN FV 8919	This study	Canadian Museum of Nature
Archosauromorpha	*Euparkeria capensis*	SAM-PK-7696	Gabriela Sobral, and the Digital Collection of the Museum für Naturkunde Berlin	South African Museum
	Malawisaurus	Mal 202-1	Kate Andrzejewski and Mike Polcyn	Malawi Department of Antiquities
	Massospondylus	BP/1/5241	Kimberley Chapelle	University of Witwatersrand
	Falcarius utahensis	UMNH VP 15000	Stephan Lautenschlager	Natural History Museum of Utah
	Falcarius utahensis	UMNH VP 15001	Stephan Lautenschlager	Natural History Museum of Utah
	Erlikosaurus andrewsi	IGM 100/111	Stephan Lautenschlager	Geological Institute of the Mongolian Acadamy of Science
	Nothronychus mckinleyi	AZMNH-2117	Stephan Lautenschlager	Arizona Museum of Natural History
Lepidosauria	*Plioplatecarpus*	MOR 1062	Hillary Maddin	Museum of the Rockies
	Iguana iguana	MCZ 2560	Hillary Maddin	Museum of Comparative Zoology
	Pantherophis guttatus	Uncatalogued, available in the Maddin Lab	Fred Gaidies, and Hillary Maddin	Carleton University
	Typhlops	Uncatalogued, available in the Maddin Lab	Hillary Maddin	Carleton University
	Varanus niloticus	MCZ 1066	Hillary Maddin	Museum of Comparative Zoology

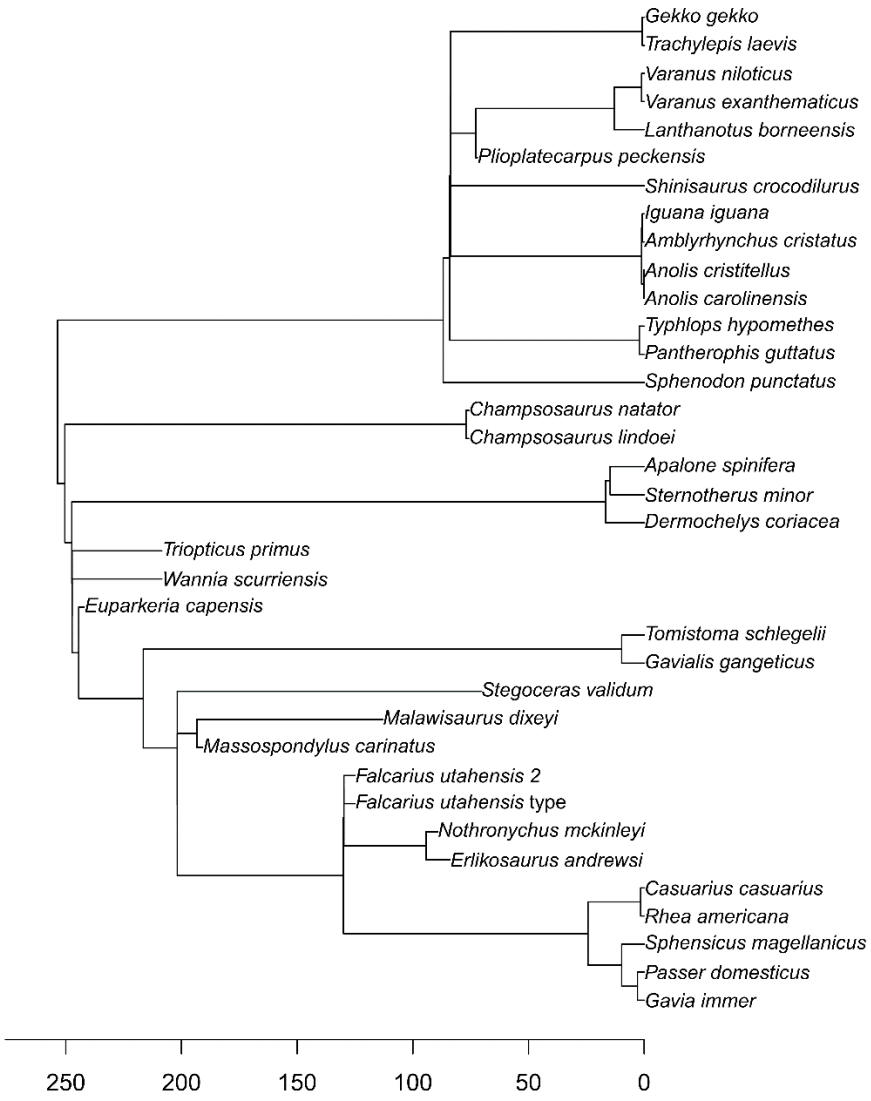

Appendix D: Time calibrated phylogeny of taxa used in the PCA.

References

Abo-Eleneen, R.E., S.I. Othman, H.M. Al-Harbi, A.M. Abdeen, A.A. Allam. 2017. Anatomical study of the skull of amphisbaenian *Diplometopon zarudnyi* (Squamata, Amphisbaenia). Saudi Journal of Biological Sciences 1:1–11.

Adams, D.C. 2014. A generalized K statistic for estimating phylogenetic signal from shape and other high-dimensional multivariate data. Systematic Biology 63(5):685-697.

Adams, D.C., M.L. Collyer, A. Kaliontzopoulou. 2019. Geomorph: Software for geometric morphometric analyses. R package version 3.1.0. https://cran.r-project.org/package=geomorph.

Alloing-Séguier, L., M.R. Sánchez-Villagra, M.S.Y. Lee, R. Lebrun. 2013. The bony labyrinth in diprotodontian marsupial mammals: Diversity in extant and extinct forms and relationships with size and phylogeny. Journal of Mammals Evolution 20:191-198.

Amiot, R., X. Wang, Z. Zhoua, X. Wang, E. Buffetaut, C. Lécuyer, Z. Ding, F. Fluteaue, T. Hibino, N. Kusuhashig, J. Moh, V. Suteethorn, Y. Wanga, X. Xua, and F. Zhang. 2011. Oxygen isotopes of East Asian dinosaurs reveal exceptionally cold Early Cretaceous climates. PNAS 108(13):5179–5183.

Anderson, J.S., R.L. Carroll, and T.B. Rowe. 2003. New information on *Lethiscus stocki* (Tetrapoda: Lepospondyli: Aistopoda) from high-resolution computed tomography and a phylogenetic analysis of Aistopoda. Canadian Journal of Earth Sciences 40:1071–1083.

Andrzejewski, K.A., M.J. Polcyn, D.A. Winkler, E.G. Chindebvu, L.L. Jacobs. 2019. The braincase of *Malawisaurus dixeyi* (Sauropoda: Titanosauria): A 3D reconstruction of the brain endocast and inner ear. PLoS ONE 14(2):e0211423

Araújo, R., V. Fernandez, M.J. Polcyn, J. Fröbisch, R.M.S. Martins. 2017. Aspects of gorgonopsian paleobiology and evolution: insights from the basicranium, occiput, osseous labyrinth, vasculature, and neuroanatomy. PeerJ 5:e3119; DOI: 10.7717/peerj.3119

Atkins, J.B., T.A. Franz-Odendaal. 2016. The evolutionary and morphological history of the parasphenoid bone in vertebrates. Acta Zoologica 97:255–263.

Atkins, J.B., R.R. Reisz, H.C. Maddin. 2019. Braincase simplification and the origin of lissamphibians. PLoS One 14(3):e0213694.

Averianov, A. 2005. The first choristoderes (Diapsida, Choristodera) from the Paleogene of Asia. Paleontological Journal 39(1):79-84.

Bailleul, A.M., J.B. Scannella, J.R. Horner, D.C. Evans. 2016. Fusion patterns in the skulls of modern archosaurs reveal that sutures are ambiguous maturity indicators for the Dinosauria. PLoS ONE 11(2):1–26.

Bapst, D.W. 2012. Paleotree: An R package for paleontological and phylogenetic analyses of evolution. Methods in Ecology and Evolution. 3: 803-807. doi:10.1111/j.2041-210X.2012.00223.x

de Beer, G. 1937. The development of the vertebrate skull. Oxford University Press. Toronto.

Bellairs, A., A.M. Kamal. 1981. The chrondrocranium and the development of the skull in recent reptiles. In: Gans C, Parsons TS, eds. Biology of the Reptilia, Vol. 11, Morphology F. New York: Academic Press, 1–283.

Bellary, S.S., A. Steinberg, N. Mirzayan, M. Shirak, R.S. Tubbs, A.A. Cohen-Gadol, M. Loukas. 2013. Wormian bones: A review. Clinical Anatomy 26:922–927.

Benson, R.B.J., G. Hunt, M.T. Carrano, N. Campione. 2018. Cope's rule and the adaptive landscape of dinosaur body size evolution. Palaeontology 61(1):13-48.

Benoit, J., S.C. Jasinoski, V. Fernandez, F. Abdala. 2017. The mystery of a missing bone: revealing the orbitosphenoid in basal *Epicynodontia* (Cynodontia, Therapsida) through computed tomography. The Science of Nature 104(66):1–6.

Bennett, K.A. 1965. The etiology and genetics of Wormian bones. American Journal of Physical Anthropology 23:255–260.

Berlin, J.C., E.C. Kirk, T.B. Rowe. 2013. Functional implications of ubiquitous semicircular canal non-orthogonality in mammals. PLoS One 8(11): e79585.

Bever, G.S. 2009. The postnatal skull of the extant North American turtle *Pseudemys texana* (Cryptodira: Emydidae), with comments on the study of discrete intraspecific variation. Journal of Morphology 270:97–128.

Bever, G.S., J.C. Bell, J.A Maisano. 2005. The ossified braincase and cephalic osteoderms on *Shinisaurus crocodilurus* (Squamta, Shinisauridae). Palaeontologia Electronica 8(1):1–36.

Bhullar, B.A.S., and G.S. Bever. 2009. An archosaur-like laterosphenoid in early turtles (Reptilia: Pantestudines). Brevoria 518:1-11.

Billet, G., L. Hautier , R.J. Asher, C. Schwarz, N. Crumpton, T. Martin I. Ruf. 2012. High morphological variation of vestibular system accompanies slow and infrequent locomotion in three-toed sloths. Proceedings of the Royal Society B 279(1744): 3932-3939.

Bloomberg, S.P., T. Garland Jr., A.R. Ives. 2003. Testing for phylogenetic signal in comparative data: behaviour traits are more labile. Evolution 57(4):717-745.

Böhme, M. 2008. Ectothermic vertebrates (Teleostei, Allocaudata, Urodela, Anura, Testudines, Choristodera, Crocodylia, Squamata) from the Upper Oligocene of Oberleichtersbach (Northern Bavaria, Germany). Courier Forschungsinstitut Senckenberg, 260:161-183.

Boistel R., A. Herrel, R. Lebrun, G. Daghfous, P. Tafforeau, J.B. Losos, B. Vanhooydonck. 2011. Shake rattle and roll: the bony labyrinth and aerial descent in squamates. Integrative and Comparative Biology. 51:957–968.

Bookstein, FL. 1991. Morphometric tools for landmark data: geometry and biology. Cambridge: Cambridge University Press.

Bowen, C.F. 1915. Stratigraphy of the Montana Group with special reference position and age of the Judith River Formation in North-Central Montana. Department of the Interior United States Geological Survey: Professional Paper 90-I.

Brinkman, D.B. 1990. Paleontology of the Judith River Formation (Campanian) of Dinosaur National Park, Alberta, Canada: evidence from vertebrate microfossil locality. Paleogeology, Paleoclimatology, Paleoecology 78:37-54.

Brinkman, D.B., and Z. Dong. 1993. New material of *Ikechosaurus sunailinae* (Reptilia: Choristodira) from the Early Cretaceous Laohongdong Formation, Ordos Basin, Inner Mongolia, and the interrelationships of the genus. Canadian Journal of Earth Sciences 30:2153-2162.

Brown, B. 1905. The osteology of *Champsosaurus* Cope. American Museum of Natural History, Memoirs 9:1-26.

Buffetaut, E., L. Jianjun, T. Haiyan, and H. Zhang. 2007. A two-headed reptile from the Cretaceous of China. Biology Letters 3:80-81.

Capshaw, C. and D. Soares. 2016. Hearing in plethodontid salamanders: A review. Copeia 104: 157–164.

Cardini, A., S. Elton. 2008. Does the skull carry a phylogenetic signal? Evolution and modularity in the guenons. Biological Journal of the Linnean Society 93:813–834.

Carroll, R.L. 1980. The hyomandibular as a supporting element in the skull of primitive tetrapods, p. 293-317. In Panchen, A. L. (ed.), The Terrestrial Environment and the Origins of Land Vertebrates. Systematics Association Special Volume No. 15. London/New York.

Carroll, R.L. 1982. Early evolution of reptiles. Annual Review of Ecology, Evolution, and Systematics 13:87-109.

Carroll, R.L., P.J. Currie. 1991. The early radiation of diapsid reptiles. In: H.P Schultze, and L Trueb, eds. Origins of the Higher Groups of Tetrapods. Ithaca: Comstock Publishing Associates 354-424.

Cerio, D.G., L.M. Witmer. 2019. Intraspecific variation and symmetry of the inner-ear labyrinth of wild turkeys: implications for paleontological reconstructions. PeerJ 7:e7355.

Cheng, Y., X. Wu, Q. Ji. 2004. Triassic marine reptiles gave birth to live young. Nature 432:383–386

Christensen, C.B., H. Lauridsen, J. Christensen-Dalsgaard, M. Pedersen, P.T. Madsen. 2015. Better than fish on land? Hearing across metamorphosis in salamanders. Proceedings of the Royal Society B. 282: 20141943.

Christensen, C.B., J. Christensen-Dalsgaard, C. Brandt, P.T. Madsen. 2012. Hearing with an atympanic ear: good vibration and poor sound-pressure detection in the royal python, Python regius. The Journal of Experimental Biology 215:331-342.

Christensen-Dalsgaard, J. C. Brandt, K.L. Willis, C.B. Christensen, D. Ketten, P. Eggs-Walton, R.R. Fay, P.T. Madsen, C.E. Carr. 2012. Specialization for underwater hearing by the tympanic middle ear of the turtle, *Trachemys scripta elegans*. Proceedings of the Royal Society B 279:2816-2824.

Chure, D.J., and S.E. Evans. 1998. A new occurrence of Cteniogenys, with comments on its distribution and abundance. Modern Geology 23:49-55.

Clack, J.A. 1997. The evolution of tetrapod ears and the fossil record. Brain, Behaviour and Evolution 50:198– 212.

Clack, J.A. 2002. Patterns and Processes in the Early Evolution of the Tetrapod Ear. Journal of Neurobiology 53(2):251-264.

Clack, J.A., and E. Allin. 2004. The evolution of single- and multiple-ossicle ears in fishes and tetrapods. In: Evolution of the vertebrate auditory system. G.A. Manley, A.N. Popper, R.R. Fay (Eds). Springer, New York, USA. p128-163.

Clack, J.A., J.S. Anderson. 2016. Early tetrapods. In Clack, JA, Fay, RR, Popper, AN, eds. Evolution of the vertebrate ear: evidence from the fossil record, p71–105. New York, Springer.

Conrad, J.L. 2008. Phylogeny and systematics of Squamata (Reptilia) based on morphology. Bulletin of the American Museum of Natural History 310:1–182.

Cope, E.D. 1876. On some extinct reptiles and Batrachia from the Judith River and Fox Hills beds of Montana. Proceedings of the Academy of Natural Sciences of Philadelphia p340-359.

Cope, E.D. 1884a. The Vertebrata of the Tertiary formations of the West (Book I). In: F.V. Hayden, (Ed.) Report of the United States Geological Survey of the Territories, Vol. III: Tertiary Vertebrata, Book I. Washington: Government Printing Office.

Cope, E.D. 1884b. The Choristodera. American Naturalist 17:815-817.

Crawford, N.G., J.F. Parham, A.B. Sellas, B.C. Faircloth, T.C. Glenn, T.J. Papenfuss, J.B. Henderson, M.H. Hansen, W.B. Simison. 2015. A phylogenomic analysis of turtles. Molecular Phylogenetics and Evolution 83:250-257.

Cremin, B., H. Goodman, J. Spranger, P. Beighton. 1982. Wormian bones in osteogenesis imperfecta and other disorders. Skeletal Radiology 8:35–38.

Cummins, S.F., J.H. Bowie. 2012. Pheromones, attractants and other chemical cues of aquatic organisms and amphibians. Natural Products Reports 29:642–658.

Currie, P.J. 1985. Cranial anatomy of *Stenonychosaurus inequalis* (Saurischia, Theropoda) and its bearing on the origin of birds. Canadian Journal of Earth Sciences 22:1643–1658.

Curtis, N., M.E.H. Jones, S.E. Evans, P. O'Higgins, M.J. Fagan. 2013. Cranial sutures work collectively to distribute strain throughout the reptile skull. Royal Society Publishing 10:1–9.

Daza, J.D., A.M. Bauer. 2010. The circumorbital bones of the Gekkota (Reptilia: Squamata). The Anatomical Record 293:402–413.

Deeming, D.C., L.B. Halstead, M. Manabe, D.M. Unwin. 1993. An ichthyosaur embryo from the Lower Lias (Jurassic: Hettangian) of Somerset, England, with comments on the reproductive biology of ichthyosaurs. Modern Geology 18:423–442.

DeLaurier, A. 2018. Evolution and development of the fish jaw skeleton. Wiley Interdisciplinary Reviews: Developmental Biology 8(2):e337.

Dickson, B.V., E. Sherratt, J.B. Losos, and S.E. Piercel. 2017. Semicircular canals in Anolis lizards: ecomorphological convergence and ectomorph affinities of fossil species. Royal Society Open Science 4:1-15.

Dieckmann, U., M. Doebeli. 1999. On the origin of species by sympatric speciation. Nature 400:354–357.

Dudgeon, T.W., H.C. Maddin, D.C. Evans, J.C. Mallon. In Revision. Computed tomography (CT) analysis of the braincase of *Champsosaurus lindoei* (Diapsida: Choristodera) and implications for the choristoderan neomorphic ossification. Journal of Anatomy.

Efimov, M.B. 1975. A champsosaurid from the Lower Cretaceous of Mongolia. In: N.N. Kramarenko (Ed.) Fossil Fauna and Flora of Mongolia. Transactions of the Joint Soviet-Mongolian Paleontological Expeditions 2:84-93.

Efimov, M.B. 1979. *Tchoiria* (Champsosauridae) from the Early Cretaceous of Khamarin-Khural, Mongolia. In: R. Barsbold et al. (Eds.) Mesozoic and Cenozoic Fauna of Mongolia. Transactions of the Joint Soviet-Mongolian Paleontological Expeditions 8:56-57.

Efimov, M.B. 1983. Champsosaurs of central Asia. Trudy Sovmestimosti Sovetsko-Mongol'skoi Paleontologi Cheskoi Ekspeditsiya 24: 67–75.

Efimov, M.B. 1996. Champsosaurid from the Lower Cretaceous of Burytia. Journal of Paleontology 1:122–123.

Efimov, M.B., G.W. Storrs. 2000. Choristodera from the Lower Cretaceous of northern Asia. In: M.J. Benton, M.A. Shishkin, D.M. Unwin, E.N. Kurochkin (Eds) The age of dinosaurs in Russia and Mongolia. Cambridge University Press, Cambridge, UK.

Endo, R. 1940. A new genus of Thecodontia from the Lycoptera beds in Manchoukuo. Bulletin of the Central National Museum of Manchoukuo, 2: 1-14.

Erickson, B.R. 1972. The lepidosaurian reptile *Champsosaurus* in North America. Science Museum of Minnesota, Monograph (Paleontology) 1: 1-9 1.

Erickson, B.R. 1981. *Champsosaurus tenuis* (Reptilia—Eosuchia): A new species from the Late Paleocene of North America. Scientific Publications of the Science Museum of Minnesota New Series 5(1):3-14.

Erickson, B.R. 1985. Aspects of some anatomical structures of *Champsosaurus* (Reptilia: Eosuchia). Journal of Vertebrate Paleontology 5(2):111-127.

Erickson, B.R. 1987. *Simoedosaurus dakotensis*, new species, a diapsid reptile (Archosauromorpha; Choristodera) from the Paleogene of North America. Journal of Vertebrate Paleontology 7(3):237-251.

Erickson, G.M., A.K. Lappin, K.A. Vliet. 2003. The ontogeny of bite-force performance in American alligator (*Alligator mississippiensis*). Journal of Zoology 260:317–327.

Estes, R. 1983. Sauria terrestrial, Amphisbaenia. In: P. Wellnhofer (Ed.), Hanbunch der Palaoherpetologie, 10A:1-249.

Estes, R., K. de Queiroz, J. Gauthier. 1988. Phylogenetic relationships within Squamata. In: Estes R, Pregill G, eds. Phylogenetic relationships of the lizard families. Stanford, California: Stanford University Press, 119–281.

Evans, D.C. 2005. New evidence on brain−endocranial cavity relationships in ornithischian dinosaurs. Acta Palaeontological Polonica 50(3):617–622.

Evans, S.E. 1988. The early history and relationships of the Diapsida. In M.J. Benton (Ed.), The phylogeny and classification of the tetrapods, 1: Amphibians, reptiles, birds. Systematics Association Special Volume, 35A: 221-253.

Evans, S.E. 1989. New Material of Cteniogenys (Reptilia: Diapsida) and a reassessment of the systematic position of the genus. Neues Jahrbuch fur Geologie and Palaontologie 181:577-589.

Evans, S.E. 1990. The skull of *Cteniogenys*, a choristodere (Reptilia: Archosauromorpha) from the Middle Jurassic of Oxfordshire. Zoological Journal of the Linnaean Society 99:205-237.

Evans, S.E, and M.K. Hecht. 1993. A history of an extinct reptilian clade, the Choristodera: longevity, Lazarus-taxa, and the fossil record. Evolutionary Biology 27: 323-338.

Evans, S.E., and M. Waldman. 1996. Small reptiles and amphibians from the Middle Jurassic of Skye, Scotland. In M. Morales (Ed.) The Continental Jurassic. Museum of Arizona Bulletin 60:219-226.

Evans, S.E., and M. Manabe. 1999. A choristoderan reptile from the Lower Cretaceous of Japan. Special Papers in Paleontology 60: 101–119.

Evans, S., and J. Klembara. 2005. A choristoderan reptile (Reptilia: Diapsida) from the lower Miocene of northwest Bohemia (Czech Republic). Journal of Vertebrate Paleontology 25(1):171-184.

Evans, S. E. 2008. The skull of lizards and Tuatara. In: The skull of Lepidosauria. C. Gans, A.S. Gaunt. Biology of the Reptilia, 20:1-347. Ithaca, NY: Society for the Study of Amphibians and Reptiles.

Ezcurra, M.D. 2016. The phylogenetic relationships of basal archosauromorphs, with an emphasis on the systematics of proterosuchian archosauriforms. PeerJ 1-385.

Ferrera, C.R., R.C. Vogt, and R.S. Sousa-Lima. 2013. Turtle vocalizations as the first evidence of posthatching parental care in chelonians. Journal of Comparative Psychology. Advance online publication. doi: 10.1037/a0029656

Foster, J.R., and K.C. Trujillo. 2000 New occurrences of *Cteniogenys* (Reptilia, Choristodera) in the late Jurassic of Wyoming and South Dakota. Bermingham Young University Geologic Studies 45:11-18.

Fox, R.C. 1968. Studies of the Late Cretaceous vertebrates: I. The braincase of *Champsosaurus* Cope (Reptilia: Eosuchia). Copeia 1: 100-109.

Fraser, N.C., K. Padian, G.M. Walkden, and A.L.M. Davis. 2002. Basal dinosauriform remains from Britain and the diagnosis of the Dinosauria. Paleontology 45(1):79-95.

Frazzetta, T.H. 1970. From hopeful monsters to bolyerine snakes? The American Naturalist 104:55–72.

Gaffney, E.S. 1980. Phylogenetic relationships of the major groups of amniotes. In A.L. Panchen (Ed.), The terrestrial environment and the origin of land vertebrates 593-610.

Gaffney, E.S. 1983. The cranial morphology of the extinct horned turtle *Meiolania platyceps* from the Pleistocene of Lord Howe Island, Australia. Bulletin of the American Museum of Natural History 175(4):1–124.

Gaffney, E.S. 1990. The comparative osteology of the Triassic turtle *Proganochelys*. Bulletin of the American Museum of Natural History 194:1–263.

Gao, C.L., J.C. Lu, J.Y. Liu, Q. Ji. 2005. New Choristodera from the Lower Cretaceous Jiufotang Formation in Chaoyang area, Liaoning China. Geological Review 51(6): 694–697.

Gao, K., and R.C. Fox. 1998. New choristoderes (Reptilia: Diapsida) from the Upper Cretaceous and Palaeocene, Alberta and Saskatchewan, Canada, and phylogenetic relationships of Choristodera. Zoological Journal of the Linnaean Society 124:303-353.

Gao K., Z. Tang, X. Wang. 1999. A long-necked diapsid reptile from the Upper Jurassic/Lower Cretaceous of Liaoning Province, northeastern China. Vertebrata Palasiatica 37: 1–8.

Gao K, S. Evans, Q. Ji, M. Norell, S. Ji. 2000. Exceptional fossil material of a semi-aquatic reptile from China: the resolution of an enigma. Journal of Vertebrate Paleontology 20: 417–421.

Gao, K., and D.B. Brinkman. 2005. Choristoderes from the park and its vicinity. In: Dinosaur Provincial Park: a spectacular ancient ecosystem revealed. (Eds) P.J. Currie and E.B. Koppelhus.

Gao, K., and R.C. Fox. 2005. A new choristodere (Reptilia: Diapsida) from the Lower Cretaceous of western Liaoning Province, China, and phylogenetic relationships of Monjurosuchidae. Zoological Journal of the Linnaean Society 145:427-444.

Gao, K., D. Ksepka, L. Hou, Y. Duan, D. Hu. 2007. Cranial morphology of an Early Cretaceous Monjurosuchid (Reptilia: Diapsida) from Liaoning Province of China and evolution of choristoderan palate. Historical Biology 19: 1–10.

Gao, K., and D.T. Ksepka. 2008. Osteology and taxonomic revision of *Hyphalosaurus* (Diapsida: Choristodera) from the Lower Cretaceous of Liaoning, China. Journal of Anatomy 212:747-768.

Gardner, N.M., C.M. Holliday, F.R. O'Keefe. 2010. The braincase of *Youngina capensis* (Reptilia, Diapsida): New insights from high-resolution CT scanning of the holotype. Palaeontologia Electronica 13(3):19A.

Gendron-Maguire, M., M. Mallo, M. Zhang, T. Gridley. 1993. *Hoxa-2* mutant mice exhibit homeotic transformation of skeletal elements derived from cranial neural crest. Cell 75(7):1317-1331.

Georgi, J.A., J.S. Sipla. 2009. Comparative and functional anatomy of balance in aquatic reptiles and birds. In: Sensory evolution on the threshold: adaptations in secondarily aquatic vertebrates. J.G.M. Thewissen, N. Sirpa (Eds.). Berkley, CA: University of California Press, p. 98.

Gervais, P. 1873. Enumeration de quelques ossements d'animaux vertébrés recueillis aux environs de Reims par M. Lemoine. Journal de Zoologie 2:351-355.

Gervais, P. 1877. Enumeration de quelques ossements d'animaux vertébrés recueillis aux environs de Reims par M. Lemoine. Journal de Zoologie 6:74-79.

Gignac, P.M., and N.J. Kley. 2014. Iodine-enhanced micro-CT imaging: Methodological refinements for the study of the soft-tissue anatomy of post-embryonic vertebrates. Journal of Experimental Zoology B Molecular and Developmental Evolution 322(3):166-176.

Giles, J.C., J. A. Davis, R.D. McCauley, G. Kuchling. 2009. Voice of the turtle: The underwater acoustic repertoire of the long-necked freshwater turtle, *Chelodina oblonga*. Journal of the Acoustical Society of America 126(1):434-443.

Gilmore, C. 1928. Fossil lizards of North America. Memoirs of the National Academy of Sciences 22:1-169.

Gittleman, J.L. 1991. Carnivore olfactory bulb size: allometry, phylogeny and ecology. Journal of Zoology, London 225:253-272.

Gleich, O., R.J. Dooling, G.A. Manley. 2005. Audiogram, body mass, and basilar papilla length: correlations in birds and predictions for extinct archosaurs.

Goswami, A., Polly, P.D. 2010. The influence of character correlations on phylogenetic analysis: a case study of the carnivoran skull. In: Goswami A, Friscia A, eds. Carnivoran evolution: new views on phylogeny, form and function. p141-164. Cambridge, Cambridge University Press.

Gould, S.J., R.C. Lewontin. 1979. The spandrels of San Marco and the Panglossian paradigm: a critique of the adaptationist programme. Proceedings of the Royal Society of London B 205:581–598.

Gow, C.E. 1972. The osteology and relationships of the Millerettidae (Reptilia: Cotylosauria). Zoological Journal of the Linnean Society 167:219-264.

Gower, D.J., A.G. Sennikov. 1996. Endocranial casts of early archosaurian reptiles. Paläontologische Zeitschrift 70(3-4):579-589.

Gower, D.J. 1997. The braincase of the early archosaurian reptile *Erythrosuchus africanus*. Journal of Zoology 242:557–576.

Gower, D.J., E. Weber. 1998. The braincase of *Euparkeria*, and the evolutionary relationships of birds and crocodilians. Biological Reviews 73:367–411.

Grande, L., T. Grande. 2008. Redescription of the type species for the genus "*Notogoneus*" (Teleostei: Gonorynchidae) based on new, well-preserved material. Journal of Paleontology 82(5):1–31.

Griffin, E.B. 1989. Pachycephalosaur paleoneurology (Archosauria: Ornithischia). Journal of Vertebrate Paleontology 9(1)67-77.

Head, J.J., P.M. Barrett, E.J. Rayfield. 2009. Neurocranial osteology and systematic relationships of *Varanus* (Megalania) *prisca* Owen, 1859 (Squamata: Varanidae). Zoological Journal of the Linnean Society 155(2):455-457.

Haddoumi, H., R. Allain, S. Meslouh, G. Metais, M. Monbaron, D. Pons, J. Rage, R. Vullo, S. Zouhri, E. Gheerbrant. 2016. Guelb el Ahmar (Bathonian, Anoual Syncline, eastern Morocco): First continental flora and fauna including mammals from the Middle Jurassic of Africa. Gondwana Research 29:290-319.

Hecht, M.K. 1992. A new choristodere (Reptilia: Diapsida) from the Oligocene of France: An example of the Lazarus effect. Geobios 25(1):115-131.

Helms, J.A., R.A. Schneider. 2003. Cranial skeleton biology. Nature 423:326-331.

Hernandez-Jaimes, C., A. Jerez, M.P. Ramirez-Pinilla. 2012. Embryonic development of the skull of the Andean lizard *Ptychoglossus bicolor* (Squamata, Gymnophthalmidae). Journal of Anatomy 221:285–302.

Hetherington, T.E., R.E. Lombard. 1983. Electromyography of the opercularis muscle of *Rana catesbeiana*: An amphibian tonic muscle. Journal of Morphology 175:17–26.

Hilton, W.A. 1949. The sound-transmitting apparatus of salamanders. Herpetologica 5:33-43.

Holliday, C.M., L.M. Witmer. 2009. The epipterygoid of crocodyliforms and its significance for the evolution of the orbitotemporal region of eusuchians. Journal of Vertebrate Paleontology 29(3):715–733.

Holloway, W.L., K.M. Claeson, F.R. O'keefe. 2013. A virtual phytosaur endocast and its implications for sensory system evolution in archosaurs. Journal of Vertebrate Paleontology. 33(4):848-857.

Hopson, J. A. 1979. Paleoneurology. In: Biology of the Reptilia. Neurology A, Volume 9. C. Gans, R.G. Northcutt, and P.S. Ulinki (Eds.). Academic Press, New York. pp. 39–146.

Hopson, J.A., G.W. Rougier. 1993. Braincase structure in the oldest known skull of a therian mammal: Implications for mammalian systematics and cranial evolution. American Journal of Science 293:268–299.

Hou, L., P. Li, D.T. Ksepka, K. Gao, and M. Norell. 2010. Implications of flexible-shelled eggs in a Cretaceous choristoderan reptile. Proceedings of the Royal Society B 277:1235-1239.

Ingram, T. 2014. Fitting Hansen models to investigate convergent evolution. R Package 'surface'.

Iordansky, N.N. 1990. Evolution of cranial kinesis in lower tetrapods. Netherlands Journal of Zoology 40:32–54.

Jablonski, D. 1986 - Causes and consequences of mass extinctions; a comparative approach. In D.K. Elliot (Ed.): Dynamics of extinction. Wiley, New York: 183-229.

James, M.S.B. 2010. The jaw adductor muscles in *Champsosaurus* and their implications for feeding mechanics. M.Sc. Thesis University of Alberta.

Jerison, H. J. 1973. Evolution of the brain and intelligence. Academic Press.

Jetz, W., G.H. Thomas, J.B. Joy, K. Hartmann, A.O. Mooers. 2012. The global diversity of birds in space and time. Nature 491:444-448.

Ji, Q., S. Ji, Y. Cheng, H. You, J. Lu, C. Yuan. 2004. The first fossil soft-shell eggs with embryos from Late Mesozoic Jehol Biota of western Liaoning, China. Acta Geoscientica Sin 25: 275–285.

Ji, Q., S. Ji, J. Lü, H. You, C. Yuan. 2006. Embryos of Early Cretaceous Choristodera (Reptilia) from the Jehol biota in western Liaoning, China. Journal of the Palaeontological Society of Korea 22(1):111-118.

Ji, Q., X.C. Wu, and Y.N. Cheng. 2010. Cretaceous choristoderan reptiles gave birth to live young. Naturwissenschaften 97:423–428.

Jollie, M.T. 1960. The head skeleton of the lizard. Acta Zoologica 1–64.

Jones, M.E.H, F. Groning, H. Dute, A. Sharp, M.J. Fagan, S.E. Evans. 2017. The biomechanical role of the chondrocranium and sutures in a lizard cranium. Royal Society Publishing 14:1–13.

Joyce, W.G., J.F. Parham, and J.A. Gauthier. 2004. Developing a protocol for the conversion of rank-based taxon names Developing a protocol for the conversion of rank-based taxon names to phylogenetically defined clade names, as exemplified by turtles. Journal of Paleontology 78(5):989-1013.

Katsura, Y. 2007. Sexual dimorphism in *Champsosaurus* (Diapsida: Choristodera). Lethaia 37:245-253.

Katsura, Y. 2010. Ontogenetic change of bone microstructures and its ethological implication in *Champsosaurus* (Diapsida, Choristodera). Historical Biology 22(4):380-386.

Ketten, D.R. 2008. Underwater ears and the physiology of impacts: Comparative liability for hearing loss in sea turtles, birds, and mammals. Bioacoustics, 17(1-3):312-315.

Kirton, A.M. 1983. A review of British Upper Jurassic ichthyosaurs. Unpublished PhD Thesis, University of Newcastle upon Tyne, Newcastle upon Tyne.

Knoll, F., L.M. Witmer, F. Ortega, R.C. Ridgely, and D. Schwarz-Wings. 2012. The braincase of the basal sauropod dinosaur *Spinophorosaurus* and 3D reconstructions of the cranial endocast and inner ear. PLoS ONE 7(1):1-12.

Kopher, R.A., J.J. Mao. 2003. Suture growth modulated by the oscillatory component of micromechanical strain. Journal of Bone and Mineral Research 18(3):521–528.

Ksepka, D.T., K. Gao, and M.A. Norell. 2005. A new choristodere from the Cretaceous of Mongolia. American Museum Novitates 3468(22):1-11.

Kuhlenbeck, H. 1977. The central nervous system of vertebrates: a general survey of its comparative anatomy with an introduction to the pertinent biologic and logical concepts. Vol. 5, Part 1. Derivatives of the prosencephalon: diencephalon and telencephalon. Karger, New York.

Kuhn, O. 1969. Handbuch der Paläoherpetologie, Teil 9. Stuttgart: Gustav Fischer Verlag.

Laaß, M. 2016. The origins of the cochlea and impedance matching hearing in synapsids. Acta Palaeontologica Polonica 61(2):267–280.

Ladich, F., H. Winkler. 2017. Acoustic communication in terrestrial and aquatic vertebrates. Journal of Experimental Biology 220:2306-2317.

Lambe, L.M. 1902. New genera and species from the Belly River Series (mid-Cretaceous). Geological Survey of Canada Contributions to Canadian Palaeontology 3(2):25-81.

Lande, R. 1976. Natural selection and random genetic drift in phenotypic evolution. Evolution 30:314–334

Langston, W. 1958. Champsosaur giants. Natural History Papers, Canadian Museum of Nature 2:1-4.

Larsell, O. 1929. The cerebellum of reptiles: Lizards and snake. The Journal of Comparative Neurology 41(1):59-94.

Laurenti, J.N. 1768. Specimen medicum, exhibens synopsin reptilium emendatam cum experimentis circa venena et antidota reptilium austriacorum. Vienna J.T.N. de Trattnern.

Lautenschlager, S., E.J. Rayfield, P. Altangerel, L.E. Zanno, L.M. Witmer. 2012. The endocranial anatomy of Therizinosauria and its implications for sensory and cognitive function. PLoS One 7(12): e52289.

Lautenschlager, S., R.J. Butler. 2016. Neural and endocranial anatomy of Triassic phytosaurian reptiles and convergence with fossil and modern crocodylians. PeerJ 4:e2251; DOI 10.7717/peerj.2251

Lautenschlager, S., G.S. Ferreira, I. Werneburg. 2018. Sensory evolution and ecology of early turtles revealed by digital endocranial reconstructions. Frontiers in Ecology and Evolution 6:7 doi: 10.3389/fevo.2018.00007.

Lauters, P., W. Caudyzer, M. Vercauteren, P. Godefroit. 2012. The brain of Iguanodon and Mantellisaurus: perspectives on ornithopod evolution. In: Bernissart dinosaurs and Early Cretaceous terrestrial ecosystems. P. Godefroit (Ed.). Indiana University Press, Indiana, USA. p. 213-224.

Lebrun, R. MorphoDig, an open-source 3D freeware dedicated to biology. IPC5, Paris, France; 07/2018

Lee, M.S.Y. 2013. Turtle origins: insights from phylogenetic retrofitting and molecular scaffolds. Journal of Evolutionary Biology 26(13):2729-2738.

Lehman, T.M., and K. Barnes. 2010. *Champsosaurus* (Diapsida: Choristodera) from the Paleocene of west Texas: paleoclimatic implications. Journal of Paleontology 84(2):341-345.

Lemoine W. 1884. Étude sur les caractères génériques du Simoedosaure reptile nouveau de la faune cernarysienne des environs de Reims. Imprimerie et Lithagaphie Matot-braine (Reims) 1884:1-38.

Lenhardt, M.L., R.C. Klinger, J.A. Musick. 1985. Marine turtle middle-ear anatomy. Journal of Auditory Research 25:66–72.

Lima, F.C., K.F. Pereira, A.S. Abe, A. Sebben. 2014. Osteologia do neurocrânio de *Iguana iguana iguana* (Squamata: Iguanidae). Pesquisa Veterinária Brasileira 34(1): 69–73.

Liu, J. 2004. A nearly complete skeleton of *Ikechosaurus pijiagouensis* sp. nov. (Reptilia: Choristodera) from the Jiufotang Formation (Lower Cretaceous) of Liaoning, China. Vertebrata Pal Asiatica 42:120–129.

Losos, J.B. 2008. Phylogenetic niche conservatism, phylogenetic signal and the relationship between phylogenetic relatedness and ecological similarity among species. Ecology Letters 11:995-1007.

Lu, J., Q. Zhu, X. Cheng, and X. Du. 1999a. Computed tomography (CT) of nasal cavity of *Ikechosaurus sunailinae* (Reptilia: Choristodera). Chinese Science Bulletin 44(24):2277-2281.

Lu, J., Y. Kobayashi, and Z. Li. 1999b. A new species of *Ikechosaurus* (Reptilia: Choristodera) from the Jiufotang Formation (Early Cretaceous) of Chifeng City, Inner Mongolia. Bulletin de l'Institut Royal des Sciences Naturelles de Belgique, Sciences de la Terre 69:37-47.

Lu, J., Y. Kobayashi, D.C. Deeming, and Y. Liu. 2014. Post-natal parental care in a Cretaceous diapsid from northeastern China. Geoscience Journal 19(2):273-280.

Maddin, H.C., A.P. Russell, J.S. Anderson. 2012. Phylogenetic implications of the morphology of the braincase of caecilian amphibians (Gymnophiona). Zoological Journal of the Linnean Society 166:160-201.

Maddin, H.C., E. Sherratt. 2014. Influence of fossoriality on inner ear morphology: insights from caecilian amphibians. 225:83-93.

Malinzak, M.D., R.F. Kaya, T.E. Hullar. 2012. Locomotor head movements and semicircular canal morphology in primates. PNAS 109(44):17914–17919.

Mao, J.J. 2002. Mechanobiology of craniofacial sutures. Journal of Dental Research 81(12):810–816.

Marek, R.D., B.C. Moon , M. Williams, M.J. Benton. 2015. The skull and endocranium of a Lower Jurassic Ichthyosaur based on digital reconstructions. Palaeontology 58:1-20.

Marugán-Lobón, J., L,M. Chiappe, A.A. Farke. 2013. The variability of inner ear orientation in saurischian dinosaurs: testing the use of semicircular canals as a reference system for comparative anatomy. PeerJ 1:e124; DOI 10.7717/peerj.124

Marti, B., D. Sirinelli, L. Maurin, E. Carpentier. 2013. Wormian bones in a general paediatric population. Diagnostic and Interventional Imaging 94:428–432.

Mason, J.M. 2007. Pathways for sound transmission to the inner ear in amphibians. In: Hearing and Sound Communication in Amphibians. P.M. Narins, A.S. Feng, R.R. Fey, A.N. Popper (Eds.). p147-183.

Matsumoto, R., S.E. Evans, M. Manabe. 2007. The choristoderan reptile *Monjurosuchus* from the Early Cretaceous of Japan. Acta Palaeontologica Polonica, 52: 329-350.

Matsumoto, R., S. Suzuki, K. Tsogtbaatar, and S.E. Evans. 2009. New material of the enigmatic reptile *Khurendukhosaurus* (Diapsida: Choristodera) from Mongolia. Naturwissenschaften, 96:233-242.

Matsumoto, R., and S.E. Evans. 2010. Choristoderes and the freshwater assemblages of Laurasia. Journal of Iberian Geology 36(2):253-274.

Matsumoto, R., E. Buffetaut, F. Escuillie, S. Hervet, and S.E. Evans. 2013. New material of the choristodere *Lazarussuchus* (Diapsida, Choristodera) from the Paleogene of France. Journal of Vertebrate Paleontology 33(2):319-339.

Matsumoto, R., and S.E. Evans. 2016. Morphology and function of the palatal dentition in Choristodera. Journal of Anatomy 228:414-429.

Matsumoto, R., L. Dong, Y. Wang, and S.E. Evans. 2019. The first record of a nearly complete choristodere (Reptilia: Diapsida) from the Upper Jurassic of Hebei Province, People's Republic of China. Journal of Systematic Palaeontology 0:1-18. doi: https://doi.org/10.1080/14772019.2018.1494220

Matthew, W.D. 1916. A marsupial from the Belly River Cretaceous with critical observations upon the affinities of the Cretaceous mammals. Bulletin of the American Museum of Natural History 35(25):477-499.

McGowan, C. 1973. The cranial morphology of the Lower Liassic latipinnate ichthyosaurs of England, Bulletin of the British Museum (Natural History). Geology 24:1–109.

Mennecart, B., and L. Costeur. 2016. Shape variation and ontogeny of the ruminant bony labyrinth, an example in Tragulidae. Journal of Anatomy 229:422-435.

Modesto SP, H.D. Sues. 2004. The skull of the Early Triassic archosauromorph reptile *Prolacerta broomi* and its phylogenetic significance. Zoological Journal of the Linnean Society 140:335-351.

Montefeltro, F.C., D.V. Andrade, H.C.E. Larsson. 2016. The evolution of the meatal chamber in crocodyliforms. Journal of Anatomy 228:838-863.

Mooney, T.A., M. Yamato, B.K. Branstetter. 2012. Hearing in cetaceans: from natural history to experimental biology. Advances in Marine Biology 63:197-246.

Müller, J., and L.A. Tsuji. 2007. Impedance-matching hearing in Paleozoic reptiles: Evidence of advanced sensory perception at an early stage of amniote evolution. PLoS one 2(9).

Müller, J., C. Bickelmann, and G. Sobral. 2018. The evolution and fossil history of sensory perception in amniote vertebrates. Annual Review of Earth and Planetary Sciences 46:495–519.

Neenan, J.M., T. Reich, S.W. Evers, P.S. Druckenmiller, D.F.A.E. Voeten, J.N. Choiniere, P.M. Barrett, S.E. Pierce, R.B.J. Benson. 2017. Evolution of the sauropterygian labyrinth with increasingly pelagic lifestyles. Current Biology 27: 3852–3858.

Oaks, J.R. 2011. A time-calibrates species tree of Crocodylia reveals a recent radiation of the true crocodiles. Evolution 65(11):3285–3297.

O'Laughlin, V.D. 2004. Effects of different kinds of cranial deformation on the incidence of wormian bones. American Journal of Physical Anthropology 123(2):146–155.

Olori, J.C. 2010. Digital endocasts of the cranial cavity and osseous labyrinth of the burrowing snake *Uropeltis woodmasoni* (Alethinophidia: Uropeltidae). Copeia 1:14-26.

Ollonen, J., F.O. Da Silva, K. Mahlow, N. Di-Poi. 2018. Skull development, ossification pattern, and adult shape in the emerging lizard model organism *Pogona vitticeps*: A comparative analysis with other squamates. Frontiers in Physiology 9:1–26.

Osborne, H. 1903. The reptilian subclasses Diapsida and Synapsida and the early history of the Diaptosauria. Memoires of the American Museum of Natural History. l(8):449-508.

Padian, K., and C.L. May. 1993. The earliest dinosaurs. New Mexico Museum of Natural History Science Bulletin 3:379-381.

Palci A., M.N. Hutchinson, M.W. Caldwell, J.D. Scanlon, M.S.Y. Lee. 2018. Palaeoecological inferences for the fossil Australian snakes *Yurlunggur* and *Wonambi* (Serpentes, Madtsoiidae). Royal Society of Open Science 5: 172012.

Paluh, D.J., A.M. Bauer. 2017. Comparative skull anatomy of terrestrial and crevice-dwelling *Trachylepis* skinks (Squamata: Scincidae) with a survey of resources in scincid cranial osteology. PLoS ONE 12(9):1–34.

Pardo, J.D., R. Holmes, J.S. Anderson. 2019. An enigmatic braincase from Five Points, Ohio (Westphalian D) further supports a stem tetrapod position for aistopods. Earth and Environmental Science Transactions of the Royal Society of Edinburgh 109:255-264.

Parks, W.A. 1927. *Champsosaurus albertensis*, a new species of rhynchocephalian from the Edmonton formation of Alberta. University of Toronto Studies, Geological Series 23:1-53.

Parks, W.A. 1933. New species of *Champsosaurus* from the Belly River Formation of Alberta, Canada. Transactions of the Royal Society of Canada 27(4):121-143.

Patel, N.H. 1994. Developmental evolution: insights from studies of insect segmentation. Science 266(5185):581–590.

Pfaff, C., T. Martin, I. Ruf. 2015. Bony labyrinth morphometry indicates locomotor adaptations in the squirrel-related clade (Rodentia, Mammalia). Proceedings of the Royal Society B 282(1809):1-9.

Piniak, W.E.D., S.A. Eckert, C.A. Harms, E.M. Stringer. 2012. Underwater hearing sensitivity of the leatherback sea turtle (*Dermochelys coriacea*): Assessing the potential effect of anthropogenic noise. U.S. Department of the Interior Bureau of Ocean Energy Management 2012-01156.

Platel, R. 1979. Brain weight-body weight relationships. In: Biology of the Reptilia, Volume 9. C. Gans, R. C. Northcutt, and P. Ulinski (Eds.). Academic Press, London and New York. pp. 147-171.

Popper, A.N., Z. Lu. 2000. Structure-function relationships in fish otolith organs. Fisheries Research 46:15-25.

Porto, A., F.B. de Oliveira, L.T. Shirai, V. de Conto, G. Marroig. 2009. The evolution of modularity in the mammalian skull I: Morphological integration patterns and magnitudes. Evolutionary Biology 36:118–135.

Pritchard, J.J., J.H. Scott, F.G. Girgis. 1956. The structure and development of cranial and facial sutures. Journal of Anatomy 90:73–86.

Rabbitt, R.D., E.R. Damiano, and J.W. Grant. 2004. Biomechanics of the Semicircular Canals and Otolith Organs. In: The Vestibular System. (Eds) S.M. Highstein, R.R. Fay, and A.N. Popper. Springer: New York.

Ren, D., L. Lu, Z. Guo, and S. Ji. 1995. Faunae and Stratigraphy of Jurassic-Cretaceous in Beijing and the Adjacent Areas. Seismological Press, Beijing.

Rieppel, O. 1976. The homology of the laterosphenoid bone in snakes. Herpetologica 32(4):426–429.

Rieppel, O. 1985. The recessus scalae tympani and its bearing on the classification of reptiles. Journal of Herpetology 19(3): 373–384.

Rieppel, O. 1994. The Braincases of *Simosaurus* and *Nothosaurus*: Monophyly of the Nothosauridae (Reptilia: Sauropterygia). Journal of Vertebrate Paleontology 14(1):9–23.

Rieppel, O., and R.R. Reisz. 1999. The origin and early evolution of turtles. Annual Review of Ecology and Systematics 30:1-22.

Rieppel, O., H. Zahar. 2000. The braincases of mosasaurs the relationships of snakes. Zoological Journal of the Linnean Society 129:489–514.

Romer, A.S. 1956. Osteology of the Reptiles. Chicago: The University of Chicago Press.

Romer, A.S., T.S. Parsons. 1977. The Vertebrate Body, 5th Edition. Toronto: W.B. Saunders Company.

Rowe, T. 1987. Definition and diagnosis in the phylogenetic system. Systematic Zoology 36(2):208-211.

Rowe, T., C.A. Brochu, M. Colbert, J.W. Merck Jr., K. Kishi, E. Saglamer, S. Warren. 1999. Alligator: Digital atlas of the skull. Society of Vertebrate Paleontology Memoir 6:1-8.

Russell, L.S. 1956. The Cretaceous Reptile *Champsosaurus natator* Parks. National Museum of Canada, Department of Northern Affairs and National Resources. Bulletin 145.

Sanchez-Lara, P.A., J.M. Graham Jr., A.V. Hing, J. Lee, M. Cunningham. 2007. The morphogenesis of Wormian bones: A study of craniosynostosis and purposeful cranial deformation. American Journal of Medical Genetics Part A 143A:3243–3251.

Sato, T., X.C. Wu , A. Tirabasso, and P. Bloskie. 2011. Braincase of a polycotylid plesiosaur (Reptilia: Sauropterygia) from the Upper Cretaceous of Manitoba, Canada. Journal of Vertebrate Paleontology 31(2):313-329.

Schmitz, L., and R. Motani. 2011. Nocturnality in dinosaurs inferred from scleral ring and orbit morphology. Science, New Series 332(6030) 705-708.

Scott, T.P., P.J. Weldon, 1990. Chemoreception in the feeding behaviour of adult American alligators, *Alligator mississippiensis*. Animal Behaviour 39(2):398-400.

Seiffert. J. 1973. Contribuicao para o conhecimento da Fauna do Kimeridgiano da Mina de Lignito Guimarota (Leiria, Portugal), 3; Upper Jurassic lizards from Central Portugal. Servicos Geologicos de Portugal 22:7-85.

Sepkoski, J.J. 1998. Rates of speciation in the fossil record. Philosophical Transactions of the Royal Society of London B 353:315-326.

Sereno, P.C. 1991. *Lesothosaurus*, "Fabrosaurids," and the early evolution of Ornithischia. Journal of Vertebrate Paleontology 11(2):168–197.

Sereno, P.C. 1999. Definitions in phylogenetic taxonomy: Critique and rationale. Systematic Biology 48(2):329–351.

Shubin, N., C. Tabin, S. Carroll. 1997. Fossils, genes and the evolution of animal limbs. Nature 388:639–649.

Sidor, C.A. 2001. Simplification as a trend in synapsid cranial evolution. Evolution 55(7):1419–1442.

Sigogneau-Russell D. 1979. Les champsosaures Européens: mise au point sur le champsosaure d'erquelinnes (landenien inferieur, Belgique). Annales de Paliontologit (Vertibris) 65: 7-62.

Sigogneau-Russell, D. 1981a. Étude ostéologique de reptile *Simoedosaurus* (Choristodera). II^{e} partie: squelette postcranien. Annales de Paléontologie (Vertébrés) 67:61-140.

Sigogneau-Russell, D. 1981b. Presence d'un Champsosauride dans le Crétacé supérieur de Chine. Comptes Rendus de 1'Academie des Sciences, Paris, 292: 1-4.

Sigogneau-Russell, D. 1985. Definition of the Type-Species of *Simoedosaurus*, *S. lemoinei* Gervais, 1877 (Choristodera, Reptilia). Journal of Paleontology 59(3):766-767.

Sigogneau-Russell, D. and D. Baird. 1978. Presence du genre *Simoedosaurus* (Reptilia, Choristodera) en Amerique du Nord. Géobios 11(2):251-255.

Sigogneau-Russell, D. and D.E. Russell. 1978. Étude ostéologique du Reptile *Simoedosaurus* (Choristodera). Annales de Paleontologie (Vertebres) 64:1-84.

Sigogneau-Russell, D., and M. Efimov. 1984. Un Choristodera (Eosuchia?) insolite du Crétacé inférieur de Mongolie. Paléontologie 58(3/4): 279-294.

Simões, T.R., M.W. Caldwell, M. Tałanda, M. Bernardi, A. Palci, O. Vernygora1, F. Bernardini, L. Mancini, and R.L. Nydam. 2018. The origin of squamates revealed by a Middle Triassic lizard from the Italian Alps. Nature 557:706-723.

Skutschas, P.P. 2008. A choristoderan reptile from the Lower Cretaceous of Transbaikalia, Russia. Neues Jahrbuch für Geologie und Paläontologie – Abhandlungen 247(1):63-78.

Skutschas, P.P., and D.D. Vitenko. 2017. Early Cretaceous choristoderes (Diapsida, Choristodera) from Siberia, Russia. Cretaceous Research 77:79-92.

Sobral, G., R.B. Sookias, B.A.S. Bhullar, R. Smith, R.J. Butler, J. Müller. 2016. New information on the braincase and inner ear of *Euparkeria capensis* Broom: implications for diapsid and archosaur evolution. Royal Society of Open Science 3:1–41.

Sobral, G., and J. Müller. 2019. The braincase of *Mesosuchus browni* (Reptilia, Archosauromorpha) with information on the inner ear and description of a pneumatic sinus. PeerJ 7:e6798 DOI 10.7717/peerj.6798

Specht, M., R. Lebrun, C.P.E. Zollikofer. 2007. Visualizing shape transformation between chimpanzee and human braincases. The Visual Computer 23:743–751.

Spoor, F.D., F. Zonneveld. 1998. Comparative review of the human bony labyrinth. Yearbook of Physical Anthropology 107(S27):211-251.

Spoor, F., S. Bajpai, S.T. Hussain, K. Kumar, J.G.M. Thewissen. 2002. Vestibular evidence for the evolution of aquatic behaviour in early cetaceans. Nature 417:163-166.

Spoor, F., T. Garland Jr., G. Krovitz, T.M. Ryan, M.T. Silcox, A. Walker. 2007. The primate semicircular canal system and locomotion. Proceedings of the National Academy of Science 104(26):10808-10812.

Stocker, M.R., S.J. Nesbitt, K.E. Criswell, W.G. Parker, L.M. Witmer, T.B. Rowe, R. Ridgely, M.A. Brown. 2016. A Dome-Headed Stem Archosaur Exemplifies Convergence among Dinosaurs and Their Distant Relatives. Current Biology: 26:2674–2680.

Storrs, G.W., and D.J. Gower. 1993. The earliest possible choristodere (Diapsida) and gaps in the fossil record of semi-aquatic reptiles. Journal of the Geological Society 150:1103-1107.

Storrs, G.W., D.J. Gower, N.F. Large. 1996. The diapsid reptile, *Pachystropheus rhaeticus*, a probable choristodere from the Rhaetian of Europe. Palaeontology 39: 323–349.

Tarduno, J.A., R.D. Cottrell, S.L. Wilkison, 1997. Magnetostratigraphy of the Late Cretaceous to Eocene Sverdrup Basin: implications for heterochroneity, deformation, and rotations in the Canadian Arctic Archipelago. Journal of Geophysical Research 102:723–746.

Tattersall, G.J., V. Cadena, and M.C. Skinner. 2006. Respiratory cooling and thermoregulatory coupling in reptiles. Respiratory Physiology and Neurobiology 154(2):302-318.

Taylor, M.P., M.J. Wedel, D. Naish. 2009. Head and neck posture in sauropod dinosaurs inferred from extant animals. Acta Palaeontologica Polonica 54(2):213–220.

Tokaryk, T.T. 2009. A partial skeleton of Champsosaurus from the Frenchman Formation (Maastrichtian) of Saskatchewan. Frenchman Formation Terrestrial Ecosystem Conference Program. Royal Saskatchewan Museum Contribution to Science Number 12, pp. 55-59.

Tonini, J.F.R., K.H. Beard, R.B. Ferreira, W. Jetz, R.A. Pyron. 2016. Fully-sampled phylogenies of squamates reveal evolutionary patterns in threat status. Biological Conservation 204:23-31.

Tucker, A.S. 2016. Major evolutionary transitions and innovations: the tympanic middle ear. Philosophical Transactions of the Royal Society B 372:20150483.

Vandermark, D., J.A. Tarduno, D.A. Brinkman. 2006. A fossil champsosaur population from the high Arctic: Implications for Late Cretaceous paleotemperatures. Palaeogeography, Palaeoclimatology, Palaeoecology 248:49–59

Vergne, A.L., M.B. Pritz, and N. Mathevon. 2009. Acoustic communication in crocodilians: From behaviour to brain. Biological Reviews 84:391-411.

von Huene, E.V. 1935. Ein Rhynchocephale aus dem rhat (Pachystropheus e.g.) Neues Jahrbuch für Minerologie. Geologie und Paläontologie 74:441-447.

Walsh, S.A., P.M. Barrett, A.C. Milner, G. Manley, and L.M. Witmer. 2009. Inner ear anatomy is a proxy for deducing auditory capability and behaviour in reptiles and birds. Proceedings of the Royal Society B. 276:1355–1360.

Wang, Z., J. Pascual-Anaya, A. Zadissa, W. Li, Y. Niimura, Z. Huang, C. Li, S. White, … N. Irie. 2013. The draft genomes of soft-shell turtle and green sea turtle yield insights into the development and evolution of the turtle-specific body plan. Nature Genetics 45(6):701-709.

Wever, E.G. 1978. The Reptile Ear. Princeton University Press, Princeton.

Willis, K.L., J. Christensen-Dalsgaard, D.R. Ketten, C.E. Carr. 2013. Middle ear cavity morphology is consistent with an aquatic origin for testudines. PLoS ONE 8(1): e54086.

Witmer, L.M., S. Chatterjee, J. Franzosa, T. Rowe. 2003. Neuroanatomy of flying reptiles and implications for flight, posture and behaviour. Nature 425:950-953.

Witmer, L.M., R.C. Ridgely. 2008. The paranasal air sinuses of predatory and armored dinosaurs (Archosauria: Theropoda and Ankylosauria) and their contribution to cephalic structure. The Anatomical Record 291:1362–1388.

Witmer, L.M., R.C. Ridgely, D.L. Dufeau, M.C. Semones. 2008. Using CT to peer into the past: 3D visualization of the brain and ear regions of birds, crocodiles, and nonavian dinosaurs. In: Anatomical imaging: Towards a new morphology. H. Endo and R. Frey (Eds.). p65-87.

Witmer, L.M., R.C. Ridgely. 2009. New insights into the brain, braincase, and ear region of tyrannosaurs (Dinosauria, Theropoda), with implications for sensory organization and behavior. The Anatomical Record 292:1266-1296.

Yi, H., M.A. Norell. 2015. The burrowing origin of modern snakes. Science Advances. 1(10):1–5.

Young, C.C. 1964. New fossil crocodiles from China. Vertebrata Pal Asiatica, 8: 189-210

Young, B.A., N. Mathevon, Y. Tang. 2014. In: Insights from comparative hearing research. (Eds.) C. Köppl, G.A. Manley, A.N. Popper, R.R. Fay. Springer, New York. p. 323-346.

Zelenitsky, D.K., F. Therrien, R.C. Ridgely, A.R. McGee, L.M. Witmer. 2011. Evolution of olfaction in non-avian theropod dinosaurs and birds. Proceedings of the Royal Society B 278:3625–3634.